New space-time domain decomposition algorithms combined with the Parareal algorithm

Duc Quang Bui

THÈSE

présenté à

L'UNIVERSITÉ SORBONNE PARIS NORD

École doctorale : Galilée

Par

Duc Quang BUI

Pour obtenir le grade de

DOCTEUR de l'UNIVERSITÉ SORBONNE PARIS NORD

Spécialité : Mathématiques Appliquées

Nouveaux algorithmes de décomposition de domaine espace-temps combinés avec l'algorithme Pararéel

Directeur de thèse : Pascal OMNES
Co-directeurs de thèse : Caroline JAPHET

Soutenue le : 28 juin 2021

Devant la commission d'examen formée de :

M. Martin GANDER	Université de Genève	Rapporteur
Mme. Laurence HALPERN	Université Sorbonne Paris Nord	Examinateur
Mme. Caroline JAPHET	Université Sorbonne Paris Nord	Co-directeur de thèse
M. Yvon MADAY	Sorbonne Université	Examinateur
Mme. Olga MULA	Université Paris Dauphine	Examinateur
M. Pascal OMNES	CEA	Directeur de thèse
M. Julien SALOMON	INRIA Paris	Rapporteur
M. Gabriel TURINICI	Université Paris Dauphine	Examinateur

DOCTORAL DISSERTATION

presented at

UNIVERSITY SORBONNE PARIS NORD

Doctoral school: Galilée

By

Duc Quang BUI

To obtain the degree of

DOCTOR of UNIVERSITY SORBONNE PARIS NORD

Speciality: Applied Mathematics

New space-time domain decomposition algorithms combined with the Parareal algorithm

Thesis advisor: Pascal OMNES

Thesis co-advisor: Caroline JAPHET

Defended on: 28 June 2021

In front of the examination committee consisting of:

M. Martin GANDER	University of Genève	Reviewer
Mme. Laurence HALPERN	University Sorbonne Paris Nord	Examiner
Mme. Caroline JAPHET	University Sorbonne Paris Nord	Thesis co-advisor
M. Yvon MADAY	Sorbonne University	Examiner
Mme. Olga MULA	University Paris Dauphine	Examiner
M. Pascal OMNES	CEA	Thesis advisor
M. Julien SALOMON	INRIA Paris	Reviewer
M. Gabriel TURINICI	University Paris Dauphine	Examiner

Résumé

Nous étudions dans cette thèse les méthodes de décomposition de domaine spatio-temporelles, en particulier la méthode Pararéele, la méthode de Relaxation d'Ondes Optimisée (OSWR) et leur couplage, appliqués à la simulation numérique des équations paraboliques et des équations de Stokes.

Nous proposons et analysons dans un premier temps un couplage de la méthode Pararéel avec la méthode OSWR. La méthode couplée Pararéel- OSWR obtenue est une méthode parallèle, à la fois en temps et en espace, avec seulement peu d'itérations OSWR dans le propagateur fin afin de réduire les coûts de calcul et avec un propagateur grossier classique déduit de la méthode d'Euler implicite. L'analyse de cette méthode couplée est présentée pour une équation d'advection-réaction-diffusion unidimensionnelle. Pour le couplage de Pararéel avec OSWR sans recouvrement, nous prouvons un résultat de convergence général via des estimations d'énergie. Des résultats numériques pour des problèmes d'advection-diffusion bidimensionnels et pour une équation de diffusion avec de fortes hétérogénéités sont présentés, pour illustrer les performances de l'algorithme couplé Pararéel-OSWR. Nous présentons ensuite également un algorithme qui couple Pararéel avec OSWR avec recouvrement, et nous analysons son facteur de convergence en utilisant la convergence linéaire de OSWR avec recouvrement que nous obtenons par une analyse de Fourier.

Pour les équations de Stokes, nous présentons un algorithme OSWR bien posé et une estimation d'énergie pour la convergence des vitesses. Ensuite, nous montrons qu'en général, la pression ne converge pas et nous proposons une correction pour remédier à cela. Une stratégie similaire basée sur la transformée de Fourier est effectuée pour obtenir la formulation du facteur de convergence. Des tests numériques suivent pour illustrer les performances de la méthode OSWR avec correction. De plus, ces résultats sont également étendus pour obtenir des résultats similaires sur l'équation d'Oseen. Enfin, nous proposons l'algorithme Pararéel et un couplage Pararéel-OSWR pour les équations de Stokes, et démontrons certaines de leurs propriétés de base.

Mots clés : Pararéel, Relaxation d'Ondes Optimisée, OSWR, équations paraboliques, équations de Stokes, équations d'Oseen.

Abstract

We study in this thesis space-time domain decomposition methods, in particular, the Parareal method, the Optimized Schwarz Waveform Relaxation (OSWR) method and their coupling, applied to the numerical simulation of parabolic equations and of the Stokes equations.

We first propose and analyze a coupling of the Parareal method with the OSWR method. The obtained coupled Parareal-OSWR method is a parallel method, both in the time and space directions, with only few OSWR iterations in the fine propagator in order to reduce computational costs and with a simple coarse propagator deduced from the Backward Euler method. The analysis of this coupled method is presented for a one-dimensional advection-reaction-diffusion equation. For the coupling of Parareal with non-overlapping OSWR, we prove a general convergence result via energy estimates. Numerical results for two-dimensional advection-diffusion problems and for a diffusion equation with strong heterogeneities are presented, to illustrate the performance of the coupled Parareal-OSWR algorithm. We then present also an algorithm that couples Parareal with overlapping OSWR, and we analyze its convergence factor by using the linear convergence of overlapping OSWR that we obtain through a Fourier analysis.

For the Stokes equations, we present a well-posed OSWR algorithm and an energy estimate for the convergence of the velocities. Then we show that, in general, the pressure does not converge and we propose a correction against this. A similar strategy based on Fourier transform is performed to get the formulation of the convergence factor. Numerical tests follow to illustrate the performance of the OSWR method with correction. In addition, these results are also extended to get similar ones on the Oseen equation. Finally, we propose the Parareal algorithm and a Parareal-OSWR coupling for the Stokes equations, and prove some of their basic properties.

Keywords: Parareal, Optimized Schwarz Waveform Relaxation, parabolic equations, Stokes equations, Oseen equations.

Acknowledgements

First and foremost, I would like to express first my deepest gratitude to my dedicated advisors Caroline Japhet and Pascal Omnes for their guidance and support during the last five years. Thank you, Caroline, for your enthusiasm and inspiration that encouraged me whenever I felt disappointed about my work. I will never forget engrossing exchanges with you which were not just about work but also about life and many other things. Thank you, Pascal, for easing the start of my journey in France with your invaluable assistance. During my PhD, it was always comfortable and fruitful to discuss with you. Your fine pedagogy and immense patience led me to understand things in depth many times.

I am also very grateful to Yvons Maday, the external collaborator in the first half of my thesis. Your kindliness and energy greatly motivated me every time we met, and I am very glad that you have accepted my invitation to be a jury member.

I am deeply indebted to Mr. Martin Gander and Mr. Julien Salomon, who generously undertook the tedious task of being rapporteurs on this thesis. Their comments and suggestions are greatly appreciated. I am also very honored to have Mrs. Laurence Halpern, Mrs. Olga Mula and Mr. Gabriel Turinici to be part of the jury and I would like to express my grateful thanks for their availability.

Sincere thanks must also go to the financial support of the project ANR-CINE-PARA, USPN and Le Cnam Paris for my thesis. Thank you for giving me a chance to fulfill my doctoral studies and for offering favorable conditions that facilitated my work.

I am also grateful to my professors and the organizers of French-Vietnam Master 2 (PUF) for the great courses and the opportunities to do research in France. Thanks to this program, I had the chance to work with my advisors, which led to this thesis.

I will not forget to thank especially Mr. Nguyen Van Dong for guiding me through my very first steps in research during university time.

I would like to extend my gratitude to the administrative team of LAGA and to Mr. Amara Ammad (SAIC) for their help during my PhD. I am also grateful to the lecturers that I worked with for sharing with me their invaluable experience and knowledge: Mr. Christian Ausoni, Mr. Didier Gamblin, Mr. Rahdi Abdelmoula, Mr. Thomas Duyckaerts, Mr. Thierry Horsin, Mr. François Dubois, Mrs. Isabelle Gil and Mrs. Agnes Carpentier. Many thanks to the secretaries of Institute Galilée (USPN), EPN06 and CFA Saint-Denis (Le Cnam) for their help on facilities for my courses.

I would like to show my appreciation to my Vietnamese friends who helped me handle daily problems during my internship and first days of my PhD: Nga, Huyen Nguyen, Huyen Nong, Phuong, Thuy, Hoang, Viet, Hieu, Thi, Diep, Nhat. I especially give thanks to Binh for having shared with me his room in the first three weeks of my PhD until I could find a decent room for myself. I also want to thank Mouna, my new

neighbor, for delicious Tunisian cakes, candies, juice and traditional dishes. And also thanks to all many dear sisters and brothers of Vietnamese friend group in University Paris 13 for all the great times and supports.

Finally, the special place is reserved for my family, especially my loving parents, my elder sister and my fiancée Trâm who have always been there for me through thick and thin. Your love and support is a source of encouragement and motivation for me to keep working and perfecting myself. Words simply fail to express my affection for you all.

Contents

List of Figures

List of Tables

Introduction

Motivation

The numerical simulation of Partial Differential Equations (PDEs) is an important domain of research and development, both in Academia (ranging from the development and analysis of new, fast, accurate and efficient numerical schemes to applications like ab initio calculation in quantum chemistry, simulation in porous media with application in ecology, computational electromagnetics and plasma physics, fluid flows in various regimes, etc) and in Industry (oil recovery in the oil industry, Computational Fluid Dynamics for example in Aeronautics, combustion in motor engineering and thermohydraulics and neutron transport in nuclear engineering, among many other fields). High performance computers are now able to simulate the fundamental laws representing the behavior of the phenomenon under consideration. Simulations are more and more reliable, close to the real experiments and have become a major tool to better understand complex situations, and then allow to optimize and control processes.

From 1970s to 2000s, the power of chips and processors increased significantly. However, this power seems to reach its limits: the power of a single CPU has not been improved much recently. Parallel computing approaches are then proposed to overcome these limits. In parallel architectures, the main objective is broken into smaller tasks that can be executed independently on different processors. The outputs are then regrouped to construct an approximate solution to the main problem. This process usually repeats several times before an acceptable solution is reached. One then has to give a good strategy to reduce the number of iterations needed.

One of the applications envisioned by the ANR CINE-PARA project that supports this thesis is the numerical studies in the nuclear industry, among which the interaction of turbulent flow with the solid structures of nuclear reactors. These matters are currently investigated by using a CFD code developed in the Nuclear Energy Division of the CEA, called `TrioCFD` (see [27], [26], [15], also [30], [13] for the applications). The code is developed for local and fine-scale calculations using especially Reynolds-Averaged Navier-Stokes (RANS) ([98]) and Large Eddy Simulation (LES) models ([14], [12]) that lead to very large systems consisting of more than 150 million cells and one billion degrees of freedom over hundreds of thousands of time steps. Therefore, massive parallelism is designed to handle such simulations, and the code `TrioCFD` may use more than 10,000 processors (see [14]).

Up to now, this parallelism only concerns the heavy algebra (matrix-vector products and vector scalar products in high dimensions) involved in the iterative algorithms (Conjugate Gradient, GMRES) used to find approximate solutions of large linear systems. The aim of this thesis is to lead preliminary studies on simpler models, such as

the advection-diffusion equations or the Stokes equations, in order to pave the way for the introduction in that code of space-time domain decomposition techniques at the PDE level that we are going to review in the next paragraphs. The aim would be to further speed-up the execution of heavy CFD computations.

Bibliography and previous studies

Parallel-in-time methods

The idea of parallelization in the time direction has a long history of more than 50 years, which is presented in details in [47]. The very first idea was introduced by Nievergelt in [94], based on a multiple shooting technique. This multiple shooting technique consists in solving the evolution problems in parallel, splitting the whole time interval into smaller sub-intervals, on which one gets smaller sub-problems. Each sub-problem can be distributed independently to a processor. As we used inaccurate inputs for these processors at the start, the output generally does not match with the solution, hence a correction process is then performed to correct those errors. The method is then formalized in a form of an iterative method, first at the discrete level by Bellen and Zennaro in [8], and then at the continuous level for dissipative ODEs by Chartier and Philippe in [31]; for the latter case, the authors also proved a quadratic convergence.

The Parareal algorithm was independently introduced first by Lions, Maday, and Turinici in their short note [82]. The long time interval is divided into smaller windows, the original problem is divided into smaller sub-problems. Instead of solving these sub-problems sequentially, one could start from random initial conditions (as input) and perform fine solvers in parallel to get new initial conditions (as output). A coarse and cheaper solver is then performed sequentially to correct and improve accuracy of those new initial conditions. This process is repeated until sufficiently accurate initial conditions are obtained. Later, in [56], Gander and Vandewalle pointed Parareal as a multiple shooting method and proved its superlinear convergence. Other important propositions and analyses on Parareal were also achieved: for non-exact fine solvers for ODEs [7]; for the non-linear case [48]; for hyperbolic equations ([37]), for Navier-Stokes equations ([107], [43]).

There is another approach for parallel-in-time method - the waveform relaxation technique. It was first introduced by Picard ([96]) and Lindelof ([81]), then an interesting variant was developed by Lelarasmee, Ruehli and Sangiovanni-Vincentelli ([79]). They defined the waveform relaxation as "an iterative method for analyzing non-linear dynamical systems in the time domain, which, at each iteration, decomposes the system into several dynamical subsystems, analyzed for the entire given time interval". Inheriting those initial ideas, Gander then showed that one can use overlapping domain decomposition to obtain a waveform relaxation algorithm ([45]).

Domain decomposition methods

The key of domain decomposition methods is to divide a large domain into smaller sub-domains, in space direction. When the model is non stationary, then the original problem is transformed into multi-domain space-time sub-problems. These ideas originated from the work of H. A. Schwarz [102] in 1870, in which he proposed an iterative method to show the existence and uniqueness of the solution for the harmonic problem

on an unusual domain made of a union of a rectangle and a disk. The algorithm starts from a trace on the interface of the left sub-domain, the solution on the left sub-domain is calculated, then used to calculate the trace on the interface of the right sub-domain. The solution on the right sub-domain is calculated, then the information is exchanged back, and the process continues. This method is now called Schwarz alternating or Schwarz multiplicative method.

In [85], P. L. Lions introduced a parallel version of this algorithm, called additive Schwarz method. This idea received much attention due to the development of parallel computer architectures and multiprocessor super-computer designs. One drawback at that time, as pointed out by Lions in [86] was that it only worked for overlapping sub-domains, which could limit the application of these methods. In consequence, he proposed to replace the Dirichlet traces by the Robin interface transmission conditions. He also noticed that in the one dimensional case, the Robin parameter can be chosen to get an optimal convergence of the method. The method was then analyzed in [71], [73], [74], [46], with Robin or Ventcell transmissions conditions, where a general methodology, based on the optimization of the convergence factor of the algorithm was proposed, to calculate the Robin or Ventcell parameters (see [46] for a review on this method). We call it the Optimized Schwarz method. More recent studies of such algorithm with Ventcell transmission conditions are given for example in [63], [114]. An extension of the optimized Schwarz method to the Stokes equations is given in [40], and in [33, 16] for the semi-discrete in time Navier-Stokes equations, in [87] for the fully discrete Navier-Stokes equations. Robin–Robin methods have also been used to improve the transmission condition for the Stokes-Darcy coupling, see [38], [32]. For domain decomposition methods on the Stokes problem for incompressible and compressible fluids, see also [97, 39].

Originally, Schwarz methods were made for spatial problems. Then, to extend their usage to evolutionary ones, a natural approach is to discretize in time to get a stationary problem for each time step, then to apply Schwarz methods on this steady problem (see, e.g. [25], [77]). This approach requires the same time discretization in all subdomains, hence limits the possibilities of using numerical approximations adapted to the physics of the subdomain problem. In the framework of parallel calculation, it is expensive as data have to be exchanged at every time step of the discretization. The Waveform Relaxation technique can be applied to overcome this downside, and the corresponding methods are called Schwarz Waveform Relaxation.
Like in the original Schwarz method, in Schwarz Waveform Relaxation methods the spatial domain is decomposed into overlapping or non overlapping subdomains. The algorithm computes independently in the subdomains on the whole time interval, exchanging space-time boundary data through transmission operators. These operators can be Dirichlet ([57]), or optimized Robin or Ventcell ([52], [91], [50]) and the method is called Optimized Schwarz Waveform Relaxation (OSWR) method. Such method is analyzed in [68], [69] in the context of mixed formulation. The algorithm being global in time, using projection techniques ([53]), one can freely choose different time discretizations for each subdomain ([64], [68], [69]). An adaptive OSWR algorithm, based on an a posteriori stopping criteria, is proposed and analyzed in [4], [5], wherein the iterations are stopped when the domain decomposition error does not affect significantly the global error.

The OSWR method have been developed and successfully used for advection reac-

tion diffusion problems ([91], [50], [9], [64]) with applications to porous media flow and transport ([61], [11], [68],[69]), hyperbolic problems ([52], [49], [62], [65]) and the viscous Shallow Water system ([92]). This approach was extended to nonlinear reaction diffusion equation in [24] and in [61] in the context of coupling transport and chemistry in porous media. Schwarz waveform relaxation method has been extended to compressible Navier-Stokes equations in [34], [35]. The OSWR method as been recently extended and analyzed in [2, 3] for a nonlinear and degenerate parabolic problem, with nonlinear and discontinuous transmission conditions on the interface. OSWR have also been used to improve the transmission condition in coupled problems, see for instance [17], [95], [109], [111, 110] for ocean–atmosphere models. However, there has not been up to now any complete study of this type of method for the time dependent incompressible Stokes and Navier-Stokes equations.

Coupling domain decomposition and Parareal type methods

Choosing suitable solvers for Parareal could significantly enhance the overall performance. At first glance, one may use domain decomposition methods as fine and coarse solvers for Parareal iterations, which allows a two-level parallelization process in both space and time direction (see [43], [36], [44], [90], [108]).

On the other hand, when iterative methods are used as solvers, the overall process would then be composed of outer Parareal iterations and inner iterations of the chosen method. To reduce the cost of the process, Maday and Turinici in [89] suggested that few inner iterations are enough for solvers, the overall convergence is still finally achieved via Parareal iterations (see, e.g., [93] for Jacobi method, [59], [55], [54] for SWR methods, [23] for Waveform Relaxation methods, and [105] for Dirichlet-Neumann/Neumann-Neumann waveform relaxation method).

Based on these two observations, we are interested in a coupling model for Parareal and the non-overlapping Optimized Schwarz Waveform Relaxation method, whose convergence analysis has not been given yet.

Aims of the thesis

In this thesis, we first study the coupling of Parareal and OSWR methods on advection reaction diffusion problems, in one and two dimensions. A remarkable challenge is that, while OSWR converges much faster than Dirichlet SWR, it also amplifies the difficulties in the convergence analysis, which cannot be performed using the same techniques as for Dirichlet SWR like in [59]. After giving a convergence analysis, we test its performance and give some comments on its parameters by performing numerical illustrations.

In the next step, we extend the proof of convergence of the OSWR method to the Stokes equations, and then, to the Oseen ones. We also take a look at the Parareal method, as well as at the Parareal-OSWR coupling, for these equations.

Outline

The thesis is organized as follows: In the first chapter, we study the coupled Parareal-OSWR method on parabolic equations. We start by presenting the model problem, then we reintroduce the Parareal method and the OSWR methods, and we extend some of their properties which we will use for our coupled method. The algorithm of the coupling of Parareal with non-overlapping OSWR is then presented, followed by an energy analysis and numerical experiments in 1D and 2D. The coupling with overlapping OSWR is introduced also, and its convergence is then given by using the convergence factor of the overlapping OSWR.

In the second chapter, we analyze the Schwarz Waveform Relaxation method for the two dimensional Stokes equations. We present first the Stokes equations, then the algorithm. Some observations are shown next to illustrate the difference with the parabolic case, which can lead to the non-converging behavior of the pressure, even though the convergence of the velocity is always guaranteed by the energy estimate. We then propose a correction that helps us quickly get a converged pressure. The convergence factor using Fourier transform follows. Next, we perform some numerical experiments to verify the method and to show the existence of optimized coefficients to be used in the Robin transmission conditions. Finally, we extend those theoretical observations to the Oseen equations, and we propose a coupled Parareal-OSWR algorithm for the Stokes equations.

Chapter 1

Coupling parareal with Optimized Schwarz waveform relaxation for parabolic problems

The Parareal algorithm is a time-parallel method that was proposed by Lions, Maday, and Turinici to solve evolutionary problems in parallel, see [82]. The algorithm is constructed using two solvers: the coarse solver, which is fast but not very accurate, and the fine solver, which is slower but more accurate. The long time interval is divided into smaller windows, the fine solver is performed on each window, using some input initial conditions. The outputs are then corrected by the coarse solver and used as the inputs for the next iteration.

In the most simplified convergence analysis, the initial value problem was considered to be an ODE, the fine solver was exact and the coarse solver was the Backward Euler method; in that analysis the outputs were computed exactly and so was the error. More complex analyses of the performance of Parareal were also achieved: for non-exact fine solvers for ODEs [7], for linear ordinary and partial differential equations [56]; for the non-linear case [48].

In the construction of Parareal, one may choose suitable coarse and fine solvers to fasten the process, for example by using an iterative method like, e.g., the Schwarz waveform relaxation (SWR) method. As Parareal itself is also an iterative method, the overall process would then be composed of outer iterations (Parareal) and inner iterations corresponding to the coarse and fine solvers. In order to save CPU resources, we might think of stopping the inner iterative solvers after a small number of iterations, well before convergence, and hope that the overall convergence could be carried through Parareal iterations. This idea was first raised in [89] for general iterative methods; it was then developed for some iterative methods: for the Jacobi method (see [93]), for SWR methods (see [59], [54]). In this contribution, we are more interested in the latter, which will be recalled next.

SWR algorithms are based on a spatial domain decomposition. The spatial domain is decomposed into overlapping or non overlapping subdomains; then the original problem is transformed into multi-domain space-time sub-problems. Starting from initial fluxes on the space-time interfaces, each sub-problem can then be solved in parallel over the whole time range; then the data are exchanged through the interfaces to create better fluxes. The transmission conditions for the fluxes play an important role in

the convergence process and several possibilities can be used, e.g., Dirichlet [57], Robin [91, 50] or Ventcell [74]. The last two types of conditions contain free parameters that can be chosen to optimize the convergence factor of the algorithm. While in the classical Schwarz method, exchanged fluxes are spatial functions only [46], the space-time fluxes in the SWR method leave a wide range of choices for the discretization method in the time direction in each sub-problem, which is quite useful in practice (see e.g. [64, 68, 69]).

With all their properties mentioned above, SWR methods are already promising choices for the solvers whenever one wants to use the Parareal methods, which allows a two-level parallelization process: one level in Parareal iterations, and the other in the SWR iterations. On the other hand, being seen as iterative methods, SWR could be even more efficient to use with Parereal in a coupling framework. The idea is also natural: as we do not run the solvers until convergence, we shall need to keep additional intermediate outputs from the solvers during Parareal iterations, which, in the case of SWR solvers, are fluxes on the interface.

As far as the coupling of Parareal with SWR is concerned, there exist up to now two main references, both use SWR with Dirichlet transmission conditions:

- The PhD thesis [59] which proposed several choices of coupling but focused on the one that uses non-converged classical SWR (i.e. with Dirichlet transmission conditions) in the fine solver and leaves the coarse solver unchanged (like in the classical Parareal).

- The article [54] (see also its earlier version, the proceeding paper [55]). In these works, the coupled methods are call Parareal Schwarz Wavform Relaxation methods, or PSWR, and the coarse and fine solvers are both modified such that the inner iterative process is now stopped after only 1 iteration.

In this chapter, we would like to couple Parareal with SWR with optimized Robin or Ventcell transmission conditions (i.e. with "Optimized SWR", also called OSWR method). It has been shown in the existing references about SWR methods that the Robin or Ventcell conditions give a much faster convergence than the Dirichlet ones. For simplicity we will present and analyze the coupled method with Robin transmission conditions. Obviously, the change in the transmission condition also amplifies the difficulties in the convergence analysis of the coupling algorithm, and we will inherit and modify the techniques used in the two existing references mentioned above. However, we will present numerical results both with Robin and Ventcell transmission conditions.

The chapter is organized as follows. In Section 1.1, we introduce the model problem and state some stability and regularity properties of the solutions of the whole space-time domain problem and of the sub-space-time-domain problems. In Section 1.2 we recall basic ingredients of the Parareal method and give some observations which will be useful to understand the numerical tests. In Section 1.3, the OSWR method is introduced and we give an extension of known convergence results that we will use for the analysis of the coupled method. In Section 1.4, we introduce the coupled Parareal-OSWR algorithm and then, prove a general convergence result for the method via energy estimates in Section 1.5. Section 1.6 is for numerical illustration in 1D, in which we also compare numerically our method to the one in [54], and in Section 1.7 we present numerical experiments in 2D. After that, in Section 1.8, we give an extension of the coupled method in the case of overlapping subdomains, where a bound for the

convergence factor can be obtained, and which is almost linear. In addition, we also get a bound for the operator matrix, by trying a different approach for the analysis.

The principal part of this chapter comes from an article in preparation, in collaboration with Caroline Japhet (University Sorbonne Paris Nord), Yvon Maday (Sorbonne University), and Pascal Omnes (CEA[1]).

1.1 Model problem

Denote $\mathscr{L}u := \partial_t u - \nu\partial_{xx}u + a\partial_x u + bu$, $\Omega = \mathscr{R}$. For $T > 0$, we consider the following problem

$$\mathscr{L}(u) = f, \quad \text{in } \Omega \times (0, T), \tag{1.1a}$$

$$u(\cdot, 0) = u_0, \quad \text{in } \Omega, \tag{1.1b}$$

where ν, a and b are constants, with $\nu > 0$ and $b > 0$. The source term f and the initial condition u_0 will be specified in Section 1.1.2.

1.1.1 Domain decomposition and notation

We consider a decomposition of Ω into two non-overlapping subdomains

$$\Omega_1 = (-\infty, 0), \quad \Omega_2 = (0, +\infty),$$

and introduce the Robin interface operator for $i = 1, 2$ as follows (see [84, 50]):

$$\mathscr{B}_1 = \nu\partial_x - \frac{a}{2} + \frac{p}{2}, \qquad \mathscr{B}_2 = -\nu\partial_x + \frac{a}{2} + \frac{p}{2}, \tag{1.2}$$

Then, problem (1.1) can be reformulated as the following equivalent multi-domain problem [86], with $f_i = f_{|\Omega_i}$, $u_i = u_{|\Omega_i}$, and $u_{0,i} = u_{0|\Omega_i}$, $i = 1, 2$:

$$\begin{aligned} \mathscr{L}u_i &= f_i & \text{in } \Omega_i \times (0, T), \\ u_i(\cdot, 0) &= u_{0,i} & \text{in } \Omega_i, & \qquad i = 1, 2, \\ (\mathscr{B}_i u_i)(0, \cdot) &= \xi_i & \text{on } (0, T), \end{aligned} \tag{1.3}$$

with

$$\xi_i := (\mathscr{B}_i u_j)(0, \cdot) \quad \text{on } (0, T), \quad j = 3 - i, \; i = 1, 2. \tag{1.4}$$

In (1.2) p is a free parameter chosen such that : a) a Robin subdomain problem of type (1.3) is well-posed, b) it leads to a fast converging algorithm (see Section 1.3). Both issues will be specified later.

In what follows we will use the notation $\boldsymbol{\xi} := (\xi_1, \xi_2)$ for the Robin data on $(0, T)$ associated to the solution u of (1.1).

1.1.2 Existence and regularity results

We introduce the following spaces corresponding to the subdomain problems,

$$\mathscr{X}_i = H^1(\Omega_i), \; i = 1, 2, \qquad \mathscr{Y} = H^{\frac{1}{4}}(0, T),$$

---

[1]The French Alternative Energies and Atomic Energy Commission

and the local-regular space

$$\mathscr{X} := \{U \in L^2(\Omega) : U_{|\Omega_i} \in \mathscr{X}_i\},$$

equipped with the norm $\|U\|_{\mathscr{X}} = \left(\sum_i \|U_{|\Omega_i}\|_{\mathscr{X}_i}^2 \right)^{\frac{1}{2}}$.

With the Robin transmission conditions, we will need more regularity in our analysis, in the anisotropic Sobolev spaces $H^{r,s}(\Omega \times (0,T)) = L^2(0,T; H^r(\Omega)) \cap H^s(0,T; L^2(\Omega))$ defined in [83].

We recall below some useful regularity properties from [84].

Lemma 1.1. *(Regularity of problem* (1.1)*)*
If $u_0 \in H^1(\Omega)$ and $f \in L^2(0,T; L^2(\Omega))$, problem (1.1) *has a unique solution u in $H^{2,1}(\Omega \times (0,T))$ and there exists a constant C independent of u_0 and f s.t.*

$$\|u\|_{H^{2,1}(\Omega \times (0,T))} \leq C(\|u_0\|_{H^1(\Omega)} + \|f\|_{L^2(0,T; L^2(\Omega))}). \tag{1.5}$$

Lemma 1.2. *(Regularity of problem* (1.3)*)*
Let $i = 1$ or $i = 2$. If $u_{0,i} \in \mathscr{X}_i$, $f_i \in L^2(0,T; L^2(\Omega_i))$ and $\xi_i \in \mathscr{Y}$, problem (1.3) *has a unique solution u_i in $H^{2,1}(\Omega_i \times (0,T))$ and there exists a constant C independent of u_0, f, and ξ_i s.t.*

$$\|u_i\|_{H^{2,1}(\Omega_i \times (0,T))} \leq C(\|u_{0,i}\|_{\mathscr{X}_i} + \|f_i\|_{L^2(0,T; L^2(\Omega_i))} + \|\xi_i\|_{\mathscr{Y}}).$$

Lemma 1.3. *(Trace theorem)*
If $u \in H^{2,1}(\Omega \times (0,T))$, then $u(\cdot, T) \in \mathscr{X}$, $(\mathscr{B}_i u)(0, \cdot) \in \mathscr{Y}$, $i = 1,2$, and there exists a constant C s.t.[2]

$$\|(\mathscr{B}_i u)(0,.)\|_{\mathscr{Y}} \leq C\|u\|_{H^{2,1}(\Omega \times (0,T))}, \quad i = 1,2.$$

Similar estimates hold by replacing Ω by Ω_i, u by u_i, and $\mathscr{X}$ by $\mathscr{X}_i$, for $i = 1,2$.

1.2 Parareal Method

The Parareal method introduced in [82] is a numerical method designed to solve evolution problems in parallel. It is based on a *decomposition in time* of $(0,T)$ into subintervals : $\overline{(0,T)} = \cup_{n=0}^{N-1} \overline{\mathscr{I}_n}$, with $\mathscr{I}_n = (T_n, T_{n+1})$, $0 \leq n \leq N-1$, and $0 = T_0 < T_1 < \ldots < T_{N-1} < T_N = T$. Over each such interval generically noted as $\mathscr{I} := (t_0, t_1)$, it uses two propagation operators :

- $\mathscr{G}(\mathscr{I}, U_0)$ that provides a rough approximation of $u(\cdot, t_1)$, where u is the solution of (1.1), with initial condition $u(\cdot, t_0) = U_0$.

- $\mathscr{F}(\mathscr{I}, U_0)$ that provides a more accurate approximation of $u(\cdot, t_1)$.

For simplicity, we will consider a regular decomposition of $(0,T)$, i.e. such that $T_{n+1} - T_n = \Delta T$, and we set $\mathscr{I}_n := (T_n, T_{n+1})$, $\forall n \in [\![0, N-1]\!]$. The plain Parareal algorithm [82] is as follows :

---

[2]Note that we have a better result : $u(\cdot, T) \in H^1(\Omega)$.

Algorithm 1 (Parareal)

Choose an initial data $(U_n^0)_{n \in [\![0,N]\!]}$ with $U_0^0 = u_0$ and U_n^0 an approximation of $u(\cdot, T_n)$, for example : $U_n^0 := \mathcal{G}(\mathcal{I}_{n-1}, U_{n-1}^0)$, for $n = 1, 2, \ldots, N$.

for $k = 0, 1, \ldots$ *(Parareal iterations)*

Set $U_0^{k+1} = u_0$ and perform the correction iterations

$$U_{n+1}^{k+1} = \mathcal{G}(\mathcal{I}_n, U_n^{k+1}) + \mathcal{F}(\mathcal{I}_n, U_n^k) - \mathcal{G}(\mathcal{I}_n, U_n^k), \quad n = 0, 1, \ldots, N-1. \qquad (1.6)$$

end for

We denote by u_n the solution of the (sequential) fine propagator at time T_n:

$$u_n = \mathcal{F}((0, T_n), u_0), \quad u_n = \mathcal{F}(\mathcal{I}_{n-1}, u_{n-1}), \quad \forall n \in [\![1, N]\!].$$

In practice, $\mathcal{F}$ will be close to exact, and thus, for the analysis presented here, we suppose that $\mathcal{F}$ is the exact propagator, i.e.: $\mathcal{F}((t_0, t_1), \tilde{u}_0) = \hat{u}(t_1)$ where $\hat{u}$ is the solution of (1.1a) with initial condition $\tilde{u}_0$ at $t = t_0$. In particular we can identify u_n with $u(\cdot, T_n)$, where u is the solution of (1.1).

1.2.1 Convergence

We recall results from [56]. Let $\mathcal{O}$ be either $L^2(\Omega)$, $H^1(\Omega)$, or $\mathcal{X}$. Suppose that there exist γ_1, γ_2 depending on $|\mathcal{I}| = t_1 - t_0$, such that, for all $w, v \in \mathcal{O}$

$$\|\mathcal{G}(\mathcal{I}, w) - \mathcal{G}(\mathcal{I}, v)\|_{\mathcal{O}} \leq \gamma_1 \|w - v\|_{\mathcal{O}}, \qquad (1.7)$$

$$\|(\mathcal{F} - \mathcal{G})(\mathcal{I}, w) - (\mathcal{F} - \mathcal{G})(\mathcal{I}, v)\|_{\mathcal{O}} \leq \gamma_2 \|w - v\|_{\mathcal{O}}. \qquad (1.8)$$

Denoting $E_n^k = U_n^k - u_n$, $1 \leq n \leq N$, $k \geq 0$, then (1.6), (1.7) and (1.8) imply

$$\|E_{n+1}^{k+1}\|_{\mathcal{O}} \leq \gamma_1 \|E_n^{k+1}\|_{\mathcal{O}} + \gamma_2 \|E_n^k\|_{\mathcal{O}}. \qquad (1.9)$$

Using the fact that $U_0^k = u_0$ for all $k \geq 0$ and the fact that $u_1 = \mathcal{F}(\mathcal{I}_0, u_0)$, we obtain from (1.6) that $E_1^{k+1} = 0$, $k \geq 0$. From this and (1.9), we obtain by induction the following bound for $k \geq 0$ and $n \geq 1$

$$\|E_{n+1}^{k+1}\|_{\mathcal{O}} \leq \gamma_2 \sum_{j=1}^{n} \gamma_1^{n-j} \|E_j^k\|_{\mathcal{O}}. \qquad (1.10)$$

For a matrix $A \in \mathbb{R}^{m \times n}$, we denote A^t the transpose of A, and we use the notation $0 \leq A$ if all elements of A are non-negative. We also use the notation $A \leq B$ if $0 \leq B - A$.
Our notation leads to the following basic properties (provided the matrix operations make sense)

$$\begin{aligned} A \leq B, \ B \leq C \quad &\Rightarrow \quad A \leq C, \\ A \leq B, \ 0 \leq C \quad &\Rightarrow \quad AC \leq BC. \end{aligned}$$

Let $\mathbf{E}^k := \left(\|E_1^k\|_{\mathcal{O}}, \|E_2^k\|_{\mathcal{O}}, \ldots, \|E_N^k\|_{\mathcal{O}}\right)^t$, and $\mathbf{M} \in \mathbb{R}^{N \times N}$ the Toeplitz matrix defined by

$$\mathbf{M}_{ij} = \begin{cases} \gamma_1^{i-1-j} & \text{if } j < i, \\ 0 & \text{if } j \geq i. \end{cases} \qquad (1.11)$$

Then (1.10) can be expressed in vector form as

$$\mathbf{E}^{k+1} \leq \gamma_2 \mathbf{M} \mathbf{E}^k, \qquad \forall k \geq 0, \tag{1.12}$$

which, by induction, implies

$$\mathbf{E}^k \leq (\gamma_2 \mathbf{M})^k \mathbf{E}^0, \qquad \forall k \geq 0. \tag{1.13}$$

We recall the following property of **M**, which is shown in [56]

Lemma 1.4. *If $\gamma_1 < 1$ then*

$$\|\mathbf{M}^i\|_\infty \leq \binom{N-1}{i}. \tag{1.14}$$

Remark 1.5. *In the classical Parareal, $\mathcal{O}$ can be $L^2(\Omega)$ or $H^1(\Omega)$. In those cases, it is easy to verify the Lipschitz properties (1.7)–(1.8) with the Lipschitz constant depending on $\mathcal{O}$. In Section 1.5 we will consider the convergence in $L^2(\Omega)$, thus we will use condition (1.7) with $\mathcal{O} = L^2(\Omega)$. In Section 1.8 we will consider the convergence in $\mathcal{X}$; in that case the Lipschitz properties of $\mathcal{G}$ still hold, and we will have a similar property for the incomplete OSWR fine solver.*

1.2.2   Some remarks on the constants γ

We recall now the homogeneous problem on a time window $(0, \Delta T)$

$$\begin{aligned}
\partial_t u - \nu \partial_{xx} u + a \partial_x u + bu &= 0, && \text{in } \mathbb{R} \times (0, \Delta T), \\
u(\cdot, 0) &= u_0, && \text{in } \mathbb{R}.
\end{aligned}$$

Under Fourier transform, denoting k the wave number, the above problem becomes the following ODE

$$\begin{aligned}
\partial_t \hat{u} + \nu k^2 \hat{u} + aik\hat{u} + b\hat{u} &= 0, \\
\hat{u}(0) &= \hat{u}_0.
\end{aligned}$$

We suppose that $\mathcal{G}$ is deduced from the one step backward Euler method. Thus, for an initial condition u_0, setting $U = \mathcal{G}(u_0)$, then $\hat{U}$ is the solution of the following equation

$$\frac{\hat{U} - \hat{u}_0}{\Delta T} + (\nu k^2 + aik + b)\hat{U} = 0,$$

whose solution is $\hat{U} = (1 + (\nu k^2 + aik + b)\Delta T)^{-1} \hat{u}_0$. If $\mathcal{F}$ is the exact solver, then $u = \mathcal{F}(u_0)$ and

$$\hat{u} = \exp(-(\nu k^2 + ail + b)\Delta T).$$

We recall here that we are looking for the Lipschitz constants γ_1 and γ_2 of $\mathcal{G}$ and $\mathcal{F} - \mathcal{G}$, i.e., such that, $\forall U, V$

$$\begin{aligned}
\|\mathcal{G}(U) - \mathcal{G}(V)\| &\leq \gamma_1 \|U - V\|, \\
\|(\mathcal{F} - \mathcal{G})(U) - (\mathcal{F} - \mathcal{G})(V)\| &\leq \gamma_2 \|U - V\|.
\end{aligned}$$

The norm can be that of L^2, H^1 or of $\mathcal{X}$, which does not change the values of γ_1 and γ_2 in this case. We then get

$$\gamma_1 = \max_k |(1 + (\nu k^2 + aik + b)\Delta T)^{-1}|,$$

$$\gamma_2 = \max_k |(1 + (\nu k^2 + aik + b)\Delta T)^{-1} - \exp(-(\nu k^2 + aik + b)\Delta T)|.$$

Through a change of unknown function in the model ODE, it is always possible to come back to the case in which $b = 0$; therefore, for the sake of simplicity, we shall restrict the study to that case.

We have also $\gamma_1 \leq 1$ and the equality happens at $k = 0$. In practice, the discrete wave number is bounded away from 0, hence we get $\gamma_1 < 1$. We only need to study γ_2. We define the function

$$\gamma_2(k) = |(1 + (\nu k^2 + aik)\Delta T)^{-1} - \exp(-(\nu k^2 + aik)\Delta T)|.$$

1.2.2.1   The heat equation case

We consider first the case $a = 0$. For this case, the function $\gamma_2(k)$ is

$$\gamma_2(k) = (1 + \nu k^2 \Delta T)^{-1} - \exp(-\nu k^2 \Delta T).$$

We have $\gamma_2(0) = \lim_{k \to \infty} \gamma_2(k) = 0$. As $\gamma_2(k)$ is continuous, the maximum can only be at the points verifying $\gamma_2'(k) = 0$. Setting $x = \nu k^2 \Delta T$ we have $\gamma_2(k) = \tilde{\gamma}_2(x) := (1 + x)^{-1} - \exp(-x)$ and we have $\tilde{\gamma}_2'(x) = -(1 + x)^{-2} + \exp(-x)$. Let x_0 be such that $\tilde{\gamma}_2'(x_0) = 0$, i.e. x_0 satisfying $\exp(-x_0) = (1 + x_0)^{-2}$. Hence, we conclude that

$$\sup_k \gamma_2(k) \leq \tilde{\gamma}_2(x_0) = (1 + x_0)^{-1} - \exp(-x_0)$$

$$= (1 + x_0)^{-1} - (1 + x_0)^{-2} = x_0(1 + x_0)^{-2} \leq \frac{1}{4}.$$

1.2.2.2   The case $a > 0$

Let

$$A(k) = \exp(-\nu k^2 \Delta T)\cos(ak\Delta T), \quad B(k) = \exp(-\nu k^2 \Delta T)\sin(ak\Delta T),$$

$$C(k) = \frac{1 + \nu k^2 \Delta T}{(1 + \nu k^2 \Delta T)^2 + a^2 k^2 \Delta T^2}, \quad D(k) = \frac{ak\Delta T}{(1 + \nu k^2 \Delta T)^2 + a^2 k^2 \Delta T^2}.$$

Then, it holds that

$$\gamma_2^2(k) = (A(k) - C(k))^2 + (B(k) - D(k))^2.$$

We shall split the analysis into three different cases

- For large wave numbers: $k \geq \dfrac{1}{\sqrt{\nu \Delta T}}$

We have that

$$\gamma_2^2(k) \leq 2(A^2(k) + B^2(k) + C^2(k) + D^2(k))$$

$$\leq 2\left[\exp(-2\nu k^2\Delta T) + \frac{1}{(1+\nu k^2\Delta T)^2 + a^2k^2\Delta T^2}\right]$$

$$\leq 2\left[\exp\left(-2\nu\Delta T\frac{1}{\nu\Delta T}\right) + \frac{1}{(1+\nu\Delta T\frac{1}{\nu\Delta T})^2 + a^2\Delta T^2\frac{1}{\nu\Delta T}}\right]$$

$$\leq 2\left(\frac{1}{e^2} + \frac{1}{4}\right) < 1$$

- For small k:

As $\gamma_2(k)$ is a continuous function in k and $\gamma_2(0) = 0$, there exists k_1 s.t., $\forall\ k \leq k_1$, $\gamma_2(k) < 1$.

- For intermediate k: consider the case $k_1 < k < \dfrac{1}{\sqrt{\nu\Delta T}}$

We suppose first that

$$a \leq \frac{\sqrt{\nu}}{\sqrt{\Delta T}}, \tag{1.15}$$

which implies $ak\Delta T \leq 1$. Then, $\cos(ak\Delta T) > 0$ and $\sin(ak\Delta T) > 0$. We next show that $0 \leq A(k) \leq 2C(k)$ and $0 \leq B(k) \leq 2D(k)$. We have

$$A(k) = \exp(-\nu k^2\Delta T)\cos(ak\Delta T) \leq \exp(-\nu k^2\Delta T) \leq \frac{1}{1+\nu k^2\Delta T}.$$

Hence, it is sufficient to show that

$$\frac{1}{1+\nu k^2\Delta T} \leq 2\frac{1+\nu k^2\Delta T}{(1+\nu k^2\Delta T)^2 + a^2k^2\Delta T^2},$$

or equivalently

$$\frac{1}{2} \leq \frac{(1+\nu k^2\Delta T)^2}{(1+\nu k^2\Delta T)^2 + a^2k^2\Delta T^2} = \frac{1}{1 + \dfrac{a^2k^2\Delta T^2}{(1+\nu k^2\Delta T)^2}}.$$

Thus, it remains to prove

$$\frac{a^2k^2\Delta T^2}{(1+\nu k^2\Delta T)^2} \leq 1,$$

which is trivial under the condition $ak\Delta T \leq 1$. Therefore, $0 \leq A(k) \leq 2C(k)$.

It remains to show that $B(k) \leq 2D(k)$. Multiplying both sides of this inequality by $\dfrac{\exp(\nu k^2\Delta T)}{ak\Delta T}$, the new equivalent inequality to be proven is then

$$\frac{\sin(ak\Delta T)}{ak\Delta T} \leq \frac{\exp(\nu k^2\Delta T)}{\frac{\nu^2k^4\Delta T^2}{2} + \nu k^2\Delta T + \frac{1}{2} + \frac{(ak\Delta T)^2}{2}} \tag{1.16}$$

The condition $ak\Delta T \leq 1$ implies $\frac{\nu^2k^4\Delta T^2}{2} + \nu k^2\Delta T + \frac{1}{2} + \frac{(ak\Delta T)^2}{2} \leq \frac{\nu^2k^4\Delta T^2}{2} + \nu k^2\Delta T + 1$.

In addition, one has $\dfrac{\sin(ak\Delta T)}{ak\Delta T} \leq 1$ and $\exp(\nu k^2\Delta T) \geq 1 + (\nu k^2\Delta T) + \dfrac{(\nu k^2\Delta T)^2}{2}$.
Therefore, the inequality (1.16) is true.

Now, we have $0 \leq B(k) \leq 2D(k)$. Therefore, we obtain

$$\gamma_2^2(k) = (A(k) - C(k))^2 + (B(k) - D(k))^2 \leq (C(k))^2 + (D(k))^2 \leq 1.$$

We have $(C(k))^2 + (D(k))^2 = 1$ if and only if $k = 0$. As k is bounded away from 0, the equality cannot happen, thus $\gamma_2 = \max_k \gamma(k) < 1$.

One may probably obtain a less restrictive bound on a than (1.15) by performing a more dedicated analysis, but an hypothesis of the type "a small enough" is necessary. Indeed, if a is large enough, there are values of k such that we have both $vk\Delta T \approx 0$, and $ak\Delta T \approx \dfrac{3\pi}{2}$. Then $A(k) \approx 0$, $B(k) \approx (-1)$ and

$$\begin{aligned}
\gamma_2^2 &\approx C^2(k) + (D(k) + 1)^2 \\
&\approx C^2(k) + D^2(k) + 2D(k) + 1 \\
&\approx \frac{1}{1 + \frac{9\pi^2}{4}} + \frac{3\pi}{1 + \frac{9\pi^2}{4}} + 1 \\
&\approx 1.44.
\end{aligned}$$

Hence, if a is arbitrary large, one can find k such that $\gamma_2(k) > 1$, i.e. $\gamma_2 > 1$.

1.3 Optimized Schwarz Waveform Relaxation Method

The OSWR method [51, 52, 91], for solving problem (1.1) is a space-time parallel method based on a *domain decomposition in space* only

$$\Omega_1 = (-\infty, 0), \quad \Omega_2 = (0, +\infty).$$

Let $\mathscr{I} = (0, T)$, and $\mathbf{I}^+$ the set of intervals of $\mathscr{R}^+$. The method solves iteratively subproblems on $\Omega_1 \times \mathscr{I}$ and $\Omega_2 \times \mathscr{I}$, exchanging space-time boundary data[3] through the Robin operators $\mathscr{B}_1$ and $\mathscr{B}_2$ (defined in (1.2)), where the parameter p is chosen to optimize the convergence factor of the algorithm. The method is thus defined using a subproblem solution operator and a transmission operator: for $i = 1, 2$:

- the solution operator $\mathscr{M}_i(\mathscr{I}, u_{0,i}, \xi_i)$, $i = 1, 2$, that maps the available Robin condition ξ_i and initial condition $u_{0,i}$ to the subdomain solution u_i[4]:

$$\mathscr{M}_i : \begin{array}{ccc} \mathbf{I}^+ \times H^1(\Omega_i) \times \mathscr{Y} & \to & H^{2,1}(\Omega_i \times \mathscr{I}) \\ (\mathscr{I}, u_{0,i}, \xi_i) & \to & u_i, \end{array} \quad (1.17)$$

where u_i is the solution of the following Robin problem in $\Omega_i \times \mathscr{I}$

$$\begin{aligned}
\mathscr{L}u_i &= f && \text{in } \Omega_i \times \mathscr{I}, \\
u_i(\cdot, 0) &= u_{0,i} && \text{in } \Omega_i, && i = 1, 2, \\
(\mathscr{B}_i u_i)(0, \cdot) &= \xi_i && \text{on } \mathscr{I}.
\end{aligned} \quad (1.18)$$

---

[3]In the 1d case considered here, the interface is reduced to one point in space, thus the exchanged data depend on time only.

[4]the operator $\mathscr{M}_i$ should depend also on f but we omit it here to simplify the notations.

- the transmission operator $\mathscr{B}_i$, $i = 1, 2$, that maps the available neighbor subdomain solution $u_j \in H^{2,1}(\Omega_j \times \mathscr{I})$, $j = 3 - i$, to a new Robin datum $\xi_i \in \mathscr{Y}$: $\xi_i = (\mathscr{B}_i u_j)(0, \cdot)$ on $\mathscr{I}$.

Using the definition of $\mathscr{M}_i$, problem (1.3)-(1.4) can be rewritten as

$$u_i = \mathscr{M}_i(\mathscr{I}, u_{0,i}, \xi_i), \ i = 1, 2, \tag{1.19a}$$

$$\xi_i = (\mathscr{B}_i u_j)(0, \cdot) \quad \text{on } \mathscr{I}, \quad j = 3 - i, \ i = 1, 2. \tag{1.19b}$$

The OSWR algorithm for solving problem (1.19) (or equivalently (1.1)) is as follows.

Algorithm 2 (OSWR)

Choose an initial Robin data $\boldsymbol{\xi}^0 = (\xi_1^0, \xi_2^0)$ on $\mathscr{I}$, for example $\xi_i^0 = (\mathscr{B}_i u_{0,i})(0, \cdot)$, on $(0, T)$, $i = 1, 2$.
for $\ell = 1, 2, \dots$ *(OSWR iterations)*
  1. Solve the local space-time Robin problems by calculating

$$u_i^\ell = \mathscr{M}_i(\mathscr{I}, u_{0,i}, \xi_i^{\ell-1}), \qquad i = 1, 2. \tag{1.20}$$

  2. Update the Robin interface term $\boldsymbol{\xi}^\ell = (\xi_1^\ell, \xi_2^\ell)$, with

$$\xi_i^\ell = (\mathscr{B}_i u_j^\ell)(0, \cdot) \quad \text{on } \mathscr{I}, \qquad j = 3 - i, \ i = 1, 2. \tag{1.21}$$

end for

Remark 1.6. *By definition of $\mathscr{M}_i$ and u_i^ℓ in (1.20), the interface condition is*

$$(\mathscr{B}_i u_i^\ell)(0, \cdot) = \xi_i^{\ell-1}, \ i = 1, 2. \tag{1.22}$$

Then, from (1.21), and using that $\mathscr{B}_i = -\mathscr{B}_j + p$, we obtain, for $\ell \geq 1$

$$\xi_i^\ell = -\xi_j^{\ell-1} + p u_j^\ell, \quad j = 3 - i, \ i = 1, 2. \tag{1.23}$$

Let $L \in \mathbb{N}^*$. In the sequel we will denote in compact form

$$(u^L, \boldsymbol{\xi}^L) = \text{OSWR}_L(\mathscr{I}, u_0, \boldsymbol{\xi}^0), \tag{1.24}$$

where $u^L \in L^2(\Omega \times \mathscr{I})$ with $u^L|_{\Omega_i} = u_i^L$, $i = 1, 2$, and $\boldsymbol{\xi}^L = (\xi_1^L, \xi_2^L)$ are the output after L iterations of algorithm (1.20)–(1.21) with initial condition u_0 and initial Robin datum $\boldsymbol{\xi}^0$ on $\mathscr{I}$.

1.3.1 Stability and convergence

We suppose that $f \in L^2(0, T; L^2(\Omega))$. For simplicity, we will use the notation $\|\cdot\|$ for the L^2-norm in Ω or in Ω_i, $i = 1, 2$, and $\|\cdot\|_{\mathscr{I}}$ for the $(L^2(\mathscr{I}))^2$-norm.
Let (u_i^ℓ, ξ_i^ℓ), $i = 1, 2$ be defined by (1.20)–(1.21). For the convergence analysis below, we introduce the following notations for the errors, for $i = 1, 2$ and $\ell \geq 1$:

$$\zeta_i^\ell := \xi_i^\ell - \xi_i, \quad \text{where } \xi_i \text{ is defined in (1.4), and we set } \boldsymbol{\zeta}^\ell := (\zeta_1^\ell, \zeta_2^\ell), \tag{1.25}$$

$$e_i^\ell := u_i^\ell - u, \quad \text{where } u \text{ is the solution of (1.1)}, \tag{1.26}$$

$$e^\ell := \text{ the function in } L^2(\Omega \times (0, T)) \text{ s.t. } e^\ell|_{\Omega_i} = e_i^\ell, \ i = 1, 2. \tag{1.27}$$

Theorem 1.7. *Let $L \in \mathbb{N}^*$. If $u_0 \in H^1(\Omega)$ and $\boldsymbol{\xi}^0 \in \mathscr{Y}^2$, then, Algorithm 2 is well-defined and we have*

$$\sum_{\ell=1}^{L} \left(\tfrac{1}{2} \|e^\ell(.,T)\|^2 + \sum_i \|e_i^\ell\|^2_{L^2(0,T,H^1(\Omega_i))} \right) + \tfrac{1}{2p} \|\boldsymbol{\zeta}^L\|^2_{\mathscr{I}} = \tfrac{1}{2p} \|\boldsymbol{\zeta}^0\|^2_{\mathscr{I}}.$$

Hence, Algorithm 2 converges for $p > 0$ in $L^\infty(0,T;L^2(\Omega_1)) \cap L^2(0,T;H^1(\Omega_1)) \times L^\infty(0,T;L^2(\Omega_2)) \cap L^2(0,T;H^1(\Omega_2))$ to the solution u of (1.1).

Proof. We proceed by recurrence. We have $u_{0,i} \in \mathscr{X}_i$ independently of ℓ. Moreover, let us suppose that $\xi_i^{\ell-1} \in \mathscr{Y}$ (this is true for $\ell = 1$). Then from Lemma 1.2 we have $u_i^\ell \in H^{2,1}(\Omega_i \times (0,T))$. Then from Lemma 1.3, or using (1.23) and the Trace theorem, we have $\xi_i^\ell \in \mathscr{Y}$, thus Algorithm 2 is well-defined. The proof of the energy estimate is done in [50] (Theorem 5.15) and we recall it in Appendix 2.11.1. □

In the context of the coupled Parareal-OSWR method in Section 1.4, incomplete iterations of the OSWR algorithm are performed at each Parareal iteration. This implies that the new initial condition for the OSWR algorithm, through Parareal iterations, will no more be in $H^1(\Omega)$, but only in $\mathscr{X}$. Therefore we need the following extended result, that will be used to prove the convergence of the coupled Parareal-OSWR method later.

We still use notations (1.25)–(1.27) for the errors. We suppose that the initial condition of Algorithm 2, denoted now by $\bar{u}_0$, verifies $\bar{u}_0 \in \mathscr{X}$, $\bar{u}_0 \neq u(\cdot,0)$ (where u is the solution of (1.1)), and we introduce the additional notation for the error at time $t = 0$:

$$e_0 := \bar{u}_0 - u(\cdot,0),$$

with $e_{0,i} := e_0|_{\Omega_i}$, $i = 1, 2$.

Theorem 1.8. *Let $L \in \mathbb{N}^*$. If the initial condition of Algorithm 2 is $\bar{u}_0 \in \mathscr{X}$, $\bar{u}_0 \neq u(\cdot,0)$, and if $\boldsymbol{\xi}^0 \in \mathscr{Y}^2$, then, Algorithm 2 is well-defined and we have*

$$\sum_{\ell=1}^{L} \left(\tfrac{1}{2} \|e^\ell(.,T)\|^2 + \sum_i \|e_i^\ell\|^2_{L^2(0,T,H^1(\Omega_i))} \right) + \tfrac{1}{2p} \|\boldsymbol{\zeta}^L\|^2_{\mathscr{I}} = \tfrac{L}{2} \|e_0\|^2 + \tfrac{1}{2p} \|\boldsymbol{\zeta}^0\|^2_{\mathscr{I}}. \quad (1.28)$$

Proof. For $i = 1, 2$, let (u_i^ℓ, ξ_i^ℓ) be defined by (1.20)–(1.21) with initial condition $\bar{u}_0$. We set $\zeta_i^\ell := \xi_i^\ell - \xi_i$, where ξ_i is defined in (1.4), and $e_i^\ell := u_i^\ell - u|_{\Omega_i}$, where u is the solution of (1.1).

With (ζ_1^0, ζ_2^0) given, the error e_i^ℓ, $i = 1, 2$, satisfies, for $\ell \geq 1$:

$$\begin{aligned}
\mathscr{L} e_i^\ell &= 0 && \text{in } \Omega_i \times \mathscr{I}, \\
e_i^\ell(\cdot,0) &= e_{0,i} && \text{in } \Omega_i, && i = 1, 2, \\
(\mathscr{B}_i e_i^\ell)(0,\cdot) &= \zeta_i^{\ell-1} && \text{on } \mathscr{I},
\end{aligned} \quad (1.29)$$

$$\text{where} \quad \zeta_i^\ell = (\mathscr{B}_i e_j^\ell)(0,\cdot), \; \ell \geq 1, \quad j = 3 - i, \; i = 1, 2. \quad (1.30)$$

Then we follow the same steps as in the proof of Theorem 1.7 in Appendix 2.11.1 until estimate (144), which is written, using that $e_i^\ell(\cdot,0) = e_{0,i}, \forall \ell \geq 1$:

$$\sum_{\ell=1}^{L} \left(\tfrac{1}{2} \|e^\ell(.,T)\|^2 + \sum_i \|e_i^\ell\|^2_{L^2(0,T,H^1(\Omega_i))} \right) + \tfrac{1}{2p} \|\boldsymbol{\zeta}^L\|^2_{\mathscr{I}} = \tfrac{L}{2} \sum_i \|e_{0,i}\|^2 + \tfrac{1}{2p} \|\boldsymbol{\zeta}^0\|^2_{\mathscr{I}},$$

which ends the proof of Theorem 1.8. □

1.3.2 Optimized Robin parameters

In this section we give the methodology to calculate the Robin parameter p involved in the OSWR method. This parameter is chosen to optimize the convergence factor of the algorithm, and is thus called "optimized parameter".

The calculation of the convergence factor extends the one of Lemma 5.7 in [50], obtained for $u_0 \in H^2(\Omega)$, to the case $u_0 \in H^1(\Omega)$. By linearity of $\mathcal{M}_i$, from (1.19a) and (1.20), the error $e_i^\ell := u_i^\ell - u$, $i = 1, 2$, at iteration ℓ of the OSWR method, satisfies $e_i^\ell = \mathcal{M}_i(\mathcal{I}, 0, \zeta_i^{\ell-1})$, with $\zeta_i^{\ell-1} = \xi_i^{\ell-1} - \xi_i$ and $f = 0$. Equivalently, e_i^ℓ is solution of the following problem

$$
\begin{aligned}
\mathcal{L} e_i^\ell &= 0 && \text{in } \Omega_i \times \mathcal{I}, \\
e_i^\ell(\cdot, 0) &= 0 && \text{in } \Omega_i, && i = 1, 2, \\
(\mathcal{B}_i e_i^\ell)(0, \cdot) &= \zeta_i^{\ell-1} && \text{on } \mathcal{I}.
\end{aligned}
\tag{1.31}
$$

From (1.19b) and (1.21), we have $\zeta_i^\ell = \mathcal{B}_i e_j^\ell(0, \cdot)$, $i = 1, 2$, and thus the transmission conditions on $\mathcal{I}$ in (1.31) also reads

$$
(\mathcal{B}_i e_i^\ell)(0, \cdot) = (\mathcal{B}_i e_j^{\ell-1})(0, \cdot) \quad \text{on } \mathcal{I}, \quad j = 3 - i, \; i = 1, 2.
\tag{1.32}
$$

Now, in order to use the Fourier transform, we extend (1.31)– (1.32) to $\mathbb{R}$ in the following way :

• for $\ell = 1$, the Robin condition in (1.31) is with $\zeta_i^0 \in \mathcal{Y}$ and we can extend ζ_i^0 by zero to $H^{\frac{1}{4}}(\mathcal{R})$ to obtain a function, denoted by $\tilde{\zeta}_i^0$, vanishing on $(-\infty, 0)$, and on $(T, +\infty)$, for $i = 1, 2$. Then we can extend equations (1.31) to $\mathcal{R}$, and their solutions, denoted by $(\tilde{e}_1^1, \tilde{e}_2^1)$, vanish on $(-\infty, 0)$ and coincide with (e_1^1, e_2^1) on $(0, T)$.

• for $\ell \geq 2$, we define the Robin trace $\tilde{\zeta}_i^{\ell-1} := (\mathcal{B}_i \tilde{e}_j^{\ell-1})(0, \cdot)$ on $\{0\} \times \mathcal{R}$, which belongs to $H^{\frac{1}{4}}(\mathcal{R})$, vanishes on $(-\infty, 0)$ and coincides with $(\mathcal{B}_i e_j^{\ell-1})(0, \cdot)$ on $\{0\} \times (0, T)$, for $i = 1, 2$. The subdomain problems (1.31) are extended on $\Omega_i \times \mathcal{R}$ as follows :

$$
\begin{aligned}
\mathcal{L} \tilde{e}_i^\ell &= 0 && \text{in } \Omega_i \times \mathcal{R}, \\
\tilde{e}_i^\ell(\cdot, 0) &= 0 && \text{in } \Omega_i, && i = 1, 2, \\
(\mathcal{B}_i \tilde{e}_i^\ell)(0, \cdot) &= \tilde{\zeta}_i^{\ell-1} && \text{on } \mathcal{R},
\end{aligned}
\tag{1.33}
$$

and their solution vanish on $(-\infty, 0)$ and coincide with (e_1^ℓ, e_2^ℓ) on $(0, T)$. In particular, by the definition of $\tilde{\zeta}_i^{\ell-1}$ above, the transmission condition (1.32) has been extended on $\{0\} \times \mathcal{R}$ in (1.33) as follows :

$$
(\mathcal{B}_i \tilde{e}_i^\ell)(0, \cdot) = (\mathcal{B}_i \tilde{e}_j^{\ell-1})(0, \cdot) \quad \text{on } \mathcal{R}, \quad j = 3 - i, \; i = 1, 2.
\tag{1.34}
$$

Note that for $\ell \geq 1$, the property $\tilde{\zeta}_i^{\ell-1} \in H^{\frac{1}{4}}(\mathcal{R})$ implies that the solution e_i^ℓ of problem (1.33) is in $H^{2,1}_{\text{loc}}(\Omega_i \times \mathcal{R})$ [5] (using Lemma 1.2), and thus the new Robin datum $\tilde{\zeta}_i^\ell$, defined above, is in $H^{\frac{1}{4}}_{\text{loc}}(\mathcal{R})$ (using Lemma 1.3).

---

[5]Here we set $H^{2,1}_{\text{loc}}(\Omega_i \times \mathcal{R}) = \left\{ H^{2,1}(\Omega_i \times (T_1, T_2)), \forall T_1, T_2 \in \mathcal{R} \right\}$, $i = 1, 2$.

In what follows, we use Fourier transform in time, in the sense of tempered distributions.

Then, we solve in each subdomain the ordinary differential equation

$$i\omega \hat{e}_i^\ell - \nu \partial_{xx} \hat{e}_i^\ell + a \partial_x \hat{e}_i^\ell + b \hat{e}_i^\ell = 0, \qquad i = 1, 2, \tag{1.35}$$

with the characterisitic roots

$$r^- = \frac{a - \sqrt{d}}{2\nu}, \qquad r^+ = \frac{a + \sqrt{d}}{2\nu}, \qquad d = a^2 + 4\nu(b + i\omega), \tag{1.36}$$

where $\sqrt{d}$ is the complex square-root with positive real part :
let $\tilde{d} = \sqrt{(a^2 + 4\nu b)^2 + 16\nu^2\omega^2}$, then

$$\sqrt{d} = \sqrt{\frac{\tilde{d} + a^2 + 4\nu b}{2}} + i\,\text{sign}(\omega)\sqrt{\frac{\tilde{d} - a^2 - 4\nu b}{2}}.$$

Thus, $\mathcal{R}e(r^+) > 0$ and $\mathcal{R}e(r^-) < 0$, and the solutions $\hat{e}_i^\ell \in L^2(\Omega_i)$, $i = 1, 2$ are given by[6]

$$\hat{e}_1^\ell = \frac{2}{\sqrt{d} + p}\hat{\zeta}_1^{\ell-1}(\omega)e^{r^+ x}, \qquad \hat{e}_2^\ell = \frac{2}{\sqrt{d} + p}\hat{\zeta}_2^{\ell-1}(\omega)e^{r^- x}, \qquad \ell \geq 1. \tag{1.37}$$

Then, replacing (1.37) in the transmission conditions (1.34) leads to

$$\forall \ell \geq 1, \quad \begin{pmatrix} \hat{\zeta}_1^\ell \\ \hat{\zeta}_2^\ell \end{pmatrix} = \left(\frac{-\sqrt{d} + p}{\sqrt{d} + p}\right)\begin{pmatrix} \hat{\zeta}_2^{\ell-1} \\ \hat{\zeta}_1^{\ell-1} \end{pmatrix}. \tag{1.38}$$

Setting $\hat{\boldsymbol{\zeta}}^\ell := (\hat{\zeta}_1^\ell, \hat{\zeta}_2^\ell)$, from (1.38), we have

$$\forall \ell \geq 2, \quad \hat{\boldsymbol{\zeta}}^\ell = \rho_0(\omega, p)\hat{\boldsymbol{\zeta}}^{\ell-2}, \qquad \text{with } \rho_0(\omega, p) := \left(\frac{-\sqrt{d} + p}{\sqrt{d} + p}\right)^2. \tag{1.39}$$

From (1.39), by induction on ℓ we obtain,

$$\hat{\boldsymbol{\zeta}}^{2\ell} = (\rho_0(\omega, p))^\ell \hat{\boldsymbol{\zeta}}^{(0)}, \qquad \forall \ell \geq 1. \tag{1.40}$$

From (1.40), the convergence factor of the algorithm is $\rho_0(\omega, p)$, defined in (1.39).

Note that from (1.38) we have, for all $\omega \in \mathcal{R}$, and for $\ell \geq 1$

$$|\hat{\zeta}_i^\ell(\omega)| \leq |\hat{\zeta}_{3-i}^{\ell-1}(\omega)|, \qquad \text{for } i = 1, 2.$$

Using that $\tilde{\boldsymbol{\zeta}}^0 \in H^{\frac{1}{4}}(\mathcal{R})$, the above inequality implies, by induction, that

$$\tilde{\boldsymbol{\zeta}}^\ell \in H^{\frac{1}{4}}(\mathcal{R}), \quad \forall \ell \geq 1.$$

While we have $\max_{\omega \in \mathcal{R}} |\rho_0(\omega, p)| = \lim_{\omega \to \infty} |\rho_0(\omega, p)| = 1$, we can use the continuous convergence factor $\rho_0(\omega, p)$ to calculate an efficient Robin parameter for the discrete setting (see e.g. [73, 91, 46, 50]).

---

[6]Note that here the term "∂_x" in $\mathcal{B}_i$ is multiplied by ν while this is not the case in [50]. Thus $\hat{e}_i^\ell$ is slightly different here, from the one of [50].

Indeed, in numerical computations, the frequency ω is bounded, i.e. we have $\omega_{\min} \leq \omega \leq \omega_{\max}$ where $\omega_{\max} = \dfrac{\pi}{\Delta t}$ is the largest discrete frequency supported by the numerical time grid, and $\omega_{\min} = \dfrac{\pi}{T}$ is smallest frequency relevant to the global time interval. Defining

$$\rho_c(p) := \max_{\frac{\pi}{T} \leq \omega \leq \frac{\pi}{\Delta t}} |\rho_0(p, \omega)|,$$

then the optimized Robin parameter p_c is chosen such that it verifies

$$\rho_c(p_c) = \min_{p>0} \rho_c(p). \tag{1.41}$$

In practice, the minimization problem (1.41) is solved numerically, using the `fminsearch` function in MATLAB.

1.4   Coupled Parareal-OSWR method

Coupling Parareal with domain decomposition was introduced in [59, 55, 54].

Like in Section 1.2, we set $(0, T) = \cup_{n=0}^{N-1} \mathscr{I}_n$. Then the Parareal-OSWR algorithm is defined using the coarse propagator $\mathscr{G}$ of Section 1.2 and the incomplete[7] fine propagator OSWR_L defined by (1.24) as follows :

Algorithm 3 (Coupled Parareal-OSWR)

---

1. Choose an initial data $(U_n^0)_{n \in [\![0,N]\!]}$ with $U_0^0 = u_0$ and U_n^0 an approximation of $u(\cdot, T_n)$, for example $U_n^0 := \mathscr{G}(\mathscr{I}_{n-1}, U_{n-1}^0)$, for $n = 1, 2, \ldots, N$.

2. Choose an initial Robin data $(\boldsymbol{\xi}_n^{0,0})_{n \in [\![0,N-1]\!]}$, with $\boldsymbol{\xi}_n^{0,0} := (\xi_{1,n}^{0,0}, \xi_{2,n}^{0,0})$ on $\mathscr{I}_n$, for example $\xi_{i,n}^{0,0} = (\mathscr{B}_i U_n^0)(0, \cdot)$, $i = 1, 2$.

for $k = 0, 1, \ldots$ *(Parareal iterations)*

  1. On each time interval $\mathscr{I}_n$, $n = 0, 1, \ldots, N-1$:

$$\text{Calculate} \quad (u_n^{k,L}, \boldsymbol{\xi}_n^{k,L}) = \text{OSWR}_L(\mathscr{I}_n, U_n^k, \boldsymbol{\xi}_n^{k,0}). \tag{1.42}$$

  2. Set $U_0^{k+1} = u_0$ and do Parareal corrections:

$$U_{n+1}^{k+1} = u_n^{k,L}(\cdot, T_{n+1}) + \mathscr{G}(\mathscr{I}_n, U_n^{k+1}) - \mathscr{G}(\mathscr{I}_n, U_n^k). \tag{1.43}$$

   Update the interface term: $\boldsymbol{\xi}_n^{k+1,0} = \boldsymbol{\xi}_n^{k,L}. \tag{1.44}$

end for

Remark 1.9. *In (1.42), if $L = \infty$, then $u_n^{k,L} \in H^1(\Omega)$, for all $n \geq 0$, $k \geq 0$. However, if $L < \infty$ and chosen small (e.g. $L = 2$), then $u_n^{k,L} \in \mathscr{X}$, for all $n \geq 0$, $k \geq 0$, but there is very few chance that $u_n^{k,L}$ be in $H^1(\Omega)$. Thus, using (1.43) and that $u_0 \in H^1(\Omega) \subset \mathscr{X}$, we will have $U_n^k \in \mathscr{X}$, for all $n \geq 0$, $k \geq 0$.*

1.5   Convergence of the Parareal-OSWR algorithm

We will consider the convergence in the $L^2(\Omega)$-norm. As in Section 1.3, $\| \cdot \|$ will stand for the L^2-norm in Ω or in Ω_i, $i = 1, 2$, and $\| \cdot \|_{\mathscr{I}}$ the $(L^2(\mathscr{I}))^2$-norm. Let $\widetilde{\mathscr{G}}$ be the coarse propagator associated to the source term $f = 0$. We have the following result

---

[7]In the sense that L will be smaller than the number of iterations required for convergence.

Theorem 1.10. *We suppose that there exists a constant γ_1 such that $\widetilde{\mathcal{G}}$ satisfies for each $n = 0, 1, \ldots, N$*

$$\|\widetilde{\mathcal{G}}(\mathscr{I}_n, U)\| \leq \gamma_1 \|U\|, \quad \forall U \in L^2(\Omega). \tag{1.45}$$

Then, when $k \to \infty$

- *U_n^k converges to $u(., T_n)$ in $L^2(\Omega)$,*

- *$u_{i,n}^{k,\ell}$ converges to $u|_{\Omega_i \times [T_n, T_{n+1}]}$ in $L^2(T_n, T_{n+1}, H^1(\Omega))$ for all $\ell = 1, 2, \ldots, L$.*

In order to prove Theorem 1.10, we first introduce some notation and prove the following lemmas.

Notation for error estimation

Let u be the solution of problem (1.1), and $(u_n^{k,\ell}, \boldsymbol{\xi}_n^{k,\ell})_{1 \leq \ell \leq L}$ be the sequence of iterates through the OSWR step (1.42). We define, for $k = 0, 1, \ldots$, and $n = 0, \ldots, N-1$:

- $E_n^k := U_n^k - u_n$, $n = 0, \ldots, N$, where $u_n = u(., T_n)$,

- $e_n^{k,\ell} := u_n^{k,\ell} - u$, the error in $L^2(\Omega \times \mathscr{I}_n)$ at each iteration ℓ inside step (1.42), with $e_{i,n}^{k,\ell} := e_n^{k,\ell}|_{\Omega_i}$, $i = 1, 2$, for $\ell = 1, \ldots, L$,

- $\boldsymbol{\zeta}_n^{k,\ell} := \boldsymbol{\xi}_n^{k,\ell} - \boldsymbol{\xi}_n$, for $\ell = 1, \ldots, L$, where $\boldsymbol{\xi}_n = ((\mathscr{B}_1 u)(0, \mathscr{I}_n), (\mathscr{B}_2 u)(0, \mathscr{I}_n))$.

Then, by linearity, the algorithm on the error reads

Algorithm 4 (Coupled Parareal-OSWR algorithm on the error)

---

1. Define initial data $(E_n^0)_{n \in [\![0,N]\!]}$ with $E_0^0 = 0$, $E_n^0 := \mathcal{G}(\mathscr{I}_{n-1}, U_{n-1}^0) - u_n$, where $U_0^0 = u_0$, $n = 1, 2, \ldots, N$.
2. Define initial Robin data $(\boldsymbol{\zeta}_n^{0,0})_{n \in [\![0,N]\!]}$, with $\boldsymbol{\zeta}_n^{0,0} := (\zeta_{1,n}^{0,0}, \zeta_{2,n}^{0,0})$ on $\mathscr{I}_n$, where $\zeta_{i,n}^{0,0} = (\mathscr{B}_i E_n^0)(0, \cdot)$, $i = 1, 2$.

for $k = 0, 1, \ldots$ *(Parareal iterations)*
  1. On each time interval $\mathscr{I}_n$, $n = 0, 1, \ldots, N-1$:

$$\text{Calculate} \quad (e_n^{k,L}, \boldsymbol{\zeta}_n^{k,L}) = \text{OSWR}_L(\mathscr{I}_n, E_n^k, \boldsymbol{\zeta}_n^{k,0}). \tag{1.46}$$

  2. Set $E_0^{k+1} = 0$ and do Parareal correction:

$$E_{n+1}^{k+1} = e_n^{k,L}(\cdot, T_{n+1}) + \widetilde{\mathcal{G}}(\mathscr{I}_n, E_n^{k+1} - E_n^k). \tag{1.47}$$

  Update the interface term: $\boldsymbol{\zeta}_n^{k+1,0} = \boldsymbol{\zeta}_n^{k,L}$. \hfill (1.48)

end for

Lemma 1.11. *For all $n \in [\![0, N-1]\!]$, we have:*

$$\sum_{k=0}^{K} \|e_n^{k,L}(\cdot, T_{n+1})\|^2 \leq L \sum_{k=0}^{K} \|E_n^k\|^2 + \frac{1}{p} \|\boldsymbol{\zeta}_n^{0,0}\|_{\mathscr{I}_n}^2. \tag{1.49}$$

Proof. Step (1.46) corresponds to the OSWR algorithm, on $\mathcal{I} := \mathcal{I}_n$, with initial condition $E_n^k \in \mathcal{X}$ (see Remark 1.9). Thus, from (1.28) with $e_0 := E_n^k$, $e_i^\ell := e_{i,n}^{k,\ell}$, and $\zeta^\ell := \zeta_n^{k,\ell}$, we obtain

$$\sum_{\ell=1}^{L} \left(\tfrac{1}{2} \|e_n^{k,\ell}(.,T_{n+1})\|^2 + \sum_i \|e_{i,n}^{k,\ell}\|^2_{L^2(T_n,T_{n+1};H^1(\Omega_i))} \right) + \tfrac{1}{2p} \|\zeta_n^{k,L}\|^2_{\mathcal{I}_n} = \tfrac{L}{2} \|E_n^k\|^2 + \tfrac{1}{2p} \|\zeta_n^{k,0}\|^2_{\mathcal{I}_n}.$$

Moreover, in our algorithm, from (1.48) we have $\zeta_n^{k,L} = \zeta_n^{k+1,0}$, thus

$$\sum_{\ell=1}^{L} \left(\tfrac{1}{2} \|e_n^{k,\ell}(.,T_{n+1})\|^2 + \sum_i \|e_{i,n}^{k,\ell}\|^2_{L^2(T_n,T_{n+1};H^1(\Omega_i))} \right) + \tfrac{1}{2p} \|\zeta_n^{k+1,0}\|^2_{\mathcal{I}_n} = \tfrac{L}{2} \|E_n^k\|^2 + \tfrac{1}{2p} \|\zeta_n^{k,0}\|^2_{\mathcal{I}_n}.$$

Summing with respect to k, from 0 to K, we get a telescopic sum on the interface and therefore

$$\sum_{k=0}^{K} \sum_{\ell=1}^{L} \left(\tfrac{1}{2} \|e_n^{k,\ell}(.,T_{n+1})\|^2 + \sum_i \|e_{i,n}^{k,\ell}\|^2_{L^2(T_n,T_{n+1};H^1(\Omega_i))} \right) + \tfrac{1}{2p} \|\zeta_n^{K+1,0}\|^2_{\mathcal{I}_n}$$
$$= \tfrac{L}{2} \sum_{k=0}^{K} \|E_n^k\|^2 + \tfrac{1}{2p} \|\zeta_n^{0,0}\|^2_{\mathcal{I}_n}, \qquad (1.50)$$

from which we obtain (1.49). $\qquad\square$

Lemma 1.12. *We suppose that $\widetilde{\mathcal{G}}$ satisfies* (1.45). *Then, for all $n \in [\![0, N-1]\!]$,*

$$\sum_{k=0}^{K} \|E_{n+1}^{k+1}\|^2 \le 8\gamma_1^2 \sum_{k=0}^{K+1} \|E_n^k\|^2 + 2\sum_{k=0}^{K} \|e_n^{k,L}(.,T_{n+1})\|^2. \qquad (1.51)$$

Proof. Using the triangle inequality in (1.47), and then (1.45), we get

$$\|E_{n+1}^{k+1}\|^2 \le 2\|\widetilde{\mathcal{G}}(\mathcal{I}_n, E_n^{k+1} - E_n^k)\|^2 + 2\|e_n^{k,L}(.,T_{n+1})\|^2,$$
$$\le 2\gamma_1^2 \|E_n^{k+1} - E_n^k\|^2 + 2\|e_n^{k,L}(.,T_{n+1})\|^2,$$
$$\le 4\gamma_1^2 \left(\|E_n^{k+1}\|^2 + \|E_n^k\|^2 \right) + 2\|e_n^{k,L}(.,T_{n+1})\|^2.$$

Then, summing with respect to k, from 0 to K, we have

$$\sum_{k=0}^{K} \|E_{n+1}^{k+1}\|^2 \le 4\gamma_1^2 \sum_{k=0}^{K} \left(\|E_n^{k+1}\|^2 + \|E_n^k\|^2 \right) + 2\sum_{k=0}^{K} \|e_n^{k,L}(.,T_{n+1})\|^2,$$

from which we deduce (1.51). $\qquad\square$

With these lemmas, we can now prove Theorem 1.10

Proof of Theorem 1.10. From Lemmas 1.11 and 1.12, we get

$$\sum_{k=0}^{K} \|E_{n+1}^{k+1}\|^2 \le 8\gamma_1^2 \sum_{k=0}^{K+1} \|E_n^k\|^2 + 2L \sum_{k=0}^{K} \|E_n^k\|^2 + \tfrac{2}{p} \|\zeta_n^{0,0}\|^2_{\mathcal{I}_n}.$$

Denoting $\gamma_2 = 8\gamma_1^2 + 2L$ and $R_n = \|E_{n+1}^0\|^2 + \frac{2}{p}\|\boldsymbol{\zeta}_n^{0,0}\|_{\mathcal{I}_n}^2$, we can rewrite this inequality as

$$\sum_{k=0}^{K+1} \|E_{n+1}^k\|^2 \le \gamma_2 \sum_{k=0}^{K+1} \|E_n^k\|^2 + R_n, \quad n \in [\![0, N-1]\!].$$

From this inequality, by induction, we obtain

$$\sum_{k=0}^{K+1} \|E_{n+1}^k\|^2 \le \gamma_2^{n+1} \sum_{k=0}^{K+1} \|E_0^k\|^2 + \sum_{j=0}^{n} \gamma_2^j R_{n-j}, \quad n \in [\![0, N-1]\!].$$

Using that $E_0^k = 0, \ \forall k \ge 0$, we finally obtain

$$\sum_{k=0}^{K+1} \|E_{n+1}^k\|^2 \le \sum_{j=0}^{n} \gamma_2^j R_{n-j}, \quad n \in [\![0, N-1]\!]. \tag{1.52}$$

Since the right-hand side of (1.52) does not depend on K, this shows that, for a given $n \in [\![0, N]\!]$, the sum $\sum_{k=0}^{K} \|E_n^k\|^2$ is bounded with respect to K. Hence E_n^k converges to 0 in the $L^2(\Omega)$-norm when $k \to \infty$. Moreover, from inequality (1.50), we obtain, for all $\ell = 1, 2, \ldots, L$

$$\sum_{k=0}^{K} \|e_{i,n}^{k,\ell}\|_{L^2(T_n, T_{n+1}; H^1(\Omega_i))}^2 \le \frac{L}{2} \sum_{k=0}^{K} \|E_n^k\|^2 + \frac{1}{2p}\|\boldsymbol{\zeta}_n^{0,0}\|_{\mathcal{I}_n}^2.$$

As the sum in the right-hand side of the above inequality is bounded with respect to K, then the sum in the left is also bounded with respect to K. Hence, $e_{i,n}^{k,\ell}$ tends to 0 in $L^2(T_n, T_{n+1}; H^1(\Omega_i))$, i.e, $u_{i,n}^{k,\ell} \to u_{i,n}$ in $L^2(T_n, T_{n+1}; H^1(\Omega_i))$, for any ℓ. $\square$

Remark 1.13. *The proof of convergence of the nonoverlapping Parareal-OSWR algorithm in Theorem 1.10 (using energy estimates) is done with $U_n^k \in \mathcal{X}$, for all $n \ge 0$, $k \ge 0$ (see Remark (1.9)). This result is obtained without any correction on U_n^k so that it is more regular (i.e. in $H^1(\Omega)$). Thus, in practice we do not need a correction on U_n^k to have a convergent algorithm.*

1.6   Numerical illustrations in 1D

In this section we give some numerical illustrations of the performance of the coupled Parareal-OSWR method in one dimension. We use here the 1D cell-centered finite volume method, with the centered discretization for the diffusion term. The advection term is based on a centered discretization (for regular advection-diffusion) or an upwind discretization (in the advection dominated case). With the cell-centered finite volume method, the domain decomposition method needs to add an additional unknown associated to the interface of the domains; we use the strategy proposed in [10] for the discretization on the interface. For the time discretization, the backward Euler method is used.

To start, we run a mono-domain solver - no domain decomposition in both space and time - to obtain a numerical solution which will be the reference solution with respect to which all the H^1-errors in the tests that follow will be calculated.

Next, in the Parareal algorithm, as well as for the coarse solver in our coupled method, we use a mono-domain solver (no domain decomposition in space). Then, we test the pure OSWR method - no decomposition in time - to validate our DD-code and to find the smallest required number of OSWR-iterations if we want to use OSWR for the fine solver. We should also clarify that it is different to consider L iterations in the OSWR solver when the latter is used as the fine solver in the pure Parareal method and to apply our coupled method with L: In the first case, one resets the Robin terms at the start of each Parareal iteration, which leads to a slower general convergence. Finally, the main part of our tests is the performance of our coupled method for different choices of L, for $L = 1, 2, 4, 8$.

We will also test the PSWR method of [54], [55], which is nothing but the case $L = 1$ coupled with an incomplete coarse solver based on only one iteration of Waveform Relaxation, either with Dirichlet or Robin boundary conditions. The PSWR method was originally proposed with initial guesses U_n^0 and ξ_n^0 constructed from the initial incomplete coarse solver, which is probably less efficient than starting from values constructed from the fully converged initial coarse solver. Here, we take the same initial values for all tests, namely initial guesses constructed from the full coarse solver. In addition, the initial values of the Robin terms are refined by applying the Robin operators to a linear interpolation between U_n^0 and U_{n+1}^0, which runs slightly faster than the classical constant initial Robin terms of OSWR.

1.6.1 Regular Advection-Diffusion with an exact testing solution

We set $\Omega =]0, 1[$, $T = 1$, and consider the 1D advection-diffusion equation with coefficients $v = a = 1$, $b = 0$. We consider the exact solution $u(x, t) = \exp(-t) \sin(\pi x)$. The domain Ω is decomposed into two sub-domains $\Omega_1 =]0, 1/2[$ and $\Omega_2 =]1/2, 1[$ and ten time sub-intervals (i.e. $N = 10$).

With the exact solution, we can calculate the scheme error e between the exact solution and the mono-domain reference numerical solution, and we stop when the relative error between the current iterative solution in the coupled algorithm and the mono-domain reference numerical solution is smaller than $\frac{e}{10}$.

The mesh and time steps are first chosen as follows :

$\Delta x = 5.10^{-3}, \Delta t = 2, 5.10^{-3}$ **(case 1)** and $\Delta x = 2, 5.10^{-3}, \Delta t = 6, 75.10^{-4}$ **(case 2)**.
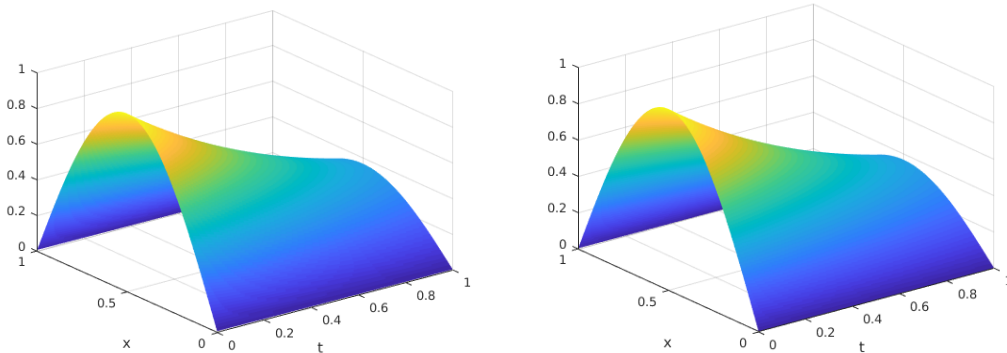
Figure 1.1: Example 1: The numerical solutions for **case 1** (left) and **case 2** (right)
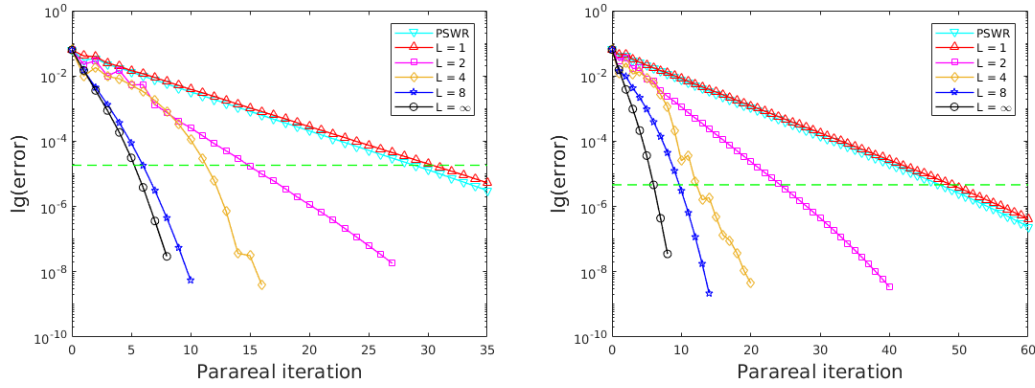
Figure 1.2: Example 1: Relative errors versus Parareal iterations for **case 1** (left) and **case 2** (right) for different values of L in the coupled method and for the pure Parareal method ($L = \infty$)

1.6.1.1   Case 1

L	PSWR	1	2	4	8	20(∞)
k	29	31	15	12	6	6
$L*k$	29	31	30	48	48	120

Table 1.1: Example 1 (case 1) Number of Parareal iterations k and total number of OSWR iterations $L*k$, versus L

solver	OSWR	Parareal	Parareal-OSWR ($L = 2$)	PSWR
iterations (n)	20	120	30	29
loss factor ($l = n/20$)	-	6	1.5	1.45
gain factor (N)	-	10	10	10
final gain factor (N/l)	-	1.33	6.67	6.9

Table 1.2: Example 1 (case 1) Gain factor for Parareal and coupled Parareal-OSWR methods compared to the OSWR solver

We first study the case $\Delta x = 5.10^{-3}, \Delta t = 2, 5.10^{-3}$. In this case, without any decomposition in the time direction (pure OSWR method), one needs at least 15 iterations of OSWR to reach the stopping criterion. Hence, we can consider $L = 20$ as $L = \infty$ (full convergence of the OSWR method).

From Figure 1.2 and Table 1.1, we observe that $L = 2$ is the best choice for our coupled method, while the PSWR method performs a little bit better. The performance of the line $L = 1$ is quite similar to the PSWR, they are almost parallel after the 4th iteration. It can be explained as the number of iterations needed for the coarse solver is small, so doing full convergence of the coarse solver or doing only one iteration are not very different. It also implies that the coarse solver plays a less important role in the overall

convergence.

The choice $L = 4$ and $L = 8$ are quite behind those smaller ones. Especially, the line $L = 4$ almost coincides with $L = 2$ in some first Parareal iterations, before falling down more rapidly. The speed-up compared to the pure OSWR of the best choice $L = 2$ is shown in Table 1.2. In that and similar tables below, we call "loss factor" the ratio of the total number of OSWR iterations in the coupled method to the number of iterations of the stand-alone OSWR method. What we call the final gain factor is actually the speed-up obtained with the coupled method with respect to the stand-alone OSWR method. It is equal to the number of time windows divided by the loss factor. Note that this speed-up value neglects the cost of the coarse solver and of the additional communications between time windows.

Other choices of L also give promising speed-up, and all choices perform a linear convergence - similarly to the convergence of OSWR. One may guess that the OSWR dominates the overall convergence.

An additional remark is that the relative performance of $L = 4$ and $L = 8$ can be improved if we decrease the stopping error: for example, in fact, the error of $L = 4$ at the 15th iteration is close to the error of $L = 2$ at the 30th iteration (so there the ratio of total iterations between $L = 2$ and $L = 4$ will be around 1, while it is 30/48 in Table 1.1).

1.6.1.2 Case 2

L	PSWR	1	2	4	8	32(∞)
k	48	49	25	13	10	6
$L*k$	48	49	50	52	80	132

Table 1.3: Example 1 (case 2) Number of Parareal iterations k and total number of OSWR iterations $L*k$, versus L

solver	OSWR	Parareal	Parareal-OSWR ($L=1$)	PSWR
iterations (n)	32	132	49	48
loss factor ($l = n/32$)	-	6	1.53	1.5
gain factor (N)	-	10	10	10
final gain factor (N/l)	-	1.67	6.54	6.67

Table 1.4: Example 1 (case 2) Gain factor for Parareal and coupled Parareal-OSWR methods compared to the OSWR solver

For $\Delta x = 2,5.10^{-3}, \Delta t = 6,75.10^{-4}$, we observe in Table 1.3 that $L = 1$ is the best choice for our coupled method, and PSWR still performs a little better. The best final gain factor, which is given in Table 1.4, is quite close to the previous case, however, the choice $L = 4$ performs much better, it is now very close to the best choice. The finer

the mesh is, the better performance for large values of L. We show next two additional simulations to strengthen this observation.

Case 3 and case 4

In this part, the mesh and time steps are :

$\Delta x = 1, 25.10^{-3}, \Delta t = 1, 69.10^{-4}$ **(case 3)** and $\Delta x = 6, 25.10^{-4}, \Delta t = 4, 22.10^{-5}$ **(case 4)**.
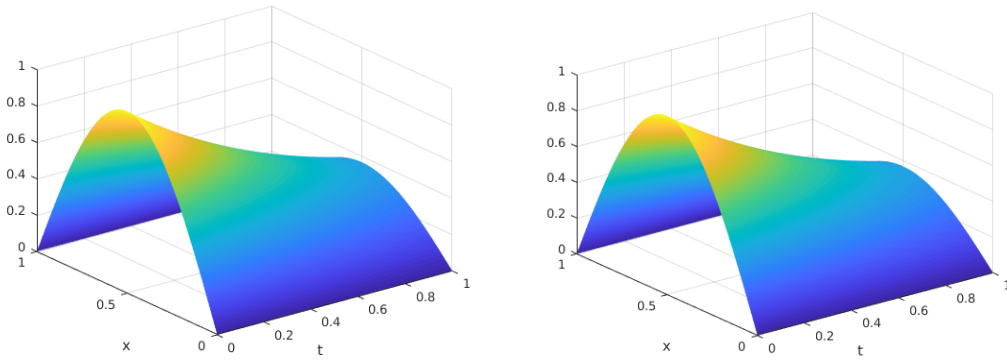
Figure 1.3: Example 1: The numerical solutions for **case 3** (left) and **case 4** (right)
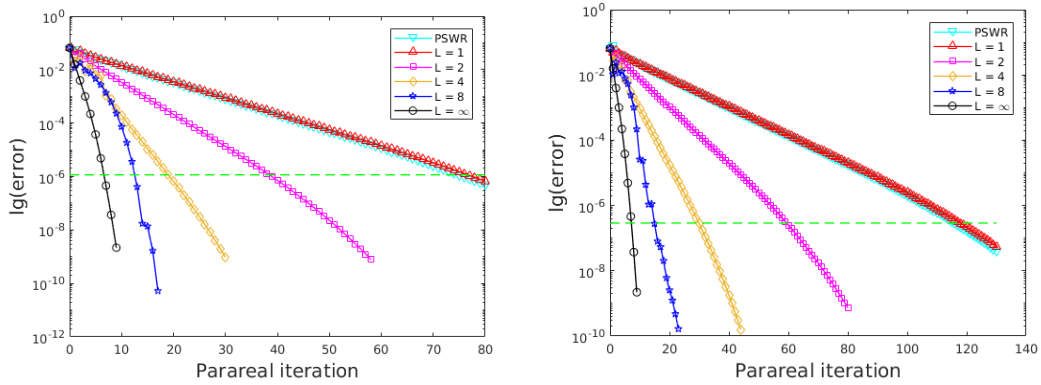
Figure 1.4: Example 1: Relative errors versus Parareal iterations for **case 3** (left) and **case 4** (right)

L	PSWR	1	2	4	8	48(∞)
k	76	77	39	19	13	7
$L*k$	77	77	78	76	104	336

Table 1.5: Example 1 (case 3) Number of Parareal iterations k and total number of OSWR iterations $L*k$, versus L

For $\Delta x = 1, 25.10^{-3}, \Delta t = 1, 69.10^{-4}$, $L = 4$ now becomes the best choice, and it performs similarly as PSWR. We see an improvement in the relative performance

solver	OSWR	Parareal	Parareal-OSWR (L = 4)	PSWR
iterations (n)	48	336	76	76
loss factor ($l = n/48$)	-	7	1.58	1.58
gain factor (N)	-	10	10	10
final gain factor (N/l)	-	1.43	6.33	6.33

Table 1.6: Example 1 (case 3) Gain factor for Parareal and coupled Parareal-OSWR methods compared to the OSWR solver

L	PSWR	1	2	4	8	72(∞)
k	117	118	60	30	15	8
$L*k$	117	118	120	120	120	576

Table 1.7: Example 1 (case 4) Number of Parareal iterations k and total number of OSWR iterations $L*k$, versus L

solver	OSWR	Parareal	Parareal-OSWR (L = 1)	PSWR
iterations (n)	72	576	118	117
loss factor ($l = n/72$)	-	8	1.64	1.63
gain factor (N)	-	10	10	10
final gain factor (N/l)	-	1.25	6.08	6.15

Table 1.8: Example 1 (case 4) Gain factor for Parareal and coupled Parareal-OSWR methods compared to the OSWR solver

of $L = 8$ (104/77 in Table 1.5 which is lower that 80/48 in Table 1.3). For $\Delta x = 6,25.10^{-4}, \Delta t = 4,22.10^{-5}$, $L = 1$ becomes the best choice again, and PSWR is a little better. On the other hand, from table 1.7, $L = 8$ now performs similarly as $L = 2$ and $L = 4$, and is very close to the best choice. From Table 1.6 and Table 1.8, one sees that the gain factors of the best choice reduce when the meshes are refined.

Before giving a brief explanation for the behavior of $L = 4$ and $L = 8$ when we refine the mesh, we recall here that, in the OSWR method, the convergence factor increases when Δt decreases, and thus more iterations are needed.

1.6.1.3 Effect of $\tilde{\rho}$ on the overall convergence

We try now to give a brief explanation on what is observed above. We first recall the inequality bound on the error of the coupled method (see Section 1.8 inequality (1.105)).

$$\mathbf{E}^k \leq (\gamma \mathbf{M} + \tilde{\rho} \mathbf{I})^k \mathbf{C}_0.$$

with $\tilde{\rho} = \rho^L$, and ρ is the convergence factor of the OSWR method. Then, the error after $2k$ Parareal iterations satisfies

$$\mathbf{E}^{2k} \leq (\gamma \mathbf{M} + \rho^L \mathbf{I})^{2k} \mathbf{C}_0. \tag{1.53}$$

On the other hand, let $\tilde{\mathbf{E}}^k$ be the error of the coupled method with $2L$ OSWR iterations in the incomplete fine solver; it satisfies the following bound

$$\tilde{\mathbf{E}}^k \leq (\gamma \mathbf{M} + \rho^{2L} \mathbf{I})^k \mathbf{C}_0. \tag{1.54}$$

Obviously, from (1.53) and (1.54), the computational costs related to the fine solver are similar because $(2k) \times L = k \times (2L)$.

At this point, we still do not know the errors $\mathbf{E}^{2k}$ and $\tilde{\mathbf{E}}^k$, however, we can try to compare their upper bounds. Then, in some ideal cases when these bounds are strict, we might get a good strategy for choosing L. We try to analyze for very small $N = 2, 3$. For $N = 2$, comparing the upper bounds in from (1.53) and (1.54), requires to compare

$$\begin{bmatrix} \rho^L & 0 \\ \gamma & \rho^L \end{bmatrix}^{2k} \mathbf{C}_0 \quad ; \quad \begin{bmatrix} \rho^{2L} & 0 \\ \gamma & \rho^{2L} \end{bmatrix}^k \mathbf{C}_0.$$

Then it remains to compare

$$\begin{bmatrix} \rho^L & 0 \\ \gamma & \rho^L \end{bmatrix}^2 \quad ; \quad \begin{bmatrix} \rho^{2L} & 0 \\ \gamma & \rho^{2L} \end{bmatrix}.$$

We calculate

$$\begin{bmatrix} \rho^L & 0 \\ \gamma & \rho^L \end{bmatrix}^2 = \begin{bmatrix} \rho^{2L} & 0 \\ 2\gamma\rho^L & \rho^{2L} \end{bmatrix}.$$

Hence, if $\rho^L < 1/2$, then $2k$ Parareal iterations coupled with L OSWR iterations might perform better than k Parareal iterations coupled with $2L$ OSWR iterations and vice versa. This is what we observe in the previous numerical tests, where low values of L perform better than large values of L, and where this more efficient behaviour tends to disappear when we refine the time step since ρ (and so ρ^L) grows with smaller Δt.

For $N = 3$: We calculate first

$$\begin{bmatrix} \rho^L & 0 & 0 \\ \gamma & \rho^L & 0 \\ \gamma\gamma_1 & \gamma & \rho^L \end{bmatrix}^2 = \begin{bmatrix} \rho^{2L} & 0 & 0 \\ 2\gamma\rho^L & \rho^{2L} & 0 \\ 2\gamma\gamma_1\rho^L + \gamma^2 & 2\gamma\rho^L & \rho^{2L} \end{bmatrix}.$$

Hence, if $\rho^L > 1/2$, then k Parareal iterations coupled with $2L$ OSWR iterations might perform better than $2k$ Parareal iterations coupled with L OSWR iterations. On the other hand, if $\rho^L < 1/2$, one might need an additional condition that $2\gamma\gamma_1\rho^L + \gamma^2 < \gamma\gamma_1$, i.e., $\rho^L < \dfrac{\gamma_1 - \gamma}{2\gamma_1}$. Now, we have a clear conclusion for $\rho^L > 1/2$ and $\rho^L < \dfrac{\gamma_1 - \gamma}{2\gamma_1} < 1/2$, but we cannot give a good conjecture for the comparison between L and $2L$ in the case $\dfrac{\gamma_1 - \gamma}{2\gamma_1} < \rho^L < 1/2$.

1.6.2 Advection-dominated test

We now try a test in which the classical Parareal does not work: the advection dominated case. We recall here that for the upwind discretization, the discrete convergence factor of OSWR is quite different from the continuous one, and so are the optimized

parameters [10]. We use here the discrete one.

We test $v = 0.001$ and $a = 1$, $b = 0$ on the domain $\Omega =]0,1[$, $T = 1$. The initial condition is $u_0(x) = x$, and Dirichlet B.C. $u(0,t) = 0$ and $u(1,t) = 1$. We show the numerical solution at the final time on Figure 1.5 to validate the upwind scheme which creates no oscillation.

The stopping criteria is based on the error between the numerical solution at the final time $t = T$ and the exact stationary solution which can be computed easily and is close to the exact stationary solution for large times.
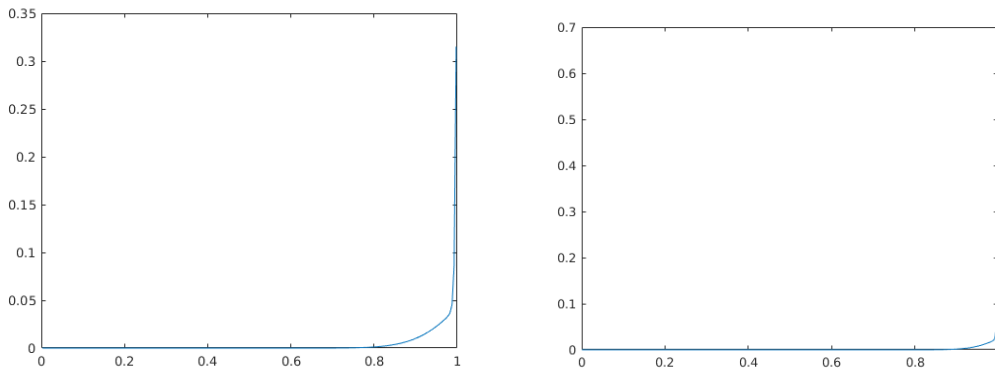
Figure 1.5: Example 2: The numerical solutions in case $\Delta x = \Delta t = 1/200$ (**case 1**, left) and case $\Delta x = \Delta t = 1/1000$ (**case 2**, right)
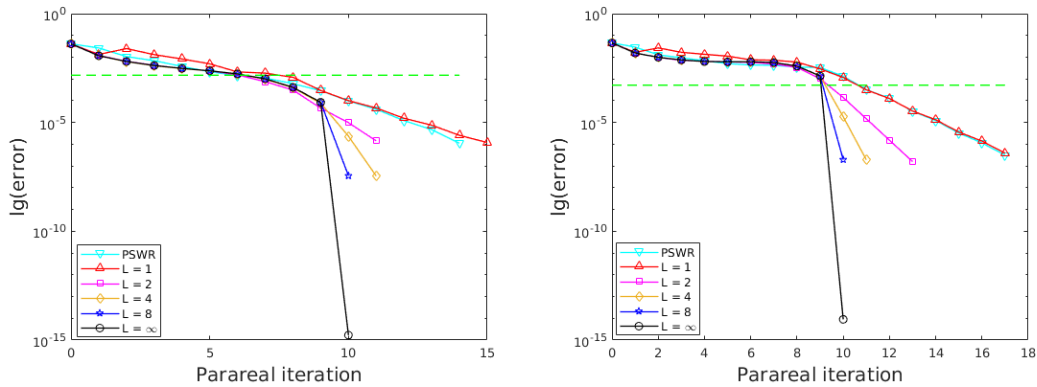
Figure 1.6: Example 2: Relative errors versus Parareal iterations in case $\Delta x = \Delta t = 1/200$ (**case 1**, left) and case $\Delta x = \Delta t = 1/1000$ (**case 2**, right)

1.6.2.1 Case 1

We first try with $\Delta x = \Delta t = 1/200$. For the monodomain solution, as the grids are not very fine, the effect of the boundary layer on the right is big (see Figure 1.5 (left)). In this test, the classical Parareal algorithm still works, even though it is quite slow, it needs 7 iterations to reach the stopping criterion. On the other hand, the OSWR method converges quite fast, it needs only 6 iterations to reach the stopping criterion. Moreover, in the coupled method, we cannot see a clear difference between the line

L	PSWR	1	2	4	$8(\infty)$
k	6	8	7	7	7
$L*k$	6	8	14	28	56

Table 1.9: Example 2 (case 1) Number of Parareal iterations k and total number of OSWR iterations $L*k$, versus L

solver	OSWR	Parareal	Parareal-OSWR ($L=1$)	PSWR
iterations (n)	6	56	8	6
loss factor ($l = n/6$)	-	9.3	1.33	1
gain factor (N)	-	10	10	10
final gain factor (N/l)	-	1.08	7.5	10

Table 1.10: Example 2 (case 1) Gain factor for Parareal and coupled Parareal-OSWR methods compared to the OSWR solver

$L = 8$ and the classical Parareal method (apart from the very last iteration because for $k = N$ the Parareal algorithm calculates the exact mono-domain solution, and this is not the case for the coupled method). This suggests that for a completely converged fine solver, one needs around 8 iterations. We choose to consider $L = 8$ to be the same as $L = \infty$.

We see from Figure 1.6 and Table 1.9 that the performance of the coupled method in this test is very different from the regular test. First, the PSWR only needs 6 iterations to converge, even fewer iterations than all other choices. One could guess that because we need very few iterations for a complete coarse solver, so putting only 1 iteration does not reduce much the accuracy while keeping the coupled method far from the classical Parareal, which performs poorly. Secondly, the final gain factors of all choices increase slightly (compare Table 1.10 to Table 1.2).

1.6.2.2   Case 2

L	PSWR	1	2	4	$8(\infty)$
k	11	11	10	10	10
$L*k$	11	11	20	40	80

Table 1.11: Example 2 (case 2) Number of Parareal iterations k and total number of OSWR iterations $L*k$, versus L

In this test case with $\Delta t = \Delta x = 1/1000$, Parareal does not work at all, since it needs full 10 iterations to converge. In consequence, the final gain factor of the best choice, shown in Table 1.12, decreases compared to case 1, so do all other choices. Figure 1.6 and table 1.11 show that there is no more singular performance in PSWR, it is now similar to the case $L = 1$, both are still the best choice. In addition, as the

solver	OSWR	Parareal	Parareal-OSWR $(L = 1)$	PSWR
iterations (n)	6	80	11	11
loss factor ($l = n/6$)	-	13.3	1.83	1.83
gain factor (N)	-	10	10	10
final gain factor (N/l)	-	0.75	5.45	5.45

Table 1.12: Example 2 (case 2) Gain factor for Parareal and coupled Parareal-OSWR methods compared to the OSWR solver

convergence factor of the OSWR becomes larger, the relative performances of large L values increase, similarly to what is observed in Section 1.6.1.

1.6.2.3 Case 3 and case 4

We repeat this test with finer grids to confirm our observations.
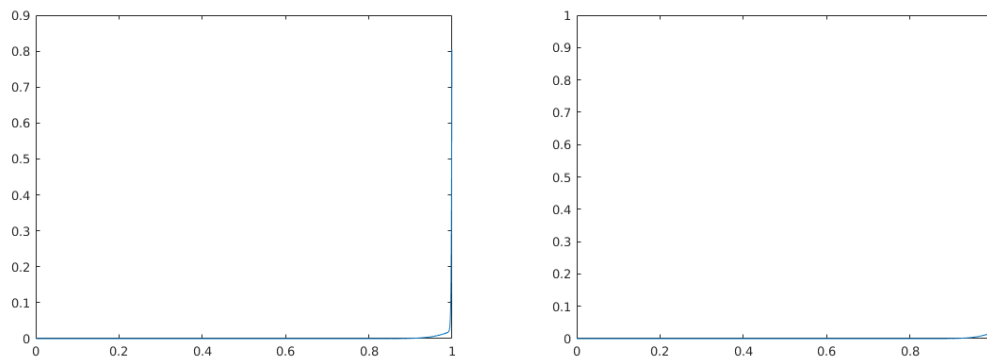
Figure 1.7: Example 2: The numerical solutions in case $\Delta x = \Delta t = 1/2000$ (left) and case $\Delta x = \Delta t = 1/5000$ (right)
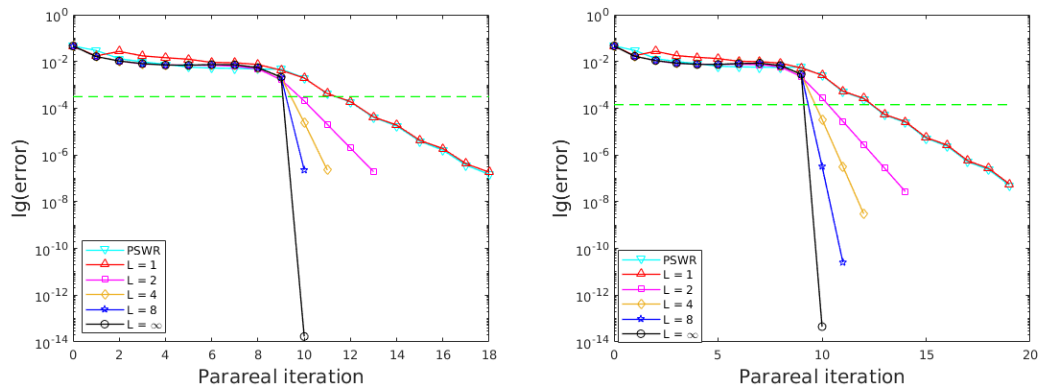
Figure 1.8: Example 2: Relative errors versus Parareal iterations in case $\Delta x = \Delta t = 1/2000$ (left) and case $\Delta x = \Delta t = 1/5000$ (right)

L	PSWR	1	2	4	$8(\infty)$
k	12	12	10	10	10
$L * k$	12	12	20	40	80

Table 1.13: Example 2 (case 3) Number of Parareal iterations k and total number of OSWR iterations $L * k$, versus L

solver	OSWR	Parareal	Parareal-OSWR ($L = 1$)	PSWR
iterations (n)	8	80	12	12
loss factor ($l = n/8$)	-	10	1.5	1.5
gain factor (N)	-	10	10	10
final gain factor (N/l)	-	1	6.83	6.83

Table 1.14: Example 2 (case 3) Gain factor for Parareal and coupled Parareal-OSWR methods compared to the OSWR solver

In case 3 with $\Delta x = \Delta t = 1/2000$, the OSWR is now really slower, it needs 8 iterations to converge. In consequence, the final gain factors of all choices increase. From table 1.13, we infer that the best choices are still PSWR and $L = 1$, while the relative performances of $L = 2$, $L = 4$ and $L = 8$ increase, but quite slightly, not as significantly as in the regular example of Section 1.6.1.

L	PSWR	1	2	4	$8(\infty)$
k	13	13	11	10	10
$L * k$	13	13	22	40	80

Table 1.15: Example 2 (case 4) Number of Parareal iterations k and total number of OSWR iterations $L * k$, versus L

solver	OSWR	Parareal	Parareal-OSWR ($L = 1$)	PSWR
iterations (n)	8	80	13	13
loss factor ($l = n/8$)	-	10	1.63	1.63
gain factor (N)	-	10	10	10
final gain factor (N/l)	-	1	6.15	6.15

Table 1.16: Example 2 (case 4) Gain factor for Parareal and coupled Parareal-OSWR methods compared to the OSWR solver

This case 4 with $\Delta t = \Delta x = 1/5000$ reproduces all observations of case 3, and from Table 1.14 and Table 1.16, we see that the final gain factors, again, decrease for finer meshes (the OSWR method still needs 8 iterations, but its convergence factor increases in fact)

1.6.2.4　When Parareal is bad and OSWR is good

We observe in the above advection dominated tests that the different choices for L do not lead to a clear separation in their convergence curves during some first Parareal iterations, before these curves go down linearly, each with a different convergence rate. We try here to give a brief explanation of this behavior by analyzing the upper bound of the error of the coupled method; at Parareal iteration $k \geq N$, we shall show below (see (1.116) in Section 1.8.6) that

$$\max_{1 \leq n \leq N} \|E_n^k\|_{\mathcal{X}} \leq C \sum_{i=0}^{N-1} \binom{k}{i} \tilde{\rho}^{k-i} \gamma^i \|\mathbf{M}^i\|_{\infty}. \tag{1.55}$$

We can write the sum in the right-hand side explicitly as

$$\sum_{i=0}^{N-1} \binom{k}{i} \tilde{\rho}^{k-i} \gamma^i \|\mathbf{M}^i\|_{\infty} = \left[\sum_{i=0}^{N-1} \binom{k}{i} \tilde{\rho}^{N-1-i} \gamma^i \|\mathbf{M}^i\|_{\infty} \right] \tilde{\rho}^{k-N+1}$$

We also recall that from the convergence result of Parareal obtained in (1.13), then after i iterations we have the following bound for the Parareal error

$$\max_{1 \leq n \leq N} \|E_n^i\|_{\mathcal{X}} \leq C \gamma_2^i \|\mathbf{M}^i\|_{\infty}.$$

For advection dominated tests, Parareal does not work well; even after $N-1$ iterations the error is still quite big. In fact, we have shown in Section 1.2.2 that when the value of the convection velocity is "large", we may have $\gamma_2 > 1$, and the above bound can get large. Using the definition of the constant γ_2 and the matrix $\mathbf{M}$, one can easily calculate γ_2 and the norm of $\|\mathbf{M}^i\|$. In this case, even though γ_2 is still smaller than 1, the term $\gamma_2^{N-1} \|\mathbf{M}^{N-1}\|$ is large.

The constant γ in the error estimate of the coupled method plays the same role as γ_2 in the pure Parareal method: they are upper bounds of the norm of the difference between the coarse solver and the (incomplete) fine solver. In our analysis, γ is not sharp, it is greater than the sum of the Lipschitz constants of $\mathcal{G}$ (which is γ_1) and $\mathcal{F}$ (which is C_2), so it is much greater than γ_2.

As OSWR converges quite fast in the above test cases, we expect that the Lipschitz constant of $(\mathcal{F} - \mathcal{G})$ and $(\tilde{\mathcal{F}} - \mathcal{G})$ are quite close to each other, regardless of the choice of L. In addition, with a small $\tilde{\rho}$, we get $\binom{k}{i} \tilde{\rho}^{N-1-i}$ very small also.

To conclude, one gets that the sum is dominated by its last term:

$$\left[\sum_{i=0}^{N-2} \binom{k}{i} \tilde{\rho}^{N-1-i} \gamma^i \|\mathbf{M}^i\|_{\infty} \right] << \gamma^{N-1} \|\mathbf{M}^{N-1}\|_{\infty}$$

or, equivalently

$$\left[\sum_{i=0}^{N-1} \binom{k}{i} \tilde{\rho}^{N-1-i} \gamma^i \|\mathbf{M}^i\|_{\infty} \right] \sim \gamma^{N-1} \|\mathbf{M}^{N-1}\|_{\infty},$$

which does not depend on $\tilde{\rho}$. This provides a bound in the right-hand side of (1.55) which behaves like

$$C \gamma^{N-1} \|\mathbf{M}^{N-1}\|_{\infty} \tilde{\rho}^{k-N+1}$$

for $k \geq N$. Therefore, in the advection dominated test case, one should not expect $k_L \times L$ to be constant (independent of L), but rather that $(k_L - N + 1) \times L$ will be more or less constant: the error after $N - 1$ iterations linearly depends on $\tilde{\rho}$. However, as $\tilde{\rho}$ is already small, the stopping criterion can be reached immediately at N iterations! However, if we decrease the stopping criteria, for example of the last test, to 5.10^{-7}, we get Table 1.17, in which we observe that all the terms $(k_L - N + 1) \times L$ are very close one to the other for all choices of L. We also see on Figure 1.8 that, after $N - 1$

L	PSWR	1	2	4	8
$(k-N+1)$	9	9	4	2	1
$L*(k-N+1)$	9	9	8	8	8

Table 1.17: Example 2 (case 3) Number of Parareal iterations after $(k - N + 1)$ and total number of OSWR iterations $(k - N + 1) * k$, versus L, stopping criteria 5.10^{-7}

iterations, all curves converge linearly.

If we follow this conjecture, then the best choice should always be $L = 1$, as it benefits from the first $N - 1$ iterations with almost no cost compared to greater values of L.

1.6.3 Large T and N

We now do another test with normal advection ($v = a = 1$) but with much larger time interval $T = 50$, the source term and initial condition are chosen in order to have the exact solution $u(x, t) = \cos(t) \sin(\pi x)$. For this big T, we take 100 time-windows, i.e. $N = 100$.
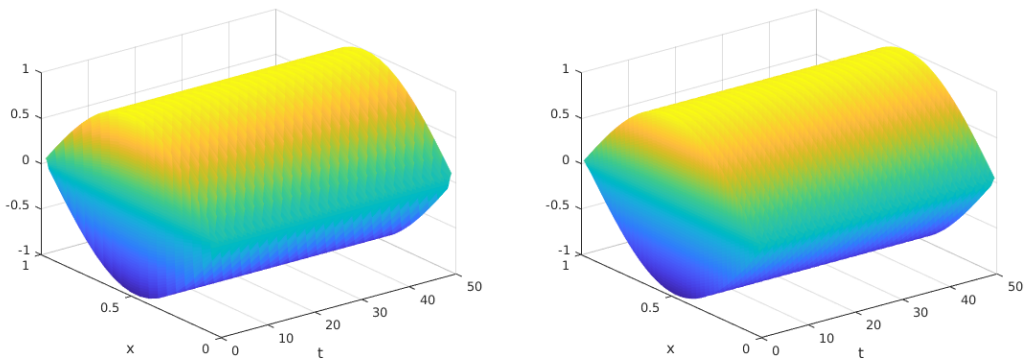
Figure 1.9: Example 3: The numerical solutions in case $\Delta x = 5.10^{-3}, \Delta t = 2.5.10^{-3}$ (left) and case $\Delta x = 2.5.10^{-3}, \Delta t = 6.25.10^{-4}$ (right)

The difference between these two cases, which are shown in Figure 1.10, are similar to the ones between the cases of Example 1. The behavior of the case $\Delta x = 2.5.10^{-3}, \Delta t = 6.25.10^{-4}$ is presented in Table 1.20 and Table 1.21. Here, we only give some remarks on the behavior of the coarser case $\Delta x = 5.10^{-3}, \Delta t = 2.5.10^{-3}$, shown in Tables 1.18 and 1.19.

With $u(x, t)$ cosine in time, the starting error for OSWR, Parareal and the coupled Parareal-OSWR are all small. We see here that the OSWR method converges very fast,
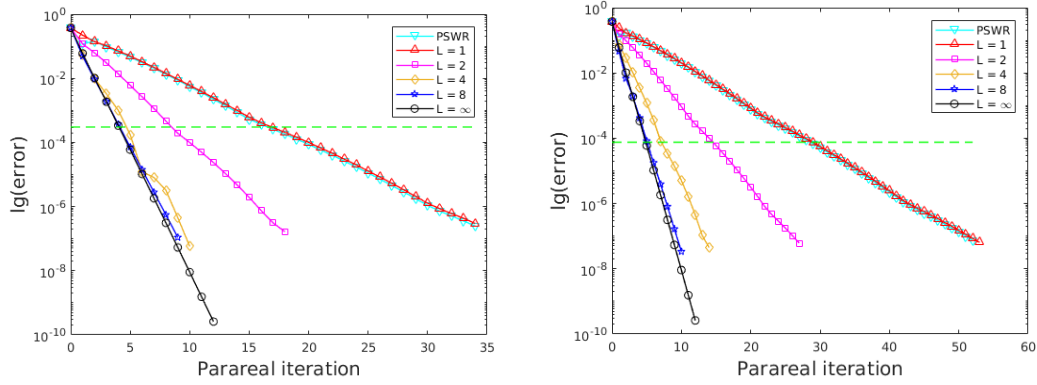
Figure 1.10: Example 3: Relative errors versus Parareal iterations in case $\Delta x = 5.10^{-3}, \Delta t = 2.5.10^{-3}$ (left) and case $\Delta x = 2.5.10^{-3}, \Delta t = 6.25.10^{-4}$ (right)

L	PSWR	1	2	4	8	$11(\infty)$
k	17	17	9	5	5	5
$L*k$	17	17	18	20	40	55

Table 1.18: Example 3 case $\Delta x = 5.10^{-3}, \Delta t = 2.5.10^{-3}$: Number of Parareal iterations k and total number of OSWR iterations $L*k$, versus L

solver	OSWR	Parareal	Parareal-OSWR $(L=1)$	PSWR
iterations (n)	11	5	17	17
loss factor ($l = n/11$)	-	5	1.55	1.55
gain factor (N)	-	100	100	100
final gain factor (N/l)	-	20	64.7	64.7

Table 1.19: Example 3 case $\Delta x = 5.10^{-3}, \Delta t = 2.5.10^{-3}$ Gain factor for Parareal and coupled Parareal-OSWR methods compared to the OSWR solver

after only 11 iterations. The Parareal method runs very fast also, it needs only 5 iterations for $N = 100$. In table 1.19, we see a great final gain factor for Parareal, using more processors. The final gain factor of the coupled choices, in consequence, greatly increases also.

The best choices are $L = 1$ and the PSWR. The lines $L = 2$ and $L = 4$ perform very well also, very close to the best one. The line $L = 8$ is not very well. Then we try to refine the mesh to see if their relative performances increase or not.

Similarly to the short time T with small N, the final gain factors of the coupled method decrease when we refine the mesh. The relative performance of $L = 8$ increases, even though it is still not as good as in the case 4 of example 1.

We can conclude now that all the observations for short T and small N are still valid for long T and large N.

L	PSWR	1	2	4	8	16(∞)
k	29	29	15	8	6	5
$L*k$	29	29	30	32	48	80

Table 1.20: Example 3 case $\Delta x = 2.5.10^{-3}, \Delta t = 6.25.10^{-4}$ Number of Parareal iterations k and total number of OSWR iterations $L*k$, versus L

solver	OSWR	Parareal	Parareal-OSWR ($L=1$)	PSWR
iterations (n)	16	80	29	29
loss factor ($l = n/16$)	-	5	1.81	1.81
gain factor (N)	-	100	100	100
final gain factor (N/l)	-	20	55.2	55.2

Table 1.21: Example 3 case $\Delta x = 2.5.10^{-3}, \Delta t = 6.25.10^{-4}$: Gain factor for Parareal and coupled Parareal-OSWR methods compared to the OSWR solver

1.7 Numerical results in 2D

In this section, we give some numerical illustrations of the performances of the coupled Parareal-OSWR method (Algorithm 3), in two space dimensions. In Section 1.7.1 and 1.7.2, these results are shown in the context of the NICEM method [72] for the space discretization, that enables the use of more efficient transmission conditions in the OSWR method (i.e. Ventcel conditions) with general domain decomposition and meshes. In section 1.7.3 we consider mixed finite elements as in [5] and Robin transmission condition. In all cases the backward Euler scheme in time is used. For the tests below with a variable advection field, the methodology to calculate the optimized Robin parameter is still based on Fourier transform, as done in Section 1.3, by a frozen coefficient approach. Another technique is proposed in [80], for a diffusion problem with variable coefficients.

In algorithm 3, a possible choice for the the initial Robin datum on $\mathscr{I}_n$ is to take $\xi_{i,n}^{0,0} = (\mathscr{B}_i U_n^0)(0)$, $i = 1,2$ (i.e. $\xi_{i,n}^{0,0}$ is constant on $\mathscr{I}_n$). A better choice, that improves the convergence of the Parareal-OSWR method, is to define V_n^0 as a linear interpolation between U_n^0 and U_{n+1}^0, and then to take $\xi_{i,n}^{0,0} = (\mathscr{B}_i V_n^0)(0)$, $i = 1,2$. Thus the latter case will be considered here.

The multi-domain problem (1.19) can actually be reformulated as an interface problem (see [39] or [68]) that can be solved by various iterative methods, such as block-Jacobi (which corresponds to the OSWR algorithm) or GMRES, the latter being our choice here (we call it "OSWRG" in what follows). Thus L will designate the number of GMRES iterations. In the Parareal algorithm, both the coarse and the fine solvers are performed using the OSWRG algorithm. For the coarse solver, as well as for the fine solver with $L = \infty$, the stopping criterion is when the jump of the optimized transmission conditions, measured in the L^2-norm on the interface, has been reduced below 10^{-13}. Otherwise, we will consider L iterations for the fine solver, with different values of L. Note that in what follows the error is mesured in the $L^\infty(0,T;H^1(\Omega))$-

norm, and that we obtain similar results in the $L^\infty(\Omega \times (0,T))$-norm.

1.7.1 A rotating velocity

We set $\Omega =]0,1[\times]0,1[$, $T = 21$, and consider the two dimensional problem

$$\partial_t u + \nabla \cdot (\boldsymbol{a} u) - \nu \Delta u = f, \quad \text{in } \Omega \times (0,T), \tag{1.56a}$$

$$u = u_D, \quad \text{on } \partial\Omega \times (0,T), \tag{1.56b}$$

$$u(\cdot, 0) = u_0, \quad \text{in } \Omega, \tag{1.56c}$$

with a rotating velocity field $\boldsymbol{a} = (a_x, a_y)$, where $a_x = -\sin\left(\pi(y - \frac{1}{2})\right)\cos\left(\pi(x - \frac{1}{2})\right)$ and $a_y = \cos\left(\pi(y - \frac{1}{2})\right)\sin\left(\pi(x - \frac{1}{2})\right)$, see Figure 1.11 on the left. We choose the
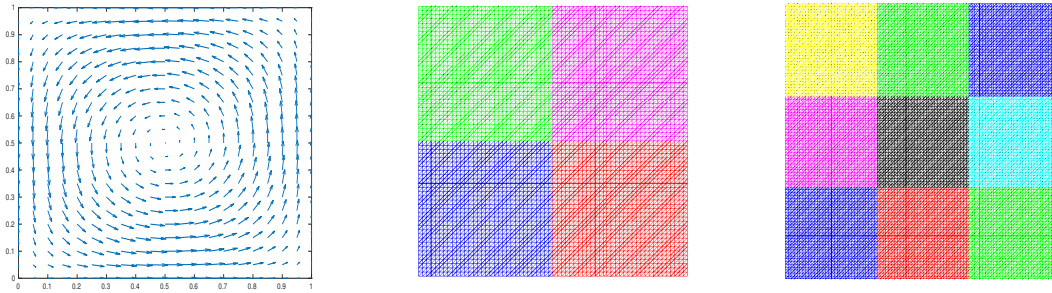
Figure 1.11: Example 1: rotating velocity (left), decomposition of Ω into 4 subdomains (middle), and decomposition of Ω into 9 subdomains (right)

right-hand side f and the values of the boundary and initial conditions so that the exact solution is given by

$$u(x,y) = \cos(\pi x)\sin(\pi y)\cos(\frac{2\pi t}{11}), \quad \forall(x,y) \in \Omega, \ \forall t \in (0,T). \tag{1.57}$$

The number of time windows for the Parareal iterations is $N = 21$. The time steps of the coarse and fine solvers are $\Delta t_C = 1$ and $\Delta t_F = 0.0156$, respectively.

In what follows we denote by e the relative scheme error, in $L^\infty(0,T;H^1(\Omega))$-norm, between the converged Parareal solution and the solution u of problem (1.56), given in (1.57). The term "OSWRG iterations" will designate the iterations for the fine solver. We will consider two cases for the diffusion and the domain decomposition in space.

In the results below, the cost of the coarse solver is negligible.

Case 1

We take $\nu = 0.05$ and a decomposition of Ω into four subdomains as in Figure 1.11 in the middle. The number of triangles in the whole domain $\bar{\Omega}$ is 8192 and the mesh size in each subdomain is 0.0221.

In Figure 1.12 (left), we plot the evolution of the relative error in the $L^\infty(0,T;H^1(\Omega))$-norm, between the Parareal-OSWRG solution and the converged

Parareal solution, as a function of the number of Parareal iterations, for different values of L. The case $L = \infty$ (black circle curve) corresponds to $L = 10$ (average value). The horizontal dashed green line represents $0.1e$ and we consider the number of iterations such that the algorithm error is smaller than this value. This is obtained after 3 iterations for Parareal or Parareal-OSWRG with $L = 8$, and after 5, 8, 18 iterations for Parareal-OSWRG with $L = 4$, $L = 2$, $L = 1$, respectively. These data are reported in Table 1.22. We observe that the fastest case is $L = 2$ with 16 OSWRG iterations globally.

Table 1.23 shows the gain (in term of fine solver iterations), when the fine solvers are performed in parallel, of the full Parareal ($L = 10$) or the coupled Parareal-OSWRG methods compared to the OSWRG algorithm for solving problem (1.56). The first column corresponds to the number of OSWRG iterations to reach $0.1e$, when the OSWRG method is used to solve (1.56). We observe that for $N = 21$ time windows, we gain a factor 10.5 for Parareal and a factor 20 for Parareal-OSWRG which is nearly the expected parallel efficiency.
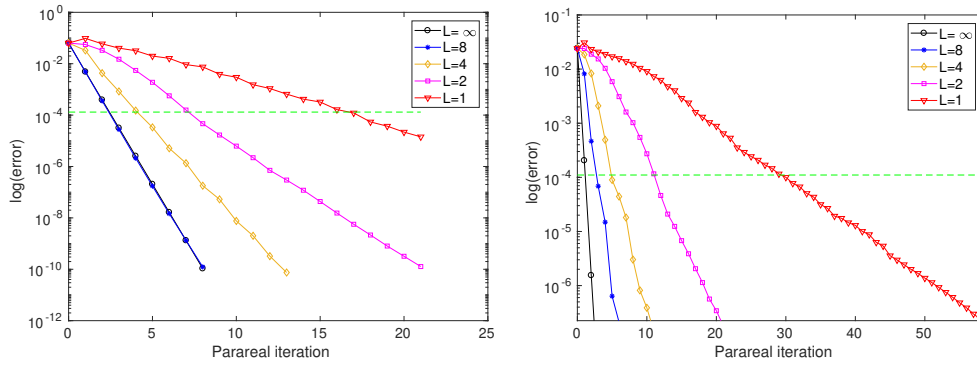
Figure 1.12: Example 1: Relative error versus Parareal iterations. Case $\nu = 0.05$ with 4 subdomains (left) and case $\nu = 0.1$ with 9 subdomains (right)

L	1	2	4	8	10 ($\approx \infty$)
k	17	8	5	3	3
$L * k$	17	16	20	24	30

Table 1.22: Example 1 (case 1): Number of Parareal iterations k and total number of OSWRG iterations $L * k$, versus L

Solver	OSWRG	Parareal	Parareal-OSWRG ($L = 2$)
iterations (n)	15	30	16
loss factor ($\ell = n/15$)	–	2	1.07
gain factor (N)	–	21	21
final gain factor (N/ℓ)	–	10.5	19.69

Table 1.23: Example 1 (case 1): Gain factor for Parareal and coupled Parareal-OSWRG methods compared to the OSWRG solver for solving problem (1.56)

Case 2

We take $\nu = 0.1$ and a decomposition of Ω into nine subdomains as in Figure 1.11 on the right. The number of triangles in the whole domain $\bar{\Omega}$ is 18432 and the mesh size in each subdomain is 0.0147.

In Figure 1.12 (right), the Parareal algorithm (black circle curve) corresponds to $L = 24$ (average value). The horizontal dashed green line represents $0.1e$, and is reached after 2 iterations for Parareal, and after 3, 5, 12, 30 iterations for Parareal-OSWRG with $L = 8$, $L = 4$, $L = 2$, $L = 1$, respectively. These data are shown in Table 1.24 and we observe that the fastest case is $L = 4$, with a total of 20 OSWRG iterations.

Table 1.25 shows the gain, when the fine solvers are performed in parallel, of the Parareal or the coupled Parareal-OSWRG methods compared to the OSWRG algorithm. In the first column we give the number of OSWRG iterations to reach $0.1e$, when it is used as a solver for problem (1.56). We observe that for $N = 21$ time windows, we gain a factor 10.94 for Parareal and a factor 26.25 for Parareal-OSWRG which represents an efficiency strictly greater than 1, since the number of processors is 21. This is notably better than the expected parallel efficiency.

L	1	2	4	8	24 $(\approx \infty)$
k	30	12	5	3	2
$L * k$	30	24	20	24	48

Table 1.24: Example 1 (case 2): Number of Parareal iterations k and total number of OSWRG iterations $L * k$, versus L

Solver	OSWRG	Parareal	Parareal-OSWRG ($L = 4$)
iterations (n)	25	48	20
loss factor ($\ell = n/25$)	–	1.92	0.8
gain factor (N)	–	21	21
final gain factor (N/ℓ)	–	10.94	26.25

Table 1.25: Example 1 (case 2): Gain factor for Parareal and coupled Parareal-OSWRG methods compared to the OSWRG solver for solving problem (1.56)

1.7.2   A boundary layer case with vorticies

We consider problem (1.56) with $f = 0$, $u_0(x, y) = 1 - x$, $u_D(x, y) = 1$ on $\{x = 0\}$ and $u_D(x, y) = 0$ elsewhere, and the following velocity field proposed in [104]: $\boldsymbol{a} = 0.32\pi\big(\sin(4\pi x)\sin(4\pi y), \cos(4\pi x)\cos(4\pi y)\big)$, see Figure 1.13 on the left. The diffusion coefficient is $\nu = 0.01$ and the final time is $T = 51$. The number of time windows for the Parareal iterations is $N = 51$. The time step of the coarse solver is $\Delta t_C = 1$.

In what follows we consider a decomposition of Ω into nine subdomains and consider a uniform mesh (case 1) and then a nonconforming mesh adapted to the physics (case 2).

Case 1

We consider a uniform mesh as in Figure 1.11 on the right, with a mesh size in each subdomain equal to 0.0147. The time step of the fine solver is $\Delta t_F = 0.0156$. The computed Parareal-OSWRG solution at final time $t = T$ is shown in Figure 1.13 on the right.
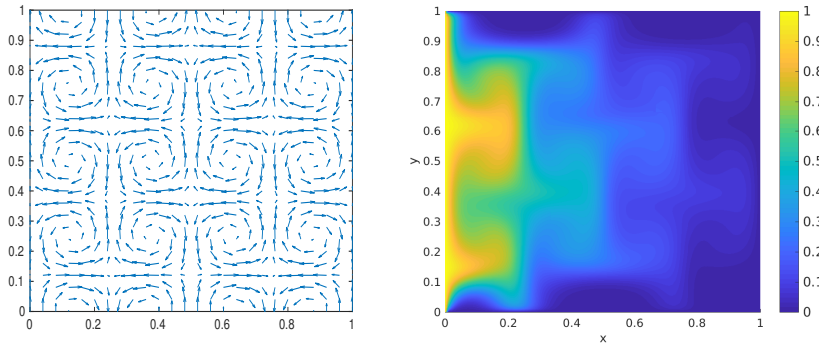
Figure 1.13: Example 2: velocity field (left), and computed Parareal-OSWRG solution at final time (right) for a uniform mesh

In Figure 1.14, we plot the evolution of the relative error in $L^\infty(0, T; H^1(\Omega))$-norm, between the Parareal-OSWRG solution and the converged Parareal solution, as a function of the number of Parareal iterations, for different values of L. The Parareal algorithm corresponds to $L = 10$ and we will compare the other cases of L to this case. We do not know the solution of problem (1.56) and thus the relative scheme error e, however we expect that e is between 10^{-1} and 10^{-3}, and thus $0.1e$ between 10^{-2} and 10^{-4}. Consequently, in Figure 1.14, the horizontal dashed green lines represent three possible values for $0.1e$, and Table 1.26 shows the number of Parareal and total OS-WRG iterations to reach these different values, for $L = 1, 2, 4, 8, 10$. We observe that the fastest case is $L = 2$.
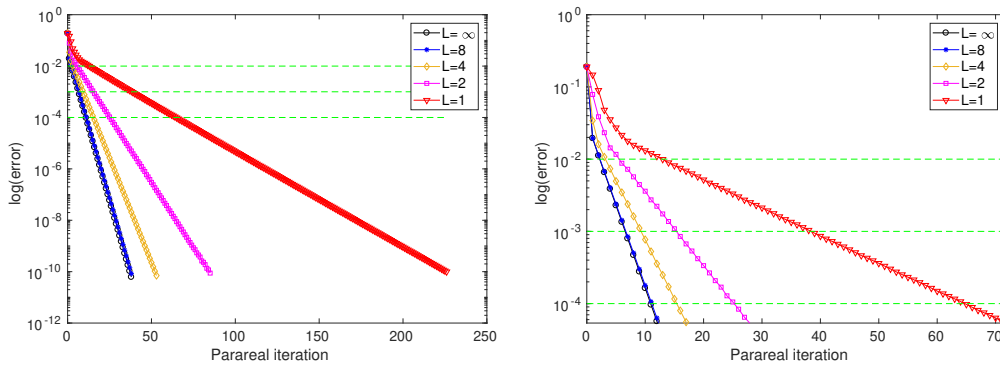
Figure 1.14: Example 2 (case 1): Relative error versus Parareal iterations, with a zoom on the first iterations on the right

The OSWRG algorithm used as a solver for problem (1.56) will need 22, 36 and 49 iterations to get a relative error in $L^\infty(0, T; H^1(\Omega))$-norm (between the iterate solution and the converged OSWRG solution) smaller than 10^{-2}, 10^{-3} and 10^{-4}, respectively. Table 1.27 shows the gain, when the fine solvers are performed in parallel, of the

Parareal or the coupled Parareal-OSWRG methods compared to the OSWRG algorithm. In this table we take the values obtained for $e = 10^{-2}$ (note that these values correspond also to those obtained with a mean value of the values for $e = 10^{-1}$, $e = 10^{-2}$ and $e = 10^{-3}$). We observe that for $N = 51$ time windows, we gain approximately a factor 26.29 for Parareal and a factor 57.38 for Parareal-OSWRG which is slightly better than the expected parallel efficiency.

L	1	2	4	8	10 ($\approx \infty$)
k	13	6	4	3	3
$L * k$	13	12	16	24	30

L	1	2	4	8	10 ($\approx \infty$)
k	39	16	10	7	7
$L * k$	39	32	40	56	70

L	1	2	4	8	10 ($\approx \infty$)
k	65	26	16	11	11
$L * k$	65	52	64	88	110

Table 1.26: Example 2 (case 1): Number of Parareal iterations k and total number of OSWRG iterations $L * k$, versus L to reach 3 different relative accuracy values: 10^{-2} (top left), 10^{-3} (top right) and 10^{-4} (bottom)

Solver	OSWRG	Parareal	Parareal-OSWRG ($L = 2$)
iterations (n)	36	70	32
loss factor ($\ell = n/36$)	–	1.94	0.89
gain factor (N)	–	51	51
final gain factor (N/ℓ)	–	26.29	57.38

Table 1.27: Example 2 (case 1): Gain factor for Parareal and coupled Parareal-OSWRG methods compared to the OSWRG solver for solving problem (1.56)

Case 2

We consider nonconforming meshes, refined in the region of the boudary layer, see Figure 1.15 on the left, with a mesh size equal to 0.0065, 0.0131, and 0.0295, for the subdomains with a boundary along $\{x = 0\}$, those with boundaries along $\{x = \frac{1}{3}\}$ and $\{x = \frac{2}{3}\}$, and those with a boundary along $\{x = 1\}$, respectively. The time step of the fine solver is $\Delta t_F = 0.01$. The computed Parareal-OSWRG solution at final time $t = T$ is shown in Figure 1.15 on the right, and is similar to the one obtained with a uniform mesh (see Figure 1.13 on the right).

In Figure 1.16, we plot the evolution of the relative error in $L^\infty(0, T; H^1(\Omega))$-norm, between the Parareal-OSWRG solution and the converged Parareal solution, as a function of the number of Parareal iterations, for different values of L. The Parareal algorithm ($L = \infty$) corresponds to the case $L = 12$, and we will compare the other cases of L to this case. As for Case 1, the horizontal dashed green lines represent three possible values of 10% of the error, and Table 1.28 shows the number of Parareal
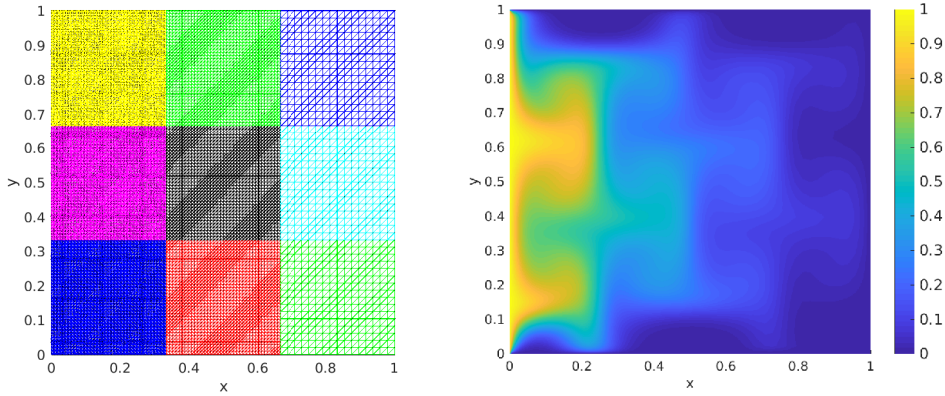
Figure 1.15: Example 2 (case 2): nonconforming meshes (left), and computed Parareal-OSWRG solution at final time (right)

and total OSWRG iterations to reach these different values, for $L = 1, 2, 4, 8, 12$. We observe that $L = 2$ is the case with the fewest iterations.
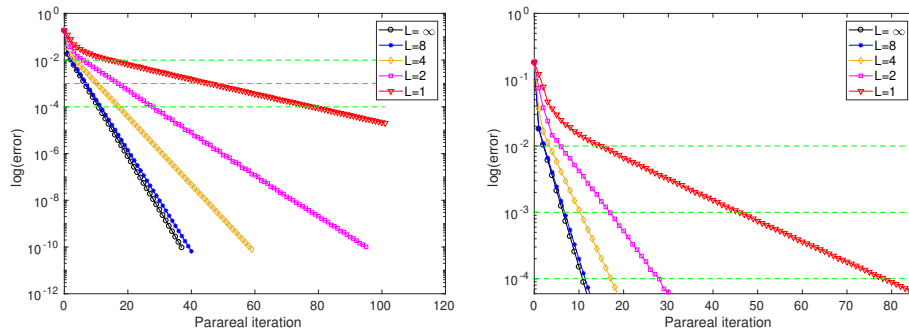
Figure 1.16: Example 2 (case 2): Relative error versus Parareal iterations, with a zoom on the first iterations on the right

The OSWRG algorithm used as a solver for problem (1.56) will need 24, 40 and 56 iterations to get a relative error in $L^\infty(0, T; H^1(\Omega))$-norm (between the iterative solution and the converged OSWRG solution) smaller than 10^{-2}, 10^{-3} and 10^{-4}, respectively. Table 1.29 shows the gain, when the fine solvers are performed in parallel, of the Parareal or the coupled Parareal-OSWRG methods compared to the OSWRG algorithm. In this table we take the values obtained for $e = 10^{-2}$ (note that these values correspond also to those obtained with a mean value of the values for $e = 10^{-1}$, $e = 10^{-2}$ and $e = 10^{-3}$). We observe that for $N = 51$ time windows, the results with a conforming mesh (Table 1.27) or with nonconforming meshes (Table 1.29) are very close and slightly better for nonconforming meshes adapted to the physics. Indeed, the gain is approximately a factor 24.28 for Parareal and a factor 60 for Parareal-OSWRG which is significantly better than the expected parallel efficiency.

L	1	2	4	8	$12\,(\approx \infty)$	L	1	2	4	8	$12\,(\approx \infty)$
k	16	6	4	3	3	k	47	17	11	7	
$L*k$	16	12	16	24	36	$L*k$	47	34	44	56	84

L	1	2	4	8	$12\,(\approx \infty)$
k	79	28	17	11	
$L*k$	79	56	68	88	132

Table 1.28: Example 2 (case 2): Number of Parareal iterations k and total number of OSWRG iterations $L*k$, versus L to reach 3 different values: 10^{-2} (top left), 10^{-3} (top right) and 10^{-4} (bottom)

Solver	OSWRG	Parareal	Parareal-OSWRG ($L=2$)
iterations (n)	40	84	34
loss factor ($\ell = n/40$)	–	2.1	0.85
gain factor (N)	–	51	51
final gain factor (N/ℓ)	–	24.28	60

Table 1.29: Example 2 (case 2): Gain factor for Parareal and coupled Parareal-OSWRG methods compared to the OSWRG solver for solving problem (1.56)

Remark 1.14. *Note that in the results above, the number of OSWRG iterations to reach full convergence, inside each time window in the Parareal iterations, is smaller than the one needed to reach full convergence on $(0,T)$ with OSWR method as a solver, probably because the time windows are smaller.*

Remark 1.15. *Another coupled algorithm is proposed in [54], involving incomplete (only one) iteration of OSWR both for the coarse and fine solvers (instead of incomplete iteration for the fine solver and a converged coarse solver as in our algorithm). The 2D simulations of this section don't show a comparison with that algorithm, however we have observed that the case $L=1$ is not the optimal choice of L, and that doing also incomplete iterations for the coarse solver will lead to similar or slower convergence than using a converged coarse solver.*

1.7.3   Example in an industrial context

We consider a simplified model problem given by ANDRA, the French National Agency for Radioactive Waste Management (see also [68, 4, 5]), that simulates the transport of a contaminant in and around a nuclear waste repository site. The simulation domain is depicted in Figure 1.17 (left) (not at scale). The nuclear waste is stored in the repository (yellow), which is a 2950m by 10m rectangle located in the center of a clay domain of 3950m by 140m (light brown). In this example, we are concerned with the following time-dependent diffusion problem in mixed formulation:

$$\boldsymbol{\sigma} = -\boldsymbol{S}\nabla u \quad \text{in} \quad \Omega \times (0,T), \tag{1.58a}$$

$$\phi \frac{\partial u}{\partial t} + \nabla \cdot \boldsymbol{\sigma} = f \qquad \text{in} \quad \Omega \times (0, T), \tag{1.58b}$$

where $\Omega = [0, 3950] \times [0, 140]$, u represents the (dimensionless) concentration of the contaminant, ϕ is the porosity, and $\boldsymbol{S}$ is the time-independent diffusion tensor. We decompose Ω into nine subdomains where Ω_5 is the nuclear waste repository domain, see Figure 1.17 (right). The porosity ϕ and the tensor $\boldsymbol{S}$ are defined as follows:

$$\phi = \begin{cases} 0.2 & \text{in } \Omega_5, \\ 0.05 & \text{in } \Omega_i, \ i \neq 5, \end{cases} \qquad \boldsymbol{S} = \begin{cases} 2 \times 10^{-9} \mathbb{I} \ \text{m}^2/\text{s} & \text{in } \Omega_5, \\ 5 \times 10^{-12} \mathbb{I} \ \text{m}^2/\text{s} & \text{in } \Omega_i, \ i \neq 5, \end{cases}$$

where $\mathbb{I}$ is the identity matrix. The source term f is zero in the clay layer and

$$f = \begin{cases} 10^{-5} \ \text{years}^{-1} & \text{if } t \leq 10^5 \ \text{years}, \\ 0 & \text{if } t > 10^5 \ \text{years}, \end{cases} \quad \text{in the repository.}$$

The initial condition is $u_0 = 0$ and we set homogeneous Dirichlet conditions on the top and the bottom of Ω, and homogeneous Neumann conditions on the other sides of $\partial \Omega$. We are interested in the long-term behavior of the repository, over one million years, so that we set $T = 10^6$ years. A dimensionless form of this problem is given in [5]. The number of triangles in the mesh of $\bar{\Omega}$ is 106638 (see Figure 1.18).
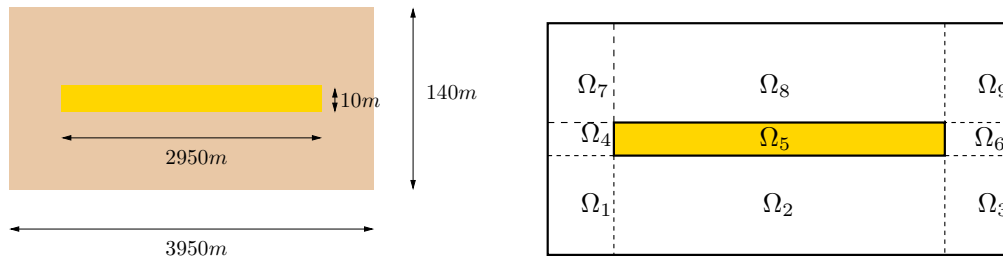
Figure 1.17: Geometry of the nuclear waste repository (yellow) and the clay layer around it (light brown) on the left and its decomposition into 9 subdomains on the right
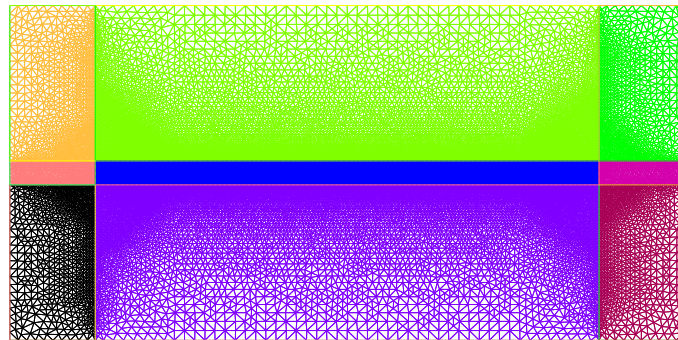
Figure 1.18: Example of a mesh used in and around a nuclear waste repository site

In Figure 1.19, we plot the evolution of the relative error in the $L^2(\Omega \times (0, T))$-norm, between the Parareal-OSWRG solution and the converged Parareal solution, as a function of the number of Parareal iterations, for different values of L. The Parareal algorithm ($L = \infty$) corresponds to $L = 10$ and we will compare the other cases of L to this case.

In [4], an a posteriori stopping criterion is given for this test case and the dashed green line shown in Figure 1.19 corresponds to this criterion. This line is reached after 3 iterations for Parareal and Parareal-OSWRG with $L = 4$, and after 12 iterations for Parareal-OSWRG with $L = 2$. The Parareal-OSWRG algorithm with $L = 1$ seems to be not convergent (at least on the first thirty iterations). These data are reported in Table 1.30 and we observe that the fastest case is $L = 4$ with a total of 12 OSWRG iterations.

Table 1.31 shows the gain, when the fine solvers are performed in parallel, of the Parareal or the coupled Parareal-OSWRG methods compared to the OSWRG algorithm. In the first column we give the number of OSWRG iterations given in [4] from the a posteriori stopping criterion, when the OSWRG method is used for solving problem (1.58). We observe that for $N = 10$ time windows, we gain a factor 3.66 for Parareal and a factor 9.17 for Parareal-OSWRG which is almost the expected parallel efficiency.
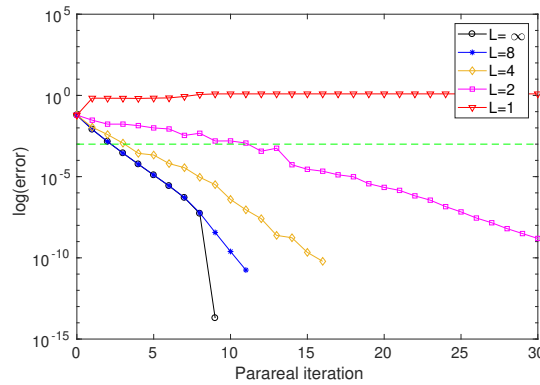
Figure 1.19: Example 3: Relative error versus Parareal iterations

L	1	2	4	8	$10\,(\approx \infty)$
k	–	12	3	3	3
$L * k$	–	24	12	24	30

Table 1.30: Example 3: Number of Parareal iterations k and total number of OSWRG iterations $L * k$, versus L

Solver	OSWRG	Parareal	Parareal-OSWRG ($L = 4$)
iterations (n)	11	30	12
loss factor ($\ell = n/11$)	–	2.73	1.09
gain factor (N)	–	10	10
final gain factor (N/ℓ)	–	3.66	9.17

Table 1.31: Example 3: Gain factor for Parareal and coupled Parareal-OSWRG methods compared to the OSWRG solver for solving problem (1.58)

1.8 Extension to overlapping subdomains : convergence factor of the Parareal-OSWR method

In this section, we provide a convergence factor of the coupled Parareal-OSWR algorithm, from the one of the OSWR method.

For nonoverlapping subdomains, as shown in Section 1.3.2, the convergence factor of the OSWR method (obtained using Fourier transform) will tend to 1 when the frequency tends to infinity, and thus we cannot derive a convergence factor of the coupled Parareal-OSWR algorithm in that case. However, in the case of overlapping subdomains, the convergence factor of the OSWR method will be strictly smaller than 1 (see Section 1.8.4 below), and we can provide a convergence factor of the coupled Parareal-OSWR algorithm. Thus, in what follows we will consider overlapping subdomains.

1.8.1 Domain decomposition and notation

We consider a decomposition of Ω into two subdomains

$$\Omega_1 = (-\infty, \delta), \quad \Omega_2 = (0, +\infty),$$

where $\delta > 0$ is the overlap between the subdomains. We set

$$\delta_1 = \delta \quad \text{and} \quad \delta_2 = 0. \tag{1.59}$$

We consider the Robin interface operator $\mathscr{B}_i$ for $i = 1, 2$ defined in (1.2). Then, problem (1.1) can be reformulated as the following equivalent multi-domain problem [39], with $u_i = u_{|\Omega_i}$, and $u_{0,i} = u_0|_{\Omega_i}$, $i = 1, 2$:

$$\begin{aligned}
\mathscr{L}u_i &= f && \text{in } \Omega_i \times (0, T), \\
u_i(\cdot, 0) &= u_{0,i} && \text{in } \Omega_i, && i = 1, 2, \\
(\mathscr{B}_i u_i)(\delta_i, \cdot) &= \xi_i && \text{on } (0, T),
\end{aligned} \tag{1.60}$$

with

$$\xi_i := (\mathscr{B}_i u_j)(\delta_i, \cdot) \quad \text{on } (0, T), \quad j = 3 - i, \ i = 1, 2. \tag{1.61}$$

As in the nonoverlapping case, in (1.2) p is a free parameter chosen such that: a) a Robin subdomain problem of type (1.60) is well-posed, b) it leads to a fast converging algorithm.

In what follows we will use the notation $\boldsymbol{\xi} := (\xi_1, \xi_2)$ for the exact Robin data on $(0, T)$ associated to the exact solution u of (1.1).

1.8.2 Existence and regularity results

We consider the spaces $\mathscr{X}_i$, $i = 1, 2$, and $\mathscr{Y}$ defined in Section 1.1.2 and the regular space $H^1(\Omega)$.

We recall below some useful regularity properties from [84].

Lemma 1.16. *(Regularity of problem (1.60))*
Let $i = 1$ or $i = 2$. If $u_0 \in \mathscr{X}_i$, $f \in L^2(0, T; L^2(\Omega_i))$ and $\xi_i \in \mathscr{Y}$, problem (1.60) has a unique solution u_i in $H^{2,1}(\Omega_i \times (0, T))$ and there exists a constant C independent of u_0, f, and ξ_i s.t.

$$\|u_i\|_{H^{2,1}(\Omega_i \times (0,T))} \leq C(\|u_0\|_{\mathscr{X}_i} + \|f\|_{L^2(0,T;L^2(\Omega_i))} + \|\xi_i\|_{\mathscr{Y}}).$$

Lemma 1.17. *(Trace theorem)*
If $u \in H^{2,1}(\Omega_i \times (0,T))$, then $u(\cdot, T) \in H^1(\Omega)$, $(\mathscr{B}_j u)(\delta_i, \cdot) \in \mathscr{Y}$, $i = 1, 2$, and there exists a constant C s.t.

$$\|(\mathscr{B}_j u)(\delta_i, .)\|_{\mathscr{Y}} \leq C \|u\|_{H^{2,1}(\Omega_i \times (0,T))}, \quad i = 1, 2.$$

and

$$\|u(., T)\|_{\mathscr{X}_i} \leq C \|u\|_{H^{2,1}(\Omega_i \times (0,T))}, \quad i = 1, 2.$$

1.8.3 Optimized Schwarz Waveform Relaxation Method

Following the notation of Section 1.3, the method is defined using, for $i = 1, 2$:

- the solution operator $\mathscr{M}_i(\mathscr{I}, u_{0,i}, \xi_i)$, $i = 1, 2$, that maps the available Robin condition ξ_i and initial condition $u_{0,i}$ to the subdomain solution u_i[8]:

$$\mathscr{M}_i : \begin{array}{ccc} \mathbf{I}^+ \times H^1(\Omega_i) \times \mathscr{Y} & \to & H^{2,1}(\Omega_i \times \mathscr{I}) \\ (\mathscr{I}, u_{0,i}, \xi_i) & \to & u_i, \end{array} \tag{1.62}$$

  where u_i is the solution of the following Robin problem in $\Omega_i \times \mathscr{I}$

$$\begin{array}{rclc} \mathscr{L} u_i = & f & \text{in } \Omega_i \times \mathscr{I}, \\ u_i(\cdot, 0) = & u_{0,i} & \text{in } \Omega_i, & i = 1, 2, \\ (\mathscr{B}_i u_i)(\delta_i, \cdot) = & \xi_i & \text{on } \mathscr{I}. \end{array} \tag{1.63}$$

- the transmission operator $\mathscr{B}_i$, $i = 1, 2$, that maps the available neighbor subdomain solution $u_j \in H^{2,1}(\Omega_j \times \mathscr{I})$, $j = 3 - i$, to a new Robin datum $\xi_i \in \mathscr{Y}$: $\xi_i = (\mathscr{B}_i u_j)(\delta_i, \cdot)$ on $\mathscr{I}$.

Using the definition of $\mathscr{M}_i$, problem (1.60)-(1.61) can be rewritten as

$$u_i = \mathscr{M}_i(\mathscr{I}, u_{0,i}, \xi_i), \ i = 1, 2, \tag{1.64a}$$

$$\xi_i = (\mathscr{B}_i u_j)(\delta_i, \cdot) \quad \text{on } \mathscr{I}, \quad j = 3 - i, \ i = 1, 2. \tag{1.64b}$$

The OSWR algorithm for solving problem (1.64) (or equivalently (1.1)) is as follows.

Algorithm 5 (OSWR)

Choose an initial Robin data $\boldsymbol{\xi}^0 = (\xi_1^0, \xi_2^0)$ on $\mathscr{I}$, for example $\xi_i^0 = (\mathscr{B}_i u_{0,i})(\delta_i, \cdot)$, $i = 1, 2$.
for $\ell = 1, 2, \ldots$ *(OSWR iterations)*
  1. Solve the local space-time Robin problems by calculating

$$u_i^\ell = \mathscr{M}_i(\mathscr{I}, u_{0,i}, \xi_i^{\ell-1}), \qquad i = 1, 2. \tag{1.65}$$

  2. Update the Robin interface term $\boldsymbol{\xi}^\ell = (\xi_1^\ell, \xi_2^\ell)$, with

$$\xi_i^\ell = (\mathscr{B}_i u_j^\ell)(\delta_i, \cdot) \quad \text{on } \mathscr{I}, \qquad j = 3 - i, \ i = 1, 2. \tag{1.66}$$

end for

Remark 1.18. *By definition of $\mathscr{M}_i$ and u_i^ℓ in (1.65), the interface condition is*

$$(\mathscr{B}_i u_i^\ell)(\delta_i, \cdot) = \xi_i^{\ell-1}, \ i = 1, 2. \tag{1.67}$$

---

[8]the operator $\mathscr{M}_i$ should depend also on f but we omit it here to simplify the notations.

1.8.4 Stability and convergence

We suppose that $f \in L^2(0, T; L^2(\Omega))$, and will use the notation of Section 1.3.1.
Let (u_i^ℓ, ξ_i^ℓ), $i = 1, 2$ be defined by (1.65)–(1.66). For the convergence analysis below, we recall the following notations of Section 1.3.1 for the errors, for $i = 1, 2$ and $\ell \geq 1$:

$$\zeta_i^\ell := \xi_i^\ell - \xi_i, \quad \text{where } \xi_i \text{ is defined in (1.61)}, \quad \text{and we set } \boldsymbol{\zeta}^\ell := (\zeta_1^\ell, \zeta_2^\ell), \quad (1.68)$$

$$e_i^\ell := u_i^\ell - u, \quad \text{where } u \text{ is the solution of (1.1)}, \quad (1.69)$$

Theorem 1.19. *Consider Algorithm 5. If $u_0 \in H^1(\Omega)$ and $\boldsymbol{\xi}^0 \in \mathscr{Y}^2$, then there exists a constant $\rho < 1$, independent of u_0 and $\boldsymbol{\xi}^0$, such that, $\forall \ell \geq 1$*

$$\|\boldsymbol{\xi}^{2\ell}\|_{\mathscr{Y}^2} \leq \check{\rho}^{2\ell} \|\boldsymbol{\xi}^0\|_{\mathscr{Y}^2} + C_1 (\|u_0\|_{H^1(\Omega)} + \|f\|_{L^2(0,T;L^2(\Omega))}) \quad (1.70)$$

$$\|u_1^{2\ell}(., T)\|_{H^1(\Omega_1)} + \|u_2^{2\ell}(., T)\|_{H^1(\Omega_2)} \leq C_2 (\check{\rho}^{2\ell-1} \|\boldsymbol{\xi}^0\|_{\mathscr{Y}^2} + \|u_0\|_{H^1(\Omega)} + \|f\|_{L^2(0,T;L^2(\Omega))}). \quad (1.71)$$

with $\check{\rho} = \sqrt{\rho}$.

Proof. The proof of Theorem 1.19 extends the one of Lemma 5.7 in [50], obtained for $u_0 \in H^2(\Omega)$, to the case $u_0 \in H^1(\Omega)$. By linearity of $\mathscr{M}_i$, from (1.64a) and (1.65), the error $e_i^\ell := u_i^\ell - u$, $i = 1, 2$, at iteration ℓ of the OSWR method, satisfies $e_i^\ell = \mathscr{M}_i(\mathscr{I}, 0, \zeta_i^{\ell-1})$, with $\zeta_i^{\ell-1} = \xi_i^{\ell-1} - \xi_i$ and $f = 0$. Equivalently, e_i^ℓ is solution of the following problem

$$\begin{aligned} \mathscr{L} e_i^\ell &= 0 && \text{in } \Omega_i \times \mathscr{I}, \\ e_i^\ell(\cdot, 0) &= 0 && \text{in } \Omega_i, && i = 1, 2, \quad (1.72) \\ \mathscr{B}_i e_i^\ell(\delta_i, \cdot) &= \zeta_i^{\ell-1} && \text{on } \mathscr{I}. \end{aligned}$$

From (1.64b) and (1.66), we have $\zeta_i^\ell = \mathscr{B}_i e_j^\ell(\delta_i, \cdot)$, $i = 1, 2$, and thus the transmission conditions on $\mathscr{I}$ in (1.72) also read

$$\mathscr{B}_i e_i^\ell(\delta_i, \cdot) = \mathscr{B}_i e_j^{\ell-1}(\delta_i, \cdot) \quad \text{on } \mathscr{I}, \quad j = 3 - i, \ i = 1, 2. \quad (1.73)$$

Now we use Fourier transform as in Section 1.3.1, and extend (1.72)–(1.73) to $\mathscr{R}$ in the following way :

• for $\ell = 1$, the Robin condition in (1.72) is with $\zeta_i^0 \in \mathscr{Y}$ and we can extend ζ_i^0 by zero to $H^{\frac{1}{4}}(\mathscr{R})$ to obtain a function, denoted by $\tilde{\zeta}_i^0$, vanishing on $(-\infty, 0)$, and on $(T, +\infty)$, for $i = 1, 2$. Then we can extend equations (1.72) to $\mathscr{R}$, and their solutions, denoted by $(\tilde{e}_1^1, \tilde{e}_2^1)$, vanish on $(-\infty, 0)$ and coincide with (e_1^1, e_2^1) on $(0, T)$.

• for $\ell \geq 2$, we define the Robin trace $\tilde{\zeta}_i^{\ell-1} := \mathscr{B}_i \tilde{e}_j^{\ell-1}(\delta_i, \cdot)$ on $\{\delta_i\} \times \mathscr{R}$, which belongs to $H^{\frac{1}{4}}(\mathscr{R})$, vanishes on $(-\infty, 0)$ and coincides with $\mathscr{B}_i e_j^{\ell-1}(\delta_i, \cdot)$ on $\{\delta_i\} \times (0, T)$, for $i = 1, 2$. The subdomain problems (1.72) are extended on $\Omega_i \times \mathscr{R}$ as follows :

$$\begin{aligned} \mathscr{L} \tilde{e}_i^\ell &= 0 && \text{in } \Omega_i \times \mathscr{R}, \\ \tilde{e}_i^\ell(\cdot, 0) &= 0 && \text{in } \Omega_i, && i = 1, 2, \quad (1.74) \\ \mathscr{B}_i \tilde{e}_i^\ell(\delta_i, \cdot) &= \tilde{\zeta}_i^{\ell-1} && \text{on } \mathscr{R}, \end{aligned}$$

and their solutions vanish on $(-\infty, 0)$ and coincide with (e_1^ℓ, e_2^ℓ) on $(0, T)$. In particular, by definition of $\tilde{\zeta}_i^{\ell-1}$ above, the transmission condition (1.73) has been extended on $\{\delta_i\} \times \mathscr{R}$ in (1.74) as follows :

$$\mathscr{B}_i \tilde{e}_i^\ell(\delta_i, \cdot) = \mathscr{B}_i \tilde{e}_j^{\ell-1}(\delta_i, \cdot) \quad \text{on } \mathscr{R}, \quad j = 3 - i, \ i = 1, 2. \tag{1.75}$$

Note that for $\ell \geq 1$, the property $\tilde{\zeta}_i^{\ell-1} \in H^{\frac{1}{4}}(\mathscr{R})$ implies that the solution e_i^ℓ of problem (1.74) is in $H^{2,1}(\Omega_i \times \mathscr{R})$, and thus the new Robin datum $\tilde{\zeta}_i^\ell$, defined above, is still in $H^{\frac{1}{4}}(\mathscr{R})$.

Then, using Fourier transform in time, we solve in each subdomain the ordinary differential equation

$$i\omega \hat{e}_i^\ell - \nu \partial_{xx} \hat{e}_i^\ell + a \partial_x \hat{e}_i^\ell + b \hat{e}_i^\ell = 0, \qquad i = 1, 2, \tag{1.76}$$

with the characteristic roots r^- and r^+ defined in (1.36), and the subdomain solutions $\hat{e}_i^\ell \in L^2(\Omega_i)$, $i = 1, 2$ are given by[9]

$$\hat{e}_1^\ell = \frac{2}{\sqrt{d}+p} \hat{\zeta}_1^{\ell-1}(\omega) e^{r^+(x-\delta)}, \qquad \hat{e}_2^\ell = \frac{2}{\sqrt{d}+p} \hat{\zeta}_2^{\ell-1}(\omega) e^{r^-x}, \qquad \ell \geq 1, \tag{1.77}$$

then, replacing (1.77) in the transmission conditions (1.75) leads to

$$\forall \ell \geq 1, \quad \begin{pmatrix} \hat{\zeta}_1^\ell \\ \hat{\zeta}_2^\ell \end{pmatrix} = \left(\frac{-\sqrt{d}+p}{\sqrt{d}+p} \right) \begin{pmatrix} e^{\delta r^-} \hat{\zeta}_2^{\ell-1} \\ e^{-\delta r^+} \hat{\zeta}_1^{\ell-1} \end{pmatrix}. \tag{1.78}$$

Using (1.36) and the following identities

$$\delta r^- = \frac{1}{2}\delta(r^- - r^+) + \frac{1}{2}\delta(r^- + r^+) = \frac{1}{2}\delta(r^- - r^+) + \frac{\delta a}{2\nu},$$

$$-\delta r^+ = \frac{1}{2}\delta(r^- - r^+) - \frac{1}{2}\delta(r^- + r^+) = \frac{1}{2}\delta(r^- - r^+) - \frac{\delta a}{2\nu},$$

one obtains

$$\hat{\zeta}_1^\ell = \sqrt{\rho_0(\omega)} e^{\delta a/(2\nu)} \hat{\zeta}_2^{\ell-1},$$
$$\hat{\zeta}_2^\ell = \sqrt{\rho_0(\omega)} e^{-\delta a/(2\nu)} \hat{\zeta}_1^{\ell-1}, \tag{1.79}$$

with $\rho_0(\omega) := \left(\frac{-\sqrt{d}+p}{\sqrt{d}+p} \right)^2 e^{\delta(r^- - r^+)}$.

Thus, setting $\hat{\boldsymbol{\zeta}}^\ell := (\hat{\zeta}_1^\ell, \hat{\zeta}_2^\ell)$, we have

$$\forall \ell \geq 2, \quad \hat{\boldsymbol{\zeta}}^\ell = \rho_0(\omega) \hat{\boldsymbol{\zeta}}^{\ell-2} \tag{1.80}$$

From (1.80), by induction we obtain,

$$\hat{\boldsymbol{\zeta}}^{2\ell} = \rho_0(\omega)^\ell \hat{\boldsymbol{\zeta}}^0, \qquad \forall \ell \geq 1. \tag{1.81}$$

Then, setting

$$\rho := \sup_{\omega \in \mathscr{R}} |\rho_0(\omega)|, \tag{1.82}$$

---

[9]Note that here the term "∂_x" in $\mathscr{B}_i$ is multiplied by ν while this is not the case in [50]. Thus $\hat{e}_i^\ell$ is slightly different here, from the one of [50].

we have $0 < \rho < 1$, and denoting $\tilde{\boldsymbol{\zeta}}^{\ell} := (\tilde{\zeta}_1^{\ell}, \tilde{\zeta}_2^{\ell})$, from (1.81) and (1.82), we get

$$\|\tilde{\boldsymbol{\zeta}}^{2\ell}\|_{\left(H^{\frac{1}{4}}(\mathscr{R})\right)^2} \leq \rho^{\ell} \|\tilde{\boldsymbol{\zeta}}^0\|_{\left(H^{\frac{1}{4}}(\mathscr{R})\right)^2}, \qquad \forall \ell \geq 1.$$

From the above inequality, and using that $\tilde{\boldsymbol{\zeta}}^0 = 0$ a.e. on $(-\infty, 0)$ and on $(T, +\infty)$, we obtain

$$\|\tilde{\boldsymbol{\zeta}}^{2\ell}\|_{\left(H^{\frac{1}{4}}(\mathscr{R})\right)^2} \leq \rho^{\ell} \|\boldsymbol{\zeta}^0\|_{\mathscr{Y}^2}, \qquad \forall \ell \geq 1.$$

Now, using that $\|\boldsymbol{\zeta}^{2\ell}\|_{\mathscr{Y}^2} \leq \|\tilde{\boldsymbol{\zeta}}^{2\ell}\|_{\left(H^{\frac{1}{4}}(\mathscr{R})\right)^2}$, then we have

$$\|\boldsymbol{\zeta}^{2\ell}\|_{\mathscr{Y}^2} \leq \rho^{\ell} \|\boldsymbol{\zeta}^0\|_{\mathscr{Y}^2}, \qquad \forall \ell \geq 1 \text{ (and also for } \ell = 0). \tag{1.83}$$

This can be rewritten by introducing explicitly the error:

$$\|\boldsymbol{\xi}^{2\ell} - \boldsymbol{\xi}\|_{\mathscr{Y}^2} \leq \rho^{\ell} \|\boldsymbol{\xi}^0 - \boldsymbol{\xi}\|_{\mathscr{Y}^2}, \qquad \forall \ell \geq 1. \tag{1.84}$$

From Lemma 1.17, the norm of ξ_i is bounded by the norm of u_i, which is itself bounded by the norm of u. Then, using Lemma 1.1, it is also bounded by the norms of u_0 and f. One then gets (1.70) using simple triangular inequalities in (1.84).

From the regularity of the subdomain problem (Lemma 1.16) for the error (1.72), we have

$$\|e_i^{2\ell}\|_{H^{2,1}(\Omega_i \times (0,T))} \leq C \|\zeta_i^{2\ell-1}\|_{\mathscr{Y}}$$

Then, from (1.79), one gets (note that the value of C changes from one inequality to the other)

$$\|e_i^{2\ell}\|_{H^{2,1}(\Omega_i \times (0,T))} \leq C \|\zeta_i^{2\ell-1}\|_{\mathscr{Y}} \leq C \check{\rho} \|\zeta_j^{2\ell-2}\|_{\mathscr{Y}} \quad \text{(with } j = 3 - i)$$

and then, with (1.83)

$$\|e_i^{2\ell}\|_{H^{2,1}(\Omega_i \times (0,T))} \leq C \check{\rho}^{2\ell-1} \|\zeta_j^0\|_{\mathscr{Y}}.$$

Then, from the triangular inequality, one has

$$\|u_i^{2\ell}\|_{H^{2,1}(\Omega_i \times (0,T))} - \|u_i\|_{H^{2,1}(\Omega_i \times (0,T))} \leq \|e_i^{2\ell}\|_{H^{2,1}(\Omega_i \times (0,T))}$$
$$\leq C \check{\rho}^{2\ell-1} (\|\xi_j^0\|_{\mathscr{Y}} + \|\xi_j\|_{\mathscr{Y}}). \tag{1.85}$$

Then, again, from Lemma 1.17, one has

$$\|u_i^{2\ell}(.,T)\|_{\mathscr{X}_i} \leq C \|u_i^{2\ell}\|_{H^{2,1}(\Omega_i \times (0,T))}. \tag{1.86}$$

Then, using again the stability results, the norms of ξ_j and u_i are bounded by those of u_0 and f, so that (1.85) and (1.86) lead to

$$\|u_i^{2\ell}(.,T)\|_{\mathscr{X}_i} \leq C_2 (\check{\rho}^{2\ell-1} \|\xi_j^0\|_{\mathscr{Y}} + \|u_0\|_{\mathscr{X}} + \|f\|_{L^2(0,T;L^2(\Omega))}),$$

which implies (1.71), with C_2 independent of ℓ, u_0 and $\boldsymbol{\xi}^0$. $\qquad\qquad \square$

Remark 1.20. *The result of Theorem 1.19 can be extended to the case* $(2\ell + 1)$. *We have first that*

$$\|u_i^{2\ell+1}(.,T)\|_{\mathscr{X}_i} \leq c_2(\check{\rho}^{2\ell}\|\xi_j^0\|_{\mathscr{Y}} + \|u_0\|_{\mathscr{X}} + \|f\|_{L^2(0,T;L^2(\Omega))}). \tag{1.87}$$

For the Robin terms, one could give a more dedicated bound

$$\begin{aligned}
\|\xi_1^{2\ell+1}\|_{\mathscr{Y}} &\leq e^{\delta a/(2\nu)}\check{\rho}^{2\ell+1}\|\xi_2^0\|_{\mathscr{Y}} + c_1(\|u_0\|_{H^1(\Omega)} + \|f\|_{L^2(0,T;L^2(\Omega))}) \\
\|\xi_2^{2\ell+1}\|_{\mathscr{Y}} &\leq e^{-\delta a/(2\nu)}\check{\rho}^{2\ell+1}\|\xi_2^0\|_{\mathscr{Y}} + c_1(\|u_0\|_{H^1(\Omega)} + \|f\|_{L^2(0,T;L^2(\Omega))})
\end{aligned} \tag{1.88}$$

As in Section 1.3, in the sequel we will denote in compact form

$$(u_1^L, u_2^L, \boldsymbol{\xi}^L) = \text{OSWR}_L(\mathscr{I}, u_0, \boldsymbol{\xi}^0), \tag{1.89}$$

where u_1^L, u_2^L, and $\boldsymbol{\xi}^L = (\xi_i^L)_{i=1,2}$ are the output after L iterations of algorithm (1.65)–(1.66) with initial condition u_0 and initial Robin data $\boldsymbol{\xi}_0$ on $\mathscr{I}$ (due to the overlap, one cannot define a global function u^L as in Section 1.3).

1.8.5 Coupled Parareal-OSWR method

In the Coupled Parareal-OSWR algorithm, incomplete iterations of the OSWR method are performed. Thus, at each parareal iteration, the output of the fine solver (i.e. the OSWR method) is not in $H^1(\Omega)$. In the case of nonoverlapping subdomains, this is not a problem since the coupled algorithm is based on initial conditions U_n^k in the local regular space $\mathscr{X}$ (defined in Section 1.1.2), at each parareal iteration k and time window $\mathscr{I}_n$ (see Section 1.4). However, in the case of overlapping subdomains considered in this section, the functional space for U_n^k is $H^1(\Omega)$. Consequently, we need a correction step that will build, from the OSWR output, a function in $H^1(\Omega)$. This correction is defined as follows : Let $\Omega_{12} :=]0, \delta[$ be the overlap, and let $u_i \in \mathscr{X}_i$, $i = 1, 2$. We define the correction operator $\mathscr{C}$ from $(\mathscr{X}_1, \mathscr{X}_2)$ to $H^1(\Omega)$ as follows :

$$\mathscr{C}(u_1, u_2) = \check{u} \quad \text{with } \check{u} = \mu_1 u_1 + \mu_2 u_2, \tag{1.90}$$

where, for $i = 1, 2$, and $j = 3 - i$,

$$\mu_1 = \begin{cases} 1 & \text{in} \quad \Omega_1 \backslash \Omega_{12}, \\ \dfrac{\delta - x}{\delta} & \text{in} \quad \Omega_{12}, \\ 0 & \text{in} \quad \Omega_2 \end{cases} \quad \text{and} \quad \mu_2 = \begin{cases} 1 & \text{in} \quad \Omega_2 \backslash \Omega_{12}, \\ \dfrac{x}{\delta} & \text{in} \quad \Omega_{12}, \\ 0 & \text{in} \quad \Omega_1. \end{cases} \tag{1.91}$$

From the formulation of the correction, one gets immediately that, if $u_1 \in H^1(\Omega_1)$ and $u_2 \in H^1(\Omega_2)$, then $\check{u} \in H^1(\Omega)$ and that there exists a constant C such that, $\forall u_1 \in H^1(\Omega_1), u_2 \in H^1(\Omega_2)$

$$\|\mathscr{C}(u_1, u_2)\|_{H_1(\Omega)} \leq C(\|u_1\|_{H^1(\Omega_1)} + \|u_2\|_{H^1(\Omega_2)}) \tag{1.92}$$

Using the notation of Section 1.4, the Parareal-OSWR algorithm with overlapping subdomains is defined, using the coarse propagator $\mathscr{G}$ of Section 1.2 and the incomplete[10] fine propagator OSWR_L defined by (1.89), as follows :

---

[10] In the sense that L will be smaller than the required number of iterations to converge.

Algorithm 6 (Coupled parareal-OSWR)

---

1. Choose an initial data $(U_n^0)_{n\in[\![0,N]\!]}$ with $U_0^0 = u_0$ and U_n^0 an approximation of $u(\cdot, T_n)$, for example $U_n^0 := \mathcal{G}(\mathscr{I}_{n-1}, U_{n-1}^0)$, for $n = 1, 2, \ldots, N$.

2. Choose an initial Robin data $(\boldsymbol{\xi}_n^{0,0})_{n\in[\![0,N]\!]}$, with $\boldsymbol{\xi}_n^{0,0} := (\xi_{1,n}^{0,0}, \xi_{2,n}^{0,0})$ on $\mathscr{I}_n$, for example $\xi_{i,n}^{0,0} = (\mathscr{B}_i U_n^0)(\delta_i, \cdot)$, $i = 1, 2$.

for $k = 0, 1, \ldots$ *(Parareal iterations)*

   1. On each time interval $\mathscr{I}_n$, $n = 0, 1, \ldots, N-1$:

$$\text{Calculate} \quad (u_{1,n}^{k,L}, u_{2,n}^{k,L}, \boldsymbol{\xi}_n^{k,L}) = \text{OSWR}_L(\mathscr{I}_n, U_n^k, \boldsymbol{\xi}_n^{k,0}). \tag{1.93}$$

   2. Perform the correction on $u_{i,n}^{k,L}$:

$$\breve{u}_n^{k,L} = \mathscr{C}(u_{1,n}^{k,L}(., T_{n+1}), u_{2,n}^{k,L}(., T_{n+1})). \tag{1.94}$$

   3. Set $U_0^{k+1} = u_0$ and do Parareal corrections:

$$U_{n+1}^{k+1} = \breve{u}_n^{k,L} + \mathscr{G}(\mathscr{I}_n, U_n^{k+1}) - \mathscr{G}(\mathscr{I}_n, U_n^k). \tag{1.95}$$

$$\text{Update the interface term:} \quad \boldsymbol{\xi}_n^{k+1,0} = \boldsymbol{\xi}_n^{k,L}. \tag{1.96}$$

   end for

1.8.6   Convergence factor of the Parareal-OSWR method

The theoretical results below are based on Theorem 1.19, and thus we suppose that the number of iterations L of the OSWR method is even, with $L \geq 2$. However, these results can be extended to the more general case of any integer $L \geq 1$, by using Remark 1.20.

As in Section 1.5, we need the following notation.

Notation for error estimation

Let u be the solution of problem (1.1), and $(u_{1,n}^{k,\ell}, u_{2,n}^{k,\ell}, \boldsymbol{\xi}_n^{k,\ell})_{1\leq \ell \leq L}$ be the sequence of iterates through the OSWR step (1.93). We define, for $k = 0, 1, \ldots$, and $n = 0, \ldots, N-1$:

- $E_n^k := U_n^k - u_n$, $n = 0, \ldots, N$, where $u_n = u(., T_n)$,

- $e_{i,n}^{k,\ell} := u_{i,n}^{k,\ell} - u|_{\Omega_i}$, the error in $H^{2,1}(\Omega_i \times (0,T))$ at each iteration ℓ inside step (1.93), $i = 1, 2$, for $\ell = 1, \ldots, L$,

- $\boldsymbol{\zeta}_n^{k,\ell} := \boldsymbol{\xi}_n^{k,\ell} - \boldsymbol{\xi}_n$, for $\ell = 1, \ldots, L$, where $\boldsymbol{\xi}_n = ((\mathscr{B}_1 u)(\delta_1, T_n), (\mathscr{B}_2 u)(\delta_2, T_n))$.

Then, by linearity, the algorithm on the error reads

Algorithm 7 (Coupled Parareal-OSWR algorithm on the error, with overlap)

---

1. Define initial data $(E_n^0)_{n \in [\![0,N]\!]}$ with $E_0^0 = 0$, $E_n^0 := \mathscr{G}(\mathscr{I}_{n-1}, U_{n-1}^0) - u_n$, $n = 1, 2, \dots, N$.
2. Define initial Robin data $(\zeta_n^{0,0})_{n \in [\![0,N]\!]}$, with $\zeta_n^{0,0} := (\zeta_{1,n}^{0,0}, \zeta_{2,n}^{0,0})$ on $\mathscr{I}_n$, where $\zeta_{i,n}^{0,0} = (\mathscr{B}_i E_n^0)(\delta_i, \cdot)$, $i = 1, 2$.

for $k = 0, 1, \dots$ *(Parareal iterations)*

   1. On each time interval $\mathscr{I}_n$, $n = 0, 1, \dots, N-1$:

$$\text{Calculate} \quad (e_{1,n}^{k,L}, e_{2,n}^{k,L}, \zeta_n^{k,L}) = \text{OSWR}_L(\mathscr{I}_n, E_n^k, \zeta_n^{k,0}). \tag{1.97}$$

   2. Perform the correction on $e_n^{k,L}$:

$$\check{e}_n^{k,L} = \mathscr{C}(e_{1,n}^{k,L}(., T_{n+1}), e_{2,n}^{k,L}(., T_{n+1})). \tag{1.98}$$

   3. Set $E_0^{k+1} = 0$ and do Parareal correction:

$$E_{n+1}^{k+1} = \check{e}_n^{k,L} + \widetilde{\mathscr{G}}(\mathscr{I}_n, E_n^{k+1} - E_n^k). \tag{1.99}$$

$$\text{Update the interface term:} \quad \zeta_n^{k+1,0} = \zeta_n^{k,L}. \tag{1.100}$$

  end for

We recall the definition

$$\check{\rho} = \sqrt{\rho}, \tag{1.101}$$

where ρ is defined by (1.82).

Convergence factor

As in Section 1.2, we set $\mathbf{E}^k := \left(\|E_1^k\|_{H^1(\Omega)}, \|E_2^k\|_{H^1(\Omega)}, \dots, \|E_N^k\|_{H^1(\Omega)} \right)^t$, and also denote $\mathscr{Y}_n = H^{\frac{1}{4}}(\mathscr{I}_n)$, $n \in [\![0, N-1]\!]$, and $\zeta^k := \left(\|\zeta_0^{k,0}\|_{\mathscr{Y}_0^2}, \|\zeta_1^{k,0}\|_{\mathscr{Y}_1^2}, \dots, \|\zeta_{N-1}^{k,0}\|_{\mathscr{Y}_{N-1}^2} \right)^t$. We will use the following element-wise notation, for $\mathbf{U}, \mathbf{V} \in \mathscr{R}^N$:

$$\mathbf{U} \leq \mathbf{V} \iff U_n \leq V_n, \ \forall n \in [\![1, N]\!],$$

$$\mathbf{W} := \max(\mathbf{U}, \mathbf{V}) \iff \mathbf{W} \in \mathscr{R}^N \text{ and } W_n = \max(U_n, V_n), \ \forall n \in [\![1, N]\!].$$

We suppose that $\widetilde{\mathscr{G}}$ is an operator on $H^1(\Omega)$ that verifies (1.45), and consider $\mathbf{M}$ defined by (see [56])

$$\mathbf{M}_{ij} = \begin{cases} \gamma_1^{i-1-j} & \text{if } j < i \\ 0 & \text{if } j \geq i \end{cases}, \qquad 1 \leq i, j \leq N.$$

Then we can prove Lemma 1.21, from which we get Theorem 1.22 and the upper estimate for the error of the Parareal-OSWR method in Corollary 1.23.

Lemma 1.21. *Let $\widetilde{\mathscr{G}}$ verify (1.45), and $\check{\rho}$ be defined by (1.101). There exist constants C_1 and C_2 such that*

$$\mathbf{E}^{k+1} \leq (\gamma_1 + C_2)\mathbf{M}\mathbf{E}^k + C_1 C_2 \check{\rho}^{-1}(\mathbf{I} + \gamma_1 \mathbf{M})\mathbf{M} \sum_{i=1}^k \check{\rho}^{iL} \mathbf{E}^{k-i} + C_2 \check{\rho}^{-1}(\mathbf{I} + \gamma_1 \mathbf{M})\check{\rho}^{(k+1)L} \zeta^0.$$

$$\tag{1.102}$$

Theorem 1.22. *Let $\breve{\rho}$ be defined by* (1.101). *We set*

$$\gamma := \max\left(C_1 C_2 \breve{\rho}^{-1}, \frac{\gamma_1 + C_2 + \sqrt{(\gamma_1 + C_2)^2 + 4\gamma_1 C_1 C_2 \breve{\rho}^{-1} \tilde{\rho}}}{2}\right), \qquad (1.103)$$

and

$$\mathbf{C}_0 := \max\left(\mathbf{E}^0, \frac{\gamma}{C_1} \zeta^0\right), \qquad (1.104)$$

with C_1, C_2 from (1.102), *and $\tilde{\rho} := \breve{\rho}^L$. Let $\mathbf{I}$ be the identity matrix in $\mathscr{R}^N$. Then*

$$\mathbf{E}^k \leq (\gamma \mathbf{M} + \tilde{\rho} \mathbf{I})^k \mathbf{C}_0, \qquad (1.105)$$

with $\tilde{\rho} < 1$.

Corollary 1.23. *Denote by $C = \|\mathbf{C}_0\|_\infty$ and $m := \max\limits_{1 \leq i \leq N-1} \|\mathbf{M}^i\|_\infty$, we have*

$$\max_{1 \leq n \leq N} \|E_n^k\|_{H^1(\Omega)} \leq Cm \max(1, \gamma^{N-1}) \sum_{i=0}^{\min(k, N-1)} \binom{k}{i} \tilde{\rho}^{k-i}, \qquad (1.106)$$

and consequently $\|E_n^k\|_{H^1(\Omega)}$ tends to 0 when k tends to infinity.

Proof of Lemma 1.21. From (1.99) the error verifies

$$\|E_{n+1}^{k+1}\|_{H^1(\Omega)} \leq \|\widetilde{\mathscr{G}}(\mathscr{I}_n, E_n^{k+1} - E_n^k)\|_{H^1(\Omega)} + \|\breve{e}_n^{k,L}\|_{H^1(\Omega)}. \qquad (1.107)$$

Here $\breve{e}_n^{k,L}$ is the error, with correction, at Pararéal iteration k and iteration L of the OSWR algorithm on $\mathscr{I} := \mathscr{I}_n$, with initial condition $E_n^k \in H^1(\Omega)$, initial Robin conditions $\zeta_n^{k,0}$. Let $L \geq 1$, then we apply (1.70) and (1.71) with $2\ell = L$, $u_i^{2\ell} := e_{i,n}^{k,L}$, $\boldsymbol{\xi}^{2\ell} := \zeta_n^{k,L}$. After that, we use the inequality on the norm of the correction (1.92) with $u_i = e_{i,n}^{k,L}(\cdot, T_{n+1})$ and $\breve{u} = \breve{e}_n^{k,L}$.

We obtain

$$\|\zeta_n^{k,L}\|_{\mathscr{Y}_n^2} \leq \breve{\rho}^L \|\zeta_n^{k,0}\|_{\mathscr{Y}_n^2} + C_1 \|E_n^k\|_{H^1(\Omega)}, \qquad (1.108)$$

$$\|\breve{e}_n^{k,L}\|_{H^1(\Omega)} \leq C_2 (\breve{\rho}^{L-1} \|\zeta_n^{k,0}\|_{\mathscr{Y}_n^2} + \|E_n^k\|_{H^1(\Omega)}). \qquad (1.109)$$

Using now condition (1.45) on $\widetilde{\mathscr{G}}$ and (1.109) in (1.107), we get

$$\|E_{n+1}^{k+1}\|_{H^1(\Omega)} \leq \gamma_1 \|E_n^{k+1} - E_n^k\|_{H^1(\Omega)} + C_2 (\breve{\rho}^{L-1} \|\zeta_n^{k,0}\|_{\mathscr{Y}_n^2} + \|E_n^k\|_{H^1(\Omega)}),$$

which implies, using the triangle inequality,

$$\|E_{n+1}^{k+1}\|_{H^1(\Omega)} \leq \gamma_1 \|E_n^{k+1}\|_{H^1(\Omega)} + (\gamma_1 + C_2) \|E_n^k\|_{H^1(\Omega)} + C_2 \breve{\rho}^{L-1} \|\zeta_n^{k,0}\|_{\mathscr{Y}_n^2}. \qquad (1.110)$$

From this we obtain, for $p = 0, 1, ..., n$, by induction on p,

$$\|E_{n+1}^{k+1}\|_{H^1(\Omega)} \leq \gamma_1^{p+1} \|E_{n-p}^{k+1}\|_{H^1(\Omega)} + (\gamma_1 + C_2) \sum_{i=0}^{p} \gamma_1^i \|E_{n-i}^k\|_{H^1(\Omega)} + C_2 \breve{\rho}^{L-1} \sum_{i=0}^{p} \gamma_1^i \|\zeta_{n-i}^{k,0}\|_{\mathscr{Y}_{n-i}^2}.$$

Using the above inequality with $p = n$, together with $\|E_0^{k+1}\|_{H^1(\Omega)} = 0$, we get, for $n = 0, 1, ..., N-1$:

$$\|E_{n+1}^{k+1}\|_{H^1(\Omega)} \leq (\gamma_1 + C_2) \sum_{i=0}^{n} \gamma_1^i \|E_{n-i}^k\|_{H^1(\Omega)} + C_2 \breve{\rho}^{L-1} \sum_{i=0}^{n} \gamma_1^i \|\zeta_{n-i}^{k,0}\|_{\mathscr{Y}_{n-i}^2},$$

or equivalently, in matrix form (using again the fact that $\|E_0^k\|_{H^1(\Omega)} = 0$),

$$\mathbf{E}^{k+1} \le (\gamma_1 + C_2)\mathbf{M}\mathbf{E}^k + C_2 \breve{\rho}^{L-1}(\mathbf{I} + \gamma_1 \mathbf{M})\boldsymbol{\zeta}^k. \tag{1.111}$$

Moreover, from (1.100) we have $\boldsymbol{\zeta}_n^{k,L} = \boldsymbol{\zeta}_n^{k+1,0}$, and thus (1.108) also reads

$$\|\boldsymbol{\zeta}_n^{k+1,0}\|_{\mathscr{Y}_n^2} \le \breve{\rho}^L \|\boldsymbol{\zeta}_n^{k,0}\|_{\mathscr{Y}_n^2} + C_1 \|E_n^k\|_{H^1(\Omega)}, \tag{1.112}$$

which implies

$$\|\boldsymbol{\zeta}_n^{k+1,0}\|_{\mathscr{Y}_n^2} \le \breve{\rho}^L \|\boldsymbol{\zeta}_n^{k,0}\|_{\mathscr{Y}_n^2} + C_1 \|E_n^k\|_{H^1(\Omega)} + C_1\gamma_1 \|E_{n-1}^k\|_{H^1(\Omega)} + \cdots + C_1 \gamma_1^{n-1} \|E_1^k\|_{H^1(\Omega)}$$

or equivalently, in matrix form,

$$\boldsymbol{\zeta}^{k+1} \le \breve{\rho}^L \boldsymbol{\zeta}^k + C_1 \mathbf{M}\mathbf{E}^k. \tag{1.113}$$

Inserting (1.113) in (1.111) we obtain, for $p = 0, \dots, k$, by induction on p,

$$\mathbf{E}^{k+1} \le (\gamma_1 + C_2)\mathbf{M}\mathbf{E}^k + C_1 C_2 \breve{\rho}^{-1}(\mathbf{I} + \gamma_1 \mathbf{M})\mathbf{M}\sum_{i=1}^{p} \breve{\rho}^{iL} \mathbf{E}^{k-i} + C_2 \breve{\rho}^{-1}(\mathbf{I} + \gamma_1 \mathbf{M})\breve{\rho}^{(p+1)L}\boldsymbol{\zeta}^{k-p}.$$

In particular, for $p = k$ we get (1.102). $\qquad\qquad\qquad\qquad\qquad\qquad\square$

Proof of Theorem 1.22. The proof is done by induction on k:

• For $k = 0$, by definition of $\mathbf{C}_0$, we have $\mathbf{E}^0 \le \mathbf{C}_0$, thus (1.105) holds for $k = 0$.

• For $k \ge 0$, we suppose that (1.105) holds up to k, and we show that it holds for $k + 1$: from (1.102) we have

$$\mathbf{E}^{k+1} \le (\gamma_1 + C_2)\mathbf{M}\mathbf{E}^k + C_1 C_2 \breve{\rho}^{-1}(\mathbf{I} + \gamma_1 \mathbf{M})\mathbf{M}\sum_{i=1}^{k} \breve{\rho}^{iL} \mathbf{E}^{k-i} + C_2 \breve{\rho}^{-1}(\mathbf{I} + \gamma_1 \mathbf{M})\breve{\rho}^{(k+1)L}\boldsymbol{\zeta}^0.$$

Using the induction hypothesis in the above inequality and $\tilde{\rho} = \breve{\rho}^L$, we obtain

$$\mathbf{E}^{k+1} \le (\gamma_1 + C_2)\mathbf{M}\big((\gamma\mathbf{M} + \tilde{\rho}\mathbf{I})^k \mathbf{C}_0\big)$$
$$+ C_1 C_2 \breve{\rho}^{-1}(\mathbf{I} + \gamma_1 \mathbf{M})\mathbf{M}\sum_{i=1}^{k} \tilde{\rho}^i \big((\gamma\mathbf{M} + \tilde{\rho}\mathbf{I})^{k-i} \mathbf{C}_0\big) + C_2 \breve{\rho}^{-1}(\mathbf{I} + \gamma_1 \mathbf{M})\tilde{\rho}^{k+1}\boldsymbol{\zeta}^0. \tag{1.114}$$

Moreover, we have

$$\gamma\mathbf{M}\sum_{i=1}^{k} \tilde{\rho}^{i-1}(\gamma\mathbf{M} + \tilde{\rho}\mathbf{I})^{k-i} = ((\gamma\mathbf{M} + \tilde{\rho}\mathbf{I}) - \tilde{\rho}\mathbf{I})\sum_{i=1}^{k} \tilde{\rho}^{i-1}(\gamma\mathbf{M} + \tilde{\rho}\mathbf{I})^{k-i}$$
$$= (\gamma\mathbf{M} + \tilde{\rho}\mathbf{I})^k - \tilde{\rho}^k\mathbf{I}. \tag{1.115}$$

Inserting (1.115) in (1.114) we get

$$\mathbf{E}^{k+1} \le (\gamma_1 + C_2)\mathbf{M}\big((\gamma\mathbf{M} + \tilde{\rho}\mathbf{I})^k \mathbf{C}_0\big)$$
$$+ \frac{C_1 C_2 \breve{\rho}^{-1}}{\gamma}(\mathbf{I} + \gamma_1 \mathbf{M})\tilde{\rho}\big((\gamma\mathbf{M} + \tilde{\rho}\mathbf{I})^k - \tilde{\rho}^k\mathbf{I}\big)\mathbf{C}_0 + C_2 \breve{\rho}^{-1}(\mathbf{I} + \gamma_1 \mathbf{M})\tilde{\rho}^{k+1}\boldsymbol{\zeta}^0,$$

or, equivalently,

$$
\mathbf{E}^{k+1} \leq \Big((\gamma_1 + C_2)\mathbf{M} + \frac{C_1 C_2 \check{\rho}^{-1}}{\gamma}(\mathbf{I} + \gamma_1 \mathbf{M})\tilde{\rho} \Big)(\gamma \mathbf{M} + \tilde{\rho}\mathbf{I})^k \mathbf{C}_0
$$
$$
+ C_2 \check{\rho}^{-1}(\mathbf{I} + \gamma_1 \mathbf{M})\tilde{\rho}^{k+1}\Big(\boldsymbol{\zeta}^0 - \frac{C_1}{\gamma}\mathbf{C}_0 \Big).
$$

By definition of $\mathbf{C}_0$ in (1.104) we have $\boldsymbol{\zeta}^0 - \dfrac{C_1}{\gamma}\mathbf{C}_0 \leq 0$. Thus we obtain

$$
\mathbf{E}^{k+1} \leq \Big((\gamma_1 + C_2)\mathbf{M} + \frac{C_1 C_2 \check{\rho}^{-1}}{\gamma}(\mathbf{I} + \gamma_1 \mathbf{M})\tilde{\rho} \Big)(\gamma \mathbf{M} + \tilde{\rho}\mathbf{I})^k \mathbf{C}_0,
$$

or equivalently,

$$
\mathbf{E}^{k+1} \leq \Big(\big(\gamma_1 + C_2 + \gamma_1 \frac{C_1 C_2 \check{\rho}^{-1}}{\gamma}\tilde{\rho}\big)\mathbf{M} + \frac{C_1 C_2 \check{\rho}^{-1}}{\gamma}\tilde{\rho}\mathbf{I} \Big)(\gamma \mathbf{M} + \tilde{\rho}\mathbf{I})^k \mathbf{C}_0.
$$

The definition of γ in (1.103) implies $\dfrac{C_1 C_2 \check{\rho}^{-1}}{\gamma} \leq 1$ and $\gamma_1 + C_2 + \gamma_1 \dfrac{C_1 C_2 \check{\rho}^{-1}}{\gamma}\tilde{\rho} \leq \gamma$, thus

$$
\mathbf{E}^{k+1} \leq (\gamma \mathbf{M} + \tilde{\rho}\mathbf{I})(\gamma \mathbf{M} + \tilde{\rho}\mathbf{I})^k \mathbf{C}_0,
$$

which gives (1.105) at step $k + 1$, and ends the proof of Theorem 1.22. $\qquad\square$

Proof of corollary 1.23. From (1.105) we have

$$
\mathbf{E}^k \leq \sum_{i=0}^{k} \binom{k}{i} \tilde{\rho}^{k-i} \gamma^i \mathbf{M}^i \mathbf{C}_0.
$$

Using that $\mathbf{M}^i = \mathbf{0}$ for $i \geq N$, the above inequality also reads

$$
\mathbf{E}^k \leq \sum_{i=0}^{\min(k,N-1)} \binom{k}{i} \tilde{\rho}^{k-i} \gamma^i \mathbf{M}^i \mathbf{C}_0.
$$

Setting $C = \|\mathbf{C}_0\|_\infty$, we obtain

$$
\max_{1 \leq n \leq N} \|E_n^k\|_{H^1(\Omega)} \leq C \sum_{i=0}^{\min(k,N-1)} \binom{k}{i} \tilde{\rho}^{k-i} \gamma^i \|\mathbf{M}^i\|_\infty. \tag{1.116}
$$

Then with $m = \max\limits_{1 \leq i \leq N-1} \|\mathbf{M}^i\|_\infty$ (note that m doesn't depend on k) we get

$$
\max_{1 \leq n \leq N} \|E_n^k\|_{H^1(\Omega)} \leq Cm \sum_{i=0}^{\min(k,N-1)} \binom{k}{i} \tilde{\rho}^{k-i} \gamma^i,
$$

from which we obtain (1.106). Using that $0 \leq i \leq N-1$, the term $\dbinom{k}{i}$ is a polynomial in k of degree less than or equal to $N-1$. Hence $\|E_n^k\|_{H^1(\Omega)}$ tends to 0 when k tends to infinity since $\tilde{\rho} < 1$. $\qquad\square$

1.8.7 From the operator view point

In this part we will try to write the algorithm using the operators between functional spaces. We then try to establish the same results as in [54].

For the error analysis, as the source term f is 0, and from the linearity, the spaces $\mathcal{Y}_n = H^{\frac{1}{4}}(T_n, T_{n+1})$ can be considered as $\mathcal{Y}_0 = H^{\frac{1}{4}}(0, \Delta T)$.

We define the following operators

$$\mathcal{G} : \mathcal{X} \to \mathcal{X}$$
$$U \mapsto \mathcal{G}(U) = u,$$

where u is the solution of the following problem

$$\frac{u - U}{\Delta T} - \nu \partial_{xx} u + a \partial_x u + bu = 0 \text{ in } \Omega$$

with homogeneous Dirichlet boundary conditions.

Let $\boldsymbol{\xi} = (\xi_1, \xi_2) \in (\mathcal{Y}_0)^2$. We recall the OSWR method with vanishing source terms using L iterations: let $(\xi_1^0, \xi_2^0) = (\xi_1, \xi_2)$, we solve, for $\ell = 1, \dots, L$: for $i = 1, 2$,

$$\begin{aligned}
\mathcal{L}(u_i^\ell) &= 0 && \text{in} && \Omega_i \times (0, \Delta T), \\
u_i^\ell(\cdot, 0) &= u_0|_{\Omega_i} && \text{in} && \Omega_i, \\
\mathcal{B}_i u_i^\ell(\delta_i, \cdot) &= \xi_i^{\ell-1} && \text{on} && (0, \Delta T),
\end{aligned}$$

with the update of the Robin data on $(0, \Delta T)$

$$\xi_i^\ell = \mathcal{B}_i u_{3-i}^\ell(\delta_i, \cdot).$$

From this we can define the incomplete fine solver operator

$$OSWR_L : \mathcal{X} \times (\mathcal{Y}_0)^2 \to \mathcal{X} \times (\mathcal{Y}_0)^2$$

that maps $(u_0, \boldsymbol{\xi})$ to $(\check{u}^L, \boldsymbol{\xi}^L)$, where $\check{u}^L = \mathcal{C}(u_1^L(., \Delta T), u_2^L(., \Delta T))$ ($\mathcal{C}$ is the correction defined in subsection 1.8.5), $\boldsymbol{\xi}^L = (\xi_1^L, \xi_2^L)$. We observe that $OSWR_L(u_0, \boldsymbol{\xi}) = OSWR_L(0, \boldsymbol{\xi}) + OSWR_L(u_0, 0)$. Here, on the right-hand side, we have four parts, the most important part here is the second component of $OSWR_L(0, \boldsymbol{\xi})$, which can be expressed as $\mathcal{Q}^L \boldsymbol{\xi}$

$$\mathcal{Q} : (\mathcal{Y}_0)^2 \to (\mathcal{Y}_0)^2, \mathcal{Q}(\zeta_1, \zeta_2) = (\mathcal{B}_1(u_2)(\delta_1), \mathcal{B}_2(u_1)(\delta_2))$$

and (u_i) is the solution of

$$\begin{aligned}
\mathcal{L}(u_i) &= 0 && \text{in} && \Omega_i \times (0, \Delta T), \\
u_i(\cdot, 0) &= 0 && \text{in} && \Omega_i, \\
\mathcal{B}_i u_i(\delta_i, \cdot) &= \zeta_i && \text{on} && (0, \Delta T).
\end{aligned}$$

In other words, $\mathcal{Q}$ is the output of one OSWR iteration, with zero initial condition and source term. It was shown before from Theorem 1.19 that $(\mathcal{Q}^k)$ tends to zero with convergence factor $\check{\rho}$.

We define also the output at final time

$$\mathcal{S}(\boldsymbol{\zeta}) = \mathcal{C}\big(u_1(\cdot, \Delta T), u_2(\cdot, \Delta T)\big)$$

Then, the first component of $OSWR_L(0, \boldsymbol{\xi})$ is $\mathcal{S}(\boldsymbol{\xi}^{L-1})$, with $\boldsymbol{\xi}^{L-1} = \mathcal{Q}^{L-1}(\boldsymbol{\xi})$.

Remark 1.24. *The arguments that follow remain valid also for the non-overlapping case, in which we do not have a convergence factor $\check{\rho} < 1$. In that case, the space $\mathscr{X}$ should be replaced by $L^2(\Omega)$, there is no correction then, and $\mathscr{S}$ is only to glue two subdomain solutions. The space of Robin terms $\mathscr{Y}$ is then replaced by $L^2(0,T)$ (not $H^{\frac{1}{4}}(0,T)$), and the sequence $\mathscr{S}\mathscr{Q}^k$ still converges to zero via an energy estimate (see Section 1.3).*

We then define the operator

$$\mathscr{P}_s : \mathscr{X} \to \mathscr{X}, \quad \mathscr{P} : \mathscr{X} \to (\mathscr{Y}_0)^2$$

which are the first and second components of $OSWR_L(u_0,0)$ respectively. We now recall briefly the incomplete fine solver on the error: provided E_n^k and $\zeta_n^{k,0}$, one solves, for $\ell = 1,2,\ldots,L$

$$
\begin{aligned}
\mathscr{L}(e_{i,n}^{k,\ell}) &= 0 && \text{in} && \Omega_i \times (0,\Delta T), \\
e_{i,n}^{k,\ell}(\cdot,0) &= E_n^k|_{\Omega_i} && \text{in} && \Omega_i, \\
\mathscr{B}_i e_{i,n}^{k,\ell}(\delta_i,\cdot) &= \zeta_{i,n}^{k,\ell-1} && \text{on} && (0,\Delta T),
\end{aligned}
$$

with

$$\zeta_{i,n}^{k,\ell} = \mathscr{B}_i e_{3-i,n}^{k,\ell}(\delta_i,\cdot), \quad \text{on } (0,\Delta T).$$

and then we define $\check{e}_n^{k,L} = \mathscr{C}(e_{i,n}^{k,L}(.,\Delta T),e_{i,n}^{k,L}(.,\Delta T))$.

Equivalently, we have

$$\left(\check{e}_n^{k,L},\zeta_n^{k,L}\right) = OSWR_L(E_n^k,\zeta_n^{k,0})$$

We can write each component as

$$
\begin{aligned}
\check{e}_n^{k,L} &= \mathscr{P}_s(E_n^k) + \mathscr{S}\mathscr{Q}^{L-1}(\zeta_n^{k,0}), \\
(\zeta_n^{k,L}) &= \mathscr{P}(E_n^k) + \mathscr{Q}^L(\zeta_n^{k,0}).
\end{aligned}
$$

Therefore we can rewrite the error formulation of the coupled Parareal-OSWR method with all the above operators, as follows :

$$E_{n+1}^{k+1} = \mathscr{G}(\mathscr{I}_n,E_n^{k+1}) - \mathscr{G}(\mathscr{I}_n,E_n^k) + \mathscr{P}_s(E_n^k) + \mathscr{S}\mathscr{Q}^{L-1}(\zeta_n^{k,0}).$$

We can simplify the above equality by using the notations $\mathscr{G}(\mathscr{I}_n,E_n^{k+1}) = \mathscr{G}(E_n^{k+1})$ and $\mathscr{R}(E_n^k) = \mathscr{P}_s(E_n^k) - \mathscr{G}(\mathscr{I}_n,E_n^k)$. Then, the error expression becomes

$$E_{n+1}^{k+1} = \mathscr{G}(E_n^{k+1}) + \mathscr{R}(E_n^k) + \mathscr{S}\mathscr{Q}^{L-1}(\zeta_n^{k,0}). \tag{1.117}$$

Moreover, from the update formulation of the Robin terms, we have

$$\zeta_n^{k+1,0} = \mathscr{P}(E_n^k) + \mathscr{Q}^L(\zeta_n^{k,0}), \tag{1.118}$$

from which one gets

$$\mathscr{Q}^L(\zeta_n^{k,0}) = \mathscr{Q}^L\mathscr{P}(E_n^{k-1}) + \mathscr{Q}^{2L}(\zeta_n^{k-1,0}),$$

$$\vdots$$

$$\mathscr{Q}^{kL}(\zeta_n^{1,0}) = \mathscr{Q}^{kL}\mathscr{P}(E_n^0) + \mathscr{Q}^{(k+1)L}(\zeta_n^{0,0}).$$

Then, summing the above expressions, we get a telescopic sum, and therefore

$$\mathscr{Q}^L(\zeta_n^{k,0}) = \sum_{i=1}^k \mathscr{Q}^{iL}\mathscr{P}(E_n^{k-i}) + \mathscr{Q}^{(k+1)L}(\zeta_n^{0,0}),$$

from which we obtain, using (1.118),

$$\zeta_n^{k+1,0} = \sum_{i=0}^k \mathscr{Q}^{(k-i)L}\mathscr{P}(E_n^i) + \mathscr{Q}^{(k+1)L}(\zeta_n^{0,0}).$$

Replacing this term in the error expression (1.117), we obtain

$$E_{n+1}^{k+1} = \mathscr{G}(E_n^{k+1}) + \mathscr{R}(E_n^k) + \sum_{i=0}^{k-1}\mathscr{S}\mathscr{Q}^{(k-i)L-1}\mathscr{P}(E_n^i) + \mathscr{S}\mathscr{Q}^{(k+1)L-1}(\zeta_n^{0,0}).$$

From this, we use the same trick as in the analysis of the Parareal method :

$$\mathscr{G}(E_n^{k+1}) = \mathscr{G}^2(E_{n-1}^{k+1}) + \mathscr{G}\mathscr{R}(E_{n-1}^k) + \mathscr{G}\sum_{i=0}^{k-1}\mathscr{S}\mathscr{Q}^{(k-i)L-1}\mathscr{P}(E_{n-1}^i) + \mathscr{G}\mathscr{S}\mathscr{Q}^{(k+1)L-1}(\zeta_{n-1}^{0,0})$$

$$\vdots$$

$$\mathscr{G}^n(E_1^{k+1}) = \mathscr{G}^{n+1}(E_0^{k+1}) + \mathscr{G}^n\mathscr{R}(E_0^k) + \mathscr{G}^n\sum_{i=0}^{k-1}\mathscr{S}\mathscr{Q}^{(k-i)L-1}\mathscr{P}(E_0^i) + \mathscr{G}^n\mathscr{S}\mathscr{Q}^{(k+1)L-1}(\zeta_0^{0,0})$$

$$= \mathscr{G}^n\mathscr{S}\mathscr{Q}^{(k+1)L-1}(\zeta_0^{0,0})$$

We obtains then by taking the telescopic sum

$$E_{n+1}^{k+1} = \sum_{q=1}^n \mathscr{G}^{n-q}\mathscr{R}(E_q^k) + \sum_{i=0}^{k-1}\sum_{q=1}^n \mathscr{G}^{n-q}\mathscr{S}\mathscr{Q}^{(k-i)L-1}\mathscr{P}(E_q^i) + \sum_{q=0}^n \mathscr{G}^{n-q}\mathscr{S}\mathscr{Q}^{(k+1)L-1}(\zeta_q^{0,0}).$$

$$(1.119)$$

We recall the error vector $\mathbf{E}^k = (E_1^k, E_2^k, \ldots, E_N^k)^t$ and the operator matrix of Parareal $\mathbf{M} : \mathscr{X}^N \to \mathscr{X}^N$

$$\mathbf{M} = \begin{pmatrix} 0 & 0 & 0 & 0 & \cdots & 0 & 0 \\ \mathrm{Id}_{\mathscr{X}} & 0 & 0 & 0 & \cdots & 0 & 0 \\ \mathscr{G} & \mathrm{Id}_{\mathscr{X}} & 0 & 0 & \cdots & 0 & 0 \\ \mathscr{G}^2 & \mathscr{G} & \mathrm{Id}_{\mathscr{X}} & 0 & \cdots & 0 & 0 \\ \vdots & \vdots & \vdots & \vdots & \ddots & \vdots & \\ \mathscr{G}^{N-3} & \mathscr{G}^{N-4} & \mathscr{G}^{N-5} & \mathscr{G}^{N-6} & \cdots & 0 & 0 \\ \mathscr{G}^{N-2} & \mathscr{G}^{N-3} & \mathscr{G}^{N-4} & \mathscr{G}^{N-5} & \cdots & \mathrm{Id}_{\mathscr{X}} & 0 \end{pmatrix}$$

We define also

$$\overline{\mathbf{M}} = \begin{pmatrix} \mathrm{Id}_{\mathscr{X}} & 0 & 0 & 0 & \cdots & 0 & 0 \\ \mathscr{G} & \mathrm{Id}_{\mathscr{X}} & 0 & 0 & \cdots & 0 & 0 \\ \mathscr{G}^2 & \mathscr{G} & \mathrm{Id}_{\mathscr{X}} & 0 & \cdots & 0 & 0 \\ \mathscr{G}^3 & \mathscr{G}^2 & \mathscr{G} & \mathrm{Id}_{\mathscr{X}} & \cdots & 0 & 0 \\ \vdots & \vdots & \vdots & \vdots & \ddots & \vdots & \\ \mathscr{G}^{N-2} & \mathscr{G}^{N-3} & \mathscr{G}^{N-4} & \mathscr{G}^{N-5} & \cdots & \mathrm{Id}_{\mathscr{X}} & 0 \\ \mathscr{G}^{N-1} & \mathscr{G}^{N-2} & \mathscr{G}^{N-3} & \mathscr{G}^{N-4} & \cdots & \mathscr{G} & \mathrm{Id}_{\mathscr{X}} \end{pmatrix}$$

Similarly, we define $\mathbf{R} : \mathcal{X}^N \to \mathcal{X}^N$, $\mathbf{S} \, ((\mathcal{Y}_0)^2)^N \to \mathcal{X}^N$

$$
\mathbf{R} = \begin{pmatrix} \mathcal{R} & 0 & 0 & \dots & 0 \\ 0 & \mathcal{R} & 0 & \dots & 0 \\ 0 & 0 & \mathcal{R} & \dots & 0 \\ \vdots & \vdots & \vdots & \ddots & \vdots \\ 0 & 0 & 0 & \dots & \mathcal{R} \end{pmatrix} ; \quad \mathbf{S} = \begin{pmatrix} \mathcal{S} & 0 & 0 & \dots & 0 \\ 0 & \mathcal{S} & 0 & \dots & 0 \\ 0 & 0 & \mathcal{S} & \dots & 0 \\ \vdots & \vdots & \vdots & \ddots & \vdots \\ 0 & 0 & 0 & \dots & \mathcal{S} \end{pmatrix} ;
$$

and $\mathbf{P} : \mathcal{X}^N \to (\mathcal{Y}_0^2)^N$, $\mathbf{Q} : (\mathcal{Y}_0^2)^N \to (\mathcal{Y}_0^2)^N$

$$
\mathbf{P} = \begin{pmatrix} \mathcal{P} & 0 & 0 & \dots & 0 \\ 0 & \mathcal{P} & 0 & \dots & 0 \\ 0 & 0 & \mathcal{P} & \dots & 0 \\ \vdots & \vdots & \vdots & \ddots & \vdots \\ 0 & 0 & 0 & \dots & \mathcal{P} \end{pmatrix} ; \quad \mathbf{Q} = \begin{pmatrix} \mathcal{Q} & 0 & 0 & \dots & 0 \\ 0 & \mathcal{Q} & 0 & \dots & 0 \\ 0 & 0 & \mathcal{Q} & \dots & 0 \\ \vdots & \vdots & \vdots & \ddots & \vdots \\ 0 & 0 & 0 & \dots & \mathcal{Q} \end{pmatrix} ;
$$

Then, from (1.119) the error in vector and operator form can be rewritten as

$$
\mathbf{E}^{k+1} = \mathbf{M} \mathbf{R} \mathbf{E}^k + \mathbf{M} \mathbf{S} \left[\sum_{i=0}^{k-1} \mathbf{Q}^{(k-i)L-1} \mathbf{P} \mathbf{E}^i \right] + \overline{\mathbf{M}} \mathbf{S} \mathbf{Q}^{(k+1)L-1} \mathbf{B}^0, \tag{1.120}
$$

with $\mathbf{B}^0 = (\boldsymbol{\zeta}_0^{0,0}, \boldsymbol{\zeta}_1^{0,0}, \dots, \boldsymbol{\zeta}_{N-1}^{0,0})$.
We have the following lemma

Lemma 1.25. *The error at iteration $k + 1$ for $k \geq 0$ can be expressed as*

$$
\mathbf{E}^{k+1} = \mathbf{M} \mathbf{C}_{k+1} \mathbf{E}^0 + \mathbf{M} \mathbf{D}_{k+1} \mathbf{B}^0 + \overline{\mathbf{M}} \mathbf{S} \mathbf{Q}^{(k+1)L-1} \mathbf{B}^0, \tag{1.121}
$$

with $\mathbf{C}_{k+1} : (\mathcal{X})^N \to (\mathcal{X})^N$, $\mathbf{D}_{k+1} : (\mathcal{Y}_0^2)^N \to (\mathcal{X})^N$ lower triangular matrices.

Proof. We prove equality (1.121) by induction on k.
For $k = 0$, we have

$$
\mathbf{E}^1 = \mathbf{M} \mathbf{R} \mathbf{E}^0 + \overline{\mathbf{M}} \mathbf{S} \mathbf{Q}^{L-1} \mathbf{B}^0.
$$

Then $\mathbf{C}_1 = \mathbf{R}$ and $\mathbf{D}_1 = 0$. The property is true for $k = 0$.
We suppose that the property is true for $1, 2, \dots, k$. We prove that it is true for $k + 1$.
Indeed, we have

$$
\mathbf{E}^{k+2} = \mathbf{M} \mathbf{R} \mathbf{E}^{k+1} + \mathbf{M} \mathbf{S} \left[\sum_{i=0}^{k} \mathbf{Q}^{(k+1-i)L-1} \mathbf{P} \mathbf{E}^i \right] + \overline{\mathbf{M}} \mathbf{S} \mathbf{Q}^{(k+2)L-1} \mathbf{B}^0.
$$

For $i \geq 1$, replacing $\mathbf{E}^i$ by the induction formulation, we get

$$
\begin{aligned}
\mathbf{E}^{k+2} = &\mathbf{M} \mathbf{R} \left[\mathbf{M} \mathbf{C}_{k+1} \mathbf{E}^0 + \mathbf{M} \mathbf{D}_{k+1} \mathbf{B}^0 + \overline{\mathbf{M}} \mathbf{S} \mathbf{Q}^{(k+1)L-1} \mathbf{B}^0 \right] \\
&+ \mathbf{M} \mathbf{S} \left[\sum_{i=1}^{k} \mathbf{Q}^{(k+1-i)L-1} \mathbf{P} \left[\mathbf{M} \mathbf{C}_i \mathbf{E}^0 + \mathbf{M} \mathbf{D}_i \mathbf{B}^0 + \overline{\mathbf{M}} \mathbf{S} \mathbf{Q}^{iL-1} \mathbf{B}^0 \right] \right] \\
&+ \mathbf{M} \mathbf{S} \mathbf{Q}^{(k+1)L-1} \mathbf{P} \mathbf{E}^0 + \overline{\mathbf{M}} \mathbf{S} \mathbf{Q}^{(k+2)L-1} \mathbf{B}^0.
\end{aligned}
$$

Therefore, we obtain

$$
\mathbf{C}_{k+2} = \mathbf{R} \mathbf{M} \mathbf{C}_{k+1} + \mathbf{S} \left[\sum_{i=1}^{k} \mathbf{Q}^{(k+1-i)L-1} \mathbf{P} \mathbf{M} \mathbf{C}_i \right] + \mathbf{S} \mathbf{Q}^{(k+1)L-1} \mathbf{P},
$$

$$\mathbf{D}_{k+2} = \mathbf{RMD}_{k+1} + \mathbf{R}\overline{\mathbf{M}}\mathbf{SQ}^{(k+1)L-1} + \mathbf{S}\sum_{i=1}^{k}\mathbf{Q}^{(k+1-i)L-1}\mathbf{P}\left[\mathbf{MD}_i + \overline{\mathbf{M}}\mathbf{SQ}^{iL-1}\right].$$

The matrices $\mathbf{C}_{k+2}$ and $\mathbf{D}_{k+2}$ are made from product and sum of lower triangular matrices, thus they are themselves lower triangular too. $\qquad\square$

To simplify the lemma, we assume that $\mathbf{B}^0$ is constructed from $\mathbf{E}^0$, that is there exists an operator $\mathscr{K} : \mathscr{X} \to (\mathscr{Y}_0)^2$ such that $\boldsymbol{\zeta}_n^{0,0} = \mathscr{K}(E_{n+1}^0)$. Denoting

$$\mathbf{K} = \begin{pmatrix} \mathscr{K} & 0 & 0 & \dots & 0 \\ 0 & \mathscr{K} & 0 & \dots & 0 \\ 0 & 0 & \mathscr{K} & \dots & 0 \\ \vdots & \vdots & \vdots & \ddots & \vdots \\ 0 & 0 & 0 & \dots & \mathscr{K} \end{pmatrix},$$

we get $\mathbf{B}^0 = \mathbf{KE}^0$. Then the expression in the lemma becomes

$$\mathbf{E}^{k+1} = \mathbf{MC}_{k+1}\mathbf{E}^0 + \mathbf{MD}_{k+1}\mathbf{KE}^0 + \overline{\mathbf{M}}\mathbf{SQ}^{(k+1)L-1}\mathbf{KE}^0.$$

Finally, setting $\mathbb{M}_k = \mathbf{MC}_k + \mathbf{MD}_k\mathbf{K} + \overline{\mathbf{M}}\mathbf{SQ}^{kL-1}\mathbf{K}$, we have $\mathbf{E}^k = \mathbb{M}_k\mathbf{E}^0$.
We obtain the following corollary

Corollary 1.26. $\mathbb{M}_k$ *is a lower triangular matrix, with the diagonal $\mathscr{S}\mathscr{Q}^{kL-1}\mathscr{K}$. Consequently, its spectral radius tends to zero at the same rate of $\check{\rho}^L$ - the convergence rate of the OSWR method.*

Proof. As $\mathbf{M}$ is strictly lower triangular, and C^k and D^k are lower triangular, then the matrix $(\mathbf{MC}_k + \mathbf{MD}_k\mathbf{K})$ is strictly lower triangular. Therefore, $\mathbb{M}_k$ is lower triangular, and its diagonal is the diagonal of $\overline{\mathbf{M}}\mathbf{SQ}^{kL-1}\mathbf{K}$, whose terms are all equal to $\mathscr{S}\mathscr{Q}^{kL-1}\mathscr{K}$. We then get that the spectral radius of $\mathbb{M}_k$ is also $\mathscr{S}\mathscr{Q}^{kL-1}\mathscr{K}$, which tends to zeros at the rate of $\mathscr{Q}^L$, i.e., $\check{\rho}^L$. $\qquad\square$

The rate of convergence of the spectral radius is quite nice and coincides with the rate of the OSWR method. However, as this spectral radius is not the norm of $\mathbb{M}_k$, the rate of convergence of this spectral radius is not the rate of convergence of the coupled algorithm. In the convergence analysis in the previous section, we showed that the error of the coupled method is bounded by $\check{\rho}^{kL}$ times a polynomial in k. In the numerical tests, one observes that this polynomial in k could affect a lot the practical convergence. In particular, for advection dominated test cases in subsection 1.6.2, it is shown that the convergence of the coupled method is singular, dominated by Parareal, and very different from the linear convergence of OSWR.

Chapter 2

Space-time domain decomposition for the incompressible Stokes problem

Several studies on spatial domain decomposition approaches have been carried out for the steady Navier-Stokes equations. These works concern various aspects of domain decomposition (DD) methods: DD as algebraic methods for the discrete matrix system (e.g. [19], [21], [20], [70], [103], [115], [75], [67], see also [101]) optimization-based DD (e.g. [60], [76], [42]); DD on vorticity equations with fourth order discretization ([106], [99], [100]); non-overlapping DD via a penalization on the interface, [28], [29]; DD for reduced order model ([112], [6]) and the Schwarz method.

Among those DD approaches, the Schwarz method interests us most. It can be done on both discrete ([58], [113], [87], see also [88] for Oseen) or continuous ([33], [16]) formulations and use Robin transmission conditions. On the other hand, when one considers applying this method on evolutionary problems, the equations have to be discretized in time first to get space problems at each time step before doing any domain decomposition. Hence, similar time-discretizations for all sub-domains are compulsory, which causes a limit on the adaptation of the method. To overcome this limit, we pay attention to the Waveform Relaxation technique for domain decomposition, which allows flexibility in time discretization on each sub-domain by exchanging data through a space-time interface. The corresponding method, called Schwarz Waveform Relaxation (SWR) Method, are wildly used and analyzed for advection reaction diffusion equation equation, as introduced in the previous chapter.

For the application of SWR on the Navier-Stokes equations, we are aware of the proceeding [34] and the PhD thesis [35] which treat the compressible Euler and Navier-Stokes equations and proposed an algorithm and various numerical experiments. However, until now, there exists no convergence analysis for the incompressible Navier-Stokes equations. We contribute to the understanding of the behavior of the method by attacking representative, though simpler, model problems. To begin with, we analyze the method on the evolutionary Stokes equations, a simplified variation of the evolu-

tionary Navier-Stokes ones in which the convection is simply discarded. We shall see later that while the convergence analysis of the SWR for the Stokes equations can be performed in a similar manner as that of parabolic equations, it has however its own obstacle related to the pressure. Next, we extend the analysis to the evolutionary Oseen equations, a linearization of the Navier-Stokes equations in which the convective velocity field is considered as a given datum.

The chapter is organized as follows. In the first section, we present the model problem, the existence and uniqueness of its solutions, and its multi-domain form. Since the multi-domain formulation leads to the study of the Stokes equations with Robin boundary conditions, we study this setting in Section 2.2. Next, section 2.3 is dedicated to the algorithm. An important observation that seems to have been overlooked in previous works will be given in section 2.4. Indeed, we show that, in general, the pressure calculated by the OSWR algorithm will not converge to the monodomain solution. In section 2.5, we obtain a convergence result on the velocity through an energy estimate, and in section 2.6, we propose a simple technique to recover the pressure from a converged velocity. In section 2.7, a Fourier analysis is done to get a formulation for the convergence factor of the OSWR algorithm. Then, numerical illustrations for the unsteady Stokes system follow in section 2.8. In the next step, in Section 2.9 we apply similar techniques to the Oseen equations. The final two sections are discussions about the Parareal and coupled Parareal-OSWR for the Stokes equations.

2.1   Presentation of the model. The multidomain formulation

For a domain $\Omega \subseteq \mathbb{R}^2$, and for a given viscosity coefficient $\nu > 0$ that we suppose constant and uniform, and for a given initial condition $\mathbf{u}_0$, we denote respectively by $\mathbf{u}$, p and $\mathbf{f}$ the velocity, the pressure and the source term in the incompressible non-stationary Stokes system:

$$
\begin{aligned}
\partial_t \mathbf{u} - \nu \Delta \mathbf{u} + \nabla p &= \mathbf{f} & \text{in} & \quad \Omega \times (0, T) \\
\nabla \cdot \mathbf{u} &= 0 & \text{in} & \quad \Omega \times (0, T) \\
\mathbf{u}(., t = 0) &= \mathbf{u}_0 & \text{in} & \quad \Omega \\
\mathbf{u} &= 0 & \text{on} & \quad \partial \Omega \times (0, T)
\end{aligned}
\tag{2.1}
$$

This system does not have a unique solution: if $(\mathbf{u}, p)$ is a solution, then $(\mathbf{u}, p + c)$ is also a solution, for any constant c. Then, for uniqueness, one needs, for example, the zero-mean condition on the pressure

$$
\int_\Omega p = 0.
\tag{2.2}
$$

We then denote by $L_0^2(\Omega) = \{p \in L^2(\Omega), \int_\Omega p = 0\}$.

Next, we shall introduce the following spaces, which are the completions, in $H^1(\Omega)$ and in $L^2(\Omega)$, respectively, of the set of compactly supported $\mathscr{C}^\infty$ functions with vanishing divergence:

$$
\begin{aligned}
V &= \left\{ \mathbf{u} \in \left[H_0^1(\Omega) \right]^2, \nabla \cdot \mathbf{u} = 0 \right\}, \\
H &= \left\{ \mathbf{u} \in \left[L^2(\Omega) \right]^2, \nabla \cdot \mathbf{u} = 0, \mathbf{u} \cdot \boldsymbol{n}_{\partial \Omega} = 0 \text{ on } \partial \Omega \right\}.
\end{aligned}
\tag{2.3}
$$

We denote by V' the dual space of V. We recall here Proposition IV.5.13 in the book [18]

Theorem 2.1. *Let Ω be a connected, bounded, Lipschitz domain of $\mathbb{R}^2$. For any $\mathbf{u}_0 \in H$ and $\mathbf{f} \in L^2_{\mathrm{loc}}([0, +\infty[, (H^{-1}(\Omega))^2)$, problem (2.1)-(2.2) has a unique solution such that, for any $T > 0$*

$$(\mathbf{u}, p) \in \left(L^2((0, T), V) \cap \mathscr{C}^0([0, T], H) \right) \times W^{-1,\infty}((0, T), L^2_0(\Omega))$$

and it holds that

$$\partial_t \mathbf{u} \in L^2((0, T), V').$$

Theorem 2.1 shows us the well-posedness of (2.1) only in the distributional sense. We recall next the existence and regularity properties of the strong solution, which is given in [78, Theorem 1, Page 86].

Theorem 2.2. *Let Ω be a bounded domain domain of $\mathbb{R}^2$ with twice continuously differentiable boundary. For any $\mathbf{u}_0 \in V$ and $\mathbf{f} \in L^2((0, T), L^2(\Omega))^2)$, problem (2.1)-(2.2) has a unique solution $(\mathbf{u}, p)$ such that*

$$\mathbf{u} \in \mathscr{C}^0([0, T], V) \cap L^2((0, T), (H^2(\Omega))^2), \ \partial_t \mathbf{u} \in L^2((0, T), L^2(\Omega))^2,$$
$$p \in L^2((0, T), H^1(\Omega)).$$

Remark 2.3. *There are other results with different hypothesis and regularities. For example, [18, Theorem V.2.1] states a regularity result for the Navier-Stokes equations that only requires a continuously differentiable boundary.*

In order to apply a domain-decomposition strategy for this problem, we decompose Ω into M non-overlapping subdomains Ω_i, i.e. $\Omega_i \cap \Omega_j = \emptyset$ and $\overline{\Omega} = \bigcup_{i=1}^{M} \overline{\Omega_i}$. For $i = 1, 2, \ldots, M$, we denote by $\mathscr{I}_i$ the set of indices of the neighbouring subdomain(s) of Ω_i: it holds that $j \in \mathscr{I}_i$ if and only if $|\partial \Omega_i \cap \partial \Omega_j| > 0$, where $|\cdot|$ denotes the one dimensional measure. We denote by Γ_{ij} the interface (if it exists) between Ω_i and Ω_j, $\mathbf{n}_{ij}$ the unit normal vector on Γ_{ij}, directed from Ω_i to Ω_j. Note that this implies that $\mathbf{n}_{ij} = -\mathbf{n}_{ji}$.

Denoting by $\mathbf{u}_i$, $(\mathbf{u}_0)_i$, p_i and $\mathbf{f}_i$ the respective restrictions of $\mathbf{u}$, $\mathbf{u}_0$, p and $\mathbf{f}$ to Ω_i, the monodomain problem is equivalent to the following multidomain one

$$
\begin{aligned}
\partial_t \mathbf{u}_i - \nu \Delta \mathbf{u}_i + \nabla p_i &= \mathbf{f}_i && \text{in} && \Omega_i \times (0, T) \\
\nabla \cdot \mathbf{u}_i &= 0 && \text{in} && \Omega_i \times (0, T) \\
\mathbf{u}_i(., t = 0) &= (\mathbf{u}_0)_i && \text{in} && \Omega_i \\
\mathbf{u}_i &= 0 && \text{on} && (\partial \Omega \cap \partial \Omega_i) \times (0, T)
\end{aligned}
\tag{2.4}
$$

with $i = 1, 2, \ldots, M$, together with the physical transmission conditions on $\Gamma_{ij} \times (0, T)$, $j \in \mathscr{I}_i$

$$
\begin{aligned}
\mathbf{u}_i &= \mathbf{u}_j \\
\nu \partial_{\mathbf{n}_{ij}} \mathbf{u}_i \times \mathbf{n}_{ij} &= \nu \partial_{\mathbf{n}_{ji}} \mathbf{u}_j \times \mathbf{n}_{ji} \\
\nu \partial_{\mathbf{n}_{ij}} \mathbf{u}_i \cdot \mathbf{n}_{ij} - p_i &= \nu \partial_{\mathbf{n}_{ji}} \mathbf{u}_j \cdot \mathbf{n}_{ji} - p_j
\end{aligned}
\tag{2.5}
$$

The condition $\mathbf{u}_i = \mathbf{u}_j$ can be rewritten as

$$\begin{aligned}
\mathbf{u}_i \cdot \boldsymbol{n}_{ij} &= -\mathbf{u}_j \cdot \boldsymbol{n}_{ji} \\
\mathbf{u}_i \times \boldsymbol{n}_{ij} &= -\mathbf{u}_j \times \boldsymbol{n}_{ji}
\end{aligned}$$

Hence we can write the transmission conditions on $\Gamma_{ij} \times (0, T)$ as

$$\begin{aligned}
\mathbf{u}_{ij} \cdot \boldsymbol{n}_{ij} &= -\mathbf{u}_{ji} \cdot \boldsymbol{n}_{ji} \\
\mathbf{u}_j \times \boldsymbol{n}_{ij} &= -\mathbf{u}_j \times \boldsymbol{n}_{ji} \\
\nu \partial_{\boldsymbol{n}_{ij}} \mathbf{u}_i \cdot \boldsymbol{n}_{ij} - p_i &= \nu \partial_{\boldsymbol{n}_{ji}} \mathbf{u}_j \cdot \boldsymbol{n}_{ji} - p_j \\
\nu \partial_{\boldsymbol{n}_{ij}} \mathbf{u}_i \times \boldsymbol{n}_{ij} &= \nu \partial_{\boldsymbol{n}_{ji}} \mathbf{u}_j \times \boldsymbol{n}_{ji}
\end{aligned} \tag{2.6}$$

For any choice of $(\alpha_{ij}, \alpha_{ji}, \beta_{ij}, \beta_{ji}) \in \left(\mathbb{R}^{+*}\right)^4$, those conditions are equivalent to the following Robin transmission conditions on $\Gamma_{ij} \times (0, T) = \Gamma_{ji} \times (0, T)$:

$$\begin{aligned}
\alpha_{ij}(\nu \partial_{\boldsymbol{n}_{ij}} \mathbf{u}_i \cdot \boldsymbol{n}_{ij} - p_i) + \mathbf{u}_i \cdot \boldsymbol{n}_{ij} &= \alpha_{ij}(\nu \partial_{\boldsymbol{n}_{ij}} \mathbf{u}_j \cdot \boldsymbol{n}_{ij} - p_j) + \mathbf{u}_j \cdot \boldsymbol{n}_{ij} \\
\alpha_{ji}(\nu \partial_{\boldsymbol{n}_{ji}} \mathbf{u}_j \cdot \boldsymbol{n}_{ji} - p_j) + \mathbf{u}_j \cdot \boldsymbol{n}_{ji} &= \alpha_{ji}(\nu \partial_{\boldsymbol{n}_{ji}} \mathbf{u}_i \cdot \boldsymbol{n}_{ji} - p_i) + \mathbf{u}_i \cdot \boldsymbol{n}_{ji} \\
\beta_{ij} \nu \partial_{\boldsymbol{n}_{ij}} \mathbf{u}_i \times \boldsymbol{n}_{ij} + \mathbf{u}_i \times \boldsymbol{n}_{ij} &= \beta_{ij} \nu \partial_{\boldsymbol{n}_{ij}} \mathbf{u}_j \times \boldsymbol{n}_{ij} + \mathbf{u}_j \times \boldsymbol{n}_{ij} \\
\beta_{ji} \nu \partial_{\boldsymbol{n}_{ji}} \mathbf{u}_j \times \boldsymbol{n}_{ji} + \mathbf{u}_j \times \boldsymbol{n}_{ji} &= \beta_{ji} \nu \partial_{\boldsymbol{n}_{ji}} \mathbf{u}_i \times \boldsymbol{n}_{ji} + \mathbf{u}_i \times \boldsymbol{n}_{ji}
\end{aligned} \tag{2.7}$$

Finally, the zero-mean condition for the pressure is equivalent to

$$\sum_{i=1}^{M} \int_{\Omega_i} p_i = 0. \tag{2.8}$$

This setting requires that we should study the Stokes system in a domain where Robin boundary conditions are applied on a part of the boundary. This is what is done in the next section.

2.2   The Stokes problem with Robin boundary conditions

We now consider a domain, still denoted by Ω, for which the boundary is decomposed into two parts: $\partial \Omega = \Gamma_D \cup \Gamma_R$, with $|\Gamma_R| > 0$. Let $\boldsymbol{n}$ be the outgoing normal vector on Γ_R; we consider the following system, with $\alpha > 0$ and $\beta > 0$

$$\begin{aligned}
\partial_t \mathbf{u} - \nu \Delta \mathbf{u} + \nabla p &= \mathbf{f} & \text{in} &\quad \Omega \times (0, T) \\
\nabla \cdot \mathbf{u} &= 0 & \text{in} &\quad \Omega \times (0, T) \\
\mathbf{u}(., t = 0) &= \mathbf{u}_0 & \text{in} &\quad \Omega \\
\mathbf{u} &= 0 & \text{on} &\quad \Gamma_D \times (0, T) \\
\alpha(\nu \partial_{\boldsymbol{n}} \mathbf{u} \cdot \boldsymbol{n} - p) + \mathbf{u} \cdot \boldsymbol{n} &= g & \text{on} &\quad \Gamma_R \times (0, T) \\
\beta \nu \partial_{\boldsymbol{n}} \mathbf{u} \times \boldsymbol{n} + \mathbf{u} \times \boldsymbol{n} &= \xi & \text{on} &\quad \Gamma_R \times (0, T)
\end{aligned} \tag{2.9}$$

where $\mathbf{f}$ is at least in $\left[L^2(\Omega \times (0, T))\right]^2$, g and ξ are at least in $\left[L^2(\Gamma_R \times (0, T))\right]$. In order to set this problem under an appropriate (parabolic) variational form, we perform the following calculations: Let $\mathbf{v}$ be a (smooth enough) test function that vanishes on Γ_D, and whose divergence vanishes on Ω; we have, on the one hand

$$-\nu \int_{\Omega} \Delta \mathbf{u} \cdot \mathbf{v} = \nu \int_{\Omega} \nabla \mathbf{u} : \nabla \mathbf{v} - \nu \int_{\partial \Omega} \partial_{\boldsymbol{n}} \mathbf{u} \cdot \mathbf{v}$$

$$= \nu \int_\Omega \nabla \mathbf{u} : \nabla \mathbf{v} - \nu \int_{\Gamma_R} \partial_n \mathbf{u} \cdot \mathbf{v}$$

$$= \nu \int_\Omega \nabla \mathbf{u} : \nabla \mathbf{v} - \nu \int_{\Gamma_R} (\partial_n \mathbf{u} \times \mathbf{n}) \cdot (\mathbf{v} \times \mathbf{n}) - \nu \int_{\Gamma_R} (\partial_n \mathbf{u} \cdot \mathbf{n})(\mathbf{v} \cdot \mathbf{n})$$

where $\nabla \mathbf{u} : \nabla \mathbf{v} = \text{trace} \left(\nabla^t \mathbf{v} \nabla \mathbf{u} \right)$ and

$$\int_\Omega \nabla p \cdot \mathbf{v} = -\int_\Omega p \nabla \cdot \mathbf{v} + \int_{\partial \Omega} p \mathbf{v} \cdot \mathbf{n} = \int_{\Gamma_R} p \mathbf{v} \cdot \mathbf{n}$$

on the other hand. Hence, grouping integrals on Γ_R and using Robin boundary conditions, we obtain

$$-\nu \int_\Omega \Delta \mathbf{u} \cdot \mathbf{v} + \int_\Omega \nabla p \cdot \mathbf{v} = \nu \int_\Omega \nabla \mathbf{u} : \nabla \mathbf{v}$$

$$- \int_{\Gamma_R} (\nu \partial_n \mathbf{u} \times \mathbf{n}) \cdot (\mathbf{v} \times \mathbf{n}) - \int_{\Gamma_R} (\nu \partial_n \mathbf{u} \cdot \mathbf{n} - p)(\mathbf{v} \cdot \mathbf{n})$$

$$= \nu \int_\Omega \nabla \mathbf{u} : \nabla \mathbf{v} \qquad (2.10)$$

$$+ \frac{1}{\alpha} \int_{\Gamma_R} (\mathbf{u} \cdot \mathbf{n})(\mathbf{v} \cdot \mathbf{n}) + \frac{1}{\beta} \int_{\Gamma_R} (\mathbf{u} \times \mathbf{n}) \cdot (\mathbf{v} \times \mathbf{n})$$

$$- \frac{1}{\alpha} \int_{\Gamma_R} g(\mathbf{v} \cdot \mathbf{n}) - \frac{1}{\beta} \int_{\Gamma_R} \xi \cdot (\mathbf{v} \times \mathbf{n}).$$

We then define the following spaces: V_D is the subset of velocities in $\left[H^1(\Omega) \right]^2$ that vanish on the Dirichlet boundary and whose divergence vanish in Ω, and H_D is its completion in $\left[L^2(\Omega) \right]^2$

$$V_D = \left\{ \mathbf{u} \in \left[H^1(\Omega) \right]^2, \mathbf{u} = 0 \text{ on } \Gamma_D, \nabla \cdot \mathbf{u} = 0 \right\},$$
$$H_D = \left\{ \mathbf{u} \in \left[L^2(\Omega) \right]^2, \mathbf{u} \cdot \mathbf{n} = 0 \text{ on } \Gamma_D, \nabla \cdot \mathbf{u} = 0 \right\}, \qquad (2.11)$$

equipped with the H^1 and L^2 norms, respectively.

We can define the following bilinear form $a(\cdot, \cdot)$ on $V_D \times V_D$ and, for a.e. $t \in (0, T)$ the following linear form $c(\cdot)$ on V_D

$$a(\mathbf{u}, \mathbf{v}) = \nu (\nabla \mathbf{u}, \nabla \mathbf{v})_\Omega + \frac{1}{\alpha} (\mathbf{u} \cdot \mathbf{n}, \mathbf{v} \cdot \mathbf{n})_{\Gamma_R} + \frac{1}{\beta} (\mathbf{u} \times \mathbf{n}, \mathbf{v} \times \mathbf{n})_{\Gamma_R}, \qquad (2.12)$$

$$c(t, \mathbf{v}) = (\mathbf{f}(t), \mathbf{v})_\Omega + \frac{1}{\alpha} (g(t), \mathbf{v} \cdot \mathbf{n})_{\Gamma_R} + \frac{1}{\beta} (\xi(t), \mathbf{v} \times \mathbf{n})_{\Gamma_R}, \qquad (2.13)$$

where $(\cdot, \cdot)_D$ denotes, for any set D (whatever the space-dimension of D) the standard L^2 product on D. In the same way, we shall use the notation $|| \cdot ||_D$ for the associated $L^2(D)$ norm. All terms in the definition of the forms a and c are well-defined for $(\mathbf{u}, \mathbf{v}) \in V_D \times V_D$. The fact that c depends on t is due to the fact that $\mathbf{f}$, g and ξ may depend on time.

V_D is dense in H_D and the embedding $V_D \subset H_D$ is continuous. We can identify H_D with its dual space, and we are in the situation where $V_D \subset H_D \equiv H_D' \subset V_D'$, which is the classical setting for parabolic equations (see e.g. [41, Section 6.1], [22, Page 218]). In this context, these references state the following result:

Theorem 2.4. *Let a be a mapping $a : (0,T) \times V_D \times V_D \mapsto \mathbb{R}$ be such that $a(t, \cdot, \cdot)$ is bilinear for almost every $t \in (0,T)$ and such that the following properties are verified:*

- *The function $t \mapsto a(t, \mathbf{u}, \mathbf{v})$ is measurable for all $(\mathbf{u}, \mathbf{v}) \in V_D^2$*

- *$\exists M \in \mathbb{R}$ such that $|a(t, \mathbf{u}, \mathbf{v})| \leq M \|\mathbf{u}\|_{V_D} \|\mathbf{v}\|_{V_D}$ for almost every t and for all $(\mathbf{u}, \mathbf{v}) \in V_D^2$*

- *$\exists m > 0$ such that $a(t, \mathbf{u}, \mathbf{u}) \geq m \|\mathbf{u}\|_{V_D}^2$ for almost every t and for all $\mathbf{u} \in V_D$.*

Let $t \mapsto c(t, \cdot)$ be an element of $L^2((0,T), V_D')$. Then, if $\mathbf{u}_0 \in H_D$ there exists a unique solution $\mathbf{u} \in \left(L^2((0,T), V_D) \cap \mathscr{C}^0([0,T], H_D) \right)$, with $\partial_t \mathbf{u} \in L^2((0,T), V_D')$, to the following problem

$$\langle \partial_t \mathbf{u}, \mathbf{v} \rangle_{V_D', V_D} + a(t, \mathbf{u}, \mathbf{v}) = c(t, \mathbf{v}), \qquad a.e. \ t \in (0,T), \forall \mathbf{v} \in V_D, \tag{2.14}$$

$$\mathbf{u}(0) = \mathbf{u}_0. \tag{2.15}$$

We shall apply this result to our setting, with the simplification that the bilinear form defined by (2.12) does not depend on time. We obtain the following result:

Theorem 2.5. *Let $\mathbf{f} \in L^2((0,T), \left[L^2(\Omega) \right]^2)$, $g, \xi \in L^2((0,T), L^2(\Gamma_R))$, and $\mathbf{u}_0 \in H_D$. Let a and c be defined by (2.12) and (2.13), respectively. Then, problem (2.14)–(2.15) admits a unique solution $\mathbf{u} \in \left(L^2((0,T), V_D) \cap \mathscr{C}^0([0,T], H_D) \right)$, with $\partial_t \mathbf{u} \in L^2((0,T), V_D')$.*

Proof. We shall show that a and c verify the hypothesis of Theorem 2.4. First, it is well-known that, as soon as $|\Gamma_R| > 0$, then

$$\|\mathbf{u}\|_{V_D} := \left(\|\nabla \mathbf{u}\|_\Omega^2 + \|\mathbf{u}\|_{\Gamma_R}^2 \right)^{\frac{1}{2}} = \left(\|\nabla \mathbf{u}\|_\Omega^2 + \|\mathbf{u} \cdot \boldsymbol{n}\|_{\Gamma_R}^2 + \|\mathbf{u} \times \boldsymbol{n}\|_{\Gamma_R}^2 \right)^{\frac{1}{2}}$$

is a norm equivalent to the H^1 norm on V_D, and we shall therefore work with this norm.

Next, the following properties hold for the bilinear form a:

- let $M = \max\left(\nu, \dfrac{1}{\alpha}, \dfrac{1}{\beta} \right)$, then

$$|a(\mathbf{u}, \mathbf{v})| \leq M \|\mathbf{u}\|_{V_D} \|\mathbf{v}\|_{V_D}, \forall \mathbf{u}, \mathbf{v} \in V_D, \tag{2.16}$$

- let $m = \min\left(\nu, \dfrac{1}{\alpha}, \dfrac{1}{\beta} \right) > 0$, then

$$a(\mathbf{u}, \mathbf{u}) \geq m \|\mathbf{u}\|_{V_D}^2, \forall \mathbf{u} \in V_D. \tag{2.17}$$

Indeed, as far as the first inequality is concerned, we have

$$
\begin{aligned}
|a(\mathbf{u}, \mathbf{v})| &\leq \nu \|\nabla \mathbf{u}\|_\Omega \|\nabla \mathbf{v}\|_\Omega + \frac{1}{\alpha} \|\mathbf{u} \cdot \boldsymbol{n}\|_{\Gamma_R} \|\mathbf{v} \cdot \boldsymbol{n}\|_{\Gamma_R} + \frac{1}{\beta} \|\mathbf{u} \times \boldsymbol{n}\|_{\Gamma_R} \|\mathbf{v} \times \boldsymbol{n}\|_{\Gamma_R} \\
&\leq M \left(\|\nabla \mathbf{u}\|_\Omega \|\nabla \mathbf{v}\|_\Omega + \|\mathbf{u} \cdot \boldsymbol{n}\|_{\Gamma_R} \|\mathbf{v} \cdot \boldsymbol{n}\|_{\Gamma_R} + \|\mathbf{u} \times \boldsymbol{n}\|_{\Gamma_R} \|\mathbf{v} \times \boldsymbol{n}\|_{\Gamma_R} \right) \\
&\leq M \left(\|\nabla \mathbf{u}\|_\Omega^2 + \|\mathbf{u} \cdot \boldsymbol{n}\|_{\Gamma_R}^2 + \|\mathbf{u} \times \boldsymbol{n}\|_{\Gamma_R}^2 \right)^{\frac{1}{2}} \left(\|\nabla \mathbf{v}\|_\Omega^2 + \|\mathbf{v} \cdot \boldsymbol{n}\|_{\Gamma_R}^2 + \|\mathbf{v} \times \boldsymbol{n}\|_{\Gamma_R}^2 \right)^{\frac{1}{2}} \\
&\leq M \|\mathbf{u}\|_{V_D} \|\mathbf{v}\|_{V_D}.
\end{aligned}
$$

Then, as far as the second inequality is concerned, we have

$$
\begin{aligned}
a(\mathbf{u}, \mathbf{u}) &= \nu \|\nabla \mathbf{u}\|_\Omega^2 + \frac{1}{\alpha} \|\mathbf{u} \cdot \boldsymbol{n}\|_{\Gamma_R}^2 + \frac{1}{\beta} \|\mathbf{u} \times \boldsymbol{n}\|_{\Gamma_R}^2 \\
&\geq m \left(\|\nabla \mathbf{u}\|_\Omega^2 + \|\mathbf{u} \cdot \boldsymbol{n}\|_{\Gamma_R}^2 + \|\mathbf{u} \times \boldsymbol{n}\|_{\Gamma_R}^2 \right) \\
&\geq m \|\mathbf{u}\|_{V_D}^2 .
\end{aligned}
$$

We then show that, for a.e. $t \in (0, T)$, the linear form $c(t, \cdot)$ is continuous on V_D. Indeed, $\forall \mathbf{v} \in V_D$

$$
|c(t, \mathbf{v})| \leq \|\mathbf{f}(t)\|_\Omega \|\mathbf{v}\|_\Omega + \frac{1}{\alpha} \|g(t)\|_{\Gamma_R} \|\mathbf{v} \cdot \boldsymbol{n}\|_{\Gamma_R} + \frac{1}{\beta} \|\xi(t)\|_{\Gamma_R} \|\mathbf{v} \times \boldsymbol{n}\|_{\Gamma_R} .
$$

Then, by equivalence of the $H^1(\Omega)$ norm with $\| \cdot \|_{V_D}$, there exists a constant C_1 s.t. $\forall \mathbf{v} \in V_D$

$$
\|\mathbf{v}\|_\Omega \leq \|\mathbf{v}\|_{[H^1(\Omega)]^2} \leq C_1 \|\mathbf{v}\|_{V_D} .
$$

Hence, $\forall \mathbf{v} \in V_D$

$$
\begin{aligned}
|c(t, \mathbf{v})| &\leq C_1 \|\mathbf{f}(t)\|_\Omega \|\mathbf{v}\|_{V_D} + \left(\frac{1}{\alpha} \|g(t)\|_{\Gamma_R} \right) \|\mathbf{v}\|_{V_D} + \left(\frac{1}{\beta} \|\xi(t)\|_{\Gamma_R} \right) \|\mathbf{v}\|_{V_D} \\
&\leq \left[C_1 \|\mathbf{f}(t)\|_\Omega + \frac{1}{\alpha} \|g(t)\|_{\Gamma_R} + \frac{1}{\beta} \|\xi(t)\|_{\Gamma_R} \right] \|\mathbf{v}\|_{V_D} .
\end{aligned}
\tag{2.18}
$$

Moreover, thanks to the hypothesis on the time dependence of $\mathbf{f}$, g and ξ, the quantity

$$
C_1 \|\mathbf{f}(t)\|_\Omega + \frac{1}{\alpha} \|g(t)\|_{\Gamma_R} + \frac{1}{\beta} \|\xi(t)\|_{\Gamma_R}
$$

is square integrable on $(0, T)$, and we can now apply Theorem 2.4, which finishes the proof. $\qquad \square$

Remark 2.6. *Since V_D is continuously and densely embedded in H_D, the fact that $\mathbf{u} \in \mathscr{C}^0([0, T], H_D)$ is a consequence of the fact that the space*

$$
\mathscr{W}(V_D, V_D') := \left\{ \mathbf{v} : (0, T) \mapsto V_D; \mathbf{v} \in L^2((0, T), V_D); \partial_t \mathbf{v} \in L^2((0, T), V_D') \right\}
$$

is included in $\mathscr{C}^0([0, T], H_D)$, as stated, for example, by [41, Lemma 6.2] and [Theorem II.5.13][18].

This has the important implication that it is legitimate to consider $\mathbf{u}(t) \in H_D$ for all $t \in [0, T]$. Moreover, the following integral equality holds for all $t \in [0, T]$ and for all $(\mathbf{u}, \mathbf{v}) \in [\mathscr{W}(V_D, V_D')]^2$ (see [41, Lemma 6.3] and [18, Theorem II.5.12]):

$$
\int_0^t \left(\langle \partial_t \mathbf{u}(s), \mathbf{v}(s) \rangle_{V_D', V_D} + \langle \partial_t \mathbf{v}(s), \mathbf{u}(s) \rangle_{V_D', V_D} \right) ds = (\mathbf{u}(t), \mathbf{v}(t))_\Omega - (\mathbf{u}(0), \mathbf{v}(0))_\Omega . \tag{2.19}
$$

Now, since we have obtained the velocity $\mathbf{u}$ from the constrained variational problem (2.14)–(2.15), we shall construct the pressure by relaxing the divergence free condition on the velocity test functions, and we shall therefore consider the space

$$
X_D = \left\{ \mathbf{v} \in \left[H^1(\Omega) \right]^2, \mathbf{v} = 0 \text{ on } \Gamma_D \right\},
$$

equipped with the above-defined norm $\| \cdot \|_{V_D}$. Like often with the Stokes problem, we shall rely on the surjectivity of the divergence operator, and on general properties of surjective mappings in Hilbert spaces. More precisely, we shall use the following results

Lemma 2.7. *The mapping B from X_D into $L^2(\Omega)$ defined by $B(\mathbf{v}) = -\nabla \cdot \mathbf{v}$ is continuous and surjective.*

Proof. This is a special case of [41, Lemma 4.9] (with, using the notations of [41], $\partial \Omega_1 = \Gamma_D$, $\partial \Omega_2 = \emptyset$, $\partial \Omega_3 = \emptyset$ and $\partial \Omega_4 = \Gamma_R$). □

Lemma 2.8. *Let L be in $\mathscr{L}(E; F)$ and L^T be its adjoint in $\mathscr{L}(F'; E')$, then if L is surjective in F, then $\operatorname{Im} L^T$ is closed in E'.*

Before stating the next Lemma, we recall the following definition (see, e.g. [18, Definition IV.2.1]) and properties (see, e.g. [18, Remark IV.2.1])

Definition 2.9. *Let E be a Banach space with dual space E'; then for any subset $A \subset E$, we define $A^\perp \subset E'$ as follows:*

$$A^\perp := \{\phi \in E', \forall x \in A, \langle \phi, x \rangle_{E',E} = 0\}$$

Proposition 2.10. *If $A \subset C \subset E$, then $C^\perp \subset A^\perp$.*

Proposition 2.11. *If A is a linear subspace of E, then $(A^\perp)^\perp = A$ if and only if A is closed in E.*

Moreover, we also recall the following general result

Lemma 2.12. *Let L be in $\mathscr{L}(E; F)$, then $(\operatorname{Im} L^T)^\perp \subset \operatorname{Ker} L$*

Proof. If $f \in (\operatorname{Im} L^T)^\perp$, then $\langle L^T q, f \rangle_{E',E} = 0$ for all $q \in F'$. Thus $\langle q, Lf \rangle_{F',F} = 0$ for all $q \in F'$, which means that $Lf = 0$, and thus $f \in \operatorname{Ker} L$. □

From these results, we obtain the following Lemma, which will be useful in the construction of the pressure field:

Lemma 2.13. *Let B^T be the adjoint operator of B, from $L^2(\Omega)$ into X'_D. Then for any ℓ in X'_D that vanishes on V_D, there exists $P \in L^2(\Omega)$ such that $\ell = B^T P$.*

Proof. Since B is in $\mathscr{L}(X_D; L^2(\Omega))$ and since B is surjective (see Lemma 2.7), then it holds that $(\operatorname{Im} B^T)$ is closed in X'_D (see Lemma 2.8), and that $\left((\operatorname{Im} B^T)^\perp\right)^\perp = \operatorname{Im} B^T$ (see Lemma 2.11). Now, using Lemma 2.12 and Proposition 2.10, we obtain that $(\operatorname{Ker} B)^\perp \subset \left((\operatorname{Im} B^T)^\perp\right)^\perp = \operatorname{Im} B^T$. So if ℓ in X'_D vanishes on $V_D = \operatorname{Ker} B$, then ℓ is in $(\operatorname{Ker} B)^\perp$ and so in $\operatorname{Im} B^T$, which exactly means that there exists $P \in L^2(\Omega)$ such that $\ell = B^T P$. □

Using this result, we can now state

Theorem 2.14. *With $\mathbf{f} \in L^2((0, T), [L^2(\Omega)]^2)$, $\xi, g \in L^2((0, T), L^2(\Gamma_R))$ and $\mathbf{u}_0 \in H_D$, there exists unique $p \in W^{-1,\infty}((0, T), L^2(\Omega))$, $\mathbf{u} \in \left(L^2((0, T), V_D) \cap \mathscr{C}^0([0, T], H_D)\right)$, with $\partial_t \mathbf{u} \in L^2((0, T), V'_D)$ such that $(\mathbf{u}, p)$ verifies problem (2.9) in the sense that*

- **u** *verifies* (2.14)–(2.15)

- $p = \partial_t P$ *with $P \in L^\infty((0, T), L^2(\Omega))$ satisfying*

$$\int_0^t c(s, \mathbf{v}) ds - (\mathbf{u}(t), \mathbf{v})_\Omega + (\mathbf{u}_0, \mathbf{v})_\Omega - \int_0^t a(\mathbf{u}(s), \mathbf{v}) ds = -\int_\Omega P(t) \nabla \cdot \mathbf{v} \;, \;\; \forall \mathbf{v} \in X_D. \;\; (2.20)$$

Proof. Let $\mathbf{u}$ be the solution of (2.14)–(2.15), and consider, for this $\mathbf{u}$, the function $t \mapsto a(\mathbf{u}(t), \mathbf{v})$ and the function $t \mapsto c(t, \mathbf{v})$ where a and c are defined by (2.12) and (2.13). Then their definitions can be straightforwardly extended to consider $\mathbf{v} \in X_D$ and, for any $t \in (0, T)$, the following element of X_D' is well-defined:

$$b(t, \mathbf{v}) := \int_0^t c(s, \mathbf{v}) - (\mathbf{u}(t), \mathbf{v})_\Omega + (\mathbf{u}_0, \mathbf{v})_\Omega - \int_0^t a(\mathbf{u}(s), \mathbf{v})ds \ , \ \ \forall \mathbf{v} \in X_D.$$

Indeed, one has that

$$\left| \int_0^t a(\mathbf{u}(s), \mathbf{v})ds \right| \leq \int_0^t M \|\mathbf{u}(s)\|_{X_D} \|\mathbf{v}\|_{X_D} ds$$

$$\leq M \sqrt{t} \left[\int_0^t \|\mathbf{u}(s)\|_{X_D}^2 ds \right]^{\frac{1}{2}} \|\mathbf{v}\|_{X_D}$$

$$\leq M \sqrt{T} \|\mathbf{u}\|_{L^2((0,T),V_D)} \|\mathbf{v}\|_{X_D}$$

and

$$\left| \int_0^t c(s, \mathbf{v})ds \right| \leq \int_0^t \left(C_1 \|\mathbf{f}(s)\|_\Omega + \frac{1}{\alpha} \|g(s)\|_{\Gamma_R} + \frac{1}{\beta} \|\xi(s)\|_{\Gamma_R} \right) \|\mathbf{v}\|_{X_D}$$

$$\leq \gamma_1 \|\mathbf{v}\|_{X_D}$$

with

$$\gamma_1 = C_1 \sqrt{T} \|\mathbf{f}\|_{L^2((0,T),[L^2(\Omega)]^2)} + \frac{\sqrt{T}}{\alpha} \|g\|_{L^2((0,T),L^2(\Gamma_R))} + \frac{\sqrt{T}}{\beta} \|\xi\|_{L^2((0,T),L^2(\Gamma_R))}.$$

In addition, since $\mathbf{u}$ belongs to $\mathscr{C}^0([0, T], H_D)$, then

$$\left| -(\mathbf{u}(t), \mathbf{v})_\Omega + (\mathbf{u}_0, \mathbf{v})_\Omega \right| \leq 2 \|\mathbf{u}\|_{L^\infty([0,T],[L^2(\Omega)]^2)} \|\mathbf{v}\|_\Omega \leq 2 C_1 \|\mathbf{u}\|_{L^\infty([0,T],[L^2(\Omega)]^2)} \|\mathbf{v}\|_{X_D}.$$

This leads to the fact that

$$|b(t, \mathbf{v})| \leq \beta \|\mathbf{v}\|_{X_D} \tag{2.21}$$

with

$$\beta = 2 C_1 \|\mathbf{u}\|_{L^\infty([0,T],[L^2(\Omega)]^2)} + \gamma_1 + M \sqrt{T} \|\mathbf{u}\|_{L^2(0,T,V_D)}.$$

Moreover, from (2.14) and (2.19) (with $\mathbf{v}$ not depending on time), we obtain that $b(t, \mathbf{v}) = 0$ for all $\mathbf{v} \in V_D$.

Thus, using Lemma 2.13, we conclude that, for all $t \in (0, T)$, there exists $P(t) \in L^2(\Omega)$ satisfying

$$b(t, \mathbf{v}) = \langle B^T P(t), \mathbf{v} \rangle_{X_D', X_D} = -(P(t), \nabla \cdot \mathbf{v})_\Omega = -\int_\Omega P(t) \nabla \cdot \mathbf{v} \ , \ \ \forall \mathbf{v} \in X_D. \tag{2.22}$$

Moreover, the surjectivity of the divergence mapping leads to the following inf-sup condition: there exists $\gamma_2 > 0$, s.t.

$$\inf_{q \in L^2(\Omega)} \sup_{\mathbf{v} \in X_D} \frac{(B\mathbf{v}, q)_\Omega}{\|\mathbf{v}\|_{X_D} \|q\|_{L^2(\Omega)}} = \gamma_2 > 0, \tag{2.23}$$

which implies, for all $q \in L^2(\Omega)$

$$\gamma_2 \|q\|_{L^2(\Omega)} \leq \sup_{\mathbf{v} \in X_D} \frac{(B\mathbf{v}, q)_\Omega}{\|\mathbf{v}\|_{X_D}}$$

We take $q = P(t)$. From (2.22), $(B\mathbf{v}, P(t))_\Omega = \langle B^T P(t), \mathbf{v} \rangle_{X_D', X_D} = b(t, \mathbf{v})$, together with (2.21), we get

$$\|P(t)\|_{L^2(\Omega)} \leq \frac{1}{\gamma_2} \sup_{\mathbf{v} \in X_D} \frac{b(t, \mathbf{v})}{\|\mathbf{v}\|_{X_D}} \leq \frac{\beta}{\gamma_2}.$$

We conclude that $P(t) \in L^\infty((0, T), L^2(\Omega))$. Then, we define the pressure $p = \partial_t P \in H^{-1,\infty}((0, T), L^2(\Omega))$.

It remains to show that p is unique. Consider the case $\mathbf{u}_0 = 0$ and $c = 0$. Then, we have $\mathbf{u} = 0$, and (2.20) leads to $\int_\Omega P(t) \nabla \cdot \mathbf{v} = 0 \ \forall \mathbf{v} \in X_D$. From the surjectivity of the divergence mapping, one gets that , for all t, $P(t) = 0$, and then $p = 0$.   □

2.3   Optimized Schwarz Waveform Relaxation Algorithm

We consider now the OSWR algorithm based on Robin transmission conditions. Denote by $\mathbf{f}_i = \mathbf{f}|_{\Omega_i}$ and $\mathbf{u}_{0,i} = \mathbf{u}_0|_{\Omega_i}$. Provided starting Robin terms g_{ij}^0, ξ_{ij}^0, then at each step $\ell \geq 1$ of the algorithm, we solve M subdomain problems

$$
\begin{aligned}
\partial_t \mathbf{u}_i^\ell - \nu \Delta \mathbf{u}_i^\ell + \nabla p_i^\ell &= \mathbf{f}_i & \text{in} \quad & \Omega_i \times (0, T) \\
\nabla \cdot \mathbf{u}_i^\ell &= 0 & \text{in} \quad & \Omega_i \times (0, T) \\
\mathbf{u}_i^\ell(., t = 0) &= \mathbf{u}_{0,i} & \text{in} \quad & \Omega_i \\
\alpha_{ij}(\nu \partial_{\mathbf{n}_{ij}} \mathbf{u}_i^\ell \cdot \mathbf{n}_{ij} - p_i^\ell) + \mathbf{u}_i^\ell \cdot \mathbf{n}_{ij} &= g_{ij}^{\ell-1} & \text{on} \quad & \Gamma_{ij} \times (0, T) \\
\beta_{ij} \nu \partial_{\mathbf{n}_{ij}} \mathbf{u}_i^\ell \times \mathbf{n}_{ij} + \mathbf{u}_i^\ell \times \mathbf{n}_{ij} &= \xi_{ij}^{\ell-1} & \text{on} \quad & \Gamma_{ij} \times (0, T) \\
\mathbf{u}_i^\ell &= 0 & \text{on} \quad & (\partial \Omega_i \cap \partial \Omega) \times (0, T)
\end{aligned}
$$

with $i = 1, 2, \ldots, M$, and then we update the new Robin terms on the interface $\Gamma_{ij} \times (0, T)$

$$g_{ij}^\ell = \alpha_{ij}(\nu \partial_{\mathbf{n}_{ij}} \mathbf{u}_j^\ell \cdot \mathbf{n}_{ij} - p_j^\ell) + \mathbf{u}_j^\ell \cdot \mathbf{n}_{ij} \qquad (2.24)$$

$$\xi_{ij}^\ell = \beta_{ij} \nu \partial_{\mathbf{n}_{ij}} \mathbf{u}_j^\ell \times \mathbf{n}_{ij} + \mathbf{u}_j^\ell \times \mathbf{n}_{ij}, \qquad (2.25)$$

with $j \in \mathcal{I}_i$.

Remark 2.15. *As seen in the previous section, the space regularity of the velocity field is $H^1(\Omega_i)$ and that of the pressure field is $L^2(\Omega_i)$. Thus, if $g_{ij}^{\ell-1}$ and $\xi_{ij}^{\ell-1}$ have $L^2(\Gamma_{ij})$ regularity, then update formulas given by (2.24)–(2.25) would return new boundary data g_{ij}^ℓ and ξ_{ij}^ℓ with a lower regularity, which is not satisfying for an iterative algorithm. Thus, we rewrite the update formulas as follows*

$$g_{ij}^\ell = \frac{\alpha_{ij}}{\alpha_{ji}} \left(\alpha_{ji}(\nu \partial_{\mathbf{n}_{ji}} \mathbf{u}_j^\ell \cdot \mathbf{n}_{ji} - p_j^\ell) + \mathbf{u}_j^\ell \cdot \mathbf{n}_{ji} \right) - \frac{\alpha_{ij}}{\alpha_{ji}} \mathbf{u}_j^\ell \cdot \mathbf{n}_{ji} + \mathbf{u}_j^\ell \cdot \mathbf{n}_{ij}$$

$$= \frac{\alpha_{ij}}{\alpha_{ji}} g_{ji}^{\ell-1} - \frac{\alpha_{ij} + \alpha_{ji}}{\alpha_{ji}} \mathbf{u}_j^\ell \cdot \mathbf{n}_{ji} \tag{2.26}$$

$$\xi_{ij}^\ell = \frac{\beta_{ij}}{\beta_{ji}} \left(\beta_{ji} \nu \partial_{\mathbf{n}_{ji}} \mathbf{u}_j^\ell \times \mathbf{n}_{ji} + \mathbf{u}_j^\ell \times \mathbf{n}_{ji} \right) - \frac{\beta_{ij}}{\beta_{ji}} \mathbf{u}_j^\ell \times \mathbf{n}_{ji} + \mathbf{u}_j^\ell \times \mathbf{n}_{ij}$$

$$= \frac{\beta_{ij}}{\beta_{ji}} \xi_{ji}^{\ell-1} - \frac{\beta_{ij} + \beta_{ji}}{\beta_{ji}} \mathbf{u}_j^\ell \times \mathbf{n}_{ji} \tag{2.27}$$

In this update formulation, the regularities of g_{ij}^ℓ and ξ_{ij}^ℓ depend only on the regularities of $g_{ji}^{\ell-1}$, $\xi_{ji}^{\ell-1}$ and $\mathbf{u}_j^\ell$, whose trace is $L^2((0,T), H^{\frac{1}{2}}(\Gamma_{ij}))$.

Now, we may express the iterative algorithm in the following way. We first define

$$V_i = \{ \mathbf{u} \in \left[H^1(\Omega_i) \right]^2, \mathbf{u} = 0 \text{ on } \partial \Omega_i \cap \partial \Omega, \nabla \cdot \mathbf{u} = 0 \text{ in } \Omega_i \},$$

$$H_i = \{ \mathbf{u} \in \left[L^2(\Omega_i) \right]^2, \mathbf{u} \cdot \mathbf{n}_{\partial \Omega_i} = 0 \text{ on } \partial \Omega_i \cap \partial \Omega, \nabla \cdot \mathbf{u} = 0 \text{ in } \Omega_i \}.$$

$$X_i = \left\{ \mathbf{u} \in \left[H^1(\Omega_i) \right]^2, \mathbf{u} = 0 \text{ on } \partial \Omega_i \cap \partial \Omega \right\},$$

Then, we set

$$a_i(\mathbf{u}, \mathbf{v}) = \nu (\nabla \mathbf{u}, \nabla \mathbf{v})_{\Omega_i} + \sum_{j \in \mathscr{I}_i} \frac{1}{\alpha_{ij}} \left(\mathbf{u} \cdot \mathbf{n}_{ij}, \mathbf{v} \cdot \mathbf{n}_{ij} \right)_{\Gamma_{ij}} + \frac{1}{\beta_{ij}} \left(\mathbf{u} \times \mathbf{n}_{ij}, \mathbf{v} \times \mathbf{n}_{ij} \right)_{\Gamma_{ij}},$$

$$c_i^\ell(t, \mathbf{v}) = (\mathbf{f}, \mathbf{v})_{\Omega_i} + \sum_{j \in \mathscr{I}_i} \frac{1}{\alpha_{ij}} \left(g_{ij}^{\ell-1}, \mathbf{v} \cdot \mathbf{n}_{ij} \right)_{\Gamma_{ij}} + \frac{1}{\beta_{ij}} \left(\xi_{ij}^{\ell-1}, \mathbf{v} \times \mathbf{n}_{ij} \right)_{\Gamma_{ij}}, \tag{2.28}$$

and the algorithm reads: for all $\ell \geq 1$, given $g_{ij}^{\ell-1}, \xi_{ij}^{\ell-1}$ on each space-time interface $\Gamma_{ij} \times (0,T)$, solve, for each $i = 1 \ldots M$:

$$\left\langle \partial_t \mathbf{u}_i^\ell, \mathbf{v} \right\rangle_{V_i', V_i} + a_i(\mathbf{u}_i^\ell, \mathbf{v}) = c_i^\ell(t, \mathbf{v}), \qquad \text{a.e. } t \in (0,T), \forall \mathbf{v} \in V_i,$$

$$\mathbf{u}_i^\ell(0) = \mathbf{u}_{0.i} \tag{2.29}$$

and then construct $p_i^\ell = \partial_t P_i^\ell$ which is such that

$$\left(\mathbf{u}_i^\ell(t), \mathbf{v} \right)_{\Omega_i} - \left(\mathbf{u}_{0,i}, \mathbf{v} \right)_{\Omega_i} + \int_0^t a_i(\mathbf{u}_i^\ell(s), \mathbf{v}) ds - (P_i^\ell, \nabla \cdot \mathbf{v})_{\Omega_i} - \int_0^t c_i^\ell(s, \mathbf{v}) ds = 0, \tag{2.30}$$

$$\forall \mathbf{v} \in X_i.$$

Finally, update the data by using (2.26)–(2.27) on the space-time interfaces.

With this formulation, we can state the following result

Theorem 2.16. *Suppose that $g_{ij}^0, \xi_{ij}^0 \in L^2((0,T), L^2(\Gamma_{ij}))$ and $\mathbf{u}_0|_{\Omega_i} \in H_i$. Then, the OSWR algorithm is well-defined and for all ℓ, $\mathbf{u}_i^\ell \in L^2((0,T), V_i) \cap \mathscr{C}^0([0,T], H_i)$ with $\partial_t \mathbf{u}_i^\ell \in L^2((0,T), V_i')$, $p_i^\ell \in W^{-1,\infty}((0,T), L^2(\Omega_i))$ and $g_{ij}^\ell, \xi_{ij}^\ell \in L^2((0,T), L^2(\Gamma_{ij}))$*

Proof. By theorem 2.14, if $g_{ij}^{\ell-1}, \xi_{ij}^{\ell-1} \in L^2((0,T), L^2(\Gamma_{ij}))$, then one gets $\mathbf{u}_i^\ell \in L^2((0,T), V_i) \cap \mathscr{C}^0([0,T], H_i)$ with $\partial_t \mathbf{u}_i^\ell \in L^2((0,T), V_i')$ and $p_i^\ell \in W^{-1,\infty}((0,T), L^2(\Omega_i))$.

Using the trace theorem, the normal and tangent traces of $\mathbf{u}_i^\ell$ on $\Gamma_{ij} \times (0,T)$ are in $L^2((0,T), L^2(\Gamma_{ij}))$. Hence, $g_{ij}^\ell, \xi_{ij}^\ell \in L^2((0,T), L^2(\Gamma_{ij}))$.
The proof is then carried out by a simple induction. $\qquad \square$

Remark 2.17. *The OSWR algorithm is constructed without considering the last condition* (2.8)*, hence it may not converge to the exact solution. We shall show in the next section that, indeed, the pressure in each subdomain may not converge to the restriction of the monodomain pressure.*

2.4   First observations on the two subdomains case

We now take a look at the simplest case $M = 2$, in which we can use the indices $_1$ and $_2$ instead of $_{12}$ and $_{21}$ and $\Gamma = \Gamma_{12} = \Gamma_{21}$.

The divergence-free condition of the velocity in each subdomain leads to

$$\int_{\partial \Omega_i} \mathbf{u}_i^\ell \cdot \boldsymbol{n}_{\partial \Omega_i} = 0 = \int_\Gamma \mathbf{u}_i^\ell \cdot \boldsymbol{n}_i \ , \quad i = 1, 2. \tag{2.31}$$

The update of Robin terms for the normal components can also be written as

$$g_i^\ell = \frac{\alpha_i}{\alpha_j} g_j^{\ell-1} - \frac{\alpha_i + \alpha_j}{\alpha_j} \mathbf{u}_j^\ell \cdot \boldsymbol{n}_j.$$

Integrating over Γ, and taking (2.31) into account, we get

$$\int_\Gamma g_i^\ell = \frac{\alpha_i}{\alpha_j} \int_\Gamma g_j^{\ell-1} = \int_\Gamma g_i^{\ell-2}. \tag{2.32}$$

Therefore, a necessary condition for the convergence of the algorithm to the monodomain solution is

$$\int_\Gamma g_i^0 = \int_\Gamma g_i$$

with $g_i = \alpha_i(\nu \partial_{\boldsymbol{n}_i} \mathbf{u} \cdot \boldsymbol{n}_i - p) + \mathbf{u} \cdot \boldsymbol{n}_i$, in which $(\mathbf{u}, p)$ is the monodomain solution of problem (2.1). This condition cannot be achieved in practice because the quantity g_i is not known.

To understand more about the behaviour of the algorithm, we now study the one-dimensional case.

The one dimensional case

Let $\Omega = (-1, 1)$ and $\Gamma = \{x = 0\}$, the OSWR algorithm applied to the one-dimensional Stokes problem can be written for the error (difference between the monodomain solution and the iterative solution at step ℓ of the algorithm) as: provided g_1^0, g_2^0, at each step ℓ, we solve, for $i = 1, 2$

$$\begin{aligned} \partial_t \mathbf{u}_i^\ell - \nu \partial_{xx} \mathbf{u}_i^\ell + \partial_x p_i^\ell &= 0 &\text{in} \quad &\Omega_i \times (0, T) \\ \partial_x \mathbf{u}_i^\ell &= 0 &\text{in} \quad &\Omega_i \times (0, T) \\ \mathbf{u}_i^\ell(., 0) &= 0 &\text{in} \quad &\Omega_i \\ \mathbf{u}_i^\ell((-1)^i, .) &= 0 &\text{on} \quad &(0, T) \\ \alpha_i(\nu \partial_x \mathbf{u}_i^\ell(0, .) - p_i^\ell(0, .)) + (-1)^{i+1} \mathbf{u}_i^\ell(0, .) &= g_i^{\ell-1} &\text{on} \quad &(0, T) \end{aligned}$$

then update on $(0, T)$, with $j = 3 - i$

$$g_i^\ell(t) = \alpha_i(\nu \partial_x \mathbf{u}_j^\ell(0, t) - p_j^\ell(0, t)) + (-1)^{i+1} \mathbf{u}_j^\ell(0, t) \tag{2.33}$$

We check if $(\mathbf{u}_i^\ell, p_i^\ell)$ tends to zeros or not. The second and third conditions on the velocity simply lead to $\mathbf{u}_i^\ell = 0$ for all ℓ. The first equation implies then $\partial_x p_i^\ell = 0$, so $p_i^\ell(x,t) := p_i^\ell(t)$.

From (2.33) and the transmission conditions, we get

$$g_j^\ell = -\alpha_j p_i^\ell = \frac{\alpha_j}{\alpha_i} g_i^{\ell-1}$$

and then $g_i^{2\ell} = g_i^0$, $g_i^{2\ell+1} = \frac{\alpha_i}{\alpha_j} g_j^0$. Therefore, the algorithm converges if and only if $g_1^0 = g_2^0 = 0$.

This will not be the case in general since the above algorithm is written on the error and thus g_i^0 contains the Robin term of the unknown monodomain solution. Thus, we have shown that the algorithm may not converge even in the most simple case. However, these arguments point out that $\mathbf{u}_i^\ell$, $p_i^{2\ell} + \frac{1}{\alpha_j} g_j^0$ and $p_i^{2\ell+1} + \frac{1}{\alpha_i} g_i^0$ are zeros.

We will try to obtain similar results for higher dimension cases.

2.5 Convergence of the velocity via energy estimate

In this section, we prove that, under sufficient regularity conditions for the solution $(\mathbf{u}, p)$ of problem (2.1)–(2.2), then the velocity fields $\mathbf{u}_i^\ell$ converge to $\mathbf{u}|_{\Omega_i}$.

Theorem 2.18. *Let $(\mathbf{u}, p)$ be the solution of problem (2.1)–(2.2); let $\mathbf{u}_i := \mathbf{u}|_{\Omega_i}$. Suppose that all conditions in Theorem 2.2 are satisfied.*
Let g_{ij}^0 and ξ_{ij}^0 be in $L^2((0,T), L^2(\Gamma_{ij}))$ and let $\mathbf{u}_i^\ell$ be the velocity component of the solution of the OSWR algorithm defined in Section 2.3. Then, if $\alpha_{ij} = \alpha_{ji}$ and $\beta_{ij} = \beta_{ji}$, the sequence $\mathbf{u}_i^\ell$ converges to $\mathbf{u}_i$ in $\mathscr{C}^0([0,T], H_i) \cap L^2(0,T,V_i)$.

Proof. Suppose that all conditions in Theorem 2.2 are satisfied. We denote by $p_i = p|_{\Omega_i}$. Then, as $(\mathbf{u}_i, p_i)$ is regular enough, we can define on any space-time interface $\Gamma_{ij} \times (0,T)$

$$g_{ij} := \alpha_{ij}(\nu \partial_{\mathbf{n}_{ij}} \mathbf{u}_i \cdot \mathbf{n}_{ij} - p_i) + \mathbf{u}_i \cdot \mathbf{n}_{ij} \tag{2.34}$$

$$\xi_{ij} := \nu \beta_{ij} \partial_{\mathbf{n}_{ij}} \mathbf{u}_i \times \mathbf{n}_{ij} + \mathbf{u}_i \times \mathbf{n}_{ij} \tag{2.35}$$

and they both belong to $L^2((0,T), L^2(\Gamma_{ij}))$.

We recall here that the strong regularity of (u,p) leads to the multidomain transmission conditions (2.7), which implies

$$
\begin{aligned}
g_{ij} &= \frac{\alpha_{ij}}{\alpha_{ji}}\left(\alpha_{ji}(\nu \partial_{\mathbf{n}_{ji}} \mathbf{u}_j \cdot \mathbf{n}_{ji} - p_j) + \mathbf{u}_j \cdot \mathbf{n}_{ji}\right) - \frac{\alpha_{ij}}{\alpha_{ji}} \mathbf{u}_j \cdot \mathbf{n}_{ji} + \mathbf{u}_j \cdot \mathbf{n}_{ij} \\
&= \frac{\alpha_{ij}}{\alpha_{ji}} g_{ji} - \frac{\alpha_{ij} + \alpha_{ji}}{\alpha_{ji}} \mathbf{u}_j \cdot \mathbf{n}_{ji} \tag{2.36}
\end{aligned}
$$

$$
\begin{aligned}
\xi_{ij} &= \frac{\beta_{ij}}{\beta_{ji}}\left(\beta_{ji} \nu \partial_{\mathbf{n}_{ji}} \mathbf{u}_j \times \mathbf{n}_{ji} + \mathbf{u}_j \times \mathbf{n}_{ji}\right) - \frac{\beta_{ij}}{\beta_{ji}} \mathbf{u}_j \times \mathbf{n}_{ji} + \mathbf{u}_j \times \mathbf{n}_{ij} \\
&= \frac{\beta_{ij}}{\beta_{ji}} \xi_{ji} - \frac{\beta_{ij} + \beta_{ji}}{\beta_{ji}} \mathbf{u}_j \times \mathbf{n}_{ji} \tag{2.37}
\end{aligned}
$$

Moreover, $(\mathbf{u}_i, p_i)$ is the strong solution of each local Robin boundary problem

$$
\begin{aligned}
\partial_t \mathbf{u}_i - \nu \Delta \mathbf{u}_i + \nabla p_i &= \mathbf{f}_i && \text{in} && \Omega_i \times (0, T) \\
\nabla \cdot \mathbf{u}_i &= 0 && \text{in} && \Omega_i \times (0, T) \\
\mathbf{u}_i(., t = 0) &= \mathbf{u}_{0,i} && \text{in} && \Omega_i \\
\mathbf{u}_i &= 0 && \text{on} && (\partial\Omega \cap \partial\Omega_i) \times (0, T) \\
\alpha_{ij}(\nu \partial_{\boldsymbol{n}_{ij}} \mathbf{u}_i \cdot \boldsymbol{n} - p_i) + \mathbf{u}_i \cdot \boldsymbol{n}_{ij} &= g_{ij} && \text{on} && \Gamma_{ij} \times (0, T) \\
\beta_{ij} \nu \partial_{\boldsymbol{n}_{ij}} \mathbf{u}_i \times \boldsymbol{n} + \mathbf{u}_i \times \boldsymbol{n}_{ij} &= \xi_{ij} && \text{on} && \Gamma_{ij} \times (0, T)
\end{aligned}
$$

which can be set under the following variational formulation, which is very similar to (2.28)–(2.29):

$$
\begin{aligned}
\langle \partial_t \mathbf{u}_i, \mathbf{v} \rangle_{V_i', V_i} + a_i(\mathbf{u}_i, \mathbf{v}) &= c_i(t, \mathbf{v}), && \text{a.e. } t \in (0, T), \forall \mathbf{v} \in V_i, \\
\mathbf{u}_i(0) &= \mathbf{u}_{0,i}
\end{aligned}
\tag{2.38}
$$

with

$$
c_i(t, \mathbf{v}) = (\mathbf{f}, \mathbf{v})_{\Omega_i} + \sum_{j \in \mathscr{I}_i} \frac{1}{\alpha_{ij}} \left(g_{ij}, \mathbf{v} \cdot \boldsymbol{n}_{ij} \right)_{\Gamma_{ij}} + \frac{1}{\beta_{ij}} \left(\xi_{ij}, \mathbf{v} \times \boldsymbol{n}_{ij} \right)_{\Gamma_{ij}}.
\tag{2.39}
$$

Denote by

$$
\mathbf{e}_i^\ell := \mathbf{u}_i^\ell - \mathbf{u}_i , \ h_{ij}^\ell = g_{ij}^\ell - g_{ij} , \ \zeta_{ij}^\ell = \xi_{ij}^\ell - \xi_{ij}.
\tag{2.40}
$$

From (2.28), (2.29), (2.38), (2.39), then $\mathbf{e}_i^\ell$ verifies

$$
\begin{aligned}
\langle \partial_t \mathbf{e}_i^\ell, \mathbf{v} \rangle_{V_i', V_i} + a_i(\mathbf{e}_i^\ell, \mathbf{v}) &= \sum_{j \in \mathscr{I}_I} \frac{1}{\alpha_{ij}} (h_{ij}^{\ell-1}, \mathbf{v} \cdot \boldsymbol{n}_{ij})_{\Gamma_{ij}} + \sum_{j \in \mathscr{I}_I} \frac{1}{\beta_{ij}} (\zeta_{ij}^{\ell-1}, \mathbf{v} \times \boldsymbol{n}_{ij})_{\Gamma_{ij}} \\
& \qquad\qquad\qquad\qquad\qquad \text{a.e. } t \in (0, T), \forall \mathbf{v} \in V_i, \\
\mathbf{e}_i^\ell(0) &= 0 \qquad\qquad\qquad .
\end{aligned}
\tag{2.41}
$$

All integrals on Γ_{ij} are well defined since g_{ij} and ξ_{ij} are both in $L^2((0, T), L^2(\Gamma_{ij}))$, and since we have proved that this is also the case for g_{ij}^ℓ and ξ_{ij}^ℓ as soon as it is true for $\ell = 0$.

With $\alpha_{ij} = \alpha_{ji}$ and $\beta_{ij} = \beta_{ji}$, the update formulas (2.26), (2.27) and (2.36), (2.37) for the Robin terms on $\Gamma_{ij} \times (0, T)$ lead to

$$
\mathbf{e}_i^\ell \cdot \boldsymbol{n}_{ij} = \frac{1}{2} \left(h_{ij}^{\ell-1} - h_{ji}^\ell \right) , \ \mathbf{e}_i^\ell \times \boldsymbol{n}_{ij} = \frac{1}{2} \left(\zeta_{ij}^{\ell-1} - \zeta_{ji}^\ell \right).
\tag{2.42}
$$

Choosing $\mathbf{e}_i^\ell$ as test function in (2.41), one gets

$$
\begin{aligned}
\langle \partial_t \mathbf{e}_i^\ell, \mathbf{e}_i^\ell \rangle_{V_i', V_i} + \nu(\nabla \mathbf{e}_i^\ell, \nabla \mathbf{e}_i^\ell)_{\Omega_i} + \sum_{j \in \mathscr{I}_I} \frac{1}{\alpha_{ij}} (\mathbf{e}_i^\ell \cdot \boldsymbol{n}_{ij}, \mathbf{e}_i^\ell \cdot \boldsymbol{n}_{ij})_{\Gamma_{ij}} + \sum_{j \in \mathscr{I}_I} \frac{1}{\beta_{ij}} (\mathbf{e}_i^\ell \times \boldsymbol{n}_{ij}, \mathbf{e}_i^\ell \times \boldsymbol{n}_{ij})_{\Gamma_{ij}} \\
= \sum_{j \in \mathscr{I}_I} \frac{1}{\alpha_{ij}} (h_{ij}^{\ell-1}, \mathbf{e}_i^\ell \cdot \boldsymbol{n}_{ij})_{\Gamma_{ij}} + \sum_{j \in \mathscr{I}_I} \frac{1}{\beta_{ij}} (\zeta_{ij}^{\ell-1}, \mathbf{e}_i^\ell \times \boldsymbol{n}_{ij})_{\Gamma_{ij}}.
\end{aligned}
\tag{2.43}
$$

On the boundary Γ_{ij}, replacing (2.42) into (2.43), one gets

$$
\langle \partial_t \mathbf{e}_i^\ell, \mathbf{e}_i^\ell \rangle_{V_i', V_i} + \nu(\nabla \mathbf{e}_i^\ell, \nabla \mathbf{e}_i^\ell)_{\Omega_i} + \frac{1}{4} \sum_{j \in \mathscr{I}_I} \frac{1}{\alpha_{ij}} (h_{ij}^{\ell-1} - h_{ji}^\ell, h_{ij}^{\ell-1} - h_{ji}^\ell)_{\Gamma_{ij}}
$$

$$+ \frac{1}{4} \sum_{j \in \mathcal{I}_I} \frac{1}{\beta_{ij}} (\zeta_{ij}^{\ell-1} - \zeta_{ji}^{\ell}, \zeta_{ij}^{\ell-1} - \zeta_{ji}^{\ell})_{\Gamma_{ij}}$$

$$= \frac{1}{2} \sum_{j \in \mathcal{I}_I} \frac{1}{\alpha_{ij}} (h_{ij}^{\ell-1}, h_{ij}^{\ell-1} - h_{ji}^{\ell})_{\Gamma_{ij}} + \frac{1}{2} \sum_{j \in \mathcal{I}_I} \frac{1}{\beta_{ij}} (\zeta_{ij}^{\ell-1}, \zeta_{ij}^{\ell-1} - \zeta_{ji}^{\ell})_{\Gamma_{ij}}.$$

Equivalently

$$\langle \partial_t \mathbf{e}_i^{\ell}, \mathbf{e}_i^{\ell} \rangle_{V_i', V_i} + \nu \|\nabla \mathbf{e}_i^{\ell}\|_{\Omega_i}^2 + \frac{1}{4} \sum_{j \in \mathcal{I}_I} \frac{1}{\alpha_{ij}} \|h_{ji}^{\ell}\|_{\Gamma_{ij}}^2 + \frac{1}{4} \sum_{j \in \mathcal{I}_I} \frac{1}{\beta_{ij}} \|\zeta_{ji}^{\ell}\|_{\Gamma_{ij}}^2$$

$$= \frac{1}{4} \sum_{j \in \mathcal{I}_I} \frac{1}{\alpha_{ij}} \|h_{ij}^{\ell-1}\|_{\Gamma_{ij}}^2 + \frac{1}{4} \sum_{j \in \mathcal{I}_I} \frac{1}{\beta_{ij}} \|\zeta_{ij}^{\ell-1}\|_{\Gamma_{ij}}^2, \tag{2.44}$$

with the norms here denoting the L^2 norms.
Next, adapting (2.19) to Ω_i, we get

$$2 \int_0^T \langle \partial_t \mathbf{e}_i^{\ell}, \mathbf{e}_i^{\ell} \rangle_{V_i', V_i} = \|\mathbf{e}_i^{\ell}(T)\|_{\Omega_i}^2 - \|\mathbf{e}_i^{\ell}(0)\|_{\Omega_i}^2.$$

Multiplying (2.44) by 2 and integrating on $(0, T)$, we obtain

$$\|\mathbf{e}_i^{\ell}(T)\|_{\Omega_i}^2 - \|\mathbf{e}_i^{\ell}(0)\|_{\Omega_i}^2 + 2\nu \int_0^T \|\nabla \mathbf{e}_i^{\ell}\|_{\Omega_i}^2 + \sum_{j \in \mathcal{I}_I} \frac{1}{2\alpha_{ij}} \int_0^T \|h_{ji}^{\ell}\|_{\Gamma_{ij}}^2 + \sum_{j \in \mathcal{I}_I} \frac{1}{2\beta_{ij}} \int_0^T \|\zeta_{ji}^{\ell}\|_{\Gamma_{ij}}^2$$

$$= \sum_{j \in \mathcal{I}_I} \frac{1}{2\alpha_{ij}} \int_0^T \|h_{ij}^{\ell-1}\|_{\Gamma_{ij}}^2 + \sum_{j \in \mathcal{I}_I} \int_0^T \frac{1}{2\beta_{ij}} \|\zeta_{ij}^{\ell-1}\|_{\Gamma_{ij}}^2 \tag{2.45}$$

Taking into account that $\mathbf{e}_i^{\ell}(0) = 0$ and summing over all subdomains Ω_i, we get

$$\sum_{i=1}^M \|\mathbf{e}_i^{\ell}(., T)\|_{\Omega_i}^2 + 2\nu \sum_{i=1}^M \int_0^T \|\nabla \mathbf{e}_i^{\ell}\|_{\Omega_i}^2 + \sum_{i=1}^M \sum_{j \in \mathcal{I}_i} \frac{1}{2\beta_{ij}} \int_0^T \|\zeta_{ji}^{\ell}\|_{\Gamma_{ij}}^2$$

$$+ \sum_{i=1}^M \sum_{j \in \mathcal{I}_i} \frac{1}{2\alpha_{ij}} \int_0^T \|h_{ji}^{\ell}\|_{\Gamma_{ij}}^2 = \sum_{i=1}^M \sum_{j \in \mathcal{I}_i} \frac{1}{2\beta_{ij}} \int_0^T \|\zeta_{ij}^{\ell-1}\|_{\Gamma_{ij}}^2 + \sum_{i=1}^M \sum_{j \in \mathcal{I}_i} \frac{1}{2\alpha_{ij}} \int_0^T \|h_{ij}^{\ell-1}\|_{\Gamma_{ij}}^2.$$

The terms

$$\sum_{i=1}^M \sum_{j \in \mathcal{I}_i} \frac{1}{2\beta_{ij}} \int_0^T \|\zeta_{ij}^{\ell-1}\|_{\Gamma_{ij}}^2 + \sum_{i=1}^M \sum_{j \in \mathcal{I}_i} \frac{1}{2\alpha_{ij}} \int_0^T \|h_{ij}^{\ell-1}\|_{\Gamma_{ij}}^2$$

and

$$\sum_{i=1}^M \sum_{j \in \mathcal{I}_i} \frac{1}{2\beta_{ji}} \int_0^T \|\zeta_{ji}^{\ell-1}\|_{\Gamma_{ij}}^2 + \sum_{i=1}^M \sum_{j \in \mathcal{I}_i} \frac{1}{2\alpha_{ji}} \int_0^T \|h_{ji}^{\ell-1}\|_{\Gamma_{ij}}^2$$

express the same quantity: the total energies on all interfaces of all Robin terms at step $(\ell - 1)$, which we denote by $E_R^{\ell-1}$. Hence, the above energy estimate becomes

$$\sum_{i=1}^M \|\mathbf{e}_i^{\ell}(., T)\|_{\Omega_i}^2 + 2\nu \sum_{i=1}^M \int_0^T \|\nabla \mathbf{e}_i^{\ell}\|_{\Omega_i}^2 + E_R^{\ell} = E_R^{\ell-1}$$

Summing from $\ell = 1$ to $\ell = L$, we get

$$\sum_{\ell=1}^{L}\sum_{i=1}^{M}\|\mathbf{e}_i^\ell(.,T)\|_{\Omega_i}^2 + 2\nu\sum_{\ell=1}^{L}\sum_{i=1}^{M}\int_0^T\|\nabla\mathbf{e}_i^\ell\|_{\Omega_i}^2(t)dt + E_R^L = E_R^0$$

As $E_R^L \geq 0$ for all L, the sums $\displaystyle\sum_{\ell=1}^{L}\sum_{i=1}^{M}\|\mathbf{e}_i^\ell(.,T)\|_{\Omega_i}^2$ and $\displaystyle\sum_{\ell=1}^{L}\sum_{i=1}^{M}\int_0^T\|\nabla\mathbf{e}_i^\ell\|_{\Omega_i}^2$ are bounded; hence $\|\mathbf{e}_i^\ell(T)\|_{\Omega_i}^2$ and $\displaystyle\int_0^T\|\nabla\mathbf{e}_i^\ell\|_{\Omega_i}^2(t)dt$ tend to 0 when $\ell \to \infty$.

In addition, in (2.45), we can integrate on $(0,t)$ instead of $(0,T)$, and we get for all $t \in (0,T)$

$$\sum_{\ell=1}^{L}\sum_{i=1}^{M}\|\mathbf{e}_i^\ell(t)\|_{\Omega_i}^2 \leq E_R^0.$$

This first leads to the convergence of $\|\mathbf{e}_i^\ell(t)\|_{\Omega_i}$ to 0 for all t and thus to the convergence of $\mathbf{e}_i^\ell$ to 0 in $\mathscr{C}^0([0,T],H_i)$, but also to the fact that, integrating on $(0,T)$, it holds that

$$\sum_{\ell=1}^{L}\sum_{i=1}^{M}\int_0^T\|\mathbf{e}_i^\ell(t)\|_{\Omega_i}^2 dt \leq TE_R^0.$$

This implies that $\displaystyle\int_0^T\|\mathbf{e}_i^\ell(t)\|_{\Omega_i}^2 dt$ tends to 0 when $\ell \to +\infty$. Then, summing with $\displaystyle\int_0^T\|\nabla\mathbf{e}_i^\ell\|_{\Omega_i}^2(t)dt$ that also tends to 0, we have that $\displaystyle\int_0^T\|\mathbf{e}_i^\ell(t)\|_{[H^1(\Omega_i)]^2}^2 dt$ tends to 0, or, in other words, that $\mathbf{e}_i^\ell$ tends to 0 in $L^2((0,T),V_i)$. $\qquad\square$

Remark 2.19. *Unfortunately, in general, we do not have the convergence of $\partial_t\mathbf{u}_i^\ell$ in V_i'. Indeed, from the first equality in (2.41), and since $a_i(\mathbf{e}_i^\ell,\mathbf{v})$ tends to 0, the convergence of $\partial_t\mathbf{u}_i^\ell$ is equivalent to the weak convergence of h_{ij}^ℓ and ζ_{ij}^ℓ. However, we have given in Section 2.4 an example from which we infer that this is not the case, in general (see (2.32)).*

On the other hand, we notice that for all $\mathbf{v} \in \left[H_0^1(\Omega_i)\right]^2$, the right-hand side in the first equality in (2.41) vanishes. Then we get

Corollary 2.20. *Let all hypotheses of Theorem 2.18 be satisfied. Denote by $W_i = \{\mathbf{u} \in \left[H_0^1(\Omega_i)\right]^2, \nabla\cdot\mathbf{u} = 0 \text{ in } \Omega_i\}$. Then, $\partial_t\mathbf{u}_i^\ell$ tends to $\partial_t\mathbf{u}_i$ in $L^2((0,T),W_i')$.*

Proof. In the constrained formulation of the error, Eq. (2.41), taking the test functions in $W_i \subset V_i$, we get

$$\langle\partial_t\mathbf{e}_i^\ell(t),\mathbf{v}\rangle_{V_i',V_i} + a_i(\mathbf{e}_i^\ell(t),\mathbf{v}) = 0,$$

which exactly means that

$$\langle\partial_t\mathbf{e}_i^\ell(t),\mathbf{v}\rangle_{W_i',W_i} + (\nabla\mathbf{e}_i^\ell(t),\nabla\mathbf{v})_{\Omega_i} = 0.$$

Then

$$\|\partial_t\mathbf{e}_i^\ell(t)\|_{W_i'} \leq \|\nabla\mathbf{e}_i^\ell(t)\|_{\Omega_i}$$

and thus

$$\int_0^T \|\partial_t \mathbf{e}_i^\ell(t)\|_{W_i'}^2 dt \le \int_0^T \|\nabla \mathbf{e}_i^\ell(t)\|_{\Omega_i}^2 dt.$$

As the right-hand side tends to 0, this proves the corollary.   □

Now, we prove a convergence result for the pressure. We set $P(t) = \int_0^t p(s)ds$ and $P_i = P|_{\Omega_i}$ and denote the error by $D_i^\ell(t) = (P_i^\ell - P_i)(t)$. Then we can state

Corollary 2.21. *Let all hypotheses of Theorem 2.18 be satisfied. Then for all $t \in [0, T]$ it holds that $\|D_i^\ell(t) - \frac{1}{|\Omega_i|} \int_{\Omega_i} D_i^\ell(t)\|_{L_0^2(\Omega_i)} \to 0$ when $\ell \to \infty$, with $L_0^2(\Omega_i) = \{p \in L^2(\Omega_i), \int_{\Omega_i} p = 0\}$.*

Proof. As $(\mathbf{u}_i, p_i)$ is the strong solution of the Robin problem with B.C. g_{ij}, ξ_{ij}, then P_i verifies a variational formulation similar to (2.30)

$$(\mathbf{u}_i(t), \mathbf{v})_{\Omega_i} - (\mathbf{u}_{0,i}, \mathbf{v})_{\Omega_i} + \int_0^t a_i(\mathbf{u}_i(s), \mathbf{v})ds - (P_i(t), \nabla \cdot \mathbf{v})_{\Omega_i} - \int_0^t c_i(s, \mathbf{v})ds = 0 \tag{2.46}$$
$$\forall \mathbf{v} \in X_i.$$

Then, from (2.30) and (2.46), taking the test function $\mathbf{v} \in \left[H_0^1(\Omega_i) \right]^2 \subset X_i$, the boundary terms in $c_i^\ell(s, \mathbf{v})$ and $c_i(s, \mathbf{v})$ vanish and then $c_i^\ell(s, \mathbf{v}) - c_i(s, \mathbf{v})$ also vanishes. Then we get

$$(D_i^\ell(t), \nabla \cdot \mathbf{v})_{\Omega_i} = (\mathbf{e}_i^\ell(t), \mathbf{v})_{\Omega_i} + \int_0^t a_i(\mathbf{e}_i^\ell(s), \mathbf{v})ds , \forall \mathbf{v} \in \left[H_0^1(\Omega_i) \right]^2. \tag{2.47}$$

As $(c, \nabla \cdot \mathbf{v})_{\Omega_i} = 0$ for all constants c and $\mathbf{v} \in \left[H_0^1(\Omega_i) \right]^2$, the above formulation implies

$$(D_i^\ell(t) - \frac{1}{|\Omega_i|} \int_{\Omega_i} D_i^\ell(t), \nabla \cdot \mathbf{v})_{\Omega_i} = (\mathbf{e}_i^\ell(t), \mathbf{v})_{\Omega_i} + \int_0^t a_i(\mathbf{e}_i^\ell(s), \mathbf{v})ds , \forall \mathbf{v} \in \left[H_0^1(\Omega_i) \right]^2. \tag{2.48}$$

Since $(D_i^\ell - \frac{1}{|\Omega_i|} \int_{\Omega_i} D_i^\ell) \in L_0^2(\Omega_i)$, we recall that the divergence mapping from $\left[H_0^1(\Omega_i) \right]^2$ to $L_0^2(\Omega_i)$ satisfies inf-sup condition: there exists γ_3 s.t.

$$\inf_{q \in L_0^2(\Omega_i)} \sup_{\mathbf{v} \in [H_0^1(\Omega_i)]^2} \frac{\int_\Omega q \nabla \cdot \mathbf{v}}{\|\mathbf{v}\|_{[H_0^1(\Omega_i)]^2} \|q\|_{L_0^2(\Omega_i)}} = \gamma_3 > 0. \tag{2.49}$$

Hence

$$\|D_i^\ell - \frac{1}{|\Omega_i|} \int_{\Omega_i} D_i^\ell\|_{L_0^2(\Omega_i)} \le \frac{1}{\gamma_3} \sup_{\mathbf{v} \in [H_0^1(\Omega_i)]^2} \frac{|(\mathbf{e}_i^\ell(t), \mathbf{v})_{\Omega_i} + \int_0^t a_i(\mathbf{e}_i^\ell(s), \mathbf{v})ds|}{\|\mathbf{v}\|_{[H_0^1(\Omega_i)]^2}}$$

We apply again the continuity of $a_i(.,.)$

$$|\int_0^t a_i(\mathbf{e}_i^\ell(s),\mathbf{v})|ds \leq M_i \int_0^t \|\mathbf{e}_i^\ell(s)\|_{X_i} \|\mathbf{v}\|_{X_i} ds \leq M_i \|\mathbf{v}\|_{[H_0^1(\Omega_i)]^2} \sqrt{T} \|\mathbf{e}_i^\ell\|_{L^2((0,T),X_i)}$$

as well as the fact that, for all $\mathbf{v} \in \left[H_0^1(\Omega_i)\right]^2$

$$|\left(\mathbf{e}_i^\ell(t),\mathbf{v}\right)_{\Omega_i}| \leq \|\mathbf{e}_i^\ell(t)\|_{\Omega_i} \|\mathbf{v}\|_{\Omega_i} \leq C_{P_i} \|\mathbf{e}_i^\ell(t)\|_{\Omega_i} \|\mathbf{v}\|_{[H_0^1(\Omega_i)]^2}$$

Therefore

$$\|D_i^\ell - \frac{1}{|\Omega_i|} \int_{\Omega_i} D_i^\ell\|_{L_0^2(\Omega_i)} \leq \frac{1}{\gamma_3}\left[C_{P_i}\|\mathbf{e}_i^\ell(t)\|_{\Omega_i} + M_i\sqrt{T}\|\mathbf{e}_i^\ell\|_{L^2((0,T),X_i)}\right]$$

From the convergence of the velocity, we get the corollary. $\square$

2.6   Recovering the pressure

We introduce the notation $\langle p \rangle_{\mathcal{O}} = \frac{1}{|\mathcal{O}|} \int_{\mathcal{O}} p \, dx$ for the mean value of a function on a domain $\mathcal{O}$ (whatever the space dimension of $\mathcal{O}$).

   We denote by $d_i^\ell := p_i - p^\ell$. In the previous section. In this section, we suppose that, for a.e $t \in (0,T)$

- $\|d_i^\ell - \langle d_i^\ell \rangle_{\Omega_i}\|_{\Omega_i} \longrightarrow 0$ for all i when $\ell \longrightarrow +\infty$

- $(\langle d_i^\ell \rangle_{\Gamma_{ij}} - \langle d_i^\ell \rangle_{\Omega_i})$ tends to 0 for all i, all Γ_{ij}, when $\ell \longrightarrow +\infty$

- $\left(\langle h_{ij}^\ell \rangle_{\Gamma_{ij}} + \alpha_{ij}\langle d_i^\ell \rangle_{\Gamma_{ij}}\right) \longrightarrow 0$ for all i, all Γ_{ij}, when $\ell \longrightarrow +\infty$

where h_{ij}^ℓ is defined in (2.40).

Remark 2.22. *Those above hypothesis can be implied from the stronger regularity and convergence of the velocity. Indeed, suppose that $(\mathbf{e}_i^\ell, d_i^\ell)$ is the strong solution of the following Robin problem*

$$
\begin{aligned}
\partial_t \mathbf{e}_i^\ell - \nu\Delta\mathbf{e}_i^\ell + \nabla d_i^\ell &= 0 & in & \quad \Omega_i \times (0,T) \\
\nabla\cdot\mathbf{e}_i^\ell &= 0 & in & \quad \Omega_i \times (0,T) \\
\mathbf{e}_i^\ell(.,t=0) &= 0 & in & \quad \Omega_i \\
\mathbf{e}_i^\ell &= 0 & on & \quad (\partial\Omega \cap \partial\Omega_i) \times (0,T) \\
\alpha_{ij}(\nu\partial_{\mathbf{n}_{ij}}\mathbf{e}_i^\ell \cdot \mathbf{n}_{ij} - d_i^\ell) + \mathbf{e}_i^\ell \cdot \mathbf{n}_{ij} &= h_{ij}^\ell & on & \quad \Gamma_{ij} \times (0,T) \\
\beta_{ij}\nu\partial_{\mathbf{n}_{ij}}\mathbf{e}_i^\ell \times \mathbf{n} + \mathbf{e}_i^\ell \times \mathbf{n}_{ij} &= \zeta_{ij}^\ell & on & \quad \Gamma_{ij} \times (0,T)
\end{aligned}
$$

with the following convergence

$$\|\mathbf{e}_i^\ell\|_{L^\infty((0,T),[H^2(\Omega_i)]^2)} \longrightarrow 0, \quad \|\partial_t\mathbf{e}_i^\ell\|_{L^\infty((0,T),[L^2(\Omega_i)]^2)} \longrightarrow 0.$$

From this, we get, for a.e. $t \in (0,T)$, $\|\nabla d_i^\ell(t)\|_{\Omega_i} \longrightarrow 0$, which implies the first and second hypothesis.
This also implies the convergence of trace of the velocity: for a.e. $t \in (0,T)$, we have $\|\alpha_{ij}\nu\partial_{\mathbf{n}_{ij}}\mathbf{e}_i^\ell(t)\cdot\mathbf{n}_{ij} + \mathbf{e}_i^\ell(t)\cdot\mathbf{n}_{ij}\|_{\Gamma_{ij}} \longrightarrow 0$ that leads to the third hypothesis.

One can rewrite these three hypothesis on the error as

$$\|(p_i^\ell - p_i) - (\langle p_i^\ell \rangle_{\Omega_i} - \langle p_i \rangle_{\Omega_i})\|_{\Omega_i} \longrightarrow 0, \tag{2.50}$$

$$(\langle p_i^\ell - p_i \rangle_{\Gamma_{ij}}) - (\langle p_i^\ell - p_i \rangle_{\Omega_i}) \longrightarrow 0, \tag{2.51}$$

$$\left[\langle g_{ij}^\ell \rangle_{\Gamma_{ij}} - \langle g_{ij} \rangle_{\Gamma_{ij}} \right] + \alpha_{ij} \langle p_i^\ell - p_i \rangle_{\Gamma_{ij}} \longrightarrow 0. \tag{2.52}$$

Expression (2.50) shows that $p_i^\ell(t)$ will tend to $p_i(t)$ if and only if the mean-value of $p_i^\ell(t)$ on Ω_i tends to the mean value of $p_i(t)$. However, no constraint was imposed on the mean-value of $p_i^\ell(t)$ in the algorithm, since, thanks to the Robin boundary conditions, such constraint is not necessary to obtain local well-posed problems at each iteration. In Section 2.4, we observed cases in which p_i^ℓ does not converge to the monodomain solution p_i. In this section, we build a modified pressure $\tilde{p}_i^\ell$ such that $\tilde{p}_i^\ell(t)$ tends to $p_i(t)$ in $L^2(\Omega_i)$, $i = 1, \ldots, M$.

Then, we are interested first in the mean-value of $p_i(t)$, which we denote by $X_i(t) := \langle p_i(t) \rangle_{\Omega_i}$. Then, we rewrite (2.50) using these notations as

$$\|(p_i^\ell(t) - \langle p_i^\ell(t) \rangle_{\Omega_i} + X_i(t)) - p_i(t)\|_{L^2(\Omega_i)} \longrightarrow 0. \tag{2.53}$$

when $\ell \to \infty$.

From (2.53), we see that the right approximation to calculate at each iteration (that tends to $p_i(t)$) is $(p_i^\ell(t) - \langle p_i^\ell(t) \rangle_{\Omega_i} + X_i(t))$. However, we do not know how to calculate X_i, and thus to calculate $p_i^\ell(t) - \langle p_i^\ell(t) \rangle_{\Omega_i} + X_i(t)$ in (2.53). A similar question was raised in the thesis of Lissoni [87, Theorem IV.3.9] at the discrete level, within a Schwarz algorithm applied at each time step of a time marching scheme for the numerical approximation of the incompressible Navier-Stokes equations.

We introduce below a new quantity $Y_i^\ell(t)$, fully computable at any given iteration ℓ, that tends to $X_i(t)$ when ℓ tends to infinity, from which we will define $\tilde{p}_i^\ell$ which tends to p_i in $L^2(\Omega_i)$.

To ease the presentation, we shall set $|\Gamma_{ij}| = 0$, $\alpha_{ij} = 0$ and $g_{ij}^\ell = 0$ if $j \notin \mathscr{I}_i$. Moreover, we introduce the constant matrix

$$A = (a_{ij})_{1 \le i,j \le M}, \quad \text{with} \quad a_{ii} = \sum_{j=1, j \neq i}^M |\Gamma_{ij}| \alpha_{ij}, \text{ and } a_{ij} = -|\Gamma_{ji}| \alpha_{ji} \text{ if } j \neq i$$

together with the constant vector $C = (|\Omega_1|, |\Omega_2|, \ldots, |\Omega_M|)$ and the sequence of vectors $(B^\ell)_\ell$, with $B^\ell = (B_1^\ell, B_2^\ell, \ldots, B_M^\ell)^t$ defined as

$$B_i^\ell = \sum_{j=1}^M |\Gamma_{ij}| \left[\langle g_{ij}^\ell \rangle_{\Gamma_{ij}} + \alpha_{ij} \langle p_i^\ell \rangle_{\Omega_i} \right] - \sum_{j=1}^M |\Gamma_{ji}| \left[\langle g_{ji}^\ell \rangle_{\Gamma_{ji}} + \alpha_{ji} \langle p_j^\ell \rangle_{\Omega_j} \right]$$

Theorem 2.23. *We recall that we are in the case $\alpha_{ij} = \alpha_{ji}$, hence A is symmetric. We have the following*

(i) For all ℓ, the following system

$$\begin{aligned} AY^\ell &= B^\ell, \\ CY^\ell &= 0, \end{aligned} \tag{2.54}$$

has a unique solution $Y^\ell \in \mathbb{R}^M$.

(ii) Moreover, we have $Y^\ell \to X := (X_1, X_2, \cdots, X_M)$ *in* $\mathbb{R}^M$, *and for all* t

$$\|\tilde{p}_i^\ell - p_i\|_{L^2(\Omega_i)} \longrightarrow 0, \quad \text{when } \ell \to \infty, \quad \text{with } \tilde{p}_i^\ell(t) := p_i^\ell(t) - \langle p_i^\ell(t)\rangle_{\Omega_i} + Y_i^\ell(t). \tag{2.55}$$

Proof of (i). The proof of Theorem 2.23–*(i)* relies on two main steps:

  (a) Existence of solutions to the system $AY^\ell = B^\ell$,

  (b) Existence and uniqueness of a solution to system (2.54) thanks to the additional constraint $CY^\ell = 0$.

Let us start with (a). Since A is symmetric, existence of at least one solution to the system $AY^\ell = B^\ell$ is equivalent to proving that $B^\ell \in \text{Im}(A) = (\text{Ker}(A))^\perp$. Therefore, we first start with the determination of $\text{Ker}(A)$.

Let $Y = (Y_1, Y_2, \ldots, Y_M)^t \in \text{Ker}(A)$. We have $\displaystyle\sum_{j=1}^{M} a_{ij} Y_j = 0$, for all $i = 1, 2, \ldots, M$. As $\alpha_{ij} = \alpha_{ji}$, we have $\displaystyle a_{ii} = -\sum_{j=1, j\neq i}^{M} a_{ij}$, which implies

$$0 = \sum_{j=1}^{M} a_{ij} Y_j Y_i = \sum_{j=1, j\neq i}^{M} a_{ij} Y_j Y_i + a_{ii} Y_i^2 = \sum_{j=1, j\neq i}^{M} a_{ij}(Y_j Y_i - Y_i^2).$$

Summing the above expression in i, and with $a_{ij} = a_{ji}$, we obtain

$$\sum_{i=1}^{M} \sum_{j=1, j\neq i}^{M} a_{ij}(Y_j Y_i - Y_i^2) = \sum_{i<j} a_{ij}(Y_i - Y_j)^2 = 0.$$

As $a_{ij} \leq 0$ for all (i,j) with $i \neq j$, and $a_{ij} < 0$ as soon as subdomains i and j are neighbours, this implies that $Y_i = Y_j$ for any pair of neighbouring subdomains i and j. Since Ω is connected, this finally implies that all Y_i are equal i.e. $\text{Ker}(A) = \text{vect}(\mathbf{e})$ with $\mathbf{e} = (1, 1, \ldots, 1, 1)$. Then, $B^\ell \in (\text{Ker}(A))^\perp$ is simply equivalent to $B^\ell \cdot \mathbf{e} = \displaystyle\sum_{i=1}^{M} B_i^\ell = 0$.

This is proved in the following way:

$$\sum_{i=1}^{M} B_i^\ell = \sum_{i=1}^{M} \left[\sum_{j=1}^{M} |\Gamma_{ij}| \left(\langle g_{ij}^\ell \rangle_{\Gamma_{ij}} + \alpha_{ij} \langle p_i^\ell \rangle_{\Omega_i} \right) - \sum_{j=1}^{M} |\Gamma_{ji}| \left(\langle g_{ji}^\ell \rangle_{\Gamma_{ji}} + \alpha_{ji} \langle p_j^\ell \rangle_{\Omega_j} \right) \right]$$

$$= \sum_{i=1}^{M} \sum_{j=1}^{M} |\Gamma_{ij}| \langle g_{ij}^\ell \rangle_{\Gamma_{ij}} + \sum_{i=1}^{M} \sum_{j=1}^{M} |\Gamma_{ij}| \alpha_{ij} \langle p_i^\ell \rangle_{\Omega_i}$$

$$\qquad - \sum_{i=1}^{M} \sum_{j=1}^{M} |\Gamma_{ji}| \langle g_{ji}^\ell \rangle_{\Gamma_{ji}} - \sum_{i=1}^{M} \sum_{j=1}^{M} |\Gamma_{ji}| \alpha_{ji} \langle p_j^\ell \rangle_{\Omega_j}$$

$$= \sum_{1 \leq i,j \leq M} |\Gamma_{ij}| \langle g_{ij}^\ell \rangle_{\Gamma_{ij}} - \sum_{1 \leq i,j \leq M} |\Gamma_{ji}| \langle g_{ji}^\ell \rangle_{\Gamma_{ji}}$$

$$\qquad + \sum_{i=1}^{M} \left(\sum_{j=1}^{M} |\Gamma_{ij}| \alpha_{ij} \right) \langle p_i^\ell \rangle_{\Omega_i} - \sum_{j=1}^{M} \left(\sum_{i=1}^{M} |\Gamma_{ji}| \alpha_{ji} \right) \langle p_j^\ell \rangle_{\Omega_j}.$$

By denoting $Q_i = \sum_{j=1}^{M} |\Gamma_{ij}| \alpha_{ij}$, we get

$$\sum_{i=1}^{M} B_i^\ell = \sum_{i=1}^{M} Q_i \langle p_i^\ell \rangle_{\Omega_i} - \sum_{j=1}^{M} Q_j \langle p_j^\ell \rangle_{\Omega_j} = 0.$$

Let us now turn to (b). From (a), we know that there exists at least a solution to $AY^\ell = B^\ell$. Moreover, let Y^* be a given solution to this system; all other solutions may be written as $Y = Y^* + \mu \mathbf{e}$, with $\mu \in \mathbb{R}$. Existence and uniqueness of the solution to (2.54) follows from the fact that $C\mathbf{e} = |\Omega| \neq 0$: we have $CY = CY^* + \mu C\mathbf{e}$ and then, as $CY^\ell = 0$, it follows that $Y^\ell = Y^* - \dfrac{CY^*}{|\Omega|} \mathbf{e}$. This ends the proof of Theorem 2.23–(i). $\square$

Proof of Theorem 2.23–(ii). It relies on the two main results:

(c) $B^\ell \to AX$ in $\mathbb{R}^M$,

(d) $CX = 0$.

Let us prove (c): from the divergence-free property of $\mathbf{u}_i$, we have

$$0 = \int_{\Omega_i} \nabla \cdot \mathbf{u}_i = \int_{\partial \Omega_i} \mathbf{u}_i \cdot \mathbf{n}_{\partial \Omega_i} = \sum_{j \in \mathscr{I}_i} \int_{\Gamma_{ij}} \mathbf{u}_i \cdot \mathbf{n}_{ij}. \tag{2.56}$$

Moreover, from the definition of g_{ij} in (2.34) and the physical transmission conditions (2.6), we have

$$|\Gamma_{ij}| \langle g_{ij} \rangle_{\Gamma_{ij}} - |\Gamma_{ji}| \langle g_{ji} \rangle_{\Gamma_{ji}} = \int_{\Gamma_{ij}} (g_{ij} - g_{ji}) = 2 \int_{\Gamma_{ij}} \mathbf{u}_i \cdot \mathbf{n}_{ij}. \tag{2.57}$$

Hence, from (2.56) and (2.57) we get

$$\sum_{j \in \mathscr{I}_i} |\Gamma_{ij}| \langle g_{ij} \rangle_{\Gamma_{ij}} = \sum_{j \in \mathscr{I}_i} |\Gamma_{ji}| \langle g_{ji} \rangle_{\Gamma_{ji}}. \tag{2.58}$$

(2.52) is equivalent to

$$\langle g_{ij}^\ell \rangle_{\Gamma_{ij}} + \alpha_{ij} \langle p_i^\ell - p_i \rangle_{\Gamma_{ij}} \longrightarrow \langle g_{ij} \rangle_{\Gamma_{ij}}. \tag{2.59}$$

From (2.51), we may replace $\langle p_i^\ell - p_i \rangle_{\Gamma_{ij}}$ by $\langle p_i^\ell - p_i \rangle_{\Omega_i}$ in (2.59), then multiply by $|\Gamma_{ij}|$ and sum over $j \in \mathscr{I}_i$ for a given i to obtain

$$\sum_{j \in \mathscr{I}_i} |\Gamma_{ij}| \left[\langle g_{ij}^\ell \rangle_{\Gamma_{ij}} + \alpha_{ij} \langle p_i^\ell - p_i \rangle_{\Omega_i} \right] \longrightarrow \sum_{j \in \mathscr{I}_i} |\Gamma_{ij}| \langle g_{ij} \rangle_{\Gamma_{ij}}. \tag{2.60}$$

In exactly the same way, we also obtain

$$\sum_{j \in \mathscr{I}_i} |\Gamma_{ji}| \left[\langle g_{ji}^\ell \rangle_{\Gamma_{ji}} + \alpha_{ji} \langle p_j^\ell - p_j \rangle_{\Omega_j} \right] \longrightarrow \sum_{j \in \mathscr{I}_i} |\Gamma_{ji}| \langle g_{ji} \rangle_{\Gamma_{ji}}. \tag{2.61}$$

Using (2.60), (2.61) and (2.58), we obtain

$$\sum_{j \in \mathscr{I}_i} |\Gamma_{ij}| \left[\langle g_{ij}^\ell \rangle_{\Gamma_{ij}} + \alpha_{ij} \langle p_i^\ell \rangle_{\Omega_i} - \alpha_{ij} \langle p_i \rangle_{\Omega_i} \right]$$

$$-\sum_{j\in\mathscr{I}_i}|\Gamma_{ji}|\Big[\langle g_{ji}^\ell\rangle_{\Gamma_{ji}}+\alpha_{ji}\langle p_j^\ell\rangle_{\Omega_j}-\alpha_{ji}\langle p_j\rangle_{\Omega_j}\Big]\longrightarrow 0,$$

or equivalently

$$\sum_{j\in\mathscr{I}_i}|\Gamma_{ij}|\Big[\langle g_{ij}^\ell\rangle_{\Gamma_{ij}}+\alpha_{ij}\langle p_i^\ell\rangle_{\Omega_i}\Big]-\sum_{j\in\mathscr{I}_i}|\Gamma_{ji}|\Big[\langle g_{ji}^\ell\rangle_{\Gamma_{ji}}+\alpha_{ji}\langle p_j^\ell\rangle_{\Omega_j}\Big]$$
$$\longrightarrow \sum_{j\in\mathscr{I}_i}|\Gamma_{ij}|\alpha_{ij}\langle p_i\rangle_{\Omega_i}-\sum_{j\in\mathscr{I}_i}|\Gamma_{ji}|\alpha_{ji}\langle p_j\rangle_{\Omega_j}.$$

This is exactly $B^\ell\longrightarrow AX$.

Let us now prove (d): We have

$$\int_\Omega p_i=\sum_{i=1}^M\int_{\Omega_i}p_i=\sum_{i=1}^M|\Omega_i|\langle p_i\rangle_{\Omega_i}=0$$

i.e. $CX=0$.

We now prove Theorem 2.23–*(ii)*: From Theorem 2.23–*(i)*, and (c) and (d), we have $A(Y^\ell-X)\longrightarrow 0$ and $C(Y^\ell-X)=0$, which implies that $(Y^\ell-X)\longrightarrow 0$ when $\ell\to\infty$. Then, from (2.53), with a triangle inequality, we get (2.55). $\qquad\square$

Remark 2.24. *In the general case of M subdomains, the calculation of $\tilde{p}_i^\ell$ is done only once, at the last OSWR iteration. It involves solving the coarse problem (2.54) when M > 2, and is given by an explicit formula when M = 2 (see Corollary 2.26), thus the cost of calculating the modified pressure is negligible.*

Remark 2.25. *Recovering the correct pressure could also be performed from the fact that $\nabla(p_i^\ell-p_i)$ tends to zero when $\ell\to\infty$. Indeed, for a given Ω_i, choosing first an arbitrary point $\mathbf{x}_i\in\Omega_i$, then one may write*

$$p_i(\mathbf{x})=p_i(\mathbf{x}_i)+(\mathbf{x}-\mathbf{x}_i)\cdot\int_0^1\nabla p_i(\mathbf{x}_i+t(\mathbf{x}-\mathbf{x}_i))\,dt\ ,\ \forall\mathbf{x}\in\Omega_i.$$

Then, one could replace ∇p_i by ∇p_i^ℓ to obtain approximate values of the pressure at each point $\mathbf{x}$. However, this formula holds on a given subdomain Ω_i. In order to relate values of the pressures in Ω_i to those in a neighboring subdomain Ω_j through this kind of formula, one needs to choose a point on the boundary Γ_{ij} that will serve as the point $\mathbf{x}_j$ in the subdomain Ω_j, and so on. At the discrete level, there are several drawbacks to that: this requires further communications between subdomains, the pressure gradient at the boundaries may not be easy to define (e.g. when the pressure is defined as a piecewise constant field like in the Crouzeix-Raviart finite element), and finally there are many ways to go from one cell to another in the mesh, and, due to round-off errors, this may lead to different evaluations of the pressure at a given cell in particular in very large scale computations.

In the two-subdomain case, the calculation of $\tilde{p}_i^\ell$ can be done by the following explicit formula.

Corollary 2.26. *Let M = 2, in which case we denote by $_1$ and $_2$ instead of $_{12}$ and $_{21}$ and $\Gamma=\Gamma_{12}=\Gamma_{21}$. We recall also that we are in the case $\alpha=\alpha_{12}=\alpha_{21}$. We define, for $i=1,2$ and $j=3-i$,*

$$\tilde{p}_i^\ell=p_i^\ell+\frac{|\Omega_j|}{|\Omega|}\Big[\frac{1}{\alpha}(\langle g_i^\ell\rangle_\Gamma-\langle g_j^\ell\rangle_\Gamma)\Big]-\frac{|\Omega_i|}{|\Omega|}\langle p_i^\ell\rangle_{\Omega_i}-\frac{|\Omega_j|}{|\Omega|}\langle p_j^\ell\rangle_{\Omega_j}.$$

Then $\tilde{p}_i^\ell$ tends to p_i when ℓ tends to infinity.

Proof. For $M = 2$ we have

$$B_1^\ell = -B_2^\ell = |\Gamma| \left[\langle g_1^\ell \rangle_\Gamma + \alpha \langle p_1 \rangle_{\Omega_1} \right] - |\Gamma| \left[\langle g_2^\ell \rangle_\Gamma + \alpha \langle p_2 \rangle_{\Omega_2} \right],$$
$$\mathbf{A} = \begin{bmatrix} \alpha|\Gamma| & -\alpha|\Gamma| \\ -\alpha|\Gamma| & \alpha|\Gamma| \end{bmatrix},$$
$$C = \left[|\Omega_1| \quad |\Omega_2| \right].$$

System (2.54) for $M = 2$ has unique solution given by

$$Y_1^\ell = \frac{|\Omega_2|}{|\Omega|} \left[\frac{1}{\alpha} (\langle g_1^\ell \rangle_\Gamma - \langle g_2^\ell \rangle_\Gamma) + (\langle p_1^\ell \rangle_{\Omega_1} - \langle p_2^\ell \rangle_{\Omega_2}) \right],$$
$$Y_2^\ell = \frac{|\Omega_1|}{|\Omega|} \left[\frac{1}{\alpha} (\langle g_2^\ell \rangle_\Gamma - \langle g_1^\ell \rangle_\Gamma) + (\langle p_2^\ell \rangle_{\Omega_2} - \langle p_1^\ell \rangle_{\Omega_1}) \right].$$

From theorem 2.23, we have

$$p_1^\ell - \langle p_1^\ell \rangle_{\Omega_1} + Y_1^\ell = p_1^\ell + \frac{|\Omega_2|}{|\Omega|} \left[\frac{1}{\alpha} (\langle g_1^\ell \rangle_\Gamma - \langle g_2^\ell \rangle_\Gamma) \right] - \frac{|\Omega_1|}{|\Omega|} \langle p_1^\ell \rangle_{\Omega_1} - \frac{|\Omega_2|}{|\Omega|} \langle p_2^\ell \rangle_{\Omega_2} \to p_1$$
$$p_2^\ell - \langle p_2^\ell \rangle_{\Omega_2} + Y_2^\ell = p_2^\ell + \frac{|\Omega_1|}{|\Omega|} \left[\frac{1}{\alpha} (\langle g_2^\ell \rangle_\Gamma - \langle g_1^\ell \rangle_\Gamma) \right] - \frac{|\Omega_1|}{|\Omega|} \langle p_1^\ell \rangle_{\Omega_1} - \frac{|\Omega_2|}{|\Omega|} \langle p_2^\ell \rangle_{\Omega_2} \to p_2$$

$\square$

2.7 Convergence factor via Fourier transform

In this Section, differently from what was presented in Chapter one, we do not intend to study rigorously the convergence of the OSWR iterative process through Fourier transforms. We proved convergence of the velocity via energy estimates in Section 2.5 and showed how to recover the pressure in Section 2.6. The aim here is to find a way to choose conveniently the parameters (α, β) that play an important role in the actual rate of convergence in numerical experiments.

Consider $\Omega = \mathscr{R}^2$. We consider two subdomains, in which case we denote by $_1$ and $_2$ instead of $_{12}$ and $_{21}$ and $\Gamma = \Gamma_{12} = \Gamma_{21} = \{x = 0\} \times \mathbb{R}$. We denote $\mathbf{u} = (u, v)$ the two components of the velocity, $\mathbf{f} = (f_1, f_2)$. Recall here the Stokes problem

$$\begin{aligned}
\partial_t u - \nu \Delta u + \partial_x p &= f_x && \text{in} && \Omega \times (0, T) \\
\partial_t v - \nu \Delta v + \partial_y p &= f_y && \text{in} && \Omega \times (0, T) \\
\partial_x u + \partial_y v &= 0 && \text{in} && \Omega \times (0, T) \\
u(., t = 0) &= u_0 && \text{in} && \Omega \\
v(., t = 0) &= v_0 && \text{in} && \Omega \\
u, v &\to 0 && \text{when} && |(x, y)| \to \infty
\end{aligned}$$

To simplify notations, we do not use g_i^ℓ, ζ_i^ℓ, we write the OSWR algorithm as follows:

starting with u_i^0, v_i^0, p_i^0, at step $\ell \geq 1$, provided $u_i^{\ell-1}, v_i^{\ell-1}, p_i^{\ell-1}$ we solve

$$
\begin{array}{llll}
\partial_t u_1^\ell - \nu \Delta u_1^\ell + \partial_x p_1^\ell & = f_x & \text{in} & \Omega \times (0,T) \\
\partial_t v_1^\ell - \nu \Delta v_1^\ell + \partial_y p_1^\ell & = f_y & \text{in} & \Omega \times (0,T) \\
\partial_x u_1^\ell + \partial_y v_1^\ell & = 0 & \text{in} & \Omega \times (0,T) \\
u_1^\ell(.,t=0) & = u_0 & \text{in} & \Omega \\
v_1^\ell(.,t=0) & = v_0 & \text{in} & \Omega \\
\alpha_1(\nu \partial_x u_1^\ell - p_1^\ell) + u_1^\ell & = \alpha_1(\nu \partial_x u_2^{\ell-1} - p_2^{\ell-1}) + u_2^{\ell-1} & \text{on} & \Gamma \times (0,T) \\
\nu \beta_1 \partial_x v_1^\ell + v_1^\ell & = \nu \beta_1 \partial_x v_2^{\ell-1} + v_2^{\ell-1} & \text{on} & \Gamma \times (0,T) \\
u_1^\ell, v_1^\ell & \to 0 & \text{when} & |(x,y)| \to \infty
\end{array}
$$

and

$$
\begin{array}{llll}
\partial_t u_2^\ell - \nu \Delta u_2^\ell + \partial_x p_2^\ell & = f_x & \text{in} & \Omega \times (0,T) \\
\partial_t v_2^\ell - \nu \Delta v_2^\ell + \partial_y p_2^\ell & = f_y & \text{in} & \Omega \times (0,T) \\
\partial_x u_2^\ell + \partial_y v_2^\ell & = 0 & \text{in} & \Omega \times (0,T) \\
u_2^\ell(.,t=0) & = u_0 & \text{in} & \Omega \\
v_2^\ell(.,t=0) & = v_0 & \text{in} & \Omega \\
\alpha_2(\nu \partial_x u_2^\ell - p_2^\ell) - u_2^\ell & = \alpha_2(\nu \partial_x u_1^{\ell-1} - p_1^{\ell-1}) - u_1^{\ell-1} & \text{on} & \Gamma \times (0,T) \\
\nu \beta_2 \partial_x v_2^\ell - v_2^\ell & = \beta_2 \partial_x v_1^{\ell-1} - v_1^{\ell-1} & \text{on} & \Gamma \times (0,T) \\
u_2^\ell, v_2^\ell & \to 0 & \text{when} & |(x,y)| \to \infty
\end{array}
$$

By linearity, let $f_x = f_y = 0$ and $u_0 = v_0 = 0$ and u, v, p below denote the errors.

Taking the Fourier transform in time and in y-direction with time frequency ω and space frequency k, and, for simplicity, we still keep notations u, v instead of $\hat{u}, \hat{v}$, we get

$$i\omega u_1^\ell - \nu \partial_{xx} u_1^\ell + \nu k^2 u_1^\ell + \partial_x p = 0 \tag{2.62a}$$

$$i\omega v_1^\ell - \nu \partial_{xx} v_1^\ell + \nu k^2 v_1^\ell + ikp = 0 \tag{2.62b}$$

$$\partial_x u_1^\ell + ik v_1^\ell = 0 \tag{2.62c}$$

Take $\dfrac{\partial}{\partial x}(2.62a) + ik(2.62b)$ we obtain

$$i\omega \left(\partial_x u_1^\ell + ik v_1^\ell\right) - \nu \partial_{xx}\left(\partial_x u_1^\ell + ik v_1^\ell\right) + \nu k^2 \left(\partial_x u_1^\ell + ik v_1^\ell\right) + \partial_{xx} p_1^\ell - k^2 p_1^\ell = 0$$

By using (2.62c), the above equation becomes an equation involving only the pressure

$$\partial_{xx} p_1^\ell - k^2 p_1^\ell = 0 \tag{2.63}$$

whose general solution is given by

$$p_1^\ell = A^\ell \exp(|k|x) + B^\ell \exp(-|k|x).$$

As p_1^ℓ must be bounded at $x = -\infty$, this implies that $B^\ell = 0$. Thus, we have

$$p_1^\ell = A^\ell \exp(|k|x). \tag{2.64}$$

Next, equation (2.62a) can be written as

$$i\omega u_1^\ell - \nu \left(\partial_{xx} u_1^\ell - k^2 u_1^\ell\right) = -A^\ell |k| \exp(|k|x)$$

which is equivalent to

$$\partial_{xx} u_1^\ell - \left(k^2 + \frac{i\omega}{\nu} \right) u_1^\ell = \frac{A^\ell}{\nu} |k| \exp(|k|x). \tag{2.65}$$

Denote by λ the square root of $k^2 + \dfrac{i\omega}{\nu}$ with positive real part, then the solution of the homogeneous equation is given by

$$u_1^\ell = C^\ell \exp(\lambda x) + D^\ell \exp(-\lambda x).$$

As u_1^ℓ tends to 0 at infinity, the solution u_1^ℓ of the homogeneous equation is

$$u_1^\ell = C^\ell \exp(\lambda x) \tag{2.66}$$

On the other hand, we assume that one special solution of (2.65) has the form $u_{1,s}^\ell = C_s^\ell \exp(|k|x)$. We insert this solution into (2.65) and we get

$$k^2 C_s^\ell \exp(|k|x) - \lambda^2 C_s^\ell \exp(|k|x) = \frac{A^\ell}{\nu} |k| \exp(|k|x)$$

i.e.

$$-\frac{i\omega}{\nu} C_s^\ell \exp(|k|x) = \frac{A^\ell}{\nu} |k| \exp(|k|x)$$

then

$$C_s^\ell = \frac{i|k|A^\ell}{\omega}.$$

As a result, the general solution of (2.65) is given by

$$u_1^\ell = \frac{i|k|A^\ell}{\omega} \exp(|k|x) + C^\ell \exp(\lambda x). \tag{2.67}$$

We can now replace $v_1^\ell = \dfrac{i}{k} \partial_x u_1^\ell$ to get

$$v_1^\ell = \frac{-kA^\ell}{\omega} \exp(|k|x) + D^\ell \exp(\lambda x). \tag{2.68}$$

with

$$\lambda C^\ell = -ikD^\ell. \tag{2.69}$$

For $u_2^\ell, v_2^\ell, p_2^\ell$, we replace $|k|$ by $-|k|$, λ by $-\lambda$ then we get

$$p_2^\ell = B^\ell \exp(-|k|x) \tag{2.70}$$

$$u_2^\ell = \frac{-i|k|B^\ell}{\omega} \exp(-|k|x) + E^\ell \exp(-\lambda x) \tag{2.71}$$

$$v_2^\ell = \frac{-kB^\ell}{\omega} \exp(-|k|x) + F^\ell \exp(-\lambda x). \tag{2.72}$$

with the same relation

$$(-\lambda)E^\ell = -ikF^\ell. \tag{2.73}$$

On $\Gamma \times (0, T)$, in the Robin B.C., we replace $(u_1^\ell, v_1^\ell, p_1^\ell)$ and $(u_2^\ell, v_2^\ell, p_2^\ell)$ in terms of (A^ℓ, C^ℓ, D^ℓ) and (B^ℓ, E^ℓ, F^ℓ) respectively, we get

$$\alpha_1\left(\nu\frac{ik^2 A^\ell}{\omega} + \nu\lambda C^\ell - A^\ell\right) + \frac{i|k|A^\ell}{\omega} + C^\ell$$

$$= \alpha_1\left(\nu\frac{ik^2 B^{\ell-1}}{\omega} + \nu(-\lambda)E^{\ell-1} - B^{\ell-1}\right) + \frac{i(-|k|)B^{\ell-1}}{\omega} + E^{\ell-1}$$

$$\beta_1\nu\left(\frac{-k|k|A^\ell}{\omega} + \lambda D^\ell\right) + \left(\frac{-kA^\ell}{\omega} + D^\ell\right)$$

$$= \beta_1\nu\left(\frac{-k(-|k|)B^{\ell-1}}{\omega} + (-\lambda)F^{\ell-1}\right) + \left(\frac{-kB^{\ell-1}}{\omega} + F^{\ell-1}\right)$$

Reordering the terms, in each side, and using (2.69) and (2.73) we get

$$\left(\alpha_1(\nu\frac{ik^2}{\omega} - 1) + \frac{i|k|}{\omega}\right)A^\ell + \left(-\alpha_1\nu ik - \frac{ik}{\lambda}\right)D^\ell$$

$$= \left(\alpha_1(\nu\frac{i|k|^2}{\omega} - 1) - \frac{i|k|}{\omega}\right)B^{\ell-1} + \left(-\alpha_1\nu ik + \frac{ik}{\lambda}\right)F^{\ell-1}$$

$$\left(-\beta_1\nu\frac{k|k|}{\omega} - \frac{k}{\omega}\right)A^\ell + (\beta_1\nu\lambda + 1)D^\ell$$

$$= \left(\beta_1\nu\frac{k|k|}{\omega} - \frac{k}{\omega}\right)B^{\ell-1} + (-\beta_1\nu\lambda + 1)F^{\ell-1}$$

This boundary condition can be written in the matrix form

$$\mathcal{M}(\alpha_1, \beta_1)\begin{pmatrix} A^\ell \\ D^\ell \end{pmatrix} = \mathcal{N}(\alpha_1, \beta_1)\begin{pmatrix} B^{\ell-1} \\ F^{\ell-1} \end{pmatrix} \tag{2.74}$$

where

$$\mathcal{M}(\alpha_1, \beta_1) = \begin{pmatrix} \alpha_1(\nu\frac{ik^2}{\omega} - 1) + \frac{i|k|}{\omega} & -\alpha_1\nu ik - \frac{ik}{\lambda} \\ -\beta_1\nu\frac{k|k|}{\omega} - \frac{k}{\omega} & \beta_1\nu\lambda + 1 \end{pmatrix} \tag{2.75}$$

and

$$\mathcal{N}(\alpha_1, \beta_1) = \begin{pmatrix} \alpha_1(\nu\frac{ik^2}{\omega} - 1) - \frac{i|k|}{\omega} & -\alpha_1\nu ik + \frac{ik}{\lambda} \\ \beta_1\nu\frac{k|k|}{\omega} - \frac{k}{\omega} & -\beta_1\nu\lambda + 1 \end{pmatrix} \tag{2.76}$$

Doing the same for Robin B.C of Ω_2, we get

$$\alpha_2\left(\nu\frac{ik^2 B^\ell}{\omega} - \nu\lambda E^\ell - B^\ell\right) + \frac{i|k|B^\ell}{\omega} - E^\ell$$

$$= \alpha_2\left(\nu\frac{ik^2 A^{\ell-1}}{\omega} + \nu\lambda C^{\ell-1} - A^{\ell-1}\right) - \frac{i|k|A^{\ell-1}}{\omega} - C^{\ell-1}$$

$$\beta_2\nu\left(\frac{k|k|B^\ell}{\omega} - \lambda F^\ell\right) - \left(\frac{-kB^\ell}{\omega} + F^\ell\right)$$

$$= \beta_2\nu\left(\frac{-k|k|A^{\ell-1}}{\omega} + \lambda D^{\ell-1}\right) - \left(\frac{-kA^{\ell-1}}{\omega} + D^{\ell-1}\right)$$

Using the relation, in the matrix form, this boundary condition can be written as

$$\mathscr{M}(\alpha_2, \beta_2)\begin{pmatrix} B^\ell \\ F^\ell \end{pmatrix} = \mathscr{N}(\alpha_2, \beta_2)\begin{pmatrix} A^{\ell-1} \\ D^{\ell-1} \end{pmatrix} \tag{2.77}$$

where $\mathscr{M}(\alpha_2, \beta_2)$ and $\mathscr{N}(\alpha_2, \beta_2)$ are defined by replacing parameters (α_1, β_1) in (2.75) and (2.76) by (α_2, β_2).
By using (2.74) and (2.77), we obviously get

$$\begin{pmatrix} A^\ell \\ D^\ell \end{pmatrix} = \mathscr{R}(\alpha_1, \alpha_2, \beta_1, \beta_2)\begin{pmatrix} A^{\ell-2} \\ D^{\ell-2} \end{pmatrix} \tag{2.78}$$

where

$$\mathscr{R}(\alpha_1, \alpha_2, \beta_1, \beta_2) = \mathscr{M}^{-1}(\alpha_1, \beta_1)\mathscr{N}(\alpha_1, \beta_1)\mathscr{M}^{-1}(\alpha_2, \beta_2)\mathscr{N}(\alpha_2, \beta_2) \tag{2.79}$$

It is obvious to see that for $k = 0$, the matrix has an eigenvalue equal to 1, i.e., the algorithm does not converge. This observation synergies with those arguments in the one-dimensional case and the convergence through energy estimate.

One-sided case

We shall now study the case $(\alpha_1, \beta_1) = (\alpha_2, \beta_2) = (\alpha, \beta)$, in order to find a suitable expression of the eigenvalues of $\mathscr{R}$, which will be the basis for an efficient choice of (α, β). Denote

$$\mathscr{P}(\alpha) = \begin{pmatrix} \alpha\left(\nu\dfrac{ik^2}{\omega} - 1\right) & -\alpha\nu ik \\ -\dfrac{k}{\omega} & 1 \end{pmatrix} = \begin{pmatrix} \dfrac{i\alpha\nu\lambda^2}{\omega} & -i\alpha\nu k \\ -\dfrac{k}{\omega} & 1 \end{pmatrix} \tag{2.80}$$

$$\mathscr{Q}(\beta) = \begin{pmatrix} \dfrac{i|k|}{\omega} & -\dfrac{ik}{\lambda} \\ -\dfrac{\beta\nu k|k|}{\omega} & \beta\nu\lambda \end{pmatrix} \tag{2.81}$$

Then

$$\mathscr{M}(\alpha, \beta) = \mathscr{P}(\alpha) + \mathscr{Q}(\beta), \quad \mathscr{N}(\alpha, \beta) = \mathscr{P}(\alpha) - \mathscr{Q}(\beta)$$

Moreover, we have $\det(\mathscr{P}(\alpha)) = -\alpha \neq 0$, i.e. $P(\alpha)$ is always invertible. Then

$$\begin{aligned} \mathscr{M}^{-1}\mathscr{N} &= (\mathscr{P} + \mathscr{Q})^{-1}(\mathscr{P} - \mathscr{Q}) \\ &= (\mathscr{P} + \mathscr{Q})^{-1}(2\mathscr{P} - (\mathscr{P} + \mathscr{Q})) \\ &= -I + 2(\mathscr{P} + \mathscr{Q})^{-1}\mathscr{P} \\ &= -I + 2[\mathscr{P}^{-1}(\mathscr{P} + \mathscr{Q})]^{-1} \\ &= -I + 2[I + \mathscr{P}^{-1}\mathscr{Q}]^{-1} \end{aligned}$$

Hence, instead of calculating the eigenvalues of $\mathscr{M}^{-1}\mathscr{N}$, we are going to calculate those of $\mathscr{P}^{-1}\mathscr{Q}$ because if $(\mathbf{e}, \mu)$ is an eigenpair of $\mathscr{P}^{-1}\mathscr{Q}$, then it may be easily checked that

$(\mathbf{e}, \dfrac{1-\mu}{1+\mu})$ is an eigenpair of $\mathcal{M}^{-1}\mathcal{N}$.

We have first that

$$
\mathscr{P}^{-1} = \frac{-1}{\alpha}
\begin{pmatrix}
1 & i\alpha\nu k \\
\dfrac{k}{\omega} & \dfrac{i\alpha\nu\lambda^2}{\omega}
\end{pmatrix}
=
\begin{pmatrix}
\dfrac{-1}{\alpha} & -i\nu k \\
\dfrac{-k}{\alpha\omega} & \dfrac{-i\nu\lambda^2}{\omega}
\end{pmatrix}
$$

Then

$$
\mathscr{P}^{-1}\mathscr{Q} =
\begin{pmatrix}
\dfrac{1}{\alpha} & i\nu k \\
\dfrac{k}{\alpha\omega} & \dfrac{i\nu\lambda^2}{\omega}
\end{pmatrix}
\begin{pmatrix}
\dfrac{-i|k|}{\omega} & \dfrac{ik}{\lambda} \\
\dfrac{\beta\nu k|k|}{\omega} & -\beta\nu\lambda
\end{pmatrix}
$$

$$
=
\begin{pmatrix}
-\dfrac{i|k|}{\alpha\omega} + \dfrac{i\beta\nu^2 k^2|k|}{\omega} & \dfrac{ik}{\alpha\lambda} - i\beta\nu^2 k\lambda \\
-\dfrac{ik|k|}{\alpha\omega^2} + \dfrac{i\beta\nu^2\lambda^2 k|k|}{\omega^2} & \dfrac{ik^2}{\alpha\omega\lambda} - \dfrac{i\beta\nu^2\lambda^3}{\omega}
\end{pmatrix}
$$

$$
\det(\mathscr{Q}(\beta)) = \frac{\beta\nu i|k|\lambda}{\omega} - \frac{\beta\nu i k^2|k|}{\omega\lambda} = \frac{\beta\nu i|k|}{\lambda\omega}(\lambda^2 - k^2) = -\frac{\beta|k|}{\lambda}
$$

so

$$
\det(\mathscr{P}^{-1}\mathscr{Q}) = \frac{\beta|k|}{\alpha\lambda}
$$

and

$$
\mathrm{trace}(\mathscr{P}^{-1}\mathscr{Q}) = -\frac{i|k|}{\alpha\omega} + \frac{i\beta\nu^2 k^2|k|}{\omega} + \frac{ik^2}{\alpha\omega\lambda} - \frac{i\beta\nu^2\lambda^3}{\omega}
$$

Hence, the eigenvalues are the solutions of the following quadratic equation

$$
\mu^2 - \left(-\frac{i|k|}{\alpha\omega} + \frac{i\beta\nu^2 k^2|k|}{\omega} + \frac{ik^2}{\alpha\omega\lambda} - \frac{i\beta\nu^2\lambda^3}{\omega} \right)\mu + \frac{\beta|k|}{\alpha\lambda} = 0 \tag{2.82}
$$

We see immediately that in (2.82), for fixed (α, β, ω), then k and $-k$ give the same quadratic equation, hence same spectral radius for $\mathscr{R}$.

Hence

$$
\max_{k,\omega} \varrho\left(\mathscr{R}(k,\omega)\right) = \max_{k\geq 0,\omega} \varrho\left(\mathscr{R}(k,\omega)\right)
$$

with $\varrho(\mathscr{A})$ denotes the spectral radius of a matrix $\mathscr{A}$. To get a similar result for ω, we fix α, β, k and consider the above matrices with variable ω only.

Let λ and λ' be the square roots of $k^2 + \dfrac{i\omega}{\nu}$ and $k^2 - \dfrac{i\omega}{\nu}$ respectively. Then, we have $\mathbf{Re}(\lambda) = \mathbf{Re}(\lambda')$ and $\mathbf{Im}(\lambda) = -\mathbf{Im}(\lambda')$. The same is true for $\dfrac{1}{\lambda}$ and $\dfrac{1}{\lambda'}$.

In addition, one gets

$$
\mathbf{Re}\left(\mathrm{trace}\left(\mathscr{P}^{-1}\mathscr{Q}(\omega)\right)\right) = \mathbf{Re}\left(\frac{ik^2}{\alpha\omega\lambda}\right) - \mathbf{Re}\left(\frac{i\beta\nu^2\lambda^3}{\omega}\right)
$$

$$
= -\mathbf{Im}\left(\frac{k^2}{\alpha\omega\lambda}\right) - \mathbf{Re}\left(\frac{i\beta\nu^2\lambda(k^2 + i\omega)}{\omega}\right)
$$

$$= -\mathbf{Im}\left(\frac{k^2}{\alpha\omega\lambda}\right) + \mathbf{Re}\left(\beta\,\nu^2\lambda\right) + \mathbf{Im}\left(\frac{\beta\,\nu^2\lambda k^2}{\omega}\right)$$

$$= -\frac{k^2}{\alpha\omega}\mathbf{Im}\left(\frac{1}{\lambda}\right) + \beta\,\nu^2\mathbf{Re}(\lambda) + \frac{\beta\,\nu^2 k^2}{\omega}\mathbf{Im}(\lambda)$$

Replacing ω by $(-\omega)$ and then λ by λ', one has

$$\mathbf{Re}\left(\mathrm{trace}\,(\mathscr{P}^{-1}\mathscr{Q}(-\omega))\right) = -\frac{k^2}{\alpha(-\omega)}\mathbf{Im}\left(\frac{1}{\lambda'}\right) + \beta\,\nu^2\mathbf{Re}(\lambda') + \frac{\beta\,\nu^2 k^2}{-\omega}\mathbf{Im}(\lambda')$$

$$= -\frac{k^2}{\alpha\omega}\mathbf{Im}\left(\frac{1}{\lambda}\right) + \beta\,\nu^2\mathbf{Re}(\lambda) + \frac{\beta\,\nu^2 k^2}{\omega}\mathbf{Im}(\lambda)$$

$$= \mathbf{Re}(\mathrm{trace}\,(\mathscr{P}^{-1}\mathscr{Q}(\omega))).$$

Similarly, for the imaginary part

$$\mathbf{Im}(\mathrm{trace}\,(\mathscr{P}^{-1}\mathscr{Q}(\omega))) = -\frac{|k|}{\alpha\omega} + \frac{\beta\,\nu^2 k^2|k|}{\omega} + \frac{k^2}{\alpha\omega}\mathbf{Re}\left(\frac{1}{\lambda}\right) + \beta\,\nu^2\mathbf{Im}(\lambda) - \frac{\beta\,\nu^2 k^2}{\omega}\mathbf{Re}(\lambda).$$

Then,

$$\mathbf{Im}(\mathrm{trace}\,(\mathscr{P}^{-1}\mathscr{Q}(-\omega))) = -\frac{|k|}{\alpha(-\omega)} + \frac{\beta\,\nu^2 k^2|k|}{-\omega} + \frac{k^2}{\alpha(-\omega)}\mathbf{Re}\left(\frac{1}{\lambda'}\right)$$

$$+ \beta\,\nu^2\mathbf{Im}(\lambda') - \frac{\beta\,\nu^2 k^2}{-\omega}\mathbf{Re}(\lambda')$$

$$= -\mathbf{Im}(\mathrm{trace}\,(\mathscr{P}^{-1}\mathscr{Q}(\omega))).$$

In the end, we get that $\mathrm{trace}\,(\mathscr{P}^{-1}\mathscr{Q}(-\omega)) = \overline{\mathrm{trace}\,(\mathscr{P}^{-1}\mathscr{Q}(\omega))}$. Doing the same for $\det\mathscr{P}^{-1}\mathscr{Q}$, we have

$$\mathbf{Re}\left(\det\,(\mathscr{P}^{-1}\mathscr{Q}(\omega))\right) = \mathbf{Re}\left(\det\,(\mathscr{P}^{-1}\mathscr{Q}(-\omega))\right)$$

$$\mathbf{Im}\left(\det\,(\mathscr{P}^{-1}\mathscr{Q}(\omega))\right) = -\mathbf{Im}\left(\det\,(\mathscr{P}^{-1}\mathscr{Q}(-\omega))\right)$$

and thus $\det\,(\mathscr{P}^{-1}\mathscr{Q}(-\omega)) = \overline{\det\,(\mathscr{P}^{-1}\mathscr{Q}(\omega))}$.

We conclude from this that the solutions of (2.82) when we change ω to $-\omega$ are simply the conjugated of the solutions with ω.

From this argument, let μ be an eigenvalue of $\mathscr{P}^{-1}\mathscr{Q}(\omega)$ then $\overline{\mu}$ is an eigenvalue of $\mathscr{P}^{-1}\mathscr{Q}(-\omega)$. And then, since

$$\left|\frac{1-\mu}{1+\mu}\right| = \left|\frac{1-\overline{\mu}}{1+\overline{\mu}}\right|,$$

then $\mathscr{M}^{-1}\mathscr{N}(\omega)$ and $\mathscr{M}^{-1}\mathscr{N}(-\omega)$ have the same spectral radius. Then, the optimization of the convergence factor needs only to consider $k \geq 0$ and $\omega \geq 0$.

$$\max_{k,\omega}\varrho\,(\mathscr{R}(k,\omega)) = \max_{k\geq 0,\omega\geq 0}\varrho\,(\mathscr{R}(k,\omega)).$$

Stationary case

If we consider the semi-discrete problem, which is presented in the thesis of Cherel [33], one can replace $i\omega$ by $\dfrac{1}{\Delta t}$, then, the above expression becomes ($\dfrac{i}{\omega} = -\Delta t$)

$$\mu^2 - \left(\frac{\Delta t|k|}{\alpha} - \Delta t\beta\,\nu^2 k^2|k| - \frac{\Delta t k^2}{\alpha\lambda} + \Delta t\beta\,\nu^2\lambda^3\right)\mu + \frac{\beta\,|k|}{\alpha\lambda} = 0$$

with $\lambda = \sqrt{k^2 + \dfrac{1}{\nu \Delta t}} > |k|$. We have an obvious observation that

$$\left(\frac{\Delta t |k|}{\alpha} - \Delta t \beta \, \nu^2 k^2 |k| - \frac{\Delta t k^2}{\alpha \lambda} + \Delta t \beta \, \nu^2 \lambda^3 \right) \geq 0$$

and

$$\frac{\beta |k|}{\alpha \lambda} \geq 0$$

The quadratic equation has 2 roots with positive real parts. Then, we get $|\dfrac{1-\mu}{1+\mu}| \leq 1$.

It implies that the spectral radius of $\mathcal{M}^{-1}\mathcal{N}$ is less than or equal one.

We observe also that for $k = 0$, $\mu = 0$ is one solution and when $k \to \infty$, one solution tends to infinity. Hence, it is only with a bounded k, which means $0 < k_{\min} \leq k \leq k_{\max} < +\infty$ that we can have that the spectral radius of $\mathcal{M}^{-1}\mathcal{N}$ is strictly less than 1.

2.8   Numerical results

In this section, we present some numerical experiments that illustrate the performances of the OSWR method of Section 2.3, with Freefem++ [66]. For the space discretization we use the nonconforming Crouzeix-Raviart Finite Element method in 2D (i.e. piecewise linear element continuous at the midpoints of the edges of the mesh for the velocity $\mathbf{u} = (u_x, u_y)$, and piecewise constant $\mathbb{P}_0$ element for the pressure p), and the backward Euler scheme in time is considered. In the context below, we use the term "monodomain solution" to denote the discrete monodomain solution that would be obtained on the same mesh without domain decomposition.

In Section 2.8.1 some results are shown on the convergence of the OSWR algorithm, without and with modification of the pressure as in Section 2.6. In Section 2.8.2 we illustrate the influence of the choice of the Robin parameter on the convergence properties of the algorithm, and then in Section 2.8.3 we present results on a more realistic test case.

2.8.1   Recovering the pressure: a rotating velocity example

We set $\Omega =]0,1[\times]0,1[$, $\nu = 1$, $T = 1$, and consider the Stokes problem (2.1). We choose the right-hand side f and the values of the boundary and initial conditions so that the exact solution is given by

$$\mathbf{u}(\mathbf{x}, t) = (-(t^2 + 1)\cos(\pi y)\sin(\pi x), (t^2 + 1)\sin(\pi y)\cos(\pi x)), \qquad (2.83)$$

$$p(\mathbf{x}, t) = \cos(t)(x^2 - y^2), \qquad \forall \mathbf{x} \in \Omega, \ \forall t \in (0, T), \qquad (2.84)$$

see Figure 2.1.

The domain Ω is decomposed into two subdomains as in Figure 2.2, and three different meshes will be considered (as shown on Figure 2.2), with mesh sizes $h = 0.0625$, $h = 0.0312$, and $h = 0.0156$, respectively. To each mesh, the associated time step is $\Delta t = h$. The mesh sizes on the interface are $h_\Gamma = 0.0417$, $h_\Gamma = 0.0208$, and $h_\Gamma = 0.0104$, respectively.

Next, we analyse the evolution of the errors, of the pressure p and the normal and tangential components of the velocity u_x and u_y, during the OSWR algorithm.
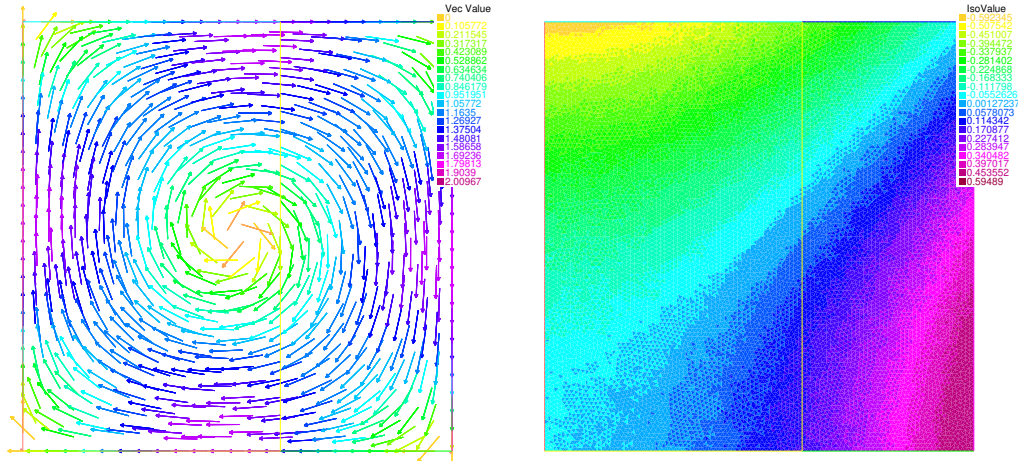
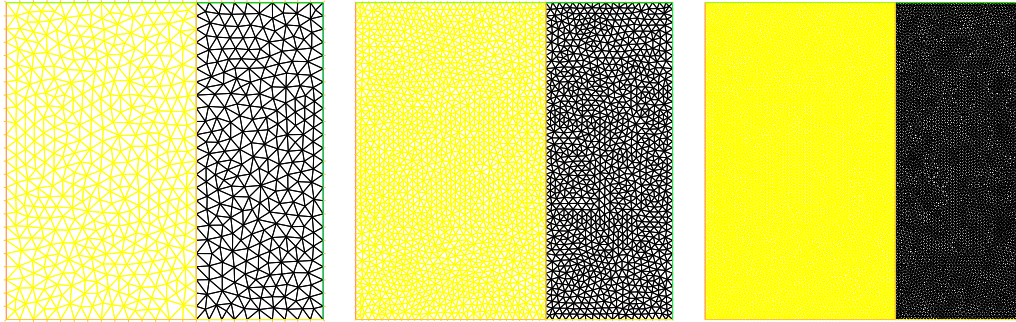Figure 2.1: Example 1: rotating velocity field (left), and pressure (right)

Figure 2.2: Example 1: mesh 1 (left), mesh 2 (middle), and mesh 3 (right)

In Figure 2.3, we plot the evolution of the relative errors, of p, u_x and u_y, in the $L^\infty(0, T; L^2(\Omega))$-norm, between the OSWR and monodomain solutions, as a function of the number of OSWR iterations, for mesh 1 and mesh 2. We observe that the method converges for the velocity but not for the pressure, as expected (see Section 2.4). In Figure 2.4, we have considered the OSWR algorithm with the modified pressure of Section 2.6, at each iteration. This figure shows the evolution of the relative error in the $L^\infty(0, T; L^2(\Omega))$-norm, between the OSWR and monodomain solutions, as a function of the number of OSWR iterations, for mesh 1, mesh 2 and mesh 3. We observe that the method now converges both for the velocity and the pressure, accordingly to the result of Section 2.6.

Remark 2.27. *Even if we calculate a modified pressure at each iteration, we do not use it in the transmission conditions of the algorithm presented in Section 2.3, thus this does not change the velocity, as shown on Figures 2.3 and 2.4 (on the top).*

Remark 2.28. *Here the pressure is modified at each iteration to illustrate the convergence of the multidomain solution to the monodomain solution. A consequence of Remark 2.24 is that in practice one needs only to modify the pressure at the last OSWR iteration, which makes the cost of the modification negligible.*
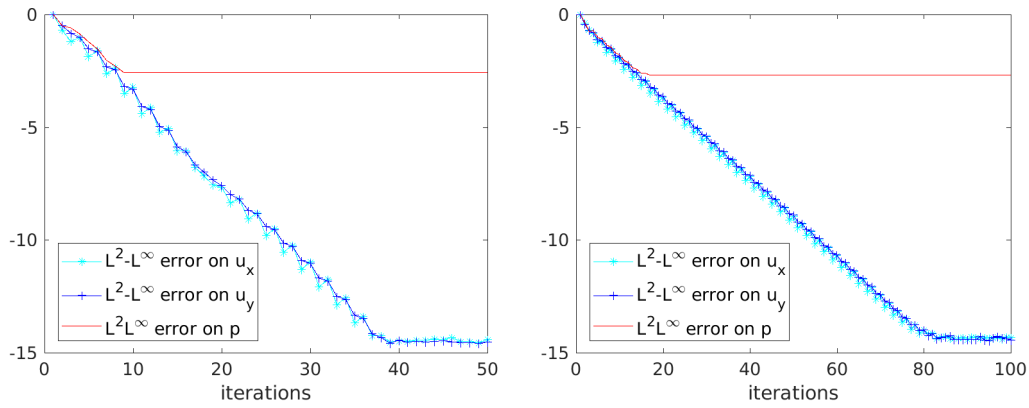
Figure 2.3: Example 1: relative errors (for u_x, u_y and p) versus iterations, for mesh 1 (left) and mesh 2 (right), with the non-modified pressure
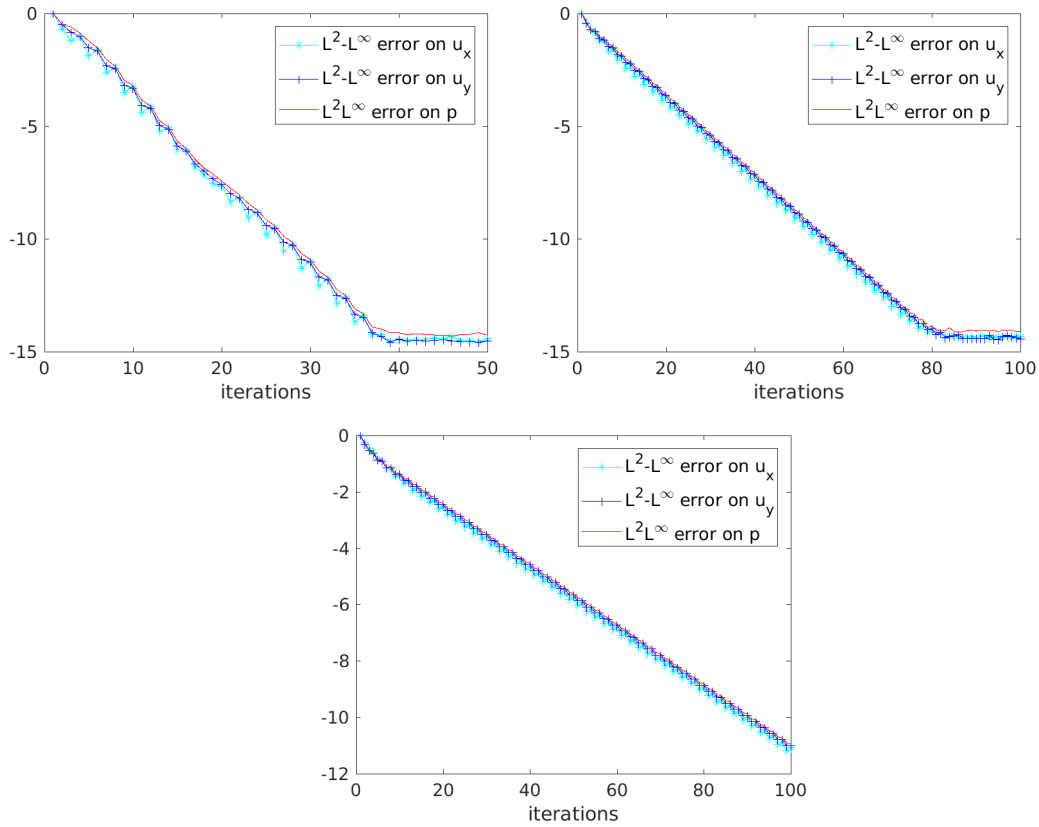
Figure 2.4: Example 1: relative errors (for u_x, u_y and p) versus iterations, for mesh 1 (top left) mesh 2 (top right) and mesh 3 (bottom), with the modified pressure

2.8.2   Optimized Robin parameters

In this section we assess the performance of the Robin parameters $\alpha_1, \alpha_2, \beta_1, \beta_2$ of the OSWR method. These parameters are chosen to optimize the convergence factor of the algorithm, and are called "optimized parameters". More precisely, they are calculated by minimizing the continuous convergence factor of Section 2.7. In the context of the Stokes problem, better results can be obtained by minimizing the semi-discrete in time

counterpart of the continuous convergence factor, as described below.

2.8.2.1 Methodology based on the convergence factor

Let us recall the definition of the matrix $\mathscr{R}$ by formula (2.79) of Section 2.7. We defnie

$$\tilde{\rho}_c(\alpha_1, \alpha_2, \beta_1, \beta_2) := \max_{\frac{\pi}{L} \leq k \leq \frac{\pi}{h}, \frac{\pi}{T} \leq \omega \leq \frac{\pi}{\Delta t}} \varrho\big(\mathscr{R}(\alpha_1, \alpha_2, \beta_1, \beta_2, k, \omega)\big),$$

where $\varrho(\mathscr{A})$ denotes the spectral radius of a matrix $\mathscr{A}$. We restrict the max over bounded strictly positive parameters to take into account the fact that in actual calculations, only a bounded range of frequencies and wavelengths are present on the numerical grid.

We consider the following cases :

- Optimized Robin parameter : $\alpha_1 = \alpha_2 = \beta_1 = \beta_2 = \alpha_c$ where α_c verifies

$$\rho_c(\alpha_c) = \min_{\alpha > 0} \rho_c(\alpha),$$

  with $\rho_c(\alpha) := \tilde{\rho}_c(\alpha, \alpha, \alpha, \alpha)$.

- Optimized Robin-2p parameters : $\alpha_1 = \alpha_2 = \alpha_c$, $\beta_1 = \beta_2 = \beta_c$ where (α_c, β_c) is such that

$$\rho_c(\alpha_c, \beta_c) = \min_{\alpha > 0, \beta > 0} \rho_c(\alpha, \beta),$$

  with $\rho_c(\alpha, \beta) := \tilde{\rho}_c(\alpha, \alpha, \beta, \beta)$.

- Optimized Robin-2sided parameters : $\alpha_1 = \beta_1 = \alpha_c$, $\alpha_2 = \beta_2 = \beta_c$ where (α_c, β_c) is such that

$$\rho_c(\alpha_c, \beta_c) = \min_{\alpha > 0, \beta > 0} \rho_c(\alpha, \beta),$$

  with $\rho_c(\alpha, \beta) := \tilde{\rho}_c(\alpha, \beta, \alpha, \beta)$.

One can also consider the semi-discrete in time counterpart of the continuous convergence factor to better capture the discrete time frequencies : we replace in the expression of $\mathscr{R}$ the term $i\omega$ by its discrete counterpart using the implicit Euler scheme, that is we replace $i\omega$ by $\dfrac{1 - e^{-i\omega\Delta t}}{\Delta t}$. Equivalently, we replace in the expression of $\mathscr{R}$ the term ω by $\overline{\omega} := -i\left(\dfrac{1 - e^{-i\omega\Delta t}}{\Delta t}\right)$, and we set

$$\mathscr{R}_{\Delta t}(\alpha_1, \alpha_2, \beta_1, \beta_2, k, \omega) := \mathscr{R}(\alpha_1, \alpha_2, \beta_1, \beta_2, k, \overline{\omega}). \tag{2.85}$$

Then, as above, we define

$$\tilde{\rho}(\alpha_1, \alpha_2, \beta_1, \beta_2) := \max_{\frac{\pi}{L} \leq k \leq \frac{\pi}{h}, \frac{\pi}{T} \leq \omega \leq \frac{\pi}{\Delta t}} \varrho\big(\mathscr{R}_{\Delta t}(\alpha_1, \alpha_2, \beta_1, \beta_2, k, \omega)\big),$$

and consider the following cases, where "SDT" means "Semi-discrete in time" :

- SDT-Optimized Robin parameter : $\alpha_1 = \alpha_2 = \beta_1 = \beta_2 = \alpha^*$ where α^* verifies

$$\rho(\alpha^*) = \min_{\alpha > 0} \rho(\alpha),$$

  with $\rho(\alpha) := \tilde{\rho}(\alpha, \alpha, \alpha, \alpha)$.

- SDT-Optimized Robin-2p parameters : $\alpha_1 = \alpha_2 = \alpha^*$, $\beta_1 = \beta_2 = \beta^*$ where (α^*, β^*) is such that

$$\rho(\alpha^*, \beta^*) = \min_{\alpha > 0, \beta > 0} \rho(\alpha, \beta),$$

with $\rho(\alpha, \beta) := \tilde{\rho}(\alpha, \alpha, \beta, \beta)$.

- SDT-Optimized Robin-2sided parameters : $\alpha_1 = \beta_1 = \alpha^*$, $\alpha_2 = \beta_2 = \beta^*$ where (α^*, β^*) is such that

$$\rho(\alpha^*, \beta^*) = \min_{\alpha > 0, \beta > 0} \rho(\alpha, \beta),$$

with $\rho(\alpha, \beta) := \tilde{\rho}(\alpha, \beta, \alpha, \beta)$.

In our experiments below, the domain Ω is decomposed into two subdomains as in Figure 2.2, and we consider either the meshes 1,2,3 of Figure 2.2, either the meshes 4,5,6 of Figure 2.5, where the mesh sizes on the interface and time steps are $h_\Gamma = \Delta t = 0.0625$, $h_\Gamma = \Delta t = 0.0312$, and $h_\Gamma = \Delta t = 0.0156$ respectively.
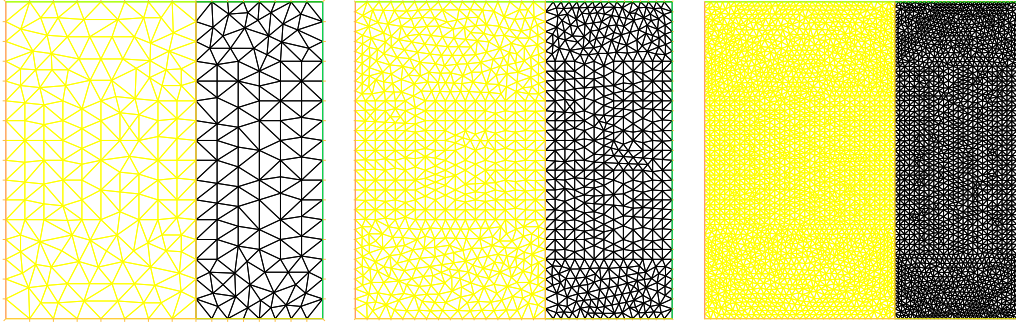

Figure 2.5: Example 2: mesh 4 (left), mesh 5 (middle), and mesh 6 (right)

Next, in order to analyze the convergence behavior of the method, we consider the Stokes problem with homogeneous initial and boundary conditions (i.e., the solution converges to zero). We start with a random Robin initial guess on the space-time interface (i.e. that contains all space-time frequencies) and compute the error in the $L^\infty(0, T; L^2(\Omega))$-norm for the pressure p and for the normal and tangential components of the velocity u_x and u_y. We show the error in p, u_x, u_y (in logarithmic scale) after fifteen OSWR iterations for various values of the optimized parameters.

Remark 2.29. *The convergence of the error on the pressure to zero can be obtained either by taking a random Robin initial guess with zero mean value on $\Gamma \times (0, T)$ (without any modification of the pressure), either by taking any random Robin initial guess on $\Gamma \times (0, T)$ and by modifying the pressure as in Section 2.6.*

2.8.2.2   Robin case

In this part, only one Robin parameter α is considered, and we take $\alpha_1 = \alpha_2 = \beta_1 = \beta_2 = \alpha$. Next, for an optimized choice of α, we consider and compare the results obtained with the optimized parameter $\alpha = \alpha_c$ and the SDT-optimized parameter $\alpha = \alpha^*$ described in section 2.8.2.1.

• **Case $\nu = 1$** - We take $\nu = 1$ and consider mesh 4 (i.e. $h_\Gamma = \Delta t = 0.0625$). In Figure 2.6, we plot the evolution of the continuous convergence factor ρ_c (on the left) and of the semi-discrete in time convergence factor ρ (on the right), as a function of the Robin parameter α. The optimized values α_c (blue circle) and α^* (red star), shown on Figure 2.6, are calculated using the function `fminsearch` of MATLAB [1].
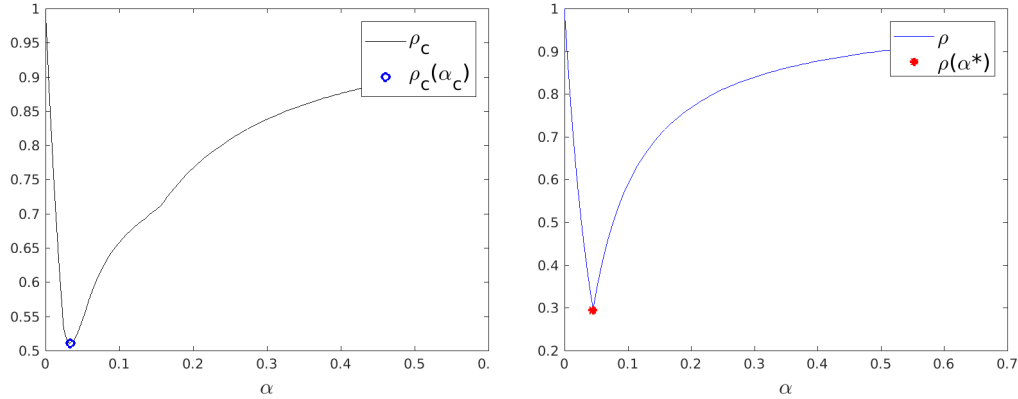

Figure 2.6: Case $\nu = 1$. Left: continuous convergence factor versus α (black curve) with theoretical optimized value α_c (blue circle); Right: SDT convergence factor versus α (blue curve) with theoretical optimized value α^* (red star)

In Figure 2.7, we plot the evolution of the relative errors, of p, u_x and u_y, in the $L^\infty(0, T; L^2(\Omega))$-norm, after fifteen OSWR iterations, for various values of the Robin parameter α. We also show the values of the errors with the optimized parameters α_c (blue circle) and α^* (red star). On the left figure we take a random Robin initial guess with zero mean value on $\Gamma \times (0, T)$ (see Remark 2.29). We see that α_c and α^* are close to the Robin values giving the smallest error after the same number of iterations. In Figure 2.7, on the right, we take any random initial guess on $\Gamma \times (0, T)$ (i.e. with all space-time frequencies) and modify the pressure as in Section 2.6. We see that α^* is again close to the Robin values giving the smallest error after fifteen iterations, while α_c gives a larger error. We also observe, for both cases, that the convergence can be significantly slower if α is not chosen well.

• **Case $\nu = 0.1$** - In Figure 2.8, we show the evolution of the continuous convergence factor ρ_c (top line) and of the semi-discrete in time convergence factor ρ (bottom line), as a function of the Robin parameter α, for mesh 4 (left), mesh 5 (middle), and mesh 6 (right), respectively. The optimized values α_c (blue circle) and α^* (red star), are shown. We observe that both α_c and α^* decrease as h_Γ and Δt decrease, and α_c and α^* differ from about a factor 5.

In Figure 2.9, we plot the evolution of the relative errors, of p, u_x and u_y, in the $L^\infty(0, T; L^2(\Omega))$-norm, after fifteen OSWR iterations, for various values of α, for mesh 4 (left), mesh 5 (middle), and mesh 6 (right), respectively. We also show the values of the errors with α_c (blue circle) and α^* (red star). We take any random initial guess on $\Gamma \times (0, T)$ (i.e. with all space-time frequencies). We see that α^* is close to the Robin values giving the smallest error after fifteen iterations, for the three meshes, while α_c gives a higher error in all cases. As for the case $\nu = 1$, we observe that the convergence can be significantly slower if α is not chosen well.
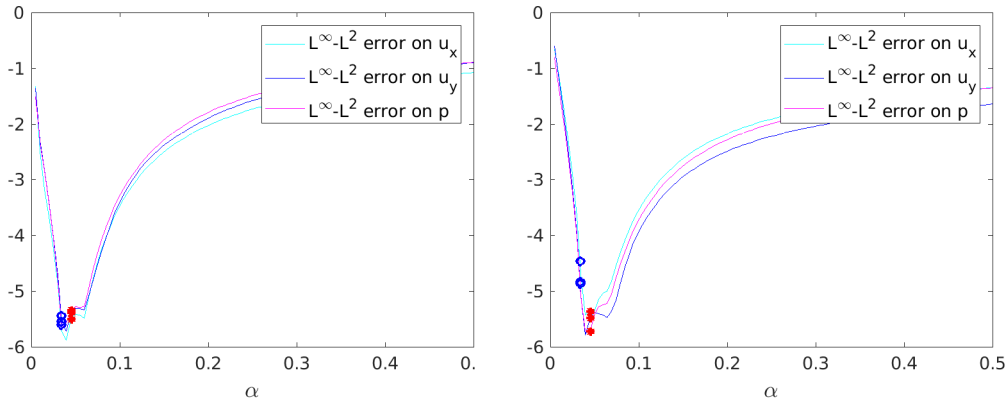
Figure 2.7: Case $\nu = 1$. Relative errors after 15 iterations (for u_x, u_y and p) versus α, with their values at α_c (blue circles) and at α^* (red stars). Left: starting from a random initial guess with a zero mean value on $\Gamma \times (0, T)$ (with non-modified pressure); Right: starting from any random initial guess on $\Gamma \times (0, T)$ (with modified pressure)
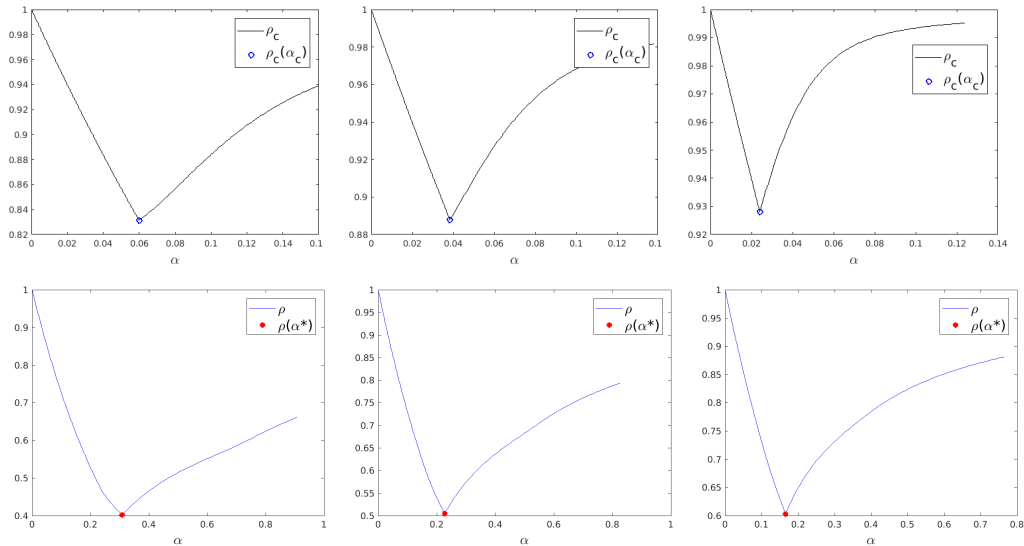
Figure 2.8: Case $\nu = 0.1$. Top: continuous convergence factor versus α (black curve) with theoretical optimized value α_c (blue circle); Bottom: SDT convergence factor versus α (blue curve) with theoretical optimized value α^* (red star); Left : mesh 4; Middle : mesh 5; Right : mesh 6

• Case $\boldsymbol{\nu = 0.01}$

We now consider the case $\nu = 0.01$ and mesh 5 (i.e. $h_\Gamma = \Delta t = 0.0312$). In Figure 2.10, we show the evolution of the continuous convergence factor ρ_c (on the left) and of the semi-discrete in time convergence factor ρ (on the middle), as a function of the Robin parameter α, as well as the optimized values α_c (blue circle) and α^* (red star). We observe that α_c is significantly smaller than α^*. We also observe from Figure 2.8 (middle) and Figure 2.10 that α_c and α^* increase as ν decrease.

In Figure 2.10, on the right, we plot the evolution of the relative errors, of p, u_x and u_y, in the $L^\infty(0, T; L^2(\Omega))$-norm, after fifteen OSWR iterations, for various values

Figure 2.9: Case $v = 0.1$. Relative errors after 15 iterations (for u_x, u_y and p) versus α, with their values at α_c (blue circles) and at α^* (red stars), starting from any random initial guess on $\Gamma \times (0, T)$ (with modified pressure); Left : mesh 4; Middle : mesh 5; Right : mesh 6
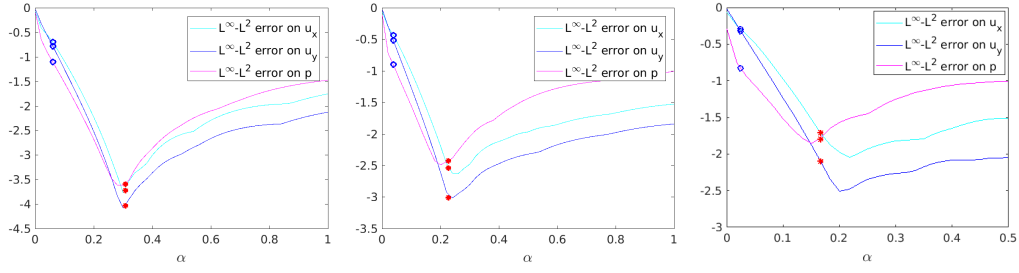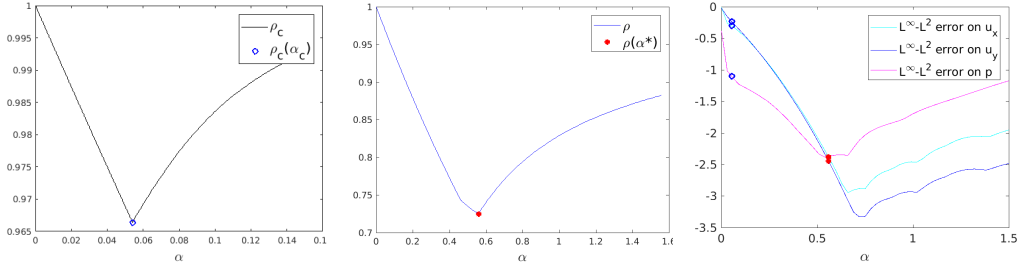

Figure 2.10: Case $v = 0.01$. Left: continuous convergence factor versus α (black curve) with theoretical optimized value α_c (blue circle); Middle: SDT convergence factor versus α (blue curve) with theoretical optimized value α^* (red star); Right: Relative errors after 15 iterations (for u_x, u_y and p) versus α, with their values at α_c (blue circles) and at α^* (red stars), starting from any random initial guess on $\Gamma \times (0, T)$ (with modified pressure)

of α, as well as the errors obtained with α_c (blue circle) and α^* (red star). We take any random initial guess on $\Gamma \times (0, T)$. We see that α^* is close to the Robin values giving the smallest error after fifteen iterations, for the pressure, and nearly close for the velocity, while α_c gives a higher error for p, u_x, u_y, far from the Robin values giving the smallest error.

2.8.2.3 Robin-2p case

In this section, two Robin parameters α and β are considered, and we take $\alpha_1 = \alpha_2 = \alpha$ and $\beta_1 = \beta_2 = \beta$. Next, for an optimized choice of α and β, we compare the results obtained with the optimized parameters $(\alpha, \beta) = (\alpha_c, \beta_c)$ and the SDT-optimized parameters $(\alpha, \beta) = (\alpha^*, \beta^*)$ described in section 2.8.2.1.

• **Case $v = 1$** - In Figure 2.11, we show the evolution of the continuous convergence factor ρ_c (on the left) and of the semi-discrete in time convergence factor ρ (on the right), as a function of the Robin parameters α and β, for mesh 1 (i.e. $h_\Gamma = 0.0417$, $\Delta t = 0.0625$). The optimized values (α_c, β_c) (blue circle, on the left figure) and (α^*, β^*) (red star, on the right figure), are also plotted.

In Figure 2.12, on the top two lines, we plot the evolution of the relative errors, of u_x (left), u_y (right), and p (middle), in the $L^\infty(0, T; L^2(\Omega))$-norm, after fifteen OSWR

iterations, for various values of α and β, for mesh 1. We also plot the values of the errors with (α_c, β_c) (blue circle) and (α^*, β^*) (red star). We take a random initial guess with zero mean value on $\Gamma \times (0, T)$ and the pressure is not modified. We see that both (α^*, β^*) and (α_c, β_c) are close to the Robin-2p values giving the smallest error after fifteen iterations.

In Figure 2.12, on the two bottom lines, we do the same simulations as on the top two lines, except that we start now from any random initial guess on $\Gamma \times (0, T)$ (i.e. with all space-time frequencies), and consider the modified pressure. We observe that the results are similar, in particular both (α^*, β^*) and (α_c, β_c) are close to the Robin-2p values giving the smallest error after fifteen iterations. As for the Robin case, we observe that the convergence can be significantly slower if α and β are not well chosen.

Figure 2.11: Case $\nu = 1$ (Robin-2p). Continuous (left) and semi-discrete in time (right) convergence factors versus α and β with their respective theoretical optimized values (α_c, β_c) (blue circle) and (α^*, β^*) (red star)
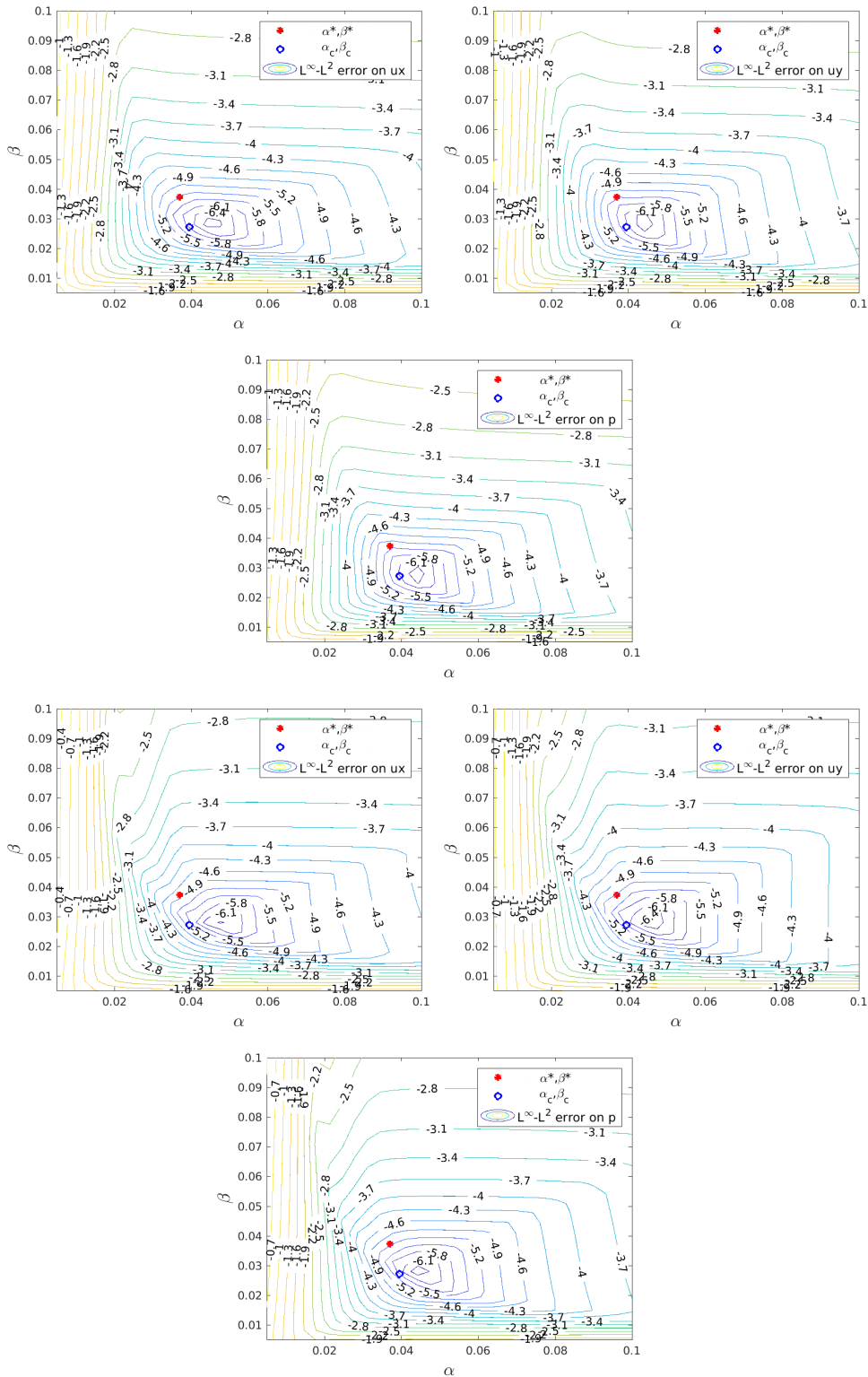
Figure 2.12: Case $\nu = 1$ (Robin-2p). Relative errors after 15 iterations versus α and β, with value at (α_c, β_c) (blue circle) and at (α^*, β^*) (red star), for u_x (left), u_y (right) and p (middle). Top two lines : random initial guess with a zero mean value on $\Gamma \times (0, T)$ and non-modified pressure; Bottom two lines: arbitrary random initial guess on $\Gamma \times (0, T)$ and modified pressure

• **Case $\nu = 0.1$** - In Figure 2.13, we plot the evolution of the continuous convergence factor ρ_c (on the left) and of the semi-discrete in time convergence factor ρ (on the right), as a function of the Robin parameters α and β, for mesh 4 (i.e. $h_\Gamma = \Delta t = 0.0625$). The optimized values (α_c, β_c) (blue circle, on the left figure) and (α^*, β^*) (red star, on the right figure), are also shown. We observe that these optimized values are very different : we have $(\alpha_c, \beta_c) = (5.9870 \, 10^{-2}, 5.9424 \, 10^{-2})$ and $(\alpha^*, \beta^*) = (3.0931 \, 10^{-1}, 2.8641 \, 10^{-1})$.

In Figure 2.14, we plot the evolution of the relative errors, with any random initial guess on $\Gamma \times (0, T)$ with modified pressure. These errors of u_x (left), u_y (right), and p (middle), in the $L^\infty(0, T; L^2(\Omega))$-norm, are calculated after fifteen OSWR iterations, for various values of α and β, for mesh 4. We also plot the values of the errors with (α_c, β_c) (blue circle) and (α^*, β^*) (red star). We observe that (α^*, β^*) is nearly close to the Robin-2p values giving the smallest error after fifteen iterations, while (α_c, β_c) is far from this value.
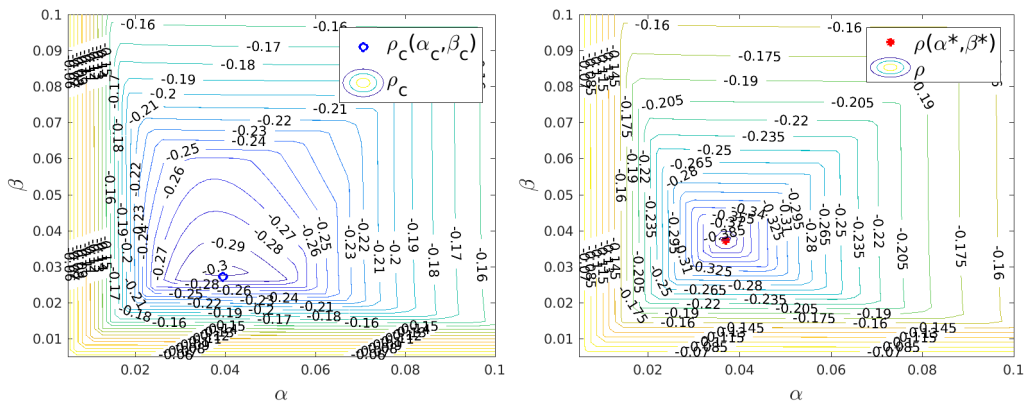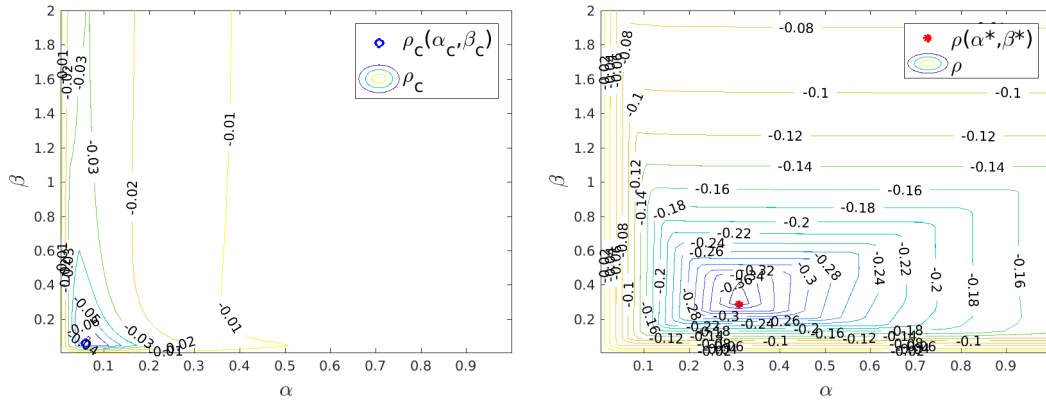

Figure 2.13: Case $\nu = 0.1$ (Robin-2p). Continuous (left) and semi-discrete in time (right) convergence factors versus α and β with their respective theoretical optimized values (α_c, β_c) (blue circle) and (α^*, β^*) (red star)
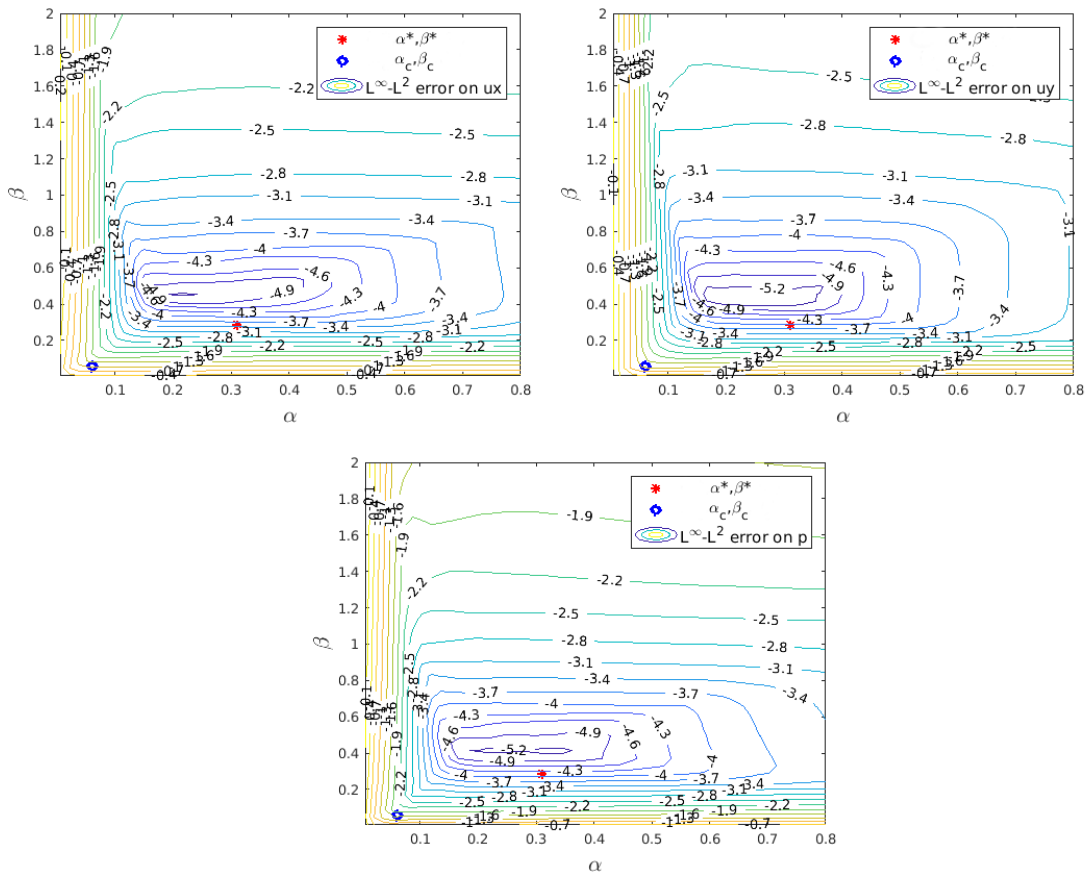
Figure 2.14: Case $\nu = 0.1$ (Robin-2p). Relative errors after 15 iterations versus α and β, with value at (α_c, β_c) (blue circle) and at (α^*, β^*) (red star), for u_x (left), u_y (right) and p (middle), starting from any random initial guess on $\Gamma \times (0, T)$ and modified pressure

2.8.2.4   Robin-2sided case

In this part, two Robin parameters α and β are again considered, and we take $\alpha_1 = \beta_1 = \alpha$ and $\alpha_2 = \beta_2 = \beta$. We compare below the results obtained with the optimized parameters $(\alpha, \beta) = (\alpha_c, \beta_c)$ and the SDT-optimized parameters $(\alpha, \beta) = (\alpha^*, \beta^*)$ described in section 2.8.2.1.

• **Case $\nu = 1$** - In Figure 2.15, we plot the evolution of the continuous convergence factor ρ_c (on the left) and of the semi-discrete in time convergence factor ρ (on the right), as a function of the Robin parameters α and β, for mesh 1, as well as the optimized values (α_c, β_c) (blue circle, on the left figure) and (α^*, β^*) (red star, on the right figure). We observe that, unlike the previous choices of the optimized parameters (Robin or Robin-2p), the numerical calculation of the SDT Robin-2sided parameter (α^*, β^*) requires to be careful in the choice of the initial data and of the number of space-time frequencies, for the inputs of the function "fminsearch" of MAT-LAB. This can be explained by the shape of the isovalues of the convergence factor ρ (see Figure 2.15 on the right). Moreover, the numerical optimized values are $(\alpha_c, \beta_c) = (3.3802\,10^{-2}, 3.3802\,10^{-2})$ and $(\alpha^*, \beta^*) = (3.7214\,10^{-2}, 3.7214\,10^{-2})$, and thus correspond to Robin values (i.e. $\alpha_c = \beta_c$ and $\alpha^* = \beta^*$). We also observe that (α_c, β_c) and (α^*, β^*) are close.
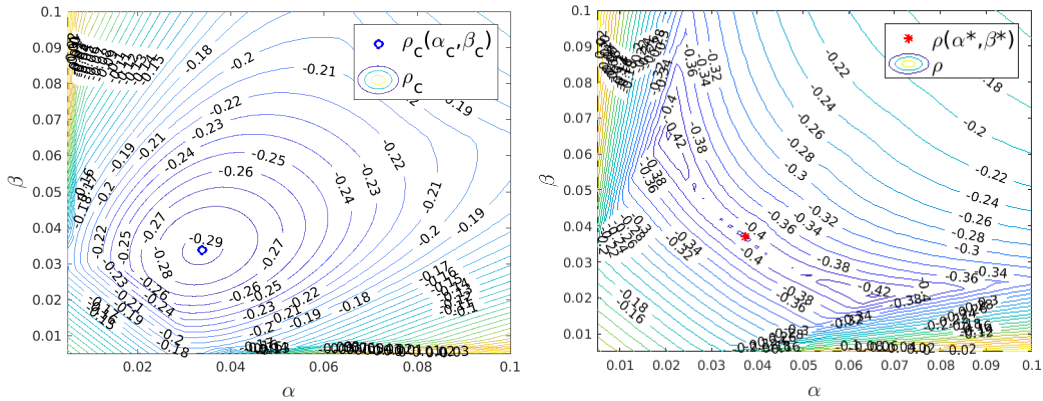
Figure 2.15: Case $\nu = 1$ (Robin-2sided). Left: continuous convergence factor versus α and β with theoretical optimized value (α_c, β_c) (blue circle); Right: SDT convergence factor versus α and β with theoretical optimized value (α^*, β^*) (red star)

In Figure 2.16, on the top two lines, we plot the evolution of the relative errors, of u_x (left), u_y (right), and p (middle), in the $L^\infty(0, T; L^2(\Omega))$-norm, after fifteen OSWR iterations, for various values of α and β, for mesh 1. We also plot the values of the errors with (α_c, β_c) (blue circle) and (α^*, β^*) (red star). We take a random initial guess with zero mean value on $\Gamma \times (0, T)$ and the pressure is not modified. We see that both (α^*, β^*) and (α_c, β_c) are close to the Robin-2sided values giving the smallest error after fifteen iterations, and that (α^*, β^*) is a little closer to these values.

In Figure 2.16, on the bottom two lines, we do the same simulation as above, except that we start now from any random initial guess on $\Gamma \times (0, T)$, with the modified pressure. While the results are similar for the velocity u_x and u_y, the shape of the errors are very different for the pressure p, with a thin layer containing several minima, where a zoom is given on Figure 2.17.

Figure 2.16: Case $\nu = 1$ (Robin-2sided). Relative errors after 15 iterations versus α and β, with value at (α_c, β_c) (blue circle) and at (α^*, β^*) (red star), for u_x (left), u_y (right) and p (middle). Top two lines: random initial guess with a zero mean value on $\Gamma \times (0, T)$ and non-modified pressure; Bottom two lines : arbitrary random initial guess on $\Gamma \times (0, T)$ and modified pressure
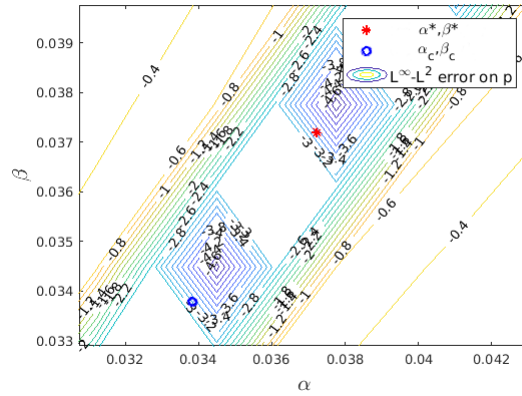
Figure 2.17: Case $\nu = 1$ (Robin-2sided). Zoom on the last line of Figure 2.16

• **Case $\nu = 0.1$** - In Figure 2.18, we plot the evolution of the continuous convergence factor ρ_c (on the left) and of the semi-discrete in time convergence factor ρ (on the right), as a function of the Robin parameters α and β, for mesh 4, as well as the optimized values (α_c, β_c) (blue circle, on the left figure) and (α^*, β^*) (red star, on the right figure). The numerical optimized values are $(\alpha_c, \beta_c) = (5.9818\,10^{-2}, 5.9818\,10^{-2})$ and $(\alpha^*, \beta^*) = (3.0832\,10^{-1}, 3.0832\,10^{-1})$, and thus correspond to Robin values (i.e. $\alpha_c = \beta_c$ and $\alpha^* = \beta^*$), and to the optimized Robin values found in Section 2.8.2.2.
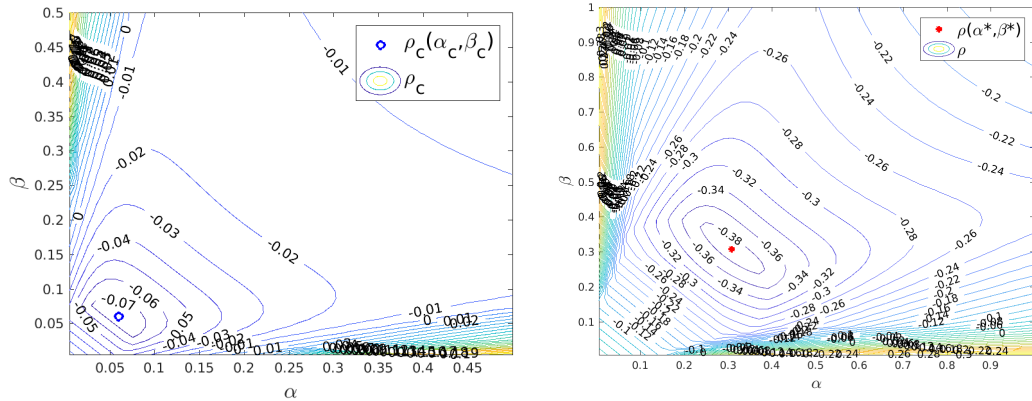
Figure 2.18: Case $\nu = 0.1$ (Robin-2sided). Left: continuous convergence factor versus α and β with theoretical optimized value (α_c, β_c) (blue circle); Right: SDT convergence factor versus α and β with theoretical optimized value (α^*, β^*) (red star)

In Figure 2.19, we show the evolution of the relative errors, of u_x (left), u_y (right), and p (middle), in the $L^\infty(0, T; L^2(\Omega))$-norm, after fifteen OSWR iterations, for various values of α and β, for mesh 4. We also plot the values of the errors with (α_c, β_c) (blue circle) and (α^*, β^*) (red star). We take any random initial guess on $\Gamma \times (0, T)$ and the pressure is modified. We see that (α^*, β^*) is close to the Robin-2sided values giving the smallest error after fifteen iterations, while (α_c, β_c) is far from these values. Moreover, as for the case $\nu = 1$ above, we observe that the shape of the errors are very different for the pressure p, with a thin layer containing several minima.
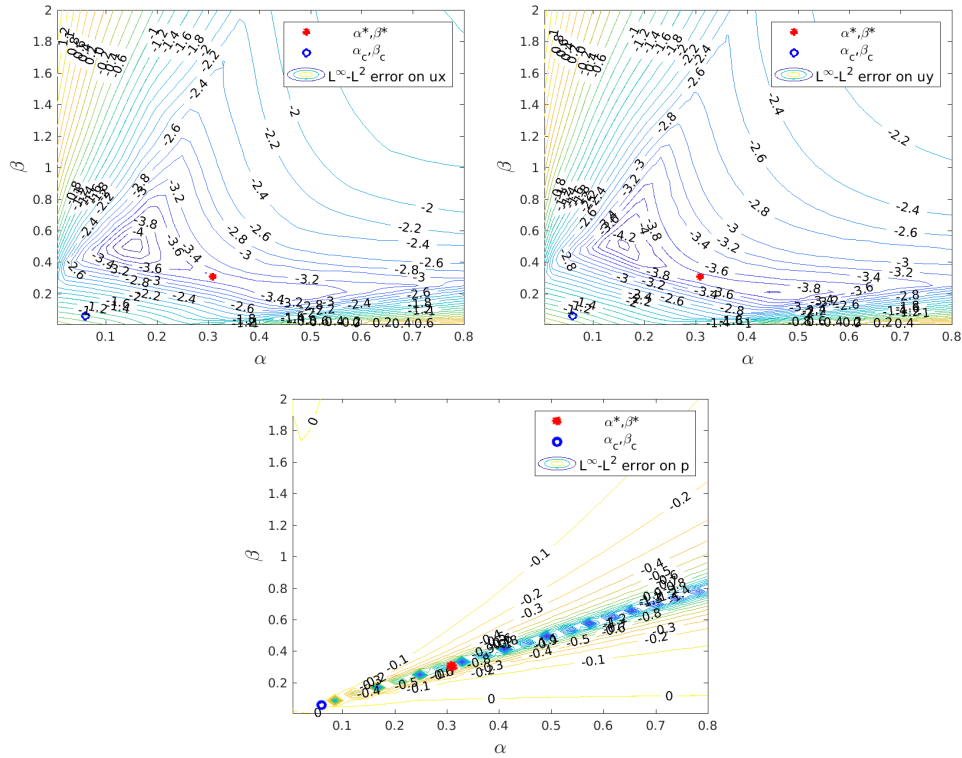
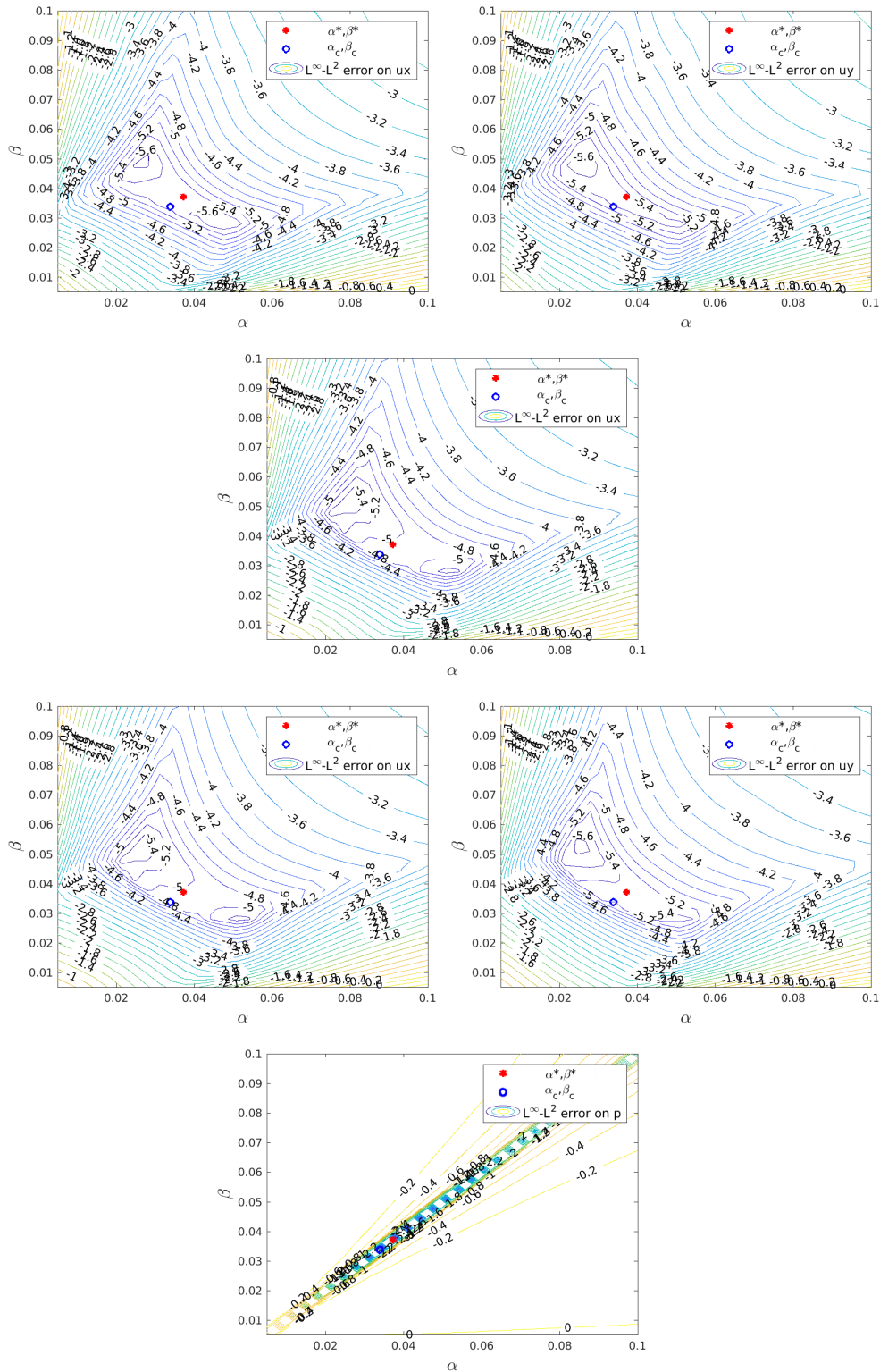Figure 2.19: Case $\nu = 0.1$ (Robin-2sided). Relative errors after 15 iterations versus α and β, with value at (α_c, β_c) (blue circle) and at (α^*, β^*) (red star), for u_x (left), u_y (right) and p (middle), starting from any random initial guess on $\Gamma \times (0, T)$ (with modified pressure)

2.8.3 A more realistic test case

In this example we take $\nu = \dfrac{1}{\mathscr{R}e}$ with $\mathscr{R}e = 200$, and $T = 5$. The mesh is given on Figure 2.20, with 22232 mesh elements. The domain is decomposed into two subdomains, with the interface at $y = -0.9$, see Figure 2.20, where domain 1 corresponds to the green and yellow parts, and domain 2 to the black part. The time step is $\Delta t = 0.05$.

We set $\Omega_f = [-2.625, 1.625] \times [-0.9, -0.6] \times (0, T)$. The domain $[-2.625, 1.625] \times [-0.9, -0.6]$ corresponds to the yellow part of the mesh on Figure 2.20 and corresponds to the location where the source term $\mathbf{f}$ in the Stokes equations does not vanish. Two different values for this source term will be used in the numerical tests that follow.
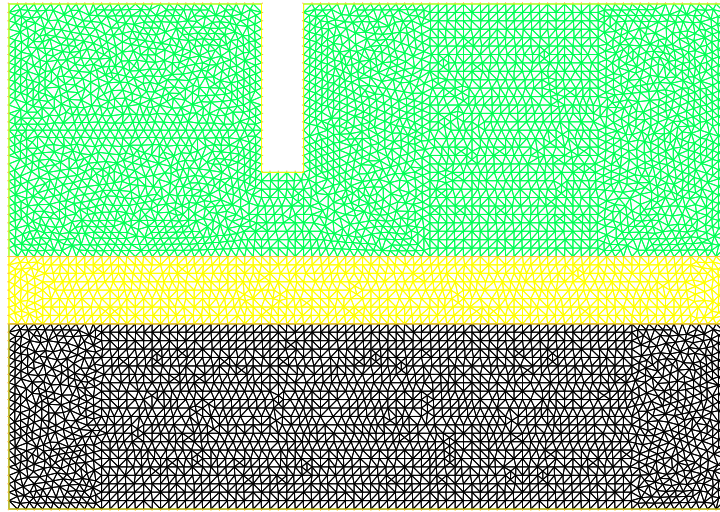
Figure 2.20: Example 3: mesh and domain decomposition into 2 subdomains (green and yellow parts for domain 1, and black part for domain 2)

2.8.3.1   Optimized Robin parameters

In this part we discuss the choice of the Optimized Robin parameters. If not specified, the initial data for the function `fminsearch` of MATLAB is $\alpha = 0$ (Robin) or $(\alpha, \beta) = (0, 0)$ (Robin-2p or Robin-2sided).

In Figure 2.21, we consider the Robin case (i.e. $\alpha_1 = \alpha_2 = \beta_1 = \beta_2 = \alpha$) and plot the evolution of the continuous convergence factor ρ_c (on the left) and of the semi-discrete in time convergence factor ρ (on the right), as a function of the Robin parameter α, as well as the optimized values α_c (blue circle, on the left figure) and α^* (red star, on the right figure). The numerical optimized values are $\alpha_c = 3.2283\,10^{-2}$ and $\alpha^* = 6.6063\,10^{-1}$, and differ from about a factor 20.
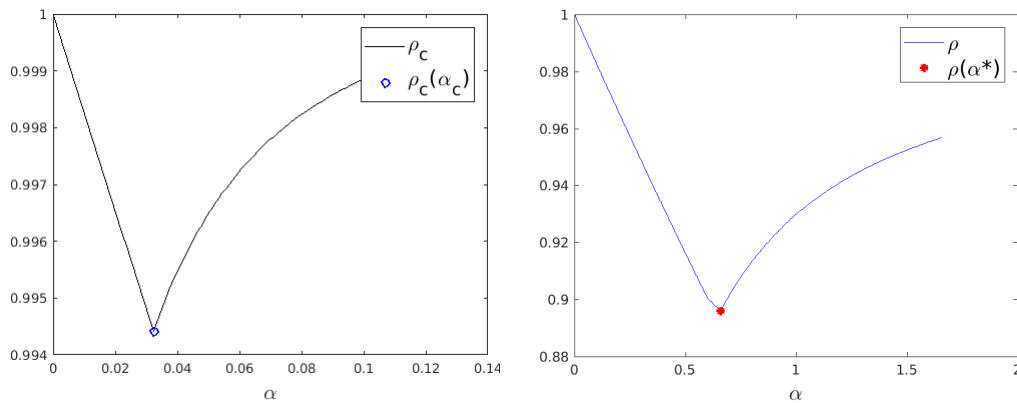
Figure 2.21: Example 3 (Robin). Left: continuous convergence factor versus α with theoretical optimized value α_c (blue circle); Right: SDT convergence factor versus α with theoretical optimized value α^* (red star)

In Figure 2.22, the Robin-2p case (i.e. $\alpha_1 = \alpha_2 = \alpha$ and $\beta_1 = \beta_2 = \beta$) is considered and we show the evolution of the continuous convergence factor ρ_c (on the left) and of the semi-discrete in time convergence factor ρ (on the right), as a function of the

Robin parameters α and β, as well as the optimized values (α_c, β_c) (blue circle, on the left figure) and (α^*, β^*) (red star, on the right figure). The numerical optimized values are $(\alpha_c, \beta_c) = (3.2284\,10^{-2}, 3.2256\,10^{-2})$ and $(\alpha^*, \beta^*) = (6.6035\,10^{-1}, 6.2908\,10^{-1})$, and thus are nearly close to the optimized Robin values (i.e. on the axis $\alpha = \beta$).

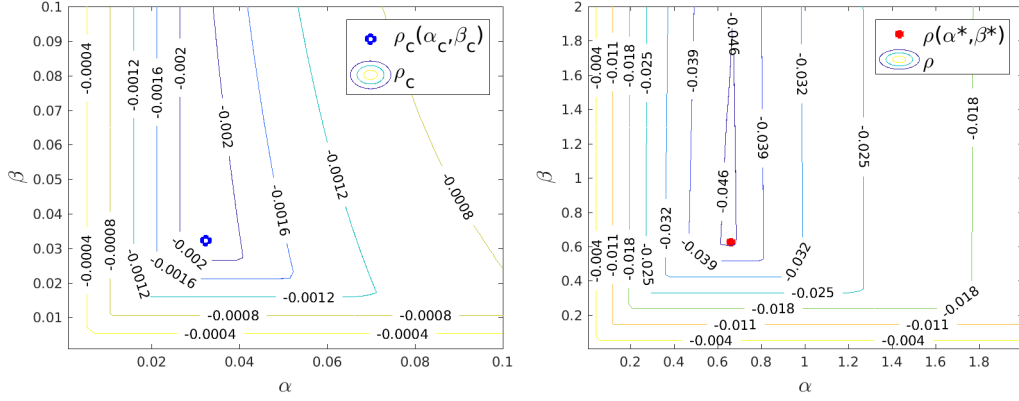Figure 2.22: Example 3 (Robin-2p). Left: continuous convergence factor versus α and β with theoretical optimized value (α_c, β_c) (blue circle); Right: SDT convergence factor versus α and β with theoretical optimized value (α^*, β^*) (red star)

In Figure 2.23, the Robin-2sided case (i.e. $\alpha_1 = \beta_1 = \alpha$ and $\alpha_2 = \beta_2 = \beta$) is considered and we plot the evolution of the continuous convergence factor ρ_c (on the left) and of the semi-discrete in time convergence factor ρ (on the right), as a function of the Robin parameters α and β. For the optimized value (α_c, β_c) (on left figure), we consider two initial inputs for the function fminsearch of MATLAB : $(\alpha, \beta) = (0, 0)$ that gives the optimized value $(\alpha_c^0, \beta_c^0) = (1.2732\,10^{-2}, 5.7254\,10^{-2})$ (blue circle), and $(\alpha, \beta) = (0.03, 0.03)$ that gives the value $(\alpha_c^1, \beta_c^1) = (5.7254\,10^{-2}, 1.2732\,10^{-2})$ (green diamond). This is due to the symmetrical shape of the convergence factor ρ_c. A conjecture is that the true optimized value (α_c, β_c) is on the axis $\alpha = \beta$ (i.e. corresponds to the optimized Robin value above), and that fminsearch find wrong values. There is no longer this problem for the optimized value (α^*, β^*) (red star, on the right figure), whose numerical value obtained with fminsearch is $(\alpha^*, \beta^*) = (6.6063\,10^{-1}, 6.6063\,10^{-1})$. It corresponds to the optimized Robin values above, of Figure 2.21.

In conclusion, for this example, we expect that using more than on parameter (Robin-2p or Robin-2sided) will not give a significant improvement compared to the Robin case, and thus we will consider only optimized Robin parameters in what follows.

2.8.3.2 Case f constant

In this example we take $\mathbf{f} = -2$ in Ω_f.

In Figures 2.24 and 2.25, we plot the evolution of the horizontal and vertical components of the velocity respectively, at times $t = 1, 2, 3, 4, 5$, with a fixed colorbar. We observe that the stationary state is not reached yet. In Figure 2.26, the pressure is also shown, at times $t = 1$ and $t = 5$.
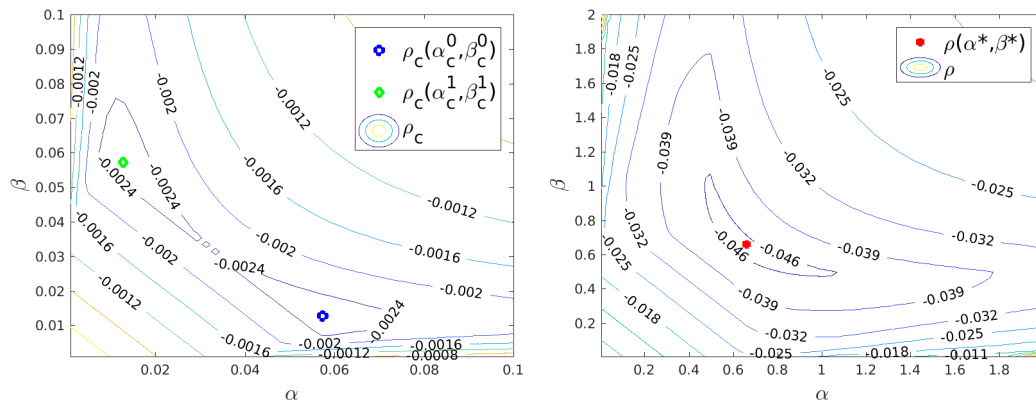
Figure 2.23: Example 3 (Robin-2sided). Left: continuous convergence factor versus α and β with theoretical optimized values (α_c^0, β_c^0) (blue circle) and (α_c^1, β_c^1) (green diamond); Right: SDT convergence factor versus α and β with theoretical optimized value (α^*, β^*) (red star)

Figure 2.24: (Case **f** constant) - Horizontal component of the velocity u_x at $t = 1, 2, 3, 4$ and at final time $t = T = 5$. The colorbar is the same for all figure and is shown on the bottom right
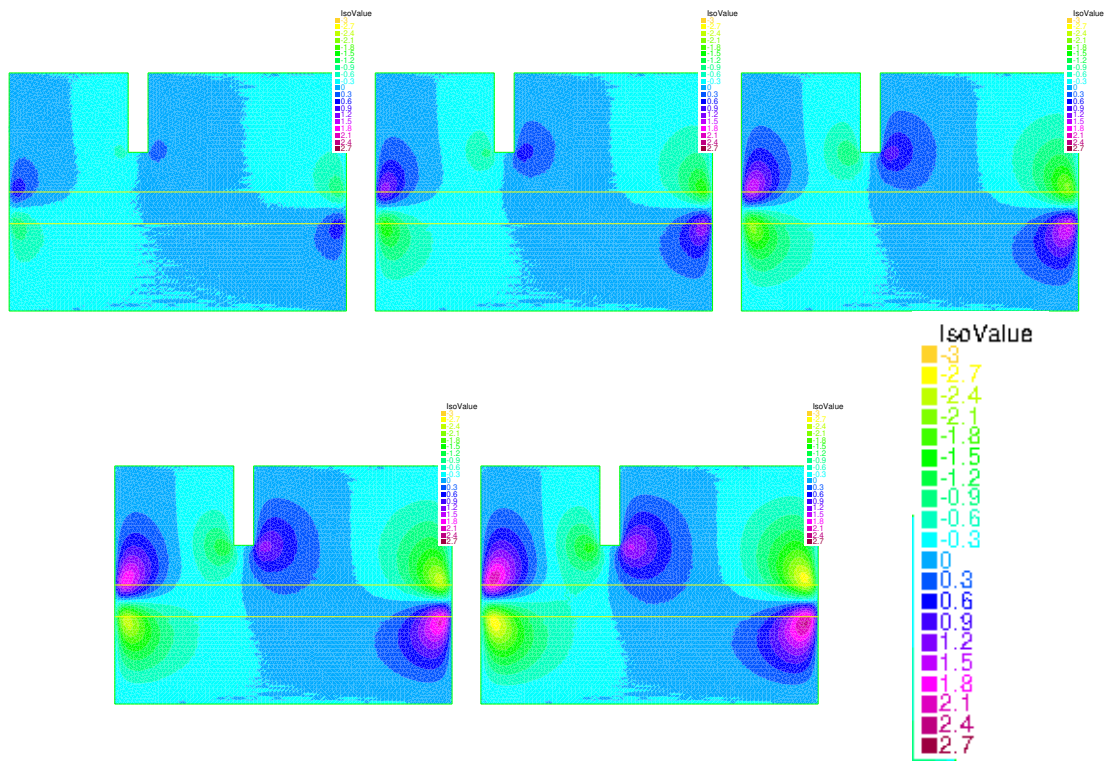
Figure 2.25: (Case **f** constant) - Vertical component of the velocity u_y at $t = 1, 2, 3, 4$ and at final time $t = T = 5$. The colorbar is the same for all figure and is shown on the bottom right
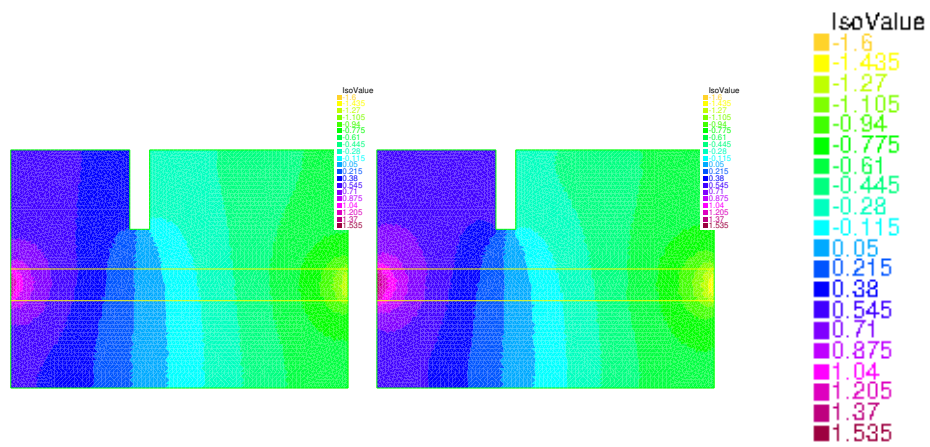
Figure 2.26: (Case **f** constant) - Pressure p at $t = 1$ and at final time $t = T = 5$

In Figure 2.27, we consider the Robin case and show the evolution of the relative errors, between the OSWR and monodomain solutions, of u_x, u_y, and p, in the $L^\infty(0, T; L^2(\Omega))$-norm, versus OSWR iterations, for $\alpha = \alpha_c = 3.2283\, 10^{-2}$ (blue, red, and cyan curves) and $\alpha = \alpha^* = 6.6063\, 10^{-1}$. For $\alpha = \alpha^*$, the curves of u_x and p are quite close, with a faster convergence for u_y. For $\alpha = \alpha_c$, the curves of u_x and u_y have almost the same speed of convergence, with a slower convergence for p for the first iterations. Moreover, the convergence is much slower with $\alpha = \alpha_c$ than with $\alpha = \alpha^*$. This illustrates the importance of the effect of the numerical scheme used in the time direction.

Figure 2.27: (Case **f** constant) - Relative errors (for u_x, u_y and p) versus iterations, with modified pressure and optimized Robin parameters α_c (blue, red, and cyan curves) and α^* (green, magenta and black curves)

2.8.3.3   Case f variable in time

In this example we take $\mathbf{f} = -2\,(\sin(\pi t) + \cos(4\pi t))$ in Ω_f.

In Figures 2.28 and 2.30, we plot the evolution of the horizontal and vertical components the velocity respectively, at times $t = 1, 2, 3, 4, 5$, with a fixed colorbar. In Figure 2.29, the pressure is also plotted, at times $t = 1$ and $t = 5$.
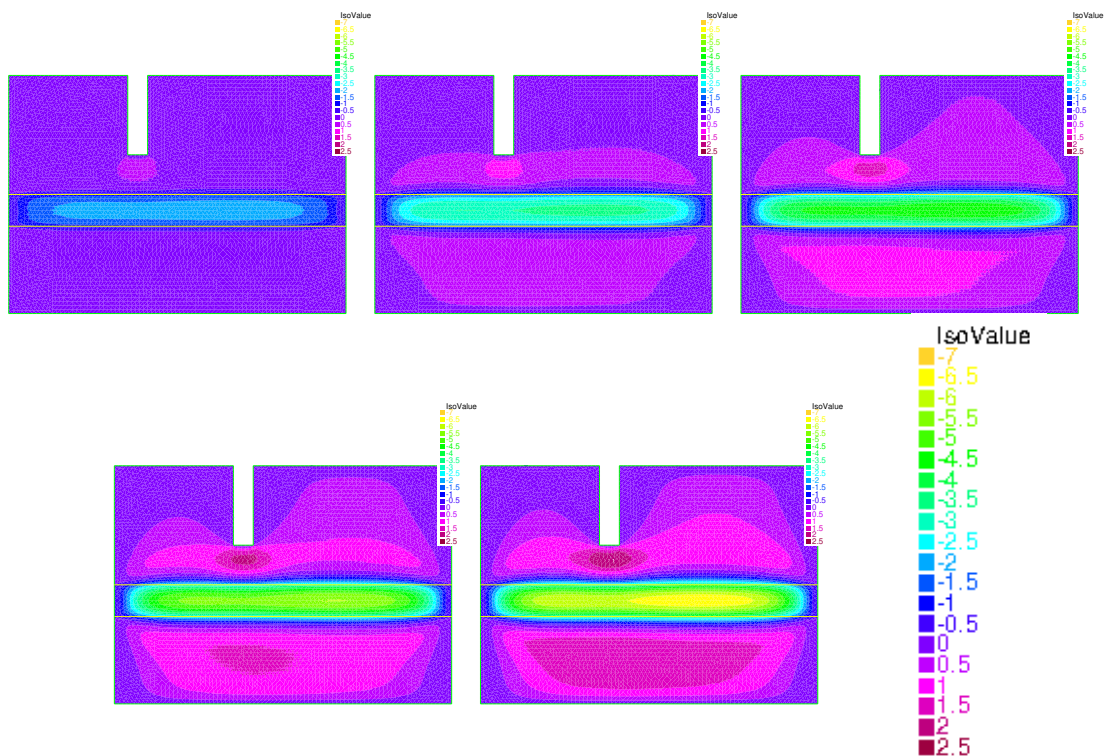
In Figure 2.31, we plot the evolution of the relative errors, between the OSWR and monodomain solutions, of u_x, u_y, and p, in the $L^\infty(0, T; L^2(\Omega))$-norm, versus OSWR iterations, for the optimized Robin parameters $\alpha = \alpha_c = 3.2283\, 10^{-2}$ (blue, red, and cyan curves) and $\alpha = \alpha^* = 6.6063\, 10^{-1}$ (green, magenta and black curves). For $\alpha = \alpha^*$, the curves of u_x, u_y and p are quite close. For $\alpha = \alpha_c$, the convergence is much slower than the one with $\alpha = \alpha^*$. This illustrates once again the importance of the effect of the numerical scheme used in the time direction.
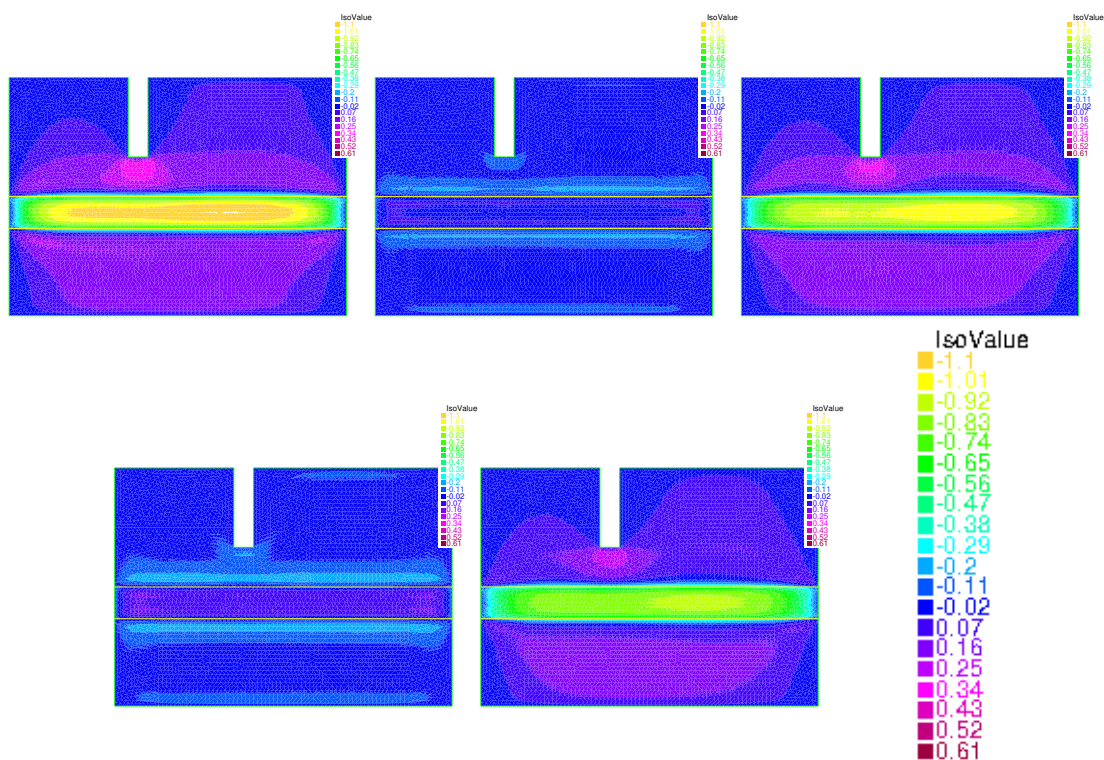
Figure 2.28: (Case **f** variable in time) - Horizontal component of the velocity u_x at $t = 1, 2, 3, 4$ and at final time $t = T = 5$. The colobar is the same for all figure and is shown on the bottom right


Figure 2.29: (Case **f** variable in time) - Pressure p at $t = 1$ and at final time $t = T = 5$
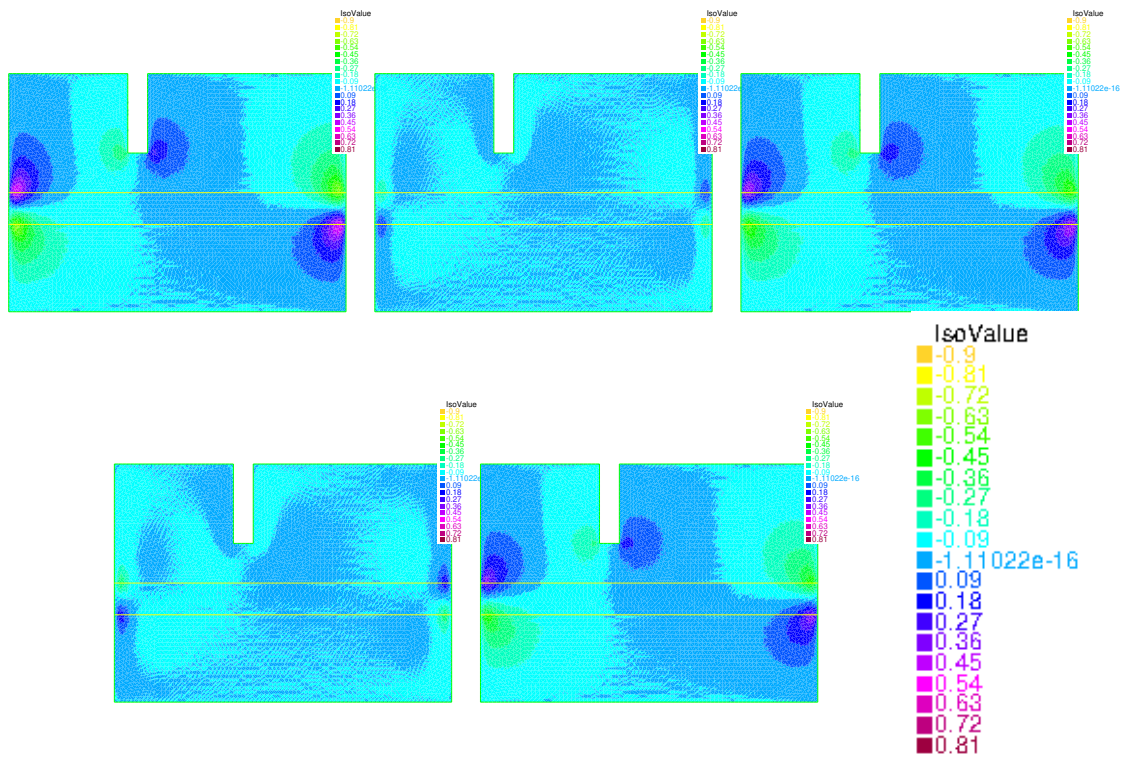
Figure 2.30: (Case **f** variable in time) - Vertical component of the velocity u_y at $t = 1, 2, 3, 4$ and at final time $t = T = 5$. The colobar is the same for all figure and is shown on the bottom right
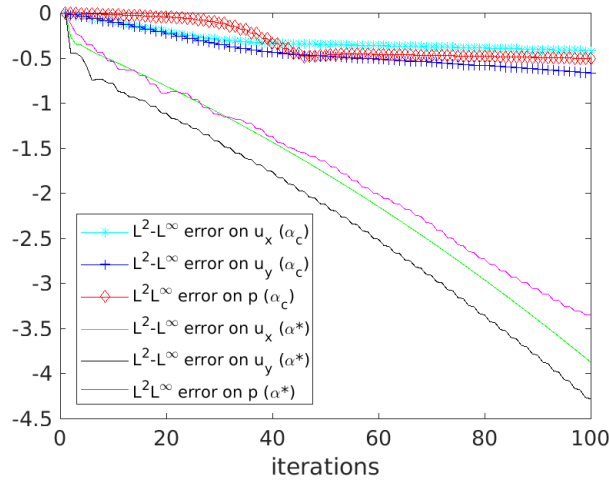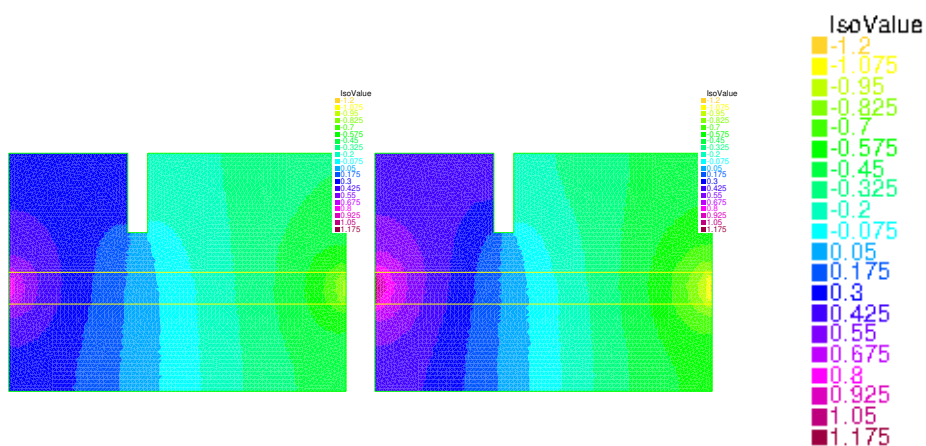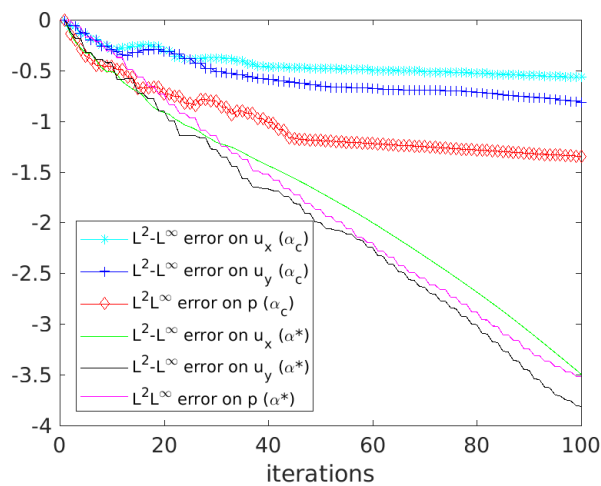

Figure 2.31: (Case **f** variable) - Relative errors (for u_x, u_y and p) versus iterations, with modified pressure and optimized Robin parameters α_c (blue, red, and cyan curves) and α^* (green, magenta and black curves)

2.9   Extension to Oseen equation

In this subsection we extend the OSWR approach to the time-dependent Oseen equation. As in the case of the Stokes equations, we write the multi-domain formulation, we study the well-posedness in the subdomains using Robin boundary conditions, we write the SWR algorithm and then we prove the velocity convergence through an energy estimate and perform a Fourier transform to get the formulation of the convergence factor.

2.9.1   The Oseen equations. Multidomain formulation

The time-dependent Oseen equation has the following form

$$
\begin{aligned}
\partial_t \mathbf{u} - \nu\Delta\mathbf{u} + (\mathbf{b}\cdot\nabla)\mathbf{u} + \nabla p &= \mathbf{f} && \text{in} && \Omega\times(0,T) \\
\nabla\!\cdot\!\mathbf{u} &= 0 && \text{in} && \Omega\times(0,T) \\
\mathbf{u}(.,t=0) &= \mathbf{u}_0 && \text{in} && \Omega \\
\mathbf{u} &= 0 && \text{on} && \partial\Omega\times(0,T)
\end{aligned}
\tag{2.86}
$$

with the divergence-free convection field $\mathbf{b}\in L^\infty((0,T),L^\infty(\Omega))$.
We recall the following spaces

$$
\begin{aligned}
V &= \left\{\mathbf{u}\in\left[H_0^1(\Omega)\right]^2, \nabla\!\cdot\!\mathbf{u}=0\right\}, \\
H &= \left\{\mathbf{u}\in\left[L^2(\Omega)\right]^2, \mathbf{u}\cdot\boldsymbol{n}=0 \text{ on } \partial\Omega, \nabla\!\cdot\!\mathbf{u}=0\right\}, \\
X &= \left\{\mathbf{u}\in\left[H_0^1(\Omega)\right]^2\right\},
\end{aligned}
\tag{2.87}
$$

For $\mathbf{u},\mathbf{v}\in V$, one has the following expression

$$
((\mathbf{b}\cdot\nabla)\mathbf{u},\mathbf{v})_\Omega = \frac{1}{2}(\mathbf{b}\cdot\nabla\mathbf{u},\mathbf{v})_\Omega - \frac{1}{2}(\mathbf{b}\cdot\nabla\mathbf{v},\mathbf{u})_\Omega
$$

Then, we can write the constrained variational form of (2.86) as:
find $(\mathbf{u},p)\in L^2((0,T),V)\cap\mathscr{C}((0,T),H)\times W^{-1,\infty}((0,T),L_0^2(\Omega))$ such that

- $\partial_t\mathbf{u}\in L^2((0,T),V')$ and $\mathbf{u}$ verifies

$$
\begin{aligned}
\langle\partial_t\mathbf{u},\mathbf{v}\rangle_{V,V'} + A(\mathbf{u},\mathbf{v}) &= (\mathbf{f},\mathbf{v})_\Omega, \quad \forall\mathbf{v}\in V \\
\mathbf{u}(t=0) &= \mathbf{u}_0,
\end{aligned}
\tag{2.88}
$$

  with $A(.,.)$ a bilinear form defined on $X\supset V$

$$
A(\mathbf{u},\mathbf{v}) = \nu(\nabla\mathbf{u},\nabla\mathbf{v})_\Omega + \frac{1}{2}(\mathbf{b}\cdot\nabla\mathbf{u},\mathbf{v})_\Omega - \frac{1}{2}(\mathbf{b}\cdot\nabla\mathbf{v},\mathbf{u})_\Omega
$$

- $p = \partial_t P$, with $P\in L^\infty((0,T),L_0^2(\Omega))$ satisfying

$$
(\mathbf{u}(t),\mathbf{v})_\Omega - (\mathbf{u}_0,\mathbf{v})_\Omega + \int_0^t A(\mathbf{u}(s),\mathbf{v}) - (\nabla\!\cdot\!\mathbf{v},P(t))_\Omega = \int_0^t (\mathbf{f}(s),\mathbf{v})_\Omega, \quad \forall\mathbf{v}\in X
\tag{2.89}
$$

Theorem 2.30. *When $\mathbf{u}_0\in H$, problem (2.88)–(2.89) admits a unique solution.*

Proof. One has

$$A(\mathbf{u}, \mathbf{u}) = \nu (\nabla \mathbf{u}, \nabla \mathbf{u})_\Omega,$$

hence $A(.,.)$ is coercive. In addition, the inequality

$$|\frac{1}{2}(\mathbf{b}\cdot\nabla\mathbf{u}, \mathbf{v})_\Omega - \frac{1}{2}(\mathbf{b}\cdot\nabla\mathbf{v}, \mathbf{u})_\Omega| \le C\|\mathbf{b}\|_{L^\infty((0,T),L^\infty(\Omega)^2)}(\|\nabla\mathbf{u}\|_\Omega\|\mathbf{v}\|_\Omega + \|\nabla\mathbf{v}\|_\Omega\|\mathbf{u}\|_\Omega)$$

implies the continuity of $A(.,.)$. Then, following similar arguments as in Section 2.2, one gets the well-posedness of (2.88) and the existence of the pressure satisfying (2.89).   □

We have now the solution of the variational Oseen equation. However, in order to define the Robin transmission conditions, we need more regularity. Unfortunately, the analysis for the time-dependent Oseen equations are not well-presented in the current literature. The Oseen equations themselves in fact are usually considered as a simplified version of the Navier-Stokes system, whose strong regularity has been studied well; it is generally believed that the results obtained for the latter are also valid for the former. Therefore, at this point, we suppose that we have the following strong regularity.

Hypothesis 2.31. *With the domain Ω, the advection $\mathbf{b}$, the source term $\mathbf{f}$ and the initial condition $\mathbf{u}_0$ regular enough, the Oseen equation(2.86) admits a unique solution $\mathbf{u} \in L^2((0,T),V) \cap L^2((0,T),H^2(\Omega)^2)$, $p \in L^2((0,T),L_0^2(\Omega)) \cap L^2((0,T),H^1(\Omega)$ with $\partial_t \mathbf{u} \in L^2((0,T),H)$.*

The above regularity hypothesis allow us to rewrite the monodomain problem into the following equivalent multidomain one. We denote by $b_{ij} = \mathbf{b}\cdot\mathbf{n}_{ij}$.

$$
\begin{aligned}
\partial_t \mathbf{u}_i - \nu\Delta\mathbf{u}_i + (\mathbf{b}\cdot\nabla)\mathbf{u}_i + \nabla p_i &= \mathbf{f}_i & \text{in} \quad & \Omega_i \times (0,T) \\
\nabla\cdot\mathbf{u}_i &= 0 & \text{in} \quad & \Omega_i \times (0,T) \\
\mathbf{u}_i(.,t=0) &= (\mathbf{u}_0)_i & \text{in} \quad & \Omega_i \\
\mathbf{u}_i &= 0 & \text{on} \quad & (\partial\Omega \cap \partial\Omega_i) \times (0,T)
\end{aligned}
\tag{2.90}
$$

with $i = 1, 2, \ldots, M$, together with Robin transmission conditions on $\Gamma_{ij} \times (0,T)$

$$
\alpha_{ij}\left(\nu\partial_{\mathbf{n}_{ij}}\mathbf{u}_i \cdot \mathbf{n}_{ij} - p_i - \frac{1}{2}b_{ij}\mathbf{u}_i \cdot \mathbf{n}_{ij}\right) + \mathbf{u}_i \cdot \mathbf{n}_{ij}
$$
$$
= \alpha_{ij}\left(\nu\partial_{\mathbf{n}_{ij}}\mathbf{u}_j \cdot \mathbf{n}_{ij} - p_j - \frac{1}{2}b_{ij}\mathbf{u}_j \cdot \mathbf{n}_{ij}\right) + \mathbf{u}_j \cdot \mathbf{n}_{ij}
$$
$$
\alpha_{ji}\left(\nu\partial_{\mathbf{n}_{ji}}\mathbf{u}_j \cdot \mathbf{n}_{ji} - p_j - \frac{1}{2}b_{ji}\mathbf{u}_j \cdot \mathbf{n}_{ji}\right) + \mathbf{u}_j \cdot \mathbf{n}_{ji}
$$
$$
= \alpha_{ji}\left(\nu\partial_{\mathbf{n}_{ji}}\mathbf{u}_i \cdot \mathbf{n}_{ji} - p_i - \frac{1}{2}b_{ji}\mathbf{u}_i \cdot \mathbf{n}_{ji}\right) + \mathbf{u}_i \cdot \mathbf{n}_{ji}
$$
$$
\beta_{ij}\left(\nu\partial_{\mathbf{n}_{ij}}\mathbf{u}_i \times \mathbf{n}_{ij} - \frac{1}{2}b_{ij}\mathbf{u}_i \times \mathbf{n}_{ij}\right) + \mathbf{u}_i \times \mathbf{n}_{ij}
$$
$$
= \beta_{ij}\left(\nu\partial_{\mathbf{n}_{ij}}\mathbf{u}_j \times \mathbf{n}_{ij} - \frac{1}{2}b_{ij}\mathbf{u}_j \times \mathbf{n}_{ij}\right) + \mathbf{u}_j \times \mathbf{n}_{ij}
$$
$$
\beta_{ji}\left(\nu\partial_{\mathbf{n}_{ji}}\mathbf{u}_j \times \mathbf{n}_{ji} - \frac{1}{2}b_{ji}\mathbf{u}_j \times \mathbf{n}_{ji}\right) + \mathbf{u}_j \times \mathbf{n}_{ji}
$$
$$
= \beta_{ji}\left(\nu\partial_{\mathbf{n}_{ji}}\mathbf{u}_i \times \mathbf{n}_{ji} - \frac{1}{2}b_{ji}\mathbf{u}_i \times \mathbf{n}_{ji}\right) + \mathbf{u}_i \times \mathbf{n}_{ji}
$$

$$\tag{2.91}$$

2.9.2 Oseen equation with Robin boundary condition

We now consider a domain, still denoted by Ω, for which the boundary is decomposed into two parts: $\partial\Omega = \Gamma_D \cup \Gamma_R$, with $|\Gamma_R| > 0$. Let $\boldsymbol{n}$ be the outgoing normal vector on Γ_R; we consider the following system, with $\alpha > 0$ and $\beta > 0$

$$
\begin{aligned}
\partial_t \mathbf{u} - \nu\Delta\mathbf{u} + (\mathbf{b}\cdot\nabla)\mathbf{u} + \nabla p &= \mathbf{f} &&\text{in} &&\Omega \times (0, T) \\
\nabla\cdot\mathbf{u} &= 0 &&\text{in} &&\Omega \times (0, T) \\
\mathbf{u}(., t = 0) &= \mathbf{u}_0 &&\text{in} &&\Omega \\
\mathbf{u} &= 0 &&\text{on} &&\Gamma_D \times (0, T) \\
\alpha\left(\nu\partial_{\boldsymbol{n}}\mathbf{u}\cdot\boldsymbol{n} - p - \tfrac{1}{2}(\mathbf{b}\cdot\boldsymbol{n})\mathbf{u}\cdot\boldsymbol{n}\right) + \mathbf{u}\cdot\boldsymbol{n} &= g &&\text{on} &&\Gamma_R \times (0, T) \\
\beta\left(\nu\partial_{\boldsymbol{n}}\mathbf{u}\times\boldsymbol{n} - \tfrac{1}{2}(\mathbf{b}\cdot\boldsymbol{n})\mathbf{u}\times\boldsymbol{n}\right) + \mathbf{u}\times\boldsymbol{n} &= \xi &&\text{on} &&\Gamma_R \times (0, T)
\end{aligned}
\tag{2.92}
$$

We recall the spaces that were used for the Stokes problem

$$
\begin{aligned}
V_D &= \left\{\mathbf{u} \in \left[H^1(\Omega)\right]^2, \mathbf{u} = 0 \text{ on } \Gamma_D, \nabla\cdot\mathbf{u} = 0\right\}, \\
H_D &= \left\{\mathbf{u} \in \left[L^2(\Omega)\right]^2, \mathbf{u}\cdot\boldsymbol{n} = 0 \text{ on } \Gamma_D, \nabla\cdot\mathbf{u} = 0\right\}, \\
X_D &= \left\{\mathbf{u} \in \left[H^1(\Omega)\right]^2, \mathbf{u} = 0 \text{ on } \Gamma_D\right\},
\end{aligned}
\tag{2.93}
$$

equipped with the H^1 and L^2 norms, respectively.

Integrating by part and taking into account the fact that $\mathbf{b}$ is divergence free and $\mathbf{v} = 0$ on Γ_D, we obtain

$$
\begin{aligned}
(\mathbf{b}\cdot\nabla\mathbf{u}, \mathbf{v})_\Omega &= \frac{1}{2}(\mathbf{b}\cdot\nabla\mathbf{u}, \mathbf{v})_\Omega + \frac{1}{2}(\mathbf{b}\cdot\nabla\mathbf{u}, \mathbf{v})_\Omega \\
&= \frac{1}{2}(\mathbf{b}\cdot\nabla\mathbf{u}, \mathbf{v})_\Omega - \frac{1}{2}(\mathbf{b}\cdot\nabla\mathbf{v}, \mathbf{u})_\Omega + \frac{1}{2}((\mathbf{b}\cdot\boldsymbol{n})\mathbf{u}, \mathbf{v})_{\Gamma_R} \\
&= \frac{1}{2}(\mathbf{b}\cdot\nabla\mathbf{u}, \mathbf{v})_\Omega - \frac{1}{2}(\mathbf{b}\cdot\nabla\mathbf{v}, \mathbf{u})_\Omega \\
&\quad + \frac{1}{2}((\mathbf{b}\cdot\boldsymbol{n})\mathbf{u}\cdot\boldsymbol{n}, \mathbf{v}\cdot\mathbf{v})_{\Gamma_R} + \frac{1}{2}((\mathbf{b}\cdot\boldsymbol{n})\mathbf{u}\times\boldsymbol{n}, \mathbf{v}\times\mathbf{v})_{\Gamma_R}.
\end{aligned}
$$

Taking into account the boundary condition, we define the following bilinear form $a(\cdot, \cdot)$ on $V_D \times V_D$, and the linear form $c(\cdot)$ on V_D

$$
\begin{aligned}
a(\mathbf{u}, \mathbf{v}) = {}& \nu(\nabla\mathbf{u}, \nabla\mathbf{v})_\Omega + \frac{1}{2}(\mathbf{b}\cdot\nabla\mathbf{u}, \mathbf{v})_\Omega \\
& - \frac{1}{2}(\mathbf{b}\cdot\nabla\mathbf{v}, \mathbf{u})_\Omega + \frac{1}{\alpha}(\mathbf{u}\cdot\boldsymbol{n}, \mathbf{v}\cdot\boldsymbol{n})_{\Gamma_R} + \frac{1}{\beta}(\mathbf{u}\times\boldsymbol{n}, \mathbf{v}\times\boldsymbol{n})_{\Gamma_R},
\end{aligned}
\tag{2.94}
$$

$$
c(t, \mathbf{v}) = (\mathbf{f}, \mathbf{v})_\Omega + \frac{1}{\alpha}(g, \mathbf{v}\cdot\boldsymbol{n})_{\Gamma_R} + \frac{1}{\beta}(\xi, \mathbf{v}\times\boldsymbol{n})_{\Gamma_R},
\tag{2.95}
$$

Taking $\mathbf{u}$ as test function, one has

$$
a(\mathbf{u}, \mathbf{u}) = \nu(\nabla\mathbf{u}, \nabla\mathbf{u})_\Omega + \frac{1}{\alpha}(\mathbf{u}\cdot\boldsymbol{n}, \mathbf{u}\cdot\boldsymbol{n})_{\Gamma_R} + \frac{1}{\beta}(\mathbf{u}\times\boldsymbol{n}, \mathbf{u}\times\boldsymbol{n})_{\Gamma_R},
$$

hence, as shown for the Stokes equations, $a(., .)$ is coercive.

The inequality

$$
\left|\frac{1}{2}(\mathbf{b}\cdot\nabla\mathbf{u}, \mathbf{v})_\Omega - \frac{1}{2}(\mathbf{b}\cdot\nabla\mathbf{v}, \mathbf{u})_\Omega\right| \le C\|\mathbf{b}\|_{L^\infty((0,T), L^\infty(\Omega)^2)}(\|\nabla\mathbf{u}\|_\Omega\|\mathbf{v}\|_\Omega + \|\nabla\mathbf{v}\|_\Omega\|\mathbf{u}\|_\Omega)
$$

leads to the continuity of $a(.,.)$. Then, following similar arguments as for the Stokes equation, on can show that

Theorem 2.32. *There exists unique $p \in W^{-1,\infty}((0,T), L^2(\Omega))$ and $\mathbf{u} \in \left(L^2((0,T), V_D) \cap \mathscr{C}^0([0,T], H_D)\right)$, with $\partial_t \mathbf{u} \in L^2((0,T), V_D')$ such that $(\mathbf{u}, p)$ is solution of problem (2.92) in the sense that*

- **u** *verifies*

$$\langle \partial_t \mathbf{u}, \mathbf{v} \rangle_{V_D', V_D} + a(t, \mathbf{u}, \mathbf{v}) = c(t, \mathbf{v}) \text{ for almost every } t \in (0,T) \text{ and all } \mathbf{v} \in V_D,$$
(2.96)

$$\mathbf{u}(0) = \mathbf{u}_0.$$
(2.97)

- $p = \partial_t P$ *with* $P \in L^\infty((0,T), L^2(\Omega))$ *satisfying*

$$\int_0^t c(s, \mathbf{v}) - (\mathbf{u}(t), \mathbf{v})_\Omega + (\mathbf{u}_0, \mathbf{v})_\Omega - \int_0^t a(\mathbf{u}(s), \mathbf{v}) ds = -\int_\Omega P(t) \nabla \cdot \mathbf{v}, \quad \forall \mathbf{v} \in X_D. \quad (2.98)$$

2.9.3   Optimzed Schwarz Waveform Relaxation Algorithm

We can now establish a space-time DD algorithm for the Oseen equations:
Provided starting Robin terms g_{ij}^0, ξ_{ij}^0 on the interfaces $\Gamma_{ij} \times (0,T)$ (regular enough), at step $\ell \geq 1$, we solve M subdomain problems

$$
\begin{aligned}
\partial_t \mathbf{u}_i^\ell - \nu \Delta \mathbf{u}_i^\ell + (\mathbf{b} \cdot \nabla) \mathbf{u}_i^\ell + \nabla p_i^\ell &= \mathbf{f}_i && \text{in} && \Omega_i \times (0,T) \\
\nabla \cdot \mathbf{u}_i^\ell &= 0 && \text{in} && \Omega_i \times (0,T) \\
\mathbf{u}_i^\ell(., t=0) &= (\mathbf{u}_0)_i && \text{in} && \Omega_i \\
\alpha_{ij} \left(\nu \partial_{\mathbf{n}_{ij}} \mathbf{u}_i^\ell \cdot \mathbf{n}_{ij} - p_i^\ell - \frac{1}{2} b_{ij} \mathbf{u}_i^\ell \cdot \mathbf{n}_{ij} \right) + \mathbf{u}_i^\ell \cdot \mathbf{n}_{ij} &= g_{ij}^{\ell-1} && \text{on} && \Gamma_{ij} \times (0,T) \\
\beta_{ij} \left(\nu \partial_{\mathbf{n}_{ij}} \mathbf{u}_i^\ell \times \mathbf{n}_{ij} - \frac{1}{2} b_{ij} \mathbf{u}_i^\ell \times \mathbf{n}_{ij} \right) + \mathbf{u}_i^\ell \times \mathbf{n}_{ij} &= \xi_{ij}^{\ell-1} && \text{on} && \Gamma_{ij} \times (0,T) \\
\mathbf{u}_i^\ell &= 0 && \text{on} && (\partial\Omega_i \cap \partial\Omega) \times (0,T)
\end{aligned}
$$
(2.99)

with $i = 1, 2, \ldots, M$ and then we update the Robin terms on the interfaces $\Gamma_{ij} \times (0,T)$

$$
\begin{aligned}
g_{ij}^\ell &= \alpha_{ij} \left(\nu \partial_{\mathbf{n}_{ij}} \mathbf{u}_j^\ell \cdot \mathbf{n}_{ij} - p_j^\ell - \frac{1}{2} b_{ij} \mathbf{u}_j^\ell \cdot \mathbf{n}_{ij} \right) + \mathbf{u}_j^\ell \cdot \mathbf{n}_{ij} \\
\xi_{ij}^\ell &= \beta_{ij} \left(\nu \partial_{\mathbf{n}_{ij}} \mathbf{u}_j^\ell \times \mathbf{n}_{ij} - \frac{1}{2} b_{ij} \mathbf{u}_j^\ell \times \mathbf{n}_{ij} \right) + \mathbf{u}_j^\ell \times \mathbf{n}_{ij},
\end{aligned}
$$
(2.100)

with $j \in \mathscr{I}_i$.
We rewrite next the algorithm using a variational formulation. We recall the notations used for the Stokes equation

$$
\begin{aligned}
V_i &= \{\mathbf{u} \in \left[H^1(\Omega_i)\right]^2, \mathbf{u} = 0 \text{ on } \partial\Omega_i \cap \partial\Omega, \nabla \cdot \mathbf{u} = 0 \text{ in } \Omega_i\}, \\
H_i &= \{\mathbf{u} \in \left[L^2(\Omega_i)\right]^2, \mathbf{u} \cdot \mathbf{n}_{\partial\Omega_i} = 0 \text{ on } \partial\Omega_i \cap \partial\Omega, \nabla \cdot \mathbf{u} = 0 \text{ in } \Omega_i\}. \\
X_i &= \{\mathbf{u} \in \left[H^1(\Omega_i)\right]^2, \mathbf{u} = 0 \text{ on } \partial\Omega_i \cap \partial\Omega\},
\end{aligned}
$$

Then, we set

$$
a_i(\mathbf{u}, \mathbf{v}) = \nu(\nabla \mathbf{u}, \nabla \mathbf{v})_{\Omega_i} + \frac{1}{2}(\mathbf{b} \cdot \nabla \mathbf{u}, \mathbf{v})_{\Omega_i} - \frac{1}{2}(\mathbf{b} \cdot \nabla \mathbf{v}, \mathbf{u})_{\Omega_i}
$$

$$
+ \frac{1}{\alpha_{ij}}\left(\mathbf{u} \cdot \boldsymbol{n}_{ij}, \mathbf{v} \cdot \boldsymbol{n}_{ij}\right)_{\Gamma_{ij}} + \frac{1}{\beta_{ij}}\left(\mathbf{u} \times \boldsymbol{n}_{ij}, \mathbf{v} \times \boldsymbol{n}_{ij}\right)_{\Gamma_{ij}}, \tag{2.101}
$$

$$
c_i^\ell(t, \mathbf{v}) = (\mathbf{f}, \mathbf{v})_{\Omega_i} + \sum_{j \in \mathcal{I}_i} \frac{1}{\alpha_{ij}}\left(g_{ij}^{\ell-1}, \mathbf{v} \cdot \boldsymbol{n}_{ij}\right)_{\Gamma_{ij}} + \frac{1}{\beta_{ij}}\left(\xi_{ij}^{\ell-1}, \mathbf{v} \times \boldsymbol{n}_{ij}\right)_{\Gamma_{ij}},
$$

and the algorithm reads: for all $\ell \geq 1$, given $g_{ij}^{\ell-1}, \xi_{ij}^{\ell-1}$ on each space-time interface $\Gamma_{ij} \times (0, T)$, solve, for each $i = 1, \dots, M$:

$$
\left\langle \partial_t \mathbf{u}_i^\ell, \mathbf{v} \right\rangle_{V_i', V_i} + a_i(\mathbf{u}_i^\ell, \mathbf{v}) = c_i^\ell(t, \mathbf{v}), \qquad \text{a.e. } t \in (0, T), \forall \mathbf{v} \in V_i,
$$
$$
\mathbf{u}_i^\ell(0) = \mathbf{u}_{0,i} \tag{2.102}
$$

and then construct $p_i^\ell = \partial_t P_i^\ell$ which is such that

$$
\left(\mathbf{u}_i^\ell(t), \mathbf{v}\right)_{\Omega_i} - \left(\mathbf{u}_{0,i}, \mathbf{v}\right)_{\Omega_i} + \int_0^t a_i(\mathbf{u}_i^\ell(s), \mathbf{v}) ds - (P_i^\ell, \nabla \cdot \mathbf{v})_{\Omega_i} - \int_0^t c_i^\ell(s, \mathbf{v}) ds = 0, \ \forall \mathbf{v} \in X_i.
$$

After that, we update Robin terms using the same trick as in Remark 2.15

$$
g_{ij}^\ell = \frac{\alpha_{ij}}{\alpha_{ji}} g_{ji}^{\ell-1} - \frac{\alpha_{ij} + \alpha_{ji}}{\alpha_{ji}} \mathbf{u}_j^\ell \cdot \boldsymbol{n}_{ji} \tag{2.103}
$$

$$
\xi_{ij}^\ell = \frac{\beta_{ij}}{\beta_{ji}} \xi_{ji}^{\ell-1} - \frac{\beta_{ij} + \beta_{ji}}{\beta_{ji}} \mathbf{u}_j^\ell \times \boldsymbol{n}_{ji} \tag{2.104}
$$

2.9.4 Convergence of the velocity via energy estimate

Theorem 2.33. *Let $(\mathbf{u}, p)$ be the solution of the Oseen equations (2.86) which is supposed to verify Hypothesis 2.31. We denote by $\mathbf{u}_i = \mathbf{u}|_{\Omega_i}$. Then, if $\alpha_{ij} = \alpha_{ji}$ and $\beta_{ij} = \beta_{ji}$, the sequence $\mathbf{u}_i^\ell$ defined by the OSWR algorithm in Section 2.9.3 converges to $\mathbf{u}_i$ in $\mathscr{C}^0([0, T], H_i) \cap L^2((0, T), V_i)$.*

Proof. Denote by $p_i = p|_{\Omega_i}$. From Hypothesis 2.31, $(\mathbf{u}_i, p_i)$ is regular, so we can define then the following traces in $L^2((0, T), L^2(\Gamma_{ij}))$

$$
g_{ij} := \alpha_{ij}(\nu \partial_{\boldsymbol{n}_{ij}} \mathbf{u}_i \cdot \boldsymbol{n}_{ij} - p_i - \frac{1}{2}(\mathbf{b} \cdot \boldsymbol{n}_{ij}) \mathbf{u}_i \cdot \boldsymbol{n}_{ij}) + \mathbf{u}_i \cdot \boldsymbol{n}_{ij} \tag{2.105}
$$

$$
\xi_{ij} := \beta_{ij}(\nu \partial_{\boldsymbol{n}_{ij}} \mathbf{u}_i \times \boldsymbol{n}_{ij} - \frac{1}{2}(\mathbf{b} \cdot \boldsymbol{n}_{ij}) \mathbf{u}_i \times \boldsymbol{n}_{ij}) + \mathbf{u}_i \times \boldsymbol{n}_{ij} \tag{2.106}
$$

We recall here that the strong regularity of $(\mathbf{u}, p)$ leads to the multidomain transmission conditions (2.91), which implies, similarly to the Stokes section

$$
g_{ij} = \frac{\alpha_{ij}}{\alpha_{ji}} g_{ji} - \frac{\alpha_{ij} + \alpha_{ji}}{\alpha_{ji}} \mathbf{u}_j \cdot \boldsymbol{n}_{ji} \tag{2.107}
$$

$$
\xi_{ij} = \frac{\beta_{ij}}{\beta_{ji}} \xi_{ji} - \frac{\beta_{ij} + \beta_{ji}}{\beta_{ji}} \mathbf{u}_j \times \boldsymbol{n}_{ji} \tag{2.108}
$$

Moreover, $(\mathbf{u}_i, p_i)$ is the strong solution of each local Robin boundary problem

$$
\begin{aligned}
\partial_t \mathbf{u}_i - \nu \Delta \mathbf{u}_i + (\mathbf{b} \cdot \nabla)\mathbf{u}_i + \nabla p_i &= \mathbf{f}_i && \text{in} && \Omega_i \times (0, T) \\
\nabla \cdot \mathbf{u}_i &= 0 && \text{in} && \Omega_i \times (0, T) \\
\mathbf{u}_i(., t=0) &= \mathbf{u}_{0,i} && \text{in} && \Omega_i \\
\mathbf{u}_i &= 0 && \text{on} && (\partial\Omega \cap \partial\Omega_i) \times (0, T) \\
\alpha_{ij}\left(\nu \partial_{\boldsymbol{n}_{ij}} \mathbf{u}_i \cdot \boldsymbol{n}_{ij} - p_i - \frac{1}{2} b_{ij} \mathbf{u}_i \cdot \boldsymbol{n}_{ij}\right) + \mathbf{u}_i \cdot \boldsymbol{n}_{ij} &= g_{ij} && \text{on} && \Gamma_{ij} \times (0, T) \\
\beta_{ij}\nu \partial_{\boldsymbol{n}_{ij}} \mathbf{u}_i \times \boldsymbol{n}_{ij} - \frac{1}{2} b_{ij} \mathbf{u}_i \times \boldsymbol{n}_{ij} + \mathbf{u}_i \times \boldsymbol{n}_{ij} &= \xi_{ij} && \text{on} && \Gamma_{ij} \times (0, T)
\end{aligned}
$$

We have that u_i verifies the following variational formulation

$$
\begin{aligned}
&\langle \partial_t \mathbf{u}_i, \mathbf{v} \rangle_{V_i', V_i} + a_i(\mathbf{u}_i, \mathbf{v}) = c_i(t, \mathbf{v}) \text{ for almost every } t \in (0, T) \text{ and all } \mathbf{v} \in V_i, \\
&\mathbf{u}_i(0) = \mathbf{u}_0|_{\Omega_i}
\end{aligned}
\tag{2.109}
$$

with

$$
c_i(t, \mathbf{v}) = (\mathbf{f}, \mathbf{v})_{\Omega_i} + \sum_{j \in \mathscr{I}_i} \frac{1}{\alpha_{ij}}\left(g_{ij}, \mathbf{v} \cdot \boldsymbol{n}_{ij}\right)_{\Gamma_{ij}} + \frac{1}{\beta_{ij}}\left(\xi_{ij}, \mathbf{v} \times \boldsymbol{n}_{ij}\right)_{\Gamma_{ij}},
\tag{2.110}
$$

Denote by $\mathbf{e}_i^\ell := \mathbf{u}_i^\ell - \mathbf{u}_i$, $h_{ij}^\ell = g_{ij}^\ell - g_{ij}$, $\zeta_{ij}^\ell = \xi_{ij}^\ell - \xi_{ij}$.
From (2.101), (2.102), (2.109), (2.110), then $\mathbf{e}_i^\ell$ verifies

$$
\langle \partial_t \mathbf{e}_i^\ell, \mathbf{v} \rangle_{V_i', V_i} + a_i(\mathbf{e}_i^\ell, \mathbf{v}) = \sum_{j \in \mathscr{I}_I} \frac{1}{\alpha_{ij}}(h_{ij}^{\ell-1}, \mathbf{v} \cdot \boldsymbol{n}_{ij})_{\Gamma_{ij}} + \sum_{j \in \mathscr{I}_I} \frac{1}{\beta_{ij}}(\zeta_{ij}^{\ell-1}, \mathbf{v} \times \boldsymbol{n}_{ij})_{\Gamma_{ij}} \quad \forall \mathbf{v} \in V_i.
$$

$$
\mathbf{e}_i^\ell(0) = 0
\tag{2.111}
$$

All integrals on Γ_{ij} are well defined since g_{ij} and ξ_{ij} are both in $L^2((0, T), L^2(\Gamma_{ij}))$, and since we have shown that this is also the case for g_{ij}^ℓ and ξ_{ij}^ℓ as soon as it is true for $\ell = 0$.

With $\alpha_{ij} = \alpha_{ji}$ and $\beta_{ij} = \beta_{ji}$, formulas (2.103) and (2.104) (2.107) and (2.108) for the Robin terms on Γ_{ij} lead to

$$
\mathbf{e}_i^\ell \cdot \boldsymbol{n}_{ij} = \frac{1}{2}\left(h_{ij}^{\ell-1} - h_{ij}^\ell\right) \ , \ \ \mathbf{e}_i^\ell \times \boldsymbol{n}_{ij} = \frac{1}{2}\left(\zeta_{ij}^{\ell-1} - \zeta_{ji}^\ell\right).
\tag{2.112}
$$

Choosing $\mathbf{e}_i^\ell$ as test function in (2.111), one gets

$$
\begin{aligned}
&\langle \partial_t \mathbf{e}_i^\ell, \mathbf{e}_i^\ell \rangle_{V_i', V_i} + \nu(\nabla \mathbf{e}_i^\ell, \nabla \mathbf{e}_i^\ell)_{\Omega_i} + \sum_{j \in \mathscr{I}_I} \frac{1}{\alpha_{ij}}(\mathbf{e}_i^\ell \cdot \boldsymbol{n}_{ij}, \mathbf{e}_i^\ell \cdot \boldsymbol{n}_{ij})_{\Gamma_{ij}} + \sum_{j \in \mathscr{I}_I} \frac{1}{\beta_{ij}}(\mathbf{e}_i^\ell \times \boldsymbol{n}_{ij}, \mathbf{e}_i^\ell \times \boldsymbol{n}_{ij})_{\Gamma_{ij}} \\
&\qquad\qquad = \sum_{j \in \mathscr{I}_I} \frac{1}{\alpha_{ij}}(h_{ij}^{\ell-1}, \mathbf{e}_i^\ell \cdot \boldsymbol{n}_{ij})_{\Gamma_{ij}} + \sum_{j \in \mathscr{I}_I} \frac{1}{\beta_{ij}}(\zeta_{ij}^{\ell-1}, \mathbf{e}_i^\ell \times \boldsymbol{n}_{ij})_{\Gamma_{ij}}.
\end{aligned}
\tag{2.113}
$$

From here, one can follow exactly the same steps as in the energy estimate of the Stokes equations. □

Remark 2.34. *The proof above remains true when the vector field* $\mathbf{b}$ *has a negative divergence. One obtains a similar energy estimate with an additional positive term* $-\left((\nabla \cdot \mathbf{b})\mathbf{e}_i^\ell, \mathbf{e}_i^\ell\right)_{\Omega_i}$ *on the left-hand side.*

2.9.5   Convergence factor via Fourier transform

We then rewrite the algorithm on the error in exactly the same way as for the Stokes equations in Section 2.7, with additional notations for the convection terms $\mathbf{b} = (a, b)$, $a|_\Gamma = \mathbf{b} \cdot \boldsymbol{n}_\Gamma$, $a_0 = a(x = 0)$.

$$
\begin{aligned}
\partial_t u_i^\ell + a\partial_x u_i^\ell + b\partial_y u_i^\ell - \nu\Delta u_i^\ell + \partial_x p_i^\ell &= 0 && \text{in} && \Omega_i \times (0, T) \\
\partial_t v_i^\ell + a\partial_x v_i^\ell + b\partial_y v_i^\ell - \nu\Delta v_i^\ell + \partial_y p_i^\ell &= 0 && \text{in} && \Omega_i \times (0, T) \\
\partial_x u_i^\ell + \partial_y v_i^\ell &= 0 && \text{in} && \Omega_i \times (0, T) \\
u_i^\ell(., t = 0) &= 0 && \text{in} && \Omega_i \\
v_i^\ell(., t = 0) &= 0 && \text{in} && \Omega_i \\
u_i^\ell, v_i^\ell &\to 0 && \text{when} && |(x, y)| \to \infty
\end{aligned}
$$

with transmission condition on $\Gamma \times (0, T)$

$$
\begin{aligned}
\alpha_1(\nu\partial_x u_1^\ell - p_1^\ell - \tfrac{1}{2}a_0 u_1^\ell) + u_1^\ell &= \alpha_1(\nu\partial_x u_2^{\ell-1} - p_2^{\ell-1} - \tfrac{1}{2}a_0 u_2^{\ell-1}) + u_2^{\ell-1} \\
\beta_1(\nu\partial_x v_1^\ell - \tfrac{1}{2}a_0 v_1^\ell) + v_1^\ell &= \beta_1(\nu\partial_x v_2^{\ell-1} - \tfrac{1}{2}a_0 v_2^{\ell-1}) + v_2^{\ell-1} \\
\alpha_2(\nu\partial_x u_2^\ell - p_2^\ell - \tfrac{1}{2}a_0 u_2^\ell) - u_2^\ell &= \alpha_2(\nu\partial_x u_1^{\ell-1} - p_1^{\ell-1} - \tfrac{1}{2}a_0 u_1^{\ell-1}) - u_1^{\ell-1} \\
\beta_2(\nu\partial_x v_2^\ell - \tfrac{1}{2}a_0 v_2^\ell) - v_2^\ell &= \beta_2(\nu\partial_x v_1^{\ell-1} - \tfrac{1}{2}a_0 v_1^{\ell-1}) - v_1^{\ell-1}.
\end{aligned}
$$

At this point, we cannot simply take the Fourier transform: we have difficulties with a and b if they are non-constant. We can consider first the case where a, b are constant in y and t. Then we get

$$
\begin{aligned}
i\omega u_i^\ell + a\partial_x u_i^\ell + bik u_i^\ell - \nu\partial_{xx} u_i^\ell + \nu k^2 u_i^\ell + \partial_x p_i^\ell &= 0 \\
i\omega v_i^\ell + a\partial_x v_i^\ell + bik v_i^\ell - \nu\partial_{xx} v_i^\ell + \nu k^2 v_i^\ell + ik p_i^\ell &= 0 \\
\partial_x u_i^\ell + ik v_i^\ell &= 0 \\
u_i^\ell, v_i^\ell \to 0 \text{ when } |x| \to \infty &
\end{aligned}
$$

To avoid ODEs with non-constant coefficients, let a, b be constant in x also, thus $a_0 = a$. We can then write the solutions of the system as

$$
\begin{aligned}
u_1^\ell &= A^\ell \exp(|k|x) + B^\ell \exp(r_+ x) \\
p_1^\ell &= -\left(\frac{i\omega + bik}{|k|} + a\right) A^\ell \exp(|k|x) \\
v_1^\ell &= \frac{i|k|}{k} A^\ell \exp(|k|x) + \frac{ir_+}{k} B^\ell \exp(r_+ x)
\end{aligned}
$$

and

$$
\begin{aligned}
u_2^\ell &= C^\ell \exp(-|k|x) + D^\ell \exp(r_- x) \\
p_2^\ell &= \left(\frac{i\omega + bik}{|k|} - a\right) C^\ell \exp(-|k|x) \\
v_2^\ell &= -\frac{i|k|}{k} C^\ell \exp(-|k|x) + \frac{ir_-}{k} D^\ell \exp(r_- x)
\end{aligned}
$$

with r_+, r_- the roots of the equation $-\nu r^2 + ar + (i\omega + bik + \nu k^2) = 0$, i.e. $r_+ = \dfrac{a + \lambda}{2\nu}$, $r_- = \dfrac{a - \lambda}{2\nu}$, λ is the square root with positive real part of $a^2 + 4i\nu(\omega + bk) + 4\nu^2 k^2$.

Replacing these terms in the transmission conditions, one gets

$$\alpha_1\left[\nu|k|A^\ell + \nu r_+ B^\ell + \left(\frac{i\omega+bik}{|k|}+a\right)A^\ell - \frac{a}{2}A^\ell - \frac{a}{2}B^\ell\right] + A^\ell + B^\ell$$
$$= \alpha_1\left[-\nu|k|C^{\ell-1} + \nu r_- D^{\ell-1} + \left(-\frac{i\omega+bik}{|k|}+a\right)C^{\ell-1} - \frac{a}{2}C^{\ell-1} - \frac{a}{2}D^{\ell-1}\right] + C^{\ell-1} + D^{\ell-1},$$

$$\beta_1\left[\nu\frac{i|k|}{k}|k|A^\ell + \nu\frac{ir_+}{k}r_+ B^\ell - \frac{a}{2}\frac{i|k|}{k}A^\ell - \frac{a}{2}\frac{ir_+}{k}B^\ell\right] + \frac{i|k|}{k}A^\ell + \frac{ir_+}{k}B^\ell$$
$$= \beta_1\left[\frac{i|k|}{k}\nu|k|C^{\ell-1} + \nu\frac{ir_-}{k}r_- D^{\ell-1} + \frac{a}{2}\frac{i|k|}{k}C^{\ell-1} - \frac{a}{2}\frac{ir_-}{k}D^{\ell-1}\right] - \frac{i|k|}{k}C^{\ell-1} + \frac{ir_-}{k}D^{\ell-1},$$

$$\alpha_2\left[-\nu|k|C^\ell + \nu r_- D^\ell + \left(-\frac{i\omega+bik}{|k|}+a\right)C^\ell - \frac{a}{2}C^\ell - \frac{a}{2}D^\ell\right] - C^\ell - D^\ell$$
$$= \alpha_2\left[\nu|k|A^\ell + \nu r_+ B^\ell + \left(\frac{i\omega+bik}{|k|}+a\right)A^{\ell-1} - \frac{a}{2}A^{\ell-1} - \frac{a}{2}B^{\ell-1}\right] - A^{\ell-1} - B^{\ell-1},$$

$$\beta_2\left[\frac{i|k|}{k}\nu|k|C^\ell + \nu\frac{ir_-}{k}r_- D^\ell + \frac{a}{2}\frac{i|k|}{k}C^\ell - \frac{a}{2}\frac{ir_-}{k}D^\ell\right] + \frac{i|k|}{k}C^\ell - \frac{ir_-}{k}D^\ell$$
$$= \beta_2\left[\nu\frac{i|k|}{k}|k|A^{\ell-1} + \nu\frac{ir_+}{k}r_+ B^{\ell-1} - \frac{a}{2}\frac{i|k|}{k}A^{\ell-1} - \frac{a}{2}\frac{ir_+}{k}B^{\ell-1}\right] - \frac{i|k|}{k}A^{\ell-1} - \frac{ir_+}{k}B^{\ell-1}.$$

Factorizing the above expressions, we get

$$\left[\alpha_1\left(\nu|k| + \frac{i\omega+bik}{|k|} + \frac{a}{2}\right)+1\right]A^\ell + \left[\alpha_1\left(\nu r_+ - \frac{a}{2}\right)+1\right]B^\ell$$
$$= \left[\alpha_1\left(-\nu|k| - \frac{i\omega+bik}{|k|} + \frac{a}{2}\right)+1\right]C^{\ell-1} + \left[\alpha_1\left(\nu r_- - \frac{a}{2}\right)+1\right]D^{\ell-1}$$

$$\left[\beta_1\left(\nu ik - \frac{ai|k|}{2k}\right) + \frac{i|k|}{k}\right]A^\ell + \left[\beta_1\left(\nu\frac{ir_+^2}{k} - \frac{iar_+}{2k}\right) + \frac{ir_+}{k}\right]B^\ell$$
$$= \left[\beta_1\left(\nu ik + \frac{ai|k|}{2k}\right) - \frac{i|k|}{k}\right]C^{\ell-1} + \left[\beta_1\left(\nu\frac{ir_-^2}{k} - \frac{iar_-}{2k}\right) + \frac{ir_-}{k}\right]D^{\ell-1}$$

$$\left[\alpha_2\left(-\nu|k| - \frac{i\omega+bik}{|k|} + \frac{a}{2}\right)-1\right]C^\ell + \left[\alpha_2\left(\nu r_- - \frac{a}{2}\right)-1\right]D^\ell$$
$$= \left[\alpha_2\left(\nu|k| + \frac{i\omega+bik}{|k|} + \frac{a}{2}\right)-1\right]A^{\ell-1} + \left[\alpha_2\left(\nu r_+ - \frac{a}{2}\right)-1\right]B^{\ell-1}$$

$$\left[\beta_2\left(\nu ik + \frac{ai|k|}{2k}\right) + \frac{i|k|}{k}\right]C^\ell + \left[\beta_2\left(\nu\frac{ir_-^2}{k} - \frac{iar_-}{2k}\right) - \frac{ir_-}{k}\right]D^\ell$$
$$= \left[\beta_2\left(\nu ik - \frac{ai|k|}{2k}\right) - \frac{i|k|}{k}\right]A^{\ell-1} + \left[\beta_2\left(\nu\frac{ir_+^2}{k} - \frac{iar_+}{2k}\right) - \frac{ir_+}{k}\right]B^{\ell-1}$$

We change the sign of the third and fourth equations, then we can rewrite

$$\left[\alpha_1\left(\nu|k| + \frac{i\omega+bik}{|k|} + \frac{a}{2}\right)+1\right]A^\ell + \left[\alpha_1\left(\nu r_+ - \frac{a}{2}\right)+1\right]B^\ell$$
$$= \left[\alpha_1\left(-\nu|k| - \frac{i\omega+bik}{|k|} + \frac{a}{2}\right)+1\right]C^{\ell-1} + \left[\alpha_1\left(\nu r_- - \frac{a}{2}\right)+1\right]D^{\ell-1}$$

$$\left[\beta_1\left(\nu ik - \frac{ai|k|}{2k}\right) + \frac{i|k|}{k}\right]A^\ell + \left[\beta_1\left(\nu\frac{ir_+^2}{k} - \frac{iar_+}{2k}\right) + \frac{ir_+}{k}\right]B^\ell$$
$$= \left[\beta_1\left(\nu ik + \frac{ai|k|}{2k}\right) - \frac{i|k|}{k}\right]C^{\ell-1} + \left[\beta_1\left(\nu\frac{ir_-^2}{k} - \frac{iar_-}{2k}\right) + \frac{ir_-}{k}\right]D^{\ell-1}$$

$$\left[\alpha_2\left(-\nu|k|-\frac{i\omega+bik}{|k|}+\frac{a}{2}\right)-1\right]C^\ell+\left[\alpha_2\left(\nu r_--\frac{a}{2}\right)-1\right]D^\ell$$
$$=\left[\alpha_2\left(\nu|k|+\frac{i\omega+bik}{|k|}+\frac{a}{2}\right)-1\right]A^{\ell-1}+\left[\alpha_1\left(\nu r_+-\frac{a}{2}\right)-1\right]B^{\ell-1}$$

$$\left[\beta_2\left(\nu ik+\frac{ai|k|}{2k}\right)+\frac{i|k|}{k}\right]C^\ell+\left[\beta_2\left(\nu\frac{ir_-^2}{k}-\frac{iar_-}{2k}\right)-\frac{ir_-}{k}\right]D^\ell$$
$$=\left[\beta_2\left(\nu ik-\frac{ai|k|}{2k}\right)-\frac{i|k|}{k}\right]A^{\ell-1}+\left[\beta_2\left(\nu\frac{ir_+^2}{k}-\frac{iar_+}{2k}\right)-\frac{ir_+}{k}\right]B^{\ell-1}$$

We can rewrite this expression as

$$\left[1+X(\alpha_1)+\frac{\alpha_1 a}{2}\right]A^\ell+[1+Y(\alpha_1)]B^\ell$$
$$=\left[1-X(\alpha_1)+\frac{\alpha_1 a}{2}\right]C^{\ell-1}+[1-Y(\alpha_1)]D^{\ell-1}$$

$$\frac{i|k|}{k}\left[1+W(\beta_1)-\frac{\beta_1 a}{2}\right]A^\ell+\frac{ir_+}{k}[1+Y(\beta_1)]B^\ell$$
$$=\frac{-i|k|}{k}\left[1-W(\beta_1)-\frac{\beta_1 a}{2}\right]C^{\ell-1}+\frac{ir_-}{k}[1-Y(\beta_1)]D^{\ell-1}$$

$$\left[1+X(\alpha_2)-\frac{\alpha_2 a}{2}\right]C^\ell+[1+Y(\alpha_2)]D^\ell$$
$$=\left[1-X(\alpha_2)-\frac{\alpha_2 a}{2}\right]A^{\ell-1}+[1-Y(\alpha_2)]B^{\ell-1}$$

$$\frac{i|k|}{k}\left[1+W(\beta_2)+\frac{\beta_2 a}{2}\right]C^\ell+\frac{-ir_-}{k}[1+Y(\beta_2)]D^\ell$$
$$=\frac{-i|k|}{k}\left[1-W(\beta_2)+\frac{\beta_2 a}{2}\right]A^{\ell-1}+\frac{-ir_+}{k}[1-Y(\beta_2)]B^{\ell-1}$$

where

$$X(\alpha)=\alpha\left(\nu|k|+\frac{i\omega+bik}{|k|}\right),\ Y(\alpha)=\alpha\left(\nu r_+-\frac{a}{2}\right)=-\alpha\left(\nu r_--\frac{a}{2}\right),\ W(\alpha)=\alpha\nu|k|$$

From this, we define four matrices

$$\mathcal{M}(\alpha_1,\beta_1)=\begin{bmatrix}\left[1+X(\alpha_1)+\frac{\alpha_1 a}{2}\right] & [1+Y(\alpha_1)]\\ \frac{i|k|}{k}\left[1+W(\beta_1)-\frac{\beta_1 a}{2}\right] & \frac{ir_+}{k}[1+Y(\beta_1)]\end{bmatrix}$$

$$[10pt]\mathcal{N}(\alpha_1,\beta_1)=\begin{bmatrix}\left[1-X(\alpha_1)+\frac{\alpha_1 a}{2}\right] & [1-Y(\alpha_1)]\\ \frac{-i|k|}{k}\left[1-W(\beta_1)-\frac{\beta_1 a}{2}\right] & \frac{ir_-}{k}[1-Y(\beta_1)]\end{bmatrix}$$

$$[10pt]\mathcal{P}(\alpha_2,\beta_2)=\begin{bmatrix}\left[1+X(\alpha_2)-\frac{\alpha_2 a}{2}\right] & [1+Y(\alpha_2)]\\ \frac{i|k|}{k}\left[1+W(\beta_2)+\frac{\beta_2 a}{2}\right] & \frac{-ir_-}{k}[1+Y(\beta_2)]\end{bmatrix}$$

$$[10pt]\mathcal{Q}(\alpha_2,\beta_2)=\begin{bmatrix}\left[1-X(\alpha_2)-\frac{\alpha_2 a}{2}\right] & [1-Y(\alpha_2)]\\ \frac{-i|k|}{k}\left[1-W(\beta_2)+\frac{\beta_2 a}{2}\right] & \frac{-ir_+}{k}[1-Y(\beta_2)]\end{bmatrix}.$$

Then, one has

$$\mathcal{M}(\alpha_1,\beta_1)\begin{bmatrix}A^\ell\\B^\ell\end{bmatrix}=\mathcal{N}(\alpha_1,\beta_1)\begin{bmatrix}C^{\ell-1}\\D^{\ell-1}\end{bmatrix};\quad \mathcal{P}(\alpha_2,\beta_2)\begin{bmatrix}C^\ell\\D^\ell\end{bmatrix}=\mathcal{Q}(\alpha_2,\beta_2)\begin{bmatrix}A^{\ell-1}\\B^{\ell-1}\end{bmatrix}$$

and then

$$\begin{bmatrix}A^\ell\\B^\ell\end{bmatrix}=\mathcal{R}(\alpha_1,\beta_1,\alpha_2,\beta_2)\begin{bmatrix}A^{\ell-2}\\B^{\ell-2}\end{bmatrix}$$

with $\mathcal{R}(\alpha_1,\beta_1,\alpha_2,\beta_2)=\mathcal{M}^{-1}(\alpha_1,\beta_1)\mathcal{N}(\alpha_1,\beta_1)\mathcal{P}^{-1}(\alpha_2,\beta_2)\mathcal{Q}(\alpha_2,\beta_2)$. The convergence factor is the square root of the spectral radius of $\mathcal{R}$.

In this formulation, if $a=0$, then $r_+=-r_-$, which implies $\mathcal{M}(\alpha,\beta)=\mathcal{P}(\alpha,\beta)$ and $\mathcal{N}(\alpha,\beta)=\mathcal{Q}(\alpha,\beta)$. Then, like in the case of the Stokes equations, one can simplify the formula in the "Robin-2p" case $\alpha_1=\alpha_2=\alpha$ and $\beta_1=\beta_2=\beta$. In that case, we obtain $\mathcal{R}(\alpha,\beta,\alpha,\beta)=\left[\mathcal{P}^{-1}(\alpha,\beta)\mathcal{Q}(\alpha,\beta)\right]^2$. On the other hand, in the case $a\neq0$, we get $\mathcal{N}(\alpha,\beta)\neq\mathcal{Q}(\alpha,\beta)$ and $\mathcal{P}(\alpha,\beta)\neq\mathcal{Q}(\alpha,\beta)$, hence we cannot easily simplify the formulation even in the Robin-2p case.

2.10   Parareal for the Stokes equations

2.10.1   Algorithm

Consider a *decomposition in time* of $(0,T)$ into subintervals : $[0,T]=\cup_{n=0}^{N-1}\mathcal{I}_n$, with $\mathcal{I}_n=(T_n,T_{n+1}),n=0,\dots,N-1$, and $0=T_0<T_1<\dots<T_{N-1}<T_N=T$. For simplicity, we consider a regular decomposition of $(0,T)$ i.e. such that $T_{n+1}-T_n=\Delta T$.

Over each such interval generically noted as $\mathcal{I}:=(t_0,t_1)$, we shall consider two propagation operators, a coarse and a fine one. Before describing the Parareal Algorithm, we shall state an important remark that will allow us to make sure that it is well-defined. We first recall the functional spaces (2.3) that are relevant for the velocity component of the solution of the Stokes equations

$$V=\{\mathbf{u}\in\left[H_0^1(\Omega)\right]^2,\nabla\cdot\mathbf{u}=0\},$$
$$H=\{\mathbf{u}\in\left[L^2(\Omega)\right]^2,\nabla\cdot\mathbf{u}=0,\mathbf{u}\cdot\boldsymbol{n}_{\partial\Omega}=0\text{ on }\partial\Omega\}.$$

Remark 2.35. *The Stokes problem (2.1) only needs a velocity field as initial condition at $t=t_0$ (no need for an initial pressure), and Theorem 2.1 shows that if this initial velocity field belongs to the space H defined by (2.3), then we can consider the value of the solution $\mathbf{u}$ at time t_1 as an element of H, since the solution is in $\mathscr{C}^0([t_0,t_1],H)$. Therefore, we shall denote by*

- $\mathscr{G}(\mathcal{I},\mathbf{U}_0)$ *a velocity field in H that provides a rough approximation of $\mathbf{u}(\cdot,t_1)$, where $\mathbf{u}$ is the velocity component of the solution of the Stokes equations with initial condition $\mathbf{u}(\cdot,t_0)=\mathbf{U}_0\in H$.*

- $\mathscr{F}(\mathcal{I},\mathbf{U}_0)$ *a velocity field in H that provides a more accurate approximation of $\mathbf{u}(\cdot,t_1)$.*

Under the conditions that $\mathbf{u}_0 \in H$ and that both $\mathscr{G}$ and $\mathscr{F}$ have inputs and outputs in H, then, by an immediate recurrence, the following plain Parareal algorithm [82] is well-defined

---

Algorithm 8 (Parareal)

Choose an initial data $(\mathbf{U}_n^0)_{n\in[\![0,N]\!]}$ with $\mathbf{U}_0^0 = \mathbf{u}_0$ and $\mathbf{U}_n^0$ an approximation of $\mathbf{u}(\cdot, T_n)$, for example : $\mathbf{U}_n^0 := \mathscr{G}(\mathscr{I}_{n-1}, \mathbf{U}_{n-1}^0)$, for $n = 1, \ldots, N$.

for $k = 0, 1, \ldots$ *(Parareal iterations)*
   Set $\mathbf{U}_0^{k+1} = \mathbf{u}_0$ and perform the correction iterations

$$\mathbf{U}_n^{k+1} = \mathscr{G}(\mathscr{I}_{n-1}, \mathbf{U}_{n-1}^{k+1}) + \mathscr{F}(\mathscr{I}_{n-1}, \mathbf{U}_{n-1}^k) - \mathscr{G}(\mathscr{I}_{n-1}, \mathbf{U}_{n-1}^k), \quad n = 1, \ldots, N. \qquad (2.114)$$

end for

For the coarse solver, for simplicity, here we consider the one deduced from the one step Backward Euler method, i.e., $\mathscr{G}(\mathscr{I}_n, \mathbf{v}) \in H \supset V$ is the velocity component of the solution of the following equation: find $(\mathbf{u}, p) \in V \times L_0^2(\Omega)$ such that

$$\frac{\mathbf{u} - \mathbf{v}}{\Delta T} - \nu \Delta \mathbf{u} + \nabla p = \mathbf{f}(., T_{n+1}) \text{ in } \Omega$$

or, equivalently,

$$\frac{\mathbf{u}}{\Delta T} - \nu \Delta \mathbf{u} + \nabla p = \mathbf{f}(., T_{n+1}) + \frac{\mathbf{v}}{\Delta T} \text{ in } \Omega. \qquad (2.115)$$

We recall now the following classical result, given in [18, Theorem IV.8.1]

Theorem 2.36. *For $\mathbf{f} \in \left[H^{-1}(\Omega)\right]^2$ and $\lambda \geq 0$, the generalized Stokes equation*

$$\lambda \mathbf{u} - \nu \Delta \mathbf{u} + \nabla p = \mathbf{f} \qquad (2.116)$$

admits a unique solution $(\mathbf{u}, p) \in V \times L_0^2(\Omega)$ verifying

$$\|\mathbf{u}\|_{H^1} + \|p\|_{L^2} \leq \|\mathbf{f}\|_{H^{-1}}. \qquad (2.117)$$

Hence, if $\mathbf{v} \in H$ and if $\mathbf{f}(., T_{n+1})$ belongs to $\left[H^{-1}(\Omega)\right]^2$, the coarse solver is well defined since the velocity component of the solution of (2.115) is in $V \subset H$.

In what follows, we shall consider for the sake of the analysis that the fine solver is the exact one, i.e., for a given $\mathbf{v} \in H$, we define $\mathscr{F}(\mathscr{I}_n, \mathbf{v}) = \mathbf{u}(\cdot, T_{n+1})$, where $\mathbf{u}$ is the velocity component of the solution of the evolutionary Stokes equations: find $(\mathbf{u}, p) \in \left(L^2((T_n, T_{n+1}), V) \cap \mathscr{C}^0([T_n, T_{n+1}], H)\right) \times W^{-1,\infty}((T_n, T_{n+1}), L_0^2(\Omega))$ such that

$$\partial_t \mathbf{u} - \nu \Delta \mathbf{u} + \nabla p = \mathbf{f} \text{ in } \Omega \times (T_n, T_{n+1})$$
$$\mathbf{u}(\cdot, T_n) = \mathbf{v} \text{ in } \Omega. \qquad (2.118)$$

From Theorem 2.1, $\mathbf{u}(T_{n+1})$ is well-defined in H, then so is the fine solver.

Both coarse and fine solvers being well-posed and mapping H into itself, we can state the following result:

Theorem 2.37. *Consider $\mathbf{u}_0 \in H$ and $\mathbf{f} \in L^2((0, T), \left[L_0^2(\Omega)\right]^2)$. The Parareal method applied on the evolutionary Stokes equation is well-defined, furthermore, for $n = 1, 2, \ldots, N$, one has $\mathbf{U}_n^k \in H$ for all $k \in \mathbb{N}$.*

2.10.2   Convergence

Similarly as for the previous Chapter, We first obtain Lipschitz constants for the coarse and the fine solvers, that is, we show that there exist constants γ_1, γ_2, s.t., for all initial conditions $(\mathbf{u}, \mathbf{v}) \in H$

$$
\begin{aligned}
\|\mathscr{G}(\mathscr{I}, \mathbf{u}) - \mathscr{G}(\mathscr{I}, \mathbf{v})\|_H &\le \gamma_1 \|\mathbf{u} - \mathbf{v}\|_H, \\
\|(\mathscr{F} - \mathscr{G})(\mathscr{I}, \mathbf{u}) - (\mathscr{F} - \mathscr{G})(\mathscr{I}, \mathbf{v})\|_H &\le \gamma_2 \|\mathbf{u} - \mathbf{v}\|_H.
\end{aligned}
\tag{2.119}
$$

From linearity, it is sufficient to consider for $\mathscr{G}$ and $\mathscr{F}$ the case of a source term $\mathbf{f} = 0$.

Even though we do not deal in this Chapter with the evolutionary Stokes equations for the case $\Omega = \mathbb{R}^2$, we will start with this case here as we can use the Fourier transform in space for the analysis. For this case, we replace the homogeneous condition on the boundary by the condition that the fields vanish at infinity. The spaces V and H are defined similarly as before, with this modification in the boundary conditions. We admit that the evolutionary Stokes solution is well-posed and that the coarse and fine solvers are also well-defined.

Lemma 2.38. *For $\Omega = \mathbb{R}^2$, we have (2.119) with $\gamma_1 \le 1$ and $\gamma_2 < 1$.*

Proof. Denote by $\mathbf{u} = (u, v)$ and p the solution of the Stokes equations with initial condition $\mathbf{u}_0 = (u_0, v_0)$. Applying the Fourier transform in x and y directions, with wave numbers k_x, k_y, one gets

$$
\begin{aligned}
\partial_t \hat{u} + \nu(k_x^2 + k_y^2)\hat{u} + ik_x \hat{p} &= 0, \\
\partial_t \hat{v} + \nu(k_x^2 + k_y^2)\hat{v} + ik_y \hat{p} &= 0, \\
ik_x \hat{u} + ik_y \hat{v} &= 0, \\
\hat{u}(0) &= \hat{u}_0, \\
\hat{v}(0) &= \hat{v}_0.
\end{aligned}
$$

Denote by $\hat{w} = ik_x \hat{v} - ik_y \hat{u}$, then, with $\hat{w}_0 = ik_x \hat{v}_0 - ik_y \hat{u}_0$, we get the following ODE for $\hat{w}$

$$
\begin{aligned}
\partial_t \hat{w} + \nu(k_x^2 + k_y^2)\hat{w} &= 0 \\
\hat{w}(0) &= \hat{w}_0,
\end{aligned}
$$

which has the solution $\hat{w}(t) = \exp(-\nu(k_x^2 + k_y^2)t)\hat{w}_0$. Then, from the system

$$
\begin{aligned}
ik_x \hat{v} - ik_y \hat{u} &= \hat{w}, \\
ik_x \hat{u} + ik_y \hat{v} &= 0,
\end{aligned}
$$

we get

$$
\hat{u} = \frac{ik_y \hat{w}}{k_x^2 + k_y^2} = \exp(-\nu(k_x^2 + k_y^2)t)\frac{ik_y \hat{w}_0}{k_x^2 + k_y^2} = \exp(-\nu(k_x^2 + k_y^2)t)\frac{ik_y(ik_x \hat{v}_0 - ik_y \hat{u}_0)}{k_x^2 + k_y^2},
$$

$$
\hat{v} = \frac{-ik_x \hat{w}}{k_x^2 + k_y^2} = \exp(-\nu(k_x^2 + k_y^2)t)\frac{-ik_x \hat{w}_0}{k_x^2 + k_y^2} = \exp(-\nu(k_x^2 + k_y^2)t)\frac{-ik_x(ik_x \hat{v}_0 - ik_y \hat{u}_0)}{k_x^2 + k_y^2}.
$$

The divergence-free property of $\mathbf{u}_0$ under Fourier transform is $ik_x\hat{u}_0 + ik_y\hat{v}_0 = 0$. We use this in the above expressions to obtain

$$\hat{u} = \exp(-\nu(k_x^2 + k_y^2)t)\hat{u}_0,$$

$$\hat{v} = \exp(-\nu(k_x^2 + k_y^2)t)\hat{v}_0.$$

Then, for the fine solver

$$\widehat{\mathscr{F}(\mathscr{I}, \mathbf{u_0})} = \exp(-\nu(k_x^2 + k_y^2)\Delta T)\hat{\mathbf{u}}_0.$$

Similarly for $\mathscr{G}$, one gets

$$\widehat{\mathscr{G}(\mathscr{I}, \mathbf{u_0})} = \frac{1}{1 + \nu(k_x^2 + k_y^2)\Delta T}\hat{\mathbf{u}}_0.$$

In the L^2-norm, this first implies through the Plancherel equality

$$\|\mathscr{G}(\mathscr{I}, \mathbf{u_0})\|_{[L^2(\mathbb{R}^2)]^2} \leq \gamma_1 \|\mathbf{u_0}\|_{[L^2(\mathbb{R}^2)]^2}$$

with $\gamma_1 = \max_{k_x, k_y} \dfrac{1}{1 + \nu(k_x^2 + k_y^2)\Delta T}$. Generally, one gets $\gamma_1 = 1$, but in the discrete problem, when k_x, k_y are bounded away from 0, then $\gamma_1 < 1$.
In addition

$$\|(\mathscr{F} - \mathscr{G})(\mathscr{I}, \mathbf{u_0})\|_{[L^2(\mathbb{R}^2)]^2} \leq \gamma_2 \|\mathbf{u_0}\|_{[L^2(\mathbb{R}^2)]^2}$$

with $\gamma_2 = \max_{k_x, k_y} \left| \exp(-\nu(k_x^2 + k_y^2)\Delta T) - \dfrac{1}{1 + \nu(k_x^2 + k_y^2)\Delta T} \right|$. For a more detailed bound on γ_2, see Chapter 1.   □

Let us now turn to the case in which Ω is a bounded domain. We first recall the eigenvalue theory of the Stokes operators [18, Theorem IV.5.5, page 279]

Theorem 2.39. *There exists an increasing sequence of strictly positive real numbers* $(\lambda_j)_{j \in \mathbb{N}^*}$, *tending to infinity and a sequence of functions* $(\mathbf{u}_j)_{j \in \mathbb{N}^*}$ *orthonormal in H, orthogonal in V, forming a complete family in H and V, and a sequence of functions* $(p_j)_{j \in \mathbb{N}^*}$ *in* $L_0^2(\Omega)$ *that satisfy*

$$-\Delta \mathbf{u}_j + \nabla p_j = \lambda_j \mathbf{u}_j \tag{2.120}$$

Using this and (2.117), we obtain

Lemma 2.40. *For* Ω *bounded with Lipschitz boundary, we have* (2.119) *with* $\gamma_1 < 1$ *and* $\gamma_2 < 1$.

Proof. Let $\mathbf{u}_0$ be in H, we can express it using the basis $(\mathbf{u}_j)_{j \in \mathbb{N}^*}$ in (2.120)

$$\mathbf{u}_0 = \sum_{j \geq 1} \alpha_j \mathbf{u}_j$$

The solution of the evolutionary Stokes problem with initial condition $\mathbf{u}_0$ can then be expressed as

$$\mathbf{u}(t) = \sum_{j \geq 1} \alpha_j \exp(-\nu\lambda_j t)\mathbf{u}_j$$

$$p(t) = \nu \sum_{j \geq 1} \alpha_j \exp(-\nu \lambda_j t) p_j$$

Then, the exact fine solver gives

$$\mathscr{F}(\mathscr{I}, \mathbf{u_0}) = \sum_{j \geq 1} \alpha_j \exp(-\nu \lambda_j \Delta T) \mathbf{u}_j$$

In addition, the coarse propagator solves a generalized Stokes problem of form (2.116), and its solution is

$$\mathscr{G}(\mathscr{I}, \mathbf{u_0}) = \sum_{j \geq 1} \alpha_j \left(\frac{1}{1 + \nu \lambda_j \Delta T} \right) \mathbf{u}_j.$$

Using those expressions, we get the Lipschitz constant for $\mathscr{G}$ and $(\mathscr{F} - \mathscr{G})$

$$\gamma_1 = \frac{1}{(1 + \nu \lambda_1 \Delta T)} < 1, \quad \gamma_2 = \max_j \{(1 + \nu \lambda_j \Delta T)^{-1} - \exp(-\nu \lambda_j \Delta T)\} < 1.$$

$\square$

With these Lipschitz constants, we obtain now the convergence of the Parareal method applied on the evolutionary Stokes equation:

Theorem 2.41. *Consider the Stokes equation* (2.1) *with* $\mathbf{u}_0 \in H$. *The Parareal method applied on this equation converges with a rate similar to the case of the parabolic equation.*

2.11   The coupled Parareal-OSWR Algorithm for the Stokes equations

We now propose a coupled Parareal-OSWR algorithm on the Stokes equations. For simplicity, we consider here only two sub-domains Ω_1, Ω_2, and then $\Gamma_{1,2} = \Gamma_{2,1} = \Gamma$. We simplify the foot indexes $_{12}$ and $_{21}$ by $_1$ and $_2$, and denote also $\boldsymbol{\xi} = (\xi_1, \xi_2), \mathbf{g} = (g_1, g_2)$.

As in the previous Chapter, we shall choose the OSWR algorithm to be used as the fine solver in the Parareal algorithm, and perform only a few iterations of OSWR at each Parareal iteration. Since we shall use unconverged velocity fields as initial conditions in the coarse solver, their normal components will not necessarily be continuous across Γ; this has the important implication that the resulting velocity fields will not be globally divergence free on Ω, but only locally divergence free on each Ω_i. This may lead to low regularity pressure fields in the coarse solver. Fortunately, as only velocities are used during Parareal iterations, this low regularity poses no problem.

We recall the notations of Section 2.3

$$V_i = \{\mathbf{u} \in [H^1(\Omega_i)]^2, \mathbf{u} = 0 \text{ on } \partial \Omega_i \backslash \Gamma, \nabla \cdot \mathbf{u} = 0 \text{ in } \Omega_i\},$$
$$H_i = \{\mathbf{u} \in [L^2(\Omega_i)]^2, \mathbf{u} \cdot \boldsymbol{n}_{\partial \Omega_i} = 0 \text{ on } \partial \Omega_i \backslash \Gamma, \nabla \cdot \mathbf{u} = 0 \text{ in } \Omega_i\},$$
$$X_i = \left\{\mathbf{u} \in [H^1(\Omega_i)]^2, \mathbf{u} = 0 \text{ on } \partial \Omega_i \backslash \Gamma\right\}.$$

According to the above argument, we will use the following new space

$$K = \{\mathbf{u} \in [L^2(\Omega)]^2, \mathbf{u}|_{\Omega_i} \in H_i\}. \tag{2.121}$$

With an initial condition U in this space K, the coarse solver for the time-dependent Stokes problem from T_n to T_{n+1} defined from the one-step Backward Euler method is well-defined: for $\mathbf{U} \in K$, $\mathscr{G}(\mathscr{I}_n, \mathbf{U}) \in X \subset K$ is the solution of

$$\frac{\mathbf{u} - \mathbf{U}}{\Delta T} - \nu \Delta \mathbf{u} - \nabla p = \mathbf{f}_n, \quad \nabla \cdot \mathbf{u} = 0; \tag{2.122}$$

We cannot directly apply Lemma 2.40 concerning the generalized Stokes problem because $\mathbf{U} \in K$ and K is not included in H; however, using a simple energy estimate based on (2.122), one still has the following Lipschitz property: there exists a constant $\gamma_1 \leq 1$ s.t. $\forall \mathbf{u}$ and $\mathbf{v} \in K$

$$\|\mathscr{G}(\mathscr{I}, \mathbf{u}) - \mathscr{G}(\mathscr{I}, \mathbf{v})\|_K \leq \gamma_1 \|\mathbf{u} - \mathbf{v}\|_K. \tag{2.123}$$

Note that in the case of K, we do not state a Lipschitz constant that is strictly lower than 1 as in the case of space H. The norm on K is nothing but the L^2 norm, we can use the notation $\|.\|_\Omega$ instead.

Then, we set, for a.e. $t \in (T_n, T_{n+1})$

$$
\begin{aligned}
a_i(\mathbf{u}, \mathbf{v}) &= \nu (\nabla \mathbf{u}, \nabla \mathbf{v})_{\Omega_i} + \frac{1}{\alpha_i} (\mathbf{u} \cdot \mathbf{n}, \mathbf{v} \cdot \mathbf{n})_\Gamma + \frac{1}{\beta_i} (\mathbf{u} \times \mathbf{n}, \mathbf{v} \times \mathbf{n})_\Gamma, \\
c_{i,n}^{k,\ell}(t, \mathbf{v}) &= (\mathbf{f}_n, \mathbf{v})_{\Omega_i} + \frac{1}{\alpha_i} \left(g_{i,n}^{k,\ell-1}, \mathbf{v} \cdot \mathbf{n} \right)_\Gamma + \frac{1}{\beta_i} \left(\xi_{i,n}^{k,\ell-1}, \mathbf{v} \times \mathbf{n} \right)_\Gamma.
\end{aligned}
\tag{2.124}
$$

The algorithm can be written as

Algorithm 9 (Coupled Parareal-OSWR)

---

1. Choose an initial data $(\mathbf{U}_n^0)_{n \in [\![0,N]\!]}$ with $\mathbf{U}_0^0 = \mathbf{u}_0$ and $\mathbf{U}_n^0$ an approximation of $\mathbf{u}(\cdot, T_n)$, for example $\mathbf{U}_n^0 := \mathscr{G}(\mathscr{I}_{n-1}, \mathbf{U}_{n-1}^0)$, for $n = 1, \ldots, N$.

2. Choose an initial Robin data $(\xi_n^{0,0}, \mathbf{g}_n^{0,0})_{n \in [\![0,N-1]\!]}$. For example, if we have already run the coarse solver, then we also have calculated the approximate pressure P_n^0 for $n = 1, \ldots, N$, then $(\xi_n^{0,0}, \mathbf{g}_n^{0,0})$ with $n \in [\![0, N-1]\!]$ can be constructed, e.g., from $\mathbf{U}_n^0$ and P_n^0.

for $k = 0, 1, \ldots$ *(Parareal iterations)*

  1. On each time interval $\mathscr{I}_n$, $n = 0, 1, \ldots, N-1$,

  for $\ell = 1, \ldots, L$ *(OSWR iterations) solve, for each $i = 1, 2$:*

$$
\begin{aligned}
&\left\langle \partial_t \mathbf{u}_{i,n}^{k,\ell}, \mathbf{v} \right\rangle_{V_i', V_i} + a_i(\mathbf{u}_{i,n}^{k,\ell}, \mathbf{v}) = c_{i,n}^{k,\ell}(t, \mathbf{v}) \text{ for almost every } t \in]T_n, T_{n+1}[\text{ and all } \mathbf{v} \in V_i, \\
&\mathbf{u}_{i,n}^{k,\ell}(T_n) = \mathbf{U}_n^k|_{\Omega_i}
\end{aligned}
\tag{2.125}
$$

and, with $j = 3 - i$, update the Robin term as

$$g_{i,n}^{k,\ell} = \frac{\alpha_i}{\alpha_j} g_{j,n}^{k,\ell-1} - \frac{\alpha_i + \alpha_j}{\alpha_j} \mathbf{u}_{j,n}^{k,\ell} \cdot \mathbf{n}_j, \tag{2.126}$$

$$\xi_{i,n}^{k,\ell} = \frac{\beta_i}{\beta_j} \xi_{j,n}^{k,\ell-1} - \frac{\beta_i + \beta_j}{\beta_j} \mathbf{u}_{j,n}^{k,\ell} \times \mathbf{n}_j. \tag{2.127}$$

  end for

  2. Set $U_0^{k+1} = u_0$ and do Parareal corrections:

$$\mathbf{U}_{n+1}^{k+1} = \mathbf{u}_n^{k,L}(\cdot, T_{n+1}) + \mathscr{G}(\mathscr{I}_n, \mathbf{U}_n^{k+1}) - \mathscr{G}(\mathscr{I}_n, \mathbf{U}_n^k). \tag{2.128}$$

Update the interface term: $\quad \xi_n^{k+1,0} = \xi_n^{k,L}$ and $\quad \mathbf{g}_n^{k+1,0} = \mathbf{g}_n^{k,L}.$ \hfill (2.129)

  end for

In both Parareal and OSWR methods, the algorithms are written using only the velocity, so is the coupled Parareal-OSWR algorithm. If needed, the pressure can be defined in the following Remark

Remark 2.42. $p_{i,n}^{k,\ell} = \partial_t P_{i,n}^{k,\ell}$, *with $P_{i,n}^{k,\ell}$ which is such that,* $\forall \mathbf{v} \in X_i$

$$\left(\mathbf{u}_{i,n}^{k,\ell}(t),\mathbf{v}\right)_{\Omega_i} - \left(\mathbf{U}_n^k|_{\Omega_i},\mathbf{v}\right)_{\Omega_i} + \int_{T_n}^t a_i(\mathbf{u}_{i,n}^{k,\ell}(s),\mathbf{v})ds - (P_{i,n}^{k,\ell},\nabla\cdot\mathbf{v})_{\Omega_i} - \int_0^t c_{i,n}^{k,\ell}(s,\mathbf{v})ds = 0 \,.$$

(2.130)

As the coarse solver and the OSWR method are both well-defined, one gets the following result

Theorem 2.43. *Suppose that $\mathbf{u}_0 \in H$ and $\mathbf{f} \in L^2((0,T),\left[L^2(\Omega)\right]^2)$. With the starting initial conditions $\mathbf{U}_n^0 \in K$ and the Robin terms $\boldsymbol{\xi}_n^{0,0},\mathbf{g}_n^{0,0} \in \left[L^2(T_n,T_{n+1},L^2(\Gamma))\right]^2$ the coupled Parareal-OSWR method is well-defined with $\mathbf{U}_n^k \in K$; $\boldsymbol{\xi}_n^{k,\ell},\mathbf{g}_n^{k,\ell} \in \left[L^2(T_n,T_{n+1},L^2(\Gamma))\right]^2$.*

2.11.1 Convergence of the velocity via energy estimate

We consider the initial condition $\mathbf{u}_0 \in V$, with which we have regular exact solution $(\mathbf{u},p)$ as in Theorem 2.2, and then, its Robin traces on the space-time interface are well-defined and have L^2 regularity.

The proof in this section can be generalized to the case of M subdomains, similarly to the pure OSWR for the Stokes equation. We suppose that $\alpha_1 = \alpha_2 = \alpha$ and $\beta_1 = \beta_2 = \beta$.
We denote by $(\mathbf{u}_{i,n},p_{i,n})$ the restriction of $(\mathbf{u},p)$ to $\Omega_i \times (T_n,T_{n+1})$.

Notation for error estimation

Denote by $\mathbf{E}_n^k = \mathbf{U}_n^k - \mathbf{u}(.,T_n)$, $\mathbf{e}_{i,n}^{k,\ell} := \mathbf{u}_{i,n}^{k,\ell} - \mathbf{u}_{i,n}$, $d_{i,n}^{k,\ell} = p_{i,n}^{k,\ell} - p_{i,n}$, $h_{i,n}^{k,\ell} = g_{i,n}^{k,\ell} - g_{i,n}$, $\zeta_{i,n}^{k,\ell} = \xi_{i,n}^{k,\ell} - \xi_{i,n}$, with

$$g_{i,n} := \alpha(\nu\partial_{\boldsymbol{n}_i}\mathbf{u}_{i,n}\cdot\boldsymbol{n}_i - p_{i,n}) + \mathbf{u}_{i,n}\cdot\boldsymbol{n}_i \tag{2.131}$$

$$\xi_{i,n} := \beta\partial_{\boldsymbol{n}_i}\mathbf{u}_{i,n}\times\boldsymbol{n}_i + \mathbf{u}_{i,n}\times\boldsymbol{n}_i \tag{2.132}$$

We now write the algorithm for the error (only for the velocity and Robin terms)

Algorithm 10 (Coupled Parareal-OSWR algorithm for the error on the Stokes equations)

1. Choose an initial data $(\mathbf{E}_n^0)_{n\in[\![0,N]\!]}$ with $\mathbf{E}_0^0 = 0$, for example $\mathbf{E}_n^0 := \mathscr{G}(\mathscr{I}_{n-1}, \mathbf{U}_{n-1}^0) - u(., T_n)$, for $n = 1, \ldots, N$.

2. Choose an initial Robin data $(\boldsymbol{\zeta}_n^{0,0}, \mathbf{h}_n^{0,0})_{n\in[\![0,N-1]\!]}$. For example, if we have already run the coarse solver, then we also have calculated the approximate pressure d_n^0 for $n = 1, \ldots, N$, then $(\boldsymbol{\zeta}_n^{0,0}, \mathbf{h}_n^{0,0})$ with $n \in [\![0, N-1]\!]$ can be constructed, e.g., from $\mathbf{E}_n^0$ and d_n^0.

for $k = 0, 1, \ldots$ *(Parareal iterations)*
    1. On each time interval $\mathscr{I}_n$, $n = 0, 1, \ldots, N-1$,
    for $\ell = 1, \ldots L$ *(OSWR iterations) solve, for each* $i = 1, 2$:

$$\left\langle \partial_t \mathbf{e}_{i,n}^{k,\ell}, \mathbf{v} \right\rangle_{V_i', V_i} + a_i(\mathbf{e}_{i,n}^{k,\ell}, \mathbf{v}) = \frac{1}{\alpha}\left(h_{i,n}^{k,\ell-1}, \mathbf{v} \cdot \boldsymbol{n}_i\right)_\Gamma + \frac{1}{\beta}\left(\zeta_{i,n}^{k,\ell-1}, \mathbf{v} \times \boldsymbol{n}_i\right)_\Gamma, \qquad \text{a.e. } t \in \mathscr{I}_n, \forall \mathbf{v} \in V_i,$$

$$\mathbf{e}_{i,n}^{k,\ell}(T_n) = \mathbf{E}_n^k|_{\Omega_i}$$

(2.133)

and, with $j = 3 - i$, update the Robin term as

$$h_{i,n}^{k,\ell} = h_{j,n}^{k,\ell-1} - 2\mathbf{e}_{j,n}^{k,\ell} \cdot \boldsymbol{n}_j, \tag{2.134}$$

$$\zeta_{i,n}^{k,\ell} = \zeta_{j,n}^{k,\ell-1} - 2\mathbf{e}_{j,n}^{k,\ell} \times \boldsymbol{n}_j. \tag{2.135}$$

    end for
    2. Set $\mathbf{E}_0^{k+1} = 0$ and do Parareal corrections:

$$\mathbf{E}_{n+1}^{k+1} = \mathbf{e}_n^{k,L}(\cdot, T_{n+1}) + \tilde{\mathscr{G}}(\mathscr{I}_n, \mathbf{E}_n^{k+1} - \mathbf{E}_n^k). \tag{2.136}$$

Update the interface term: $\zeta_n^{k+1,0} = \zeta_n^{k,L}$ and $h_n^{k+1,0} = h_n^{k,L}.$ (2.137)

end for

We can obtain a similar lemma as for the parabolic problem.

Lemma 2.44. *Denote by* $\mathbf{e}_n^{k,\ell} \in \left[L^2(\Omega)\right]^2$ *the function whose restrictions are* $\mathbf{e}_n^{k,\ell}|_{\Omega_i} = \mathbf{e}_{i,n}^{k,\ell}$. *We have*

$$\sum_{\ell=1}^{L} \|\mathbf{e}_n^{k,\ell}(T_{n+1})\|_\Omega^2 + 2\nu \sum_{\ell=1}^{L} \sum_{i=1,2} \int_{\mathscr{I}_n} \|\nabla \mathbf{e}_{i,n}^{k,\ell}\|_{\Omega_i}^2 + \frac{1}{2\alpha} \sum_{i=1,2} \int_{\mathscr{I}_n} \|h_{i,n}^{k,L}\|_\Gamma^2 + \frac{1}{2\beta} \sum_{i=1,2} \int_{\mathscr{I}_n} \|\zeta_{i,n}^{k,L}\|_\Gamma^2$$

$$= L\|\mathbf{E}_n^k\|_\Omega^2 + \frac{1}{2\alpha} \sum_{i=1,2} \int_{\mathscr{I}_n} \|h_{i,n}^{k,0}\|_\Gamma^2 + \frac{1}{2\beta} \sum_{i=1,2} \int_{\mathscr{I}_n} \|\zeta_{i,n}^{k,0}\|_\Gamma^2$$

Proof. Choosing the test function $\mathbf{v} = \mathbf{e}_{i,n}^{k,\ell}$ in (2.133) we have

$$\langle \partial_t \mathbf{e}_{i,n}^{k,\ell}, \mathbf{e}_{i,n}^{k,\ell}\rangle_{V_i', V_i} + \nu(\nabla \mathbf{e}_{i,n}^{k,\ell}, \nabla \mathbf{e}_{i,n}^{k,\ell})_{\Omega_i} + \frac{1}{\alpha}(\mathbf{e}_{i,n}^{k,\ell} \cdot \boldsymbol{n}_i, \mathbf{e}_{i,n}^{k,\ell} \cdot \boldsymbol{n}_i)_\Gamma + \frac{1}{\beta}(\mathbf{e}_{i,n}^{k,\ell} \times \boldsymbol{n}_i, \mathbf{e}_{i,n}^{k,\ell} \times \boldsymbol{n}_i)_\Gamma$$

$$= \frac{1}{\alpha}(h_{i,n}^{k,\ell-1}, \mathbf{e}_{i,n}^{k,\ell} \cdot \boldsymbol{n}_i)_\Gamma + \frac{1}{\beta}(\zeta_{i,n}^{k,\ell-1}, \mathbf{e}_{i,n}^{k,\ell} \times \boldsymbol{n}_i)_\Gamma. \tag{2.138}$$

On the boundary Γ, replacing the error by the Robin terms from (2.134) and (2.135), one gets

$$\langle \partial_t \mathbf{e}_{i,n}^{k,\ell}, \mathbf{e}_{i,n}^{k,\ell}\rangle_{V_i', V_i} + \nu(\nabla \mathbf{e}_{i,n}^{k,\ell}, \nabla \mathbf{e}_{i,n}^{k,\ell})_{\Omega_i} + \frac{1}{4\alpha}(h_{i,n}^{k,\ell-1} - h_{j,n}^{k,\ell}, h_{i,n}^{k,\ell-1} - h_{j,n}^{k,\ell})_\Gamma$$

$$+ \frac{1}{4\beta}(\zeta_{i,n}^{k,\ell-1} - \zeta_{j,n}^{k,\ell}, \zeta_{i,n}^{k,\ell-1} - \zeta_{j,n}^{k,\ell})_\Gamma$$

$$= \frac{1}{2\alpha}(h_{i,n}^{k,\ell-1}, h_{i,n}^{k,\ell-1} - h_{j,n}^{k,\ell})_\Gamma + \frac{1}{2\beta}(\zeta_{i,n}^{k,\ell-1}, \zeta_{i,n}^{k,\ell-1} - \zeta_{j,n}^{k,\ell})_\Gamma,$$

or equivalently

$$\langle \partial_t \mathbf{e}_{i,n}^{k,\ell}, \mathbf{e}_{i,n}^{k,\ell} \rangle_{V_i', V_i} + \nu \|\nabla \mathbf{e}_{i,n}^{k,\ell}\|_{\Omega_i}^2 + \frac{1}{4\alpha}\|h_{j,n}^{k,\ell}\|_\Gamma^2 + \frac{1}{4\beta}\|\zeta_{j,n}^{k,\ell}\|_\Gamma^2 = \frac{1}{4\alpha}\|h_{i,n}^{k,\ell-1}\|_\Gamma^2 + \frac{1}{4\beta}\|\zeta_{i,n}^{k,\ell-1}\|_\Gamma^2.$$

Multiplying this expression by 2 and integrating on $\mathscr{I}_n$, we obtain

$$\|\mathbf{e}_{i,n}^{k,\ell}(T_{n+1})\|_{\Omega_i}^2 - \|\mathbf{e}_{i,n}^{k,\ell}(T_n)\|_{\Omega_i}^2 + 2\nu \int_{\mathscr{I}_n} \|\nabla \mathbf{e}_{i,n}^{k,\ell}\|_{\Omega_i}^2 + \frac{1}{2\alpha}\int_{\mathscr{I}_n}\|h_{j,n}^{k,\ell}\|_\Gamma^2 + \frac{1}{2\beta}\int_{\mathscr{I}_n}\|\zeta_{j,n}^{k,\ell}\|_\Gamma^2 =$$

$$\frac{1}{2\alpha}\int_{\mathscr{I}_n}\|h_{i,n}^{k,\ell-1}\|_\Gamma^2 + \int_{\mathscr{I}_n}\frac{1}{2\beta}\|\zeta_{i,n}^{k,\ell-1}\|_\Gamma^2.$$

$$(2.139)$$

From the initial condition in (2.133), we have $\mathbf{e}_{i,n}^{k,\ell}(T_n) = \mathbf{E}_n^k|_{\Omega_i}$. Then, summing for $i = 1, 2$, we get

$$\|\mathbf{e}_n^{k,\ell}(T_{n+1})\|_\Omega^2 + 2\nu \sum_{i=1,2}\int_{\mathscr{I}_n} \|\nabla \mathbf{e}_{i,n}^{k,\ell}\|_{\Omega_i}^2 + \frac{1}{2\alpha}\sum_{i=1,2}\int_{\mathscr{I}_n}\|h_{j,n}^{k,\ell}\|_\Gamma^2 + \frac{1}{2\beta}\sum_{i=1,2}\int_{\mathscr{I}_n}\|\zeta_{j,n}^{k,\ell}\|_\Gamma^2 =$$

$$\|\mathbf{E}_n^k\|_\Omega^2 + \frac{1}{2\alpha}\sum_{i=1,2}\int_{\mathscr{I}_n}\|h_{i,n}^{k,\ell-1}\|_\Gamma^2 + \sum_{i=1,2}\int_{\mathscr{I}_n}\frac{1}{2\beta}\|\zeta_{i,n}^{k,\ell-1}\|_\Gamma^2$$

One notices that, since $j = 3 - i$:

$$\sum_{i=1,2}\frac{1}{2\beta}\int_{\mathscr{I}_n}\|\zeta_{i,n}^{k,\ell}\|_\Gamma^2 + \sum_{i=1,2}\frac{1}{2\alpha}\int_{\mathscr{I}_n}\|h_{i,n}^{k,\ell}\|_\Gamma^2 = \sum_{i=1,2}\frac{1}{2\beta}\int_{\mathscr{I}_n}\|\zeta_{j,n}^{k,\ell}\|_\Gamma^2 + \sum_{i=1,2}\frac{1}{2\alpha}\int_{\mathscr{I}_n}\|h_{j,n}^{k,\ell}\|_\Gamma^2$$

which represents the total energies on the interface of all Robin terms at step ℓ. Then, summing for ℓ from 1 to L, we get the result.   □

In order to simplify notations, we shall denote $Y_n := L^2(T_n, T_{n+1}, L^2(\Gamma))$ and its norm $\|\zeta\|_{Y_n}^2 = \int_{\mathscr{I}_n} \|\zeta\|_\Gamma^2$. We also set the following notations

$$\|\boldsymbol{\zeta}\|_{(Y_n)^2} = \sum_{i=1,2}\int_{\mathscr{I}_n}\|\zeta_i\|_\Gamma^2 \ , \ \ \|\mathbf{h}\|_{(Y_n)^2} = \sum_{i=1,2}\int_{\mathscr{I}_n}\|h_i\|_\Gamma^2.$$

We build on the previous lemma to obtain the following lemma

Lemma 2.45. *We have*

$$\sum_{k=0}^{K}\sum_{\ell=1}^{L}\|\mathbf{e}_n^{k,\ell}(T_{n+1})\|_\Omega^2 + 2\nu\sum_{k=0}^{K}\sum_{\ell=1}^{L}\sum_{i=1,2}\int_{\mathscr{I}_n}\|\nabla\mathbf{e}_{i,n}^{k,\ell}\|_{\Omega_i}^2 + \frac{1}{2\alpha}\|\mathbf{h}_n^{K,L}\|_{(Y_n)^2}^2 + \frac{1}{2\beta}\|\boldsymbol{\zeta}_n^{K,L}\|_{(Y_n)^2}^2$$

$$= L\sum_{k=0}^{K}\|\mathbf{E}_n^k\|_\Omega^2 + \frac{1}{2\alpha}\|\mathbf{h}_n^{0,0}\|_{(Y_n)^2}^2 + \frac{1}{2\beta}\|\boldsymbol{\zeta}_n^{0,0}\|_{(Y_n)^2}^2$$

$$(2.140)$$

Proof. Applying the previous lemma, summing in k from 0 to K and noting that, in our algorithm, we have $\mathbf{h}_n^{k,L} = \mathbf{h}_n^{k+1,0}$ and $\boldsymbol{\zeta}_n^{k,L} = \boldsymbol{\zeta}_n^{k+1,0}$, we get

$$\sum_{k=0}^{K}\sum_{\ell=1}^{L}\|\mathbf{e}_n^{k,\ell}(T_{n+1})\|_\Omega^2 + 2\nu\sum_{k=0}^{K}\sum_{\ell=1}^{L}\sum_{i=1,2}\int_{\mathscr{I}_n}\|\nabla\mathbf{e}_{i,n}^{k,\ell}\|_{\Omega_i}^2$$

$$+\frac{1}{2\alpha}\sum_{k=0}^{K}\|\mathbf{h}_n^{k+1,0}\|_{(Y_n)^2}^2 + \frac{1}{2\beta}\sum_{k=0}^{K}\|\boldsymbol{\zeta}_n^{k+1,0}\|_{(Y_n)^2}^2 =$$

$$L\sum_{k=0}^{K}\|\mathbf{E}_n^k\|_\Omega^2 + \frac{1}{2\alpha}\sum_{k=0}^{K}\|\mathbf{h}_n^{k,0}\|_{(Y_n)^2}^2 + \frac{1}{2\beta}\sum_{k=0}^{K}\|\boldsymbol{\zeta}_n^{k,0}\|_{(Y_n)^2}^2.$$

Remarking the telescopic sum on the interface, we get (2.140). □

From the above lemma, we obtain the following convergence of the coupled Parareal-OSWR method on the Stokes equations

Theorem 2.46. *For the coupled Parareal-OSWR algorithm applied on the Stokes equations, when $k \to \infty$*

- $\mathbf{U}_n^k$ *converges to* $\mathbf{u}(T_n)$ *in K with L^2-norm.*
- $\mathbf{u}_{i,n}^{k,\ell}$ *converges to* $\mathbf{u}_{i,n}$ *in $L^2(T_n, T_{n+1}, V_i)$ for all $\ell = 1, 2, \ldots, L$.*

The proof follows similarly by using $\tilde{\mathscr{G}}$ as for the parabolic case. From (2.123), we have the following lemma:

Lemma 2.47.

$$\sum_{k=0}^{K}\|\mathbf{E}_{n+1}^{k+1}\|_\Omega^2 \le 8\gamma_1^2\sum_{k=0}^{K+1}\|\mathbf{E}_n^k\|_\Omega^2 + 2\sum_{k=0}^{K}\|\mathbf{e}_n^{k,L}(T_{n+1})\|_\Omega^2 \qquad (2.141)$$

Proof. In (2.136), using the triangle inequality and then (2.123), we get

$$\|\mathbf{E}_{n+1}^{k+1}\|_\Omega^2 \le 2\|\tilde{\mathscr{G}}(\mathscr{I}_n, \mathbf{E}_n^{k+1} - \mathbf{E}_n^k)\|_\Omega^2 + 2\|\mathbf{e}_n^{k,L}(T_{n+1})\|_\Omega^2$$

$$\le 2\gamma_1^2\|\mathbf{E}_n^{k+1} - \mathbf{E}_n^k\|_\Omega^2 + 2\|\mathbf{e}_n^{k,L}(T_{n+1})\|_\Omega^2,$$

$$\le 4\gamma_1^2\big(\|\mathbf{E}_n^{k+1}\|_\Omega^2 + \|\mathbf{E}_n^k\|_\Omega^2\big) + 2\|\mathbf{e}_n^{k,L}(T_{n+1})\|_\Omega^2.$$

Then, summing in k from 0 to K we have

$$\sum_{k=0}^{K}\|\mathbf{E}_{n+1}^{k+1}\|_\Omega^2 \le 4\gamma_1^2\sum_{k=0}^{K}\big(\|\mathbf{E}_n^{k+1}\|_\Omega^2 + \|\mathbf{E}_n^k\|_\Omega^2\big) + 2\sum_{k=0}^{K}\|\mathbf{e}_n^{k,L}(T_{n+1})\|_\Omega^2,$$

from which we deduce (2.141). □

With these lemmas, we can now prove Theorem 2.46

Proof of Theorem 2.46. From Lemmas 2.45 and 2.47, we get

$$\sum_{k=0}^{K}\|\mathbf{E}_{n+1}^{k+1}\|_\Omega^2 \le 8\gamma_1^2\sum_{k=0}^{K+1}\|\mathbf{E}_n^k\|_\Omega^2 + 2L\sum_{k=0}^{K}\|\mathbf{E}_n^k\|_\Omega^2 + \frac{1}{\alpha}\|\mathbf{h}_n^{0,0}\|_{(Y_n)^2}^2 + \frac{1}{\beta}\|\boldsymbol{\zeta}_n^{0,0}\|_{(Y_n)^2}^2.$$

Denoting $\gamma_4 = 8\gamma_1^2 + 2L$ and $R_n = \|\mathbf{E}_{n+1}^0\|_\Omega^2 + \frac{1}{\alpha}\|\mathbf{h}_n^{0,0}\|_{(Y_n)^2}^2 + \frac{1}{\beta}\|\boldsymbol{\zeta}_n^{0,0}\|_{(Y_n)^2}^2$, we can rewrite this inequality as

$$\sum_{k=0}^{K+1}\|\mathbf{E}_{n+1}^k\|_\Omega^2 \le \gamma_4 \sum_{k=0}^{K+1}\|\mathbf{E}_n^k\|_\Omega^2 + R_n, \quad n \in [\![0, N-1]\!].$$

From this inequality, by induction, we obtain

$$\sum_{k=0}^{K+1}\|\mathbf{E}_{n+1}^k\|_\Omega^2 \le \gamma_4^{n+1} \sum_{k=0}^{K+1}\|\mathbf{E}_0^k\|_\Omega^2 + \sum_{j=0}^n \gamma_4^j R_{n-j}, \quad n \in [\![0, N-1]\!].$$

Using that $\mathbf{E}_0^k = 0, \ \forall k \ge 0$, we finally obtain

$$\sum_{k=0}^{K+1}\|\mathbf{E}_{n+1}^k\|_\Omega^2 \le \sum_{j=0}^n \gamma_4^j R_{n-j}, \quad n \in [\![0, N-1]\!].$$

It shows that the sum $\displaystyle\sum_{k=0}^K \|\mathbf{E}_n^k\|_\Omega^2$ is bounded with respect to K, hence $\mathbf{E}_n^k$ converges to 0 in the $[L^2(\Omega)]^2$ norm when $k \to \infty$. Moreover, from Lemma 2.45, we obtain, for all $\ell = 1, 2, \ldots, L$

$$2\nu \sum_{k=0}^K \int_{\mathscr{I}_n} \|\nabla\mathbf{e}_{i,n}^{k,\ell}\|_{\Omega_i}^2 \le L \sum_{k=0}^K \|\mathbf{E}_n^k\|_\Omega^2 + \frac{1}{2\alpha}\|\mathbf{h}_n^{0,0}\|_{(Y_n)^2}^2 + \frac{1}{2\beta}\|\boldsymbol{\zeta}_n^{0,0}\|_{(Y_n)^2}^2$$

As the right-hand side sum is bounded, the left one is also bounded. Hence, it follows that $\displaystyle\int_{\mathscr{I}_n} \|\nabla\mathbf{e}_{i,n}^{k,\ell}\|_{\Omega_i}^2 \to 0$ when $k \to \infty$.

In addition, the expression in Lemma 2.45 is still true if we replace T_{n+1} by any $t \in (T_n, T_{n+1})$. We then get

$$\sum_{k=0}^K \|\mathbf{e}_{i,n}^{k,\ell}(t)\|_{\Omega_i}^2 \le L \sum_{k=0}^K \|\mathbf{E}_n^k\|_\Omega^2 + \frac{1}{2\alpha}\int_{T_n}^t \|\mathbf{h}_n^{0,0}\|^2 + \frac{1}{2\beta}\int_{T_n}^t \|\boldsymbol{\zeta}_n^{0,0}\|^2$$

$$\le L \sum_{k=0}^K \|\mathbf{E}_n^k\|_\Omega^2 + \frac{1}{2\alpha}\|\mathbf{h}_n^{0,0}\|_{(Y_n)^2}^2 + \frac{1}{2\beta}\|\boldsymbol{\zeta}_n^{0,0}\|_{(Y_n)^2}^2.$$

Hence, the sum $\displaystyle\sum_{k=0}^K \|\mathbf{e}_{i,n}^{k,\ell}(t)\|_{\Omega_i}^2$ is bounded by a constant independent of t. One then gets that this is also the case for $\displaystyle\sum_{k=0}^K \int_{\mathscr{I}_n} \|\mathbf{e}_{i,n}^{k,\ell}(t)\|_{\Omega_i}^2 dt$, and thus $\displaystyle\int_{\mathscr{I}_n} \|\mathbf{e}_{i,n}^{k,\ell}(t)\|_{\Omega_i}^2 dt$ tends to 0.

Hence $\mathbf{e}_{i,n}^{k,\ell}$ tends to 0 in $[L^2(T_n, T_{n+1}, V_i)]^2$, i.e, $\mathbf{u}_{i,n}^{k,\ell} \to \mathbf{u}_{i,n}$ in $[L^2(T_n, T_{n+1}, V_i)]^2$. $\square$

We now have the convergence on the velocities. As in the pure OSWR method for Stokes equation, one can recover the pressure by solving a linear system. The convergence factor can be achieved in the same manner as for the parabolic equation in Chapter 1, provided a convergence factor strictly lower that one holds for the pure OSWR.

Appendix

Proof of Theorem 1.7

Proof. The proof is done in [50] (Theorem 5.15) and we recall it here : for $\ell = 1, 2, \ldots, L$, the error $e_i^\ell := u_i^\ell - u|_{\Omega_i}$ satisfies

$$\mathscr{L}(e_i^\ell) = 0 \qquad \text{in } \Omega_i \times \mathscr{I}, \tag{142a}$$

$$e_i^\ell(.,0) = 0 \qquad \text{in } \Omega_i, \tag{142b}$$

$$\mathscr{B}_i e_i^\ell(0,.) = \zeta_i^{\ell-1} \text{ in } \mathscr{I}, \tag{142c}$$

where

$$\zeta_i^\ell = \mathscr{B}_i e_j^\ell(0,\cdot), \ \ell \geq 1. \tag{143}$$

Multiplying equation (142a) by e_i^ℓ and integrating in space on Ω_i, we obtain

$$\tfrac{1}{2}\tfrac{d}{dt}\|e_1^\ell\|^2 + \nu\|\partial_x e_1^\ell\|^2 + b\|e_1^\ell\|^2 - \big(\nu\partial_x e_1^\ell - \tfrac{a}{2}e_1^\ell\big)(0,.)e_1^\ell(0,.) = 0,$$

$$\tfrac{1}{2}\tfrac{d}{dt}\|e_2^\ell\|^2 + \nu\|\partial_x e_2^\ell\|^2 + b\|e_2^\ell\|^2 + \big(\nu\partial_x e_2^\ell - \tfrac{a}{2}e_2^\ell\big)(0,.)e_2^\ell(0,.) = 0.$$

Introducing the Robin interface operators $\mathscr{B}_i$, $i = 1, 2$, defined in (1.2), and rewriting the terms on the interface in the form

$$\big(\nu\partial_x e_i^\ell - \tfrac{a}{2}e_i^\ell\big)e_i^\ell = \tfrac{1}{2p}\big((\mathscr{B}_1 e_i^\ell)^2 - (\mathscr{B}_2 e_i^\ell)^2\big), \qquad i = 1, 2,$$

we obtain the energy estimates, for $i = 1, 2$

$$\tfrac{1}{2}\tfrac{d}{dt}\|e_i^\ell\|^2 + \nu\|\partial_x e_i^\ell\|^2 + b\|e_i^\ell\|^2 + \tfrac{1}{2p}((\mathscr{B}_j e_i^\ell)(0,.))^2 = \tfrac{1}{2p}((\mathscr{B}_i e_i^\ell)(0,.))^2, \quad j = 3 - i.$$

Replacing $(\mathscr{B}_i e_i^\ell)(0,.) = \zeta_i^{\ell-1}$, $(\mathscr{B}_j e_i^\ell)(0,.) = \zeta_j^\ell$ (from (142c) and (143)), and summing the above expression over i, we get, for all $t \in \mathscr{I}$

$$\sum_i \big(\tfrac{1}{2}\tfrac{d}{dt}\|e_i^\ell\|^2 + \nu\|\partial_x e_i^\ell\|^2 + b\|e_i^\ell\|^2\big) + \tfrac{1}{2p}\sum_i(\zeta_i^\ell)^2 = \tfrac{1}{2p}\sum_i(\zeta_i^{\ell-1})^2.$$

Then, integrating on $\mathscr{I}$, we obtain

$$\sum_i \left(\tfrac{1}{2}\big(\|e_i^\ell(.,T)\|^2 - \|e_i^\ell(.,0)\|^2\big) + \int_{\mathscr{I}} \big(\nu\|\partial_x e_i^\ell\|^2 + b\|e_i^\ell\|^2\big)\,dt \right) + \tfrac{1}{2p}\|\zeta^\ell\|_{\mathscr{I}}^2 = \tfrac{1}{2p}\|\zeta^{\ell-1}\|_{\mathscr{I}}^2.$$

In $L^2(0, T; H^1(\Omega_i))$, we consider the norm

$$\|u\|_{L^2(0,T;H^1(\Omega_i))}^2 := \int_{\mathscr{I}} \big(\nu\|\partial_x u\|^2 + b\|u\|^2\big)\,dt.$$

Then we can rewrite the above equation as

$$\sum_i \left(\tfrac{1}{2} \left(\|e_i^\ell(.,T)\|^2 - \|e_i^\ell(.,0)\|^2 \right) + \|e_i^\ell\|_{L^2(0,T;H^1(\Omega_i))}^2 \right) + \tfrac{1}{2p} \|\boldsymbol{\zeta}^\ell\|_{\mathscr{G}}^2 = \tfrac{1}{2p} \|\boldsymbol{\zeta}^{\ell-1}\|_{\mathscr{G}}^2,$$

or equivalently

$$\tfrac{1}{2} \|e^\ell(.,T)\|^2 + \sum_i \|e_i^\ell\|_{L^2(0,T,H^1(\Omega_i))}^2 + \tfrac{1}{2p} \|\boldsymbol{\zeta}^\ell\|_{\mathscr{G}}^2 = \tfrac{1}{2} \sum_i \|e_i^\ell(.,0)\|^2 + \tfrac{1}{2p} \|\boldsymbol{\zeta}^{\ell-1}\|_{\mathscr{G}}^2.$$

Summing over ℓ from 1 to L, we get a telescopic sum on the interface and thus

$$\sum_{\ell=1}^L \left(\tfrac{1}{2} \|e^\ell(.,T)\|^2 + \sum_i \|e_i^\ell\|_{L^2(0,T,H^1(\Omega_i))}^2 \right) + \tfrac{1}{2p} \|\boldsymbol{\zeta}^L\|_{\mathscr{G}}^2 = \tfrac{L}{2} \sum_i \|e_i^\ell(.,0)\|^2 + \tfrac{1}{2p} \|\boldsymbol{\zeta}^0\|_{\mathscr{G}}^2.$$

$$(144)$$

Using that $e_i^\ell(.,0) = 0$, $\forall \ell \geq 1$, $i = 1,2$, we obtain

$$\sum_{\ell=1}^L \left(\tfrac{1}{2} \|e^\ell(.,T)\|^2 + \sum_i \|e_i^\ell\|_{L^2(0,T,H^1(\Omega_i))}^2 \right) + \tfrac{1}{2p} \|\boldsymbol{\zeta}^L\|_{\mathscr{G}}^2 = \tfrac{1}{2p} \|\boldsymbol{\zeta}^0\|_{\mathscr{G}}^2.$$

Hence, the sum of the energies over all the iterates remains bounded, which implies that the energy in the iterates tends to zero when $\ell \to \infty$, which proves Theorem 1.7. □

Conclusions and future work

In the first chapter of this thesis, we analyzed the coupling of the Parareal method with OSWR methods. We introduced first the algorithm for the coupling with non-overlapping OSWR, in which case we obtained an energy estimate used to prove the general convergence of the coupled method. Then, numerical results follow to ensure that the coupled method performs efficiently in practice, especially when compared to the "pure" Parareal method or "pure" OSWR method. From these numerical observations, we gave some conjectures about how we could optimize the number of OSWR iterations in the incomplete fine solvers to fasten the process. The coupling with overlapping OSWR was introduced then, and by using the linear convergence factor of the overlapping OSWR, a general convergence result and a bound on the convergence factor were then given.

In the second chapter, we studied the application of the OSWR method on the evolutionary incompressible Stokes equations. An important result needed in the analysis is the well-posedness of the time-dependent Stokes system with Robin boundary conditions. The OSWR algorithm and its well-posedness were introduced first, followed by an energy estimate for the general convergence of the velocity. On the other hand, simple observations showed that the pressure iterates may not always converge to the monodomain pressure field. Modified pressures which converge to the exact one were then proposed, which can be cheaply calculated. Inspired by the analysis of the OSWR method for parabolic equations, we further applied the Fourier transform on the errors, and obtained the formulation of the convergence factor, which allows to numerically find optimized Robin parameters. The numerical illustrations were performed, first to verify the convergence of the velocities, then to verify the convergence of the modified pressure, and finally to assess the optimized parameters in practice. It was shown that a discrete version of the convergence factor, taking into account the implicit Euler scheme used for the time discretization, was more efficient to provide near optimal Robin parameters. In the end, we gave some observations for the OSWR method applied to the Oseen equations - a close extension of the Stokes ones -, as well as for the Parareal algorithm and the Parareal-OSWR coupling on the Stokes system itself.

This work can be taken further in various directions. For the coupled Parareal-OSWR method for parabolic equations, finding the best choice for the number of OSWR iterations for the incomplete fine solver is an attractive question, on which we put some promising conjecture but not a full theoretical answer. Designing a posteriori error estimates that combine contributions from the scheme error and from the current non converged iteration could lead to a further optimization of the costs by giving an efficient stopping criterion for the Parareal-OSWR iterations, which would enhance the application of the method.

On the other hand, one may try numerical experiments to validate the coupled Parareal-OSWR algorithm on the Stokes equations. In addition, similar techniques could be investigated to analyze the convergence behaviour of the coupling of other iterative methods with Parareal.

Finally, in the context of the OSWR method itself for the Stokes equations, industrial tests would be needed to validate the method on large scale calculations. One may also think of an extension to the Navier-Stokes equations, which would be a great challenge for the convergence analysis due to their nonlinearity.

Bibliography

[1] *MathWorks help center*. Available at https://fr.mathworks.com/help/matlab/ref/fminsearch.html.

[2] E. AHMED, S. ALI HASSAN, C. JAPHET, M. KERN, AND M. VOHRALÍK, *A posteriori error estimates and stopping criteria for space-time domain decomposition for two-phase flow between different rock types*, The SMAI journal of computational mathematics, 5 (2019), pp. 195–227.

[3] E. AHMED, C. JAPHET, AND M. KERN, *Space–time domain decomposition for two-phase flow between different rock types*, Comput. Methods Appl. Mech. Engrg., 371 (2020), pp. 113–294.

[4] S. ALI HASSAN, *A posteriori error estimates and stopping criteria for solvers using domain decomposition method and with local time stepping*, PhD thesis, Université Pierre et Marie Curie, Sorbonne Université, 2017.

[5] S. ALI HASSAN, C. JAPHET, AND M. VOHRALÍK, *A posteriori stopping criteria for space-time domain decomposition for the heat equation in mixed formulations*, Electron. Trans. Numer. Anal., 49 (2018), pp. 151–181.

[6] J. BAIGES, R. CODINA, AND S. IDELSOHN, *A domain decomposition strategy for reduced order models. application to the incompressible Navier–Stokes equations*, Computer Methods in Applied Mechanics and Engineering, 267 (2013), pp. 23 – 42.

[7] G. BAL AND Y. MADAY, *A "Parareal" time discretization for non-linear PDE's with application to the pricing of an american put*, in Recent Developments in Domain Decomposition Methods, L. F. Pavarino and A. Toselli, eds., Berlin, Heidelberg, 2002, Springer Berlin Heidelberg, pp. 189–202.

[8] A. BELLEN AND M. ZENNARO, *Parallel algorithms for initial-value problems for difference and differential equations*, J. Comput. Appl. Math., 25 (1989), pp. 341–350.

[9] D. BENNEQUIN, M. J. GANDER, AND L. HALPERN, *A homographic best approximation problem with application to optimized Schwarz waveform relaxation*, Math. Comp., 78 (2009), pp. 185–223.

[10] P.-M. BERTHE, *Méthodes de décomposition de domaine de type relaxation d'ondes optimisées pour l'équation de convection-diffusion instationnaire discrétisée par volumes finis*, PhD thesis, Université Paris XIII, 2013.

[11] P.-M. BERTHE, C. JAPHET, AND P. OMNES, *Space-Time Domain Decomposition with Finite Volumes for Porous Media Applications*, in Domain Decomposition Methods in

Science and Engineering XXI, J. Erhel, M. J. Gander, L. Halpern, G. Pichot, T. Sassi, and O. Widlund, eds., vol. 98 of Lecture Notes in Computational Science and Engineering, 2014, pp. 483–490.

[12] U. BIEDER, F. FALK, AND G. FAUCHET, *LES analysis of the flow in a simplified pwr assembly with mixing grid*, Progress in Nuclear Energy, 75 (2014), pp. 15 – 24.

[13] ———, *CFD analysis of the flow in the near wake of a generic pwr mixing grid*, Annals of Nuclear Energy, 82 (2015), pp. 169 – 178. Joint International Conference on Supercomputing in Nuclear Applications and Monte Carlo 2013, SNA + MC 2013. Pluri- and Trans-disciplinarity, Towards New Modeling and Numerical Simulation Paradigms.

[14] U. BIEDER, G. FAUCHET, AND C. CALVIN, *High performance Large Eddy Simulation of turbulent flows around pwr mixing grids*, in Proceedings of 16th IEEE International Conference on High Performance Computing and Communications (HPCC 2014), 2014.

[15] U. BIEDER AND E. GRAFFARD, *Qualification of the CFD code Trio_U for full scale reactor applications*, Nuclear Engineering and Design, 238 (2008), pp. 671 – 679. Benchmarking of CFD Codes for Application to Nuclear Reactor Safety.

[16] E. BLAYO, D. CHEREL, AND A. ROUSSEAU, *Towards optimized Schwarz methods for the Navier–Stokes equations*, Journal of Scientific Computing, 66 (2016), pp. 275–295.

[17] E. BLAYO, L. HALPERN, AND C. JAPHET, *Optimized Schwarz waveform relaxation algorithms with nonconforming time discretization for coupling convection-diffusion problems with discontinuous coefficients*, in Domain decomposition methods in science and engineering XVI, vol. 55 of Lect. Notes Comput. Sci. Eng., Springer, Berlin, 2007, pp. 267–274.

[18] F. BOYER AND P. FABRIE, *Mathematical tools for the study of the incompressible Navier-Stokes equations and related models*, Applied Mathematical Sciences, Springer New York, Nov. 2012.

[19] E. BRAKKEE, A. SEGAL, AND C. G. M. KASSELS, *A parallel domain decomposition algorithm for the incompressible Navier-Stokes equations*, Simul. Pract. Theory, 3 (1995), pp. 185–205.

[20] E. BRAKKEE, C. VUIK, AND P. WESSELING, *Domain decomposition for the incompressible Navier-Stokes equations: Solving subdomain problems accurately and inaccurately*, Domain Decomposition Methods in sciences and engineering; 8th International Conference, Beijing,, 443-451. (1997), 26 (1998).

[21] E. BRAKKEE, P. WESSELING, AND C. G. M. KASSELS, *Schwarz domain decomposition for the incompressible Navier–Stokes equations in general co-ordinates*, International Journal for Numerical Methods in Fluids, 32 (2000), pp. 141–173.

[22] H. BREZIS, *Analyse fonctionnelle. Théorie et applications*, Mathématiques appliquées pour la maîtrise, Masson, 1987.

[23] T. Cadeau and F. Magoulès, *Coupling the Parareal algorithm with the waveform relaxation method for the solution of differential algebraic equations*, in 2011 10th International Symposium on Distributed Computing and Applications to Business, Engineering and Science, 2011, pp. 15–19.

[24] F. Caetano, M. J. Gander, L. Halpern, and J. Szeftel, *Schwarz waveform relaxation algorithms for semilinear reaction-diffusion equations*, Networks and Heterogeneous Media, 5 (2010), pp. 487–505.

[25] X.-C. Cai, *Additive Schwarz algorithms for parabolic convection-diffusion equations*, Numerische Mathematik, 60 (1991), pp. 41–61.

[26] C. Calvin, O. Cueto, and P. Emonot, *An object-oriented approach to the design of fluid mechanics software*, ESAIM Mathematical Modelling and Numerical Analysis, 36 (2002), pp. 907–921.

[27] CEA/DEN/DANS/DM2S/STMF/LMSF, *Trio_U user's manual v1.7.0*, (2014).

[28] T. Chacón Rebollo and E. Chacón Vera, *Study of a non-overlapping domain decomposition method: Poisson and Stokes problems*, Applied Numerical Mathematics, 48 (2004), pp. 169 – 194.

[29] T. Chacon Rebollo and E. Chacon Vera, *Study of a non-overlapping domain decomposition method: Steady Navier–Stokes equations*, Applied Numerical Mathematics, 55 (2005), pp. 100 – 124.

[30] M. Chandesris, A. D'Hueppe, B. Mathieu, D. Jamet, and G. Benoit, *Direct numerical simulation of turbulent heat transfer in a fluid-porous domain*, Physics of Fluids, 25 (2013), p. 125110.

[31] P. Chartier and B. Philippe, *A parallel shooting technique for solving dissipative ODE's*, Computing, 51 (1993), pp. 209–236.

[32] W. Chen, M. Gunzburger, F. Hua, and X. Wang, *A parallel Robin–Robin domain decomposition method for the Stokes-–Darcy system*, SIAM Journal on Numerical Analysis, 49 (2011), pp. 1064–1084.

[33] D. Cherel, *Décomposition de domaine pour des systèmes issus des équations de Navier-Stokes*, PhD thesis, Université Grenoble Alpes, 2012.

[34] O. Ciobanu, L. Halpern, X. Juvigny, and J. Ryan, *Overlapping domain decomposition applied to the Navier-Stokes equations*, in Domain Decomposition Methods in Science and Engineering XXII, T. Dickopf, M. J. Gander, L. Halpern, R. Krause, and L. F. Pavarino, eds., Cham, 2016, Springer International Publishing, pp. 461–470.

[35] O. A. Ciobanu, *Méthode de décomposition de domaine avec adaptation de maillage en espace-temps pour les équations d'Euler et de Navier-Stokes*, PhD thesis, Université Paris 13, 2014.

[36] R. Croce, D. Ruprecht, and R. Krause, *Parallel-in-space-and-time simulation of the three-dimensional, unsteady Navier-Stokes equations for incompressible flow*, in Modeling, Simulation and Optimization of Complex Processes - HPSC 2012, H. G.

Bock, X. P. Hoang, R. Rannacher, and J. P. Schlöder, eds., Cham, 2014, Springer International Publishing, pp. 13–23.

[37] X. DAI AND Y. MADAY, *Stable Parareal in time method for first- and second-order hyperbolic systems*, SIAM Journal on Scientific Computing, 35 (2013), pp. A52–A78.

[38] M. DISCACCIATI, A. QUARTERONI, AND A. VALLI, *Robin-–Robin domain decomposition methods for the Stokes—Darcy coupling*, SIAM Journal on Numerical Analysis, 45 (2007), pp. 1246–1268.

[39] V. DOLEAN, P. JOLIVET, AND F. NATAF, *An introduction to domain decomposition methods*, Society for Industrial and Applied Mathematics (SIAM), Philadelphia, PA, 2015. Algorithms, theory, and parallel implementation.

[40] V. DOLEAN, F. NATAF, AND G. RAPIN, *Deriving a new domain decomposition method for the Stokes equations using the Smith factorization*, Mathematics of Computation, 78 (2009), pp. 789–814.

[41] A. ERN AND J.-L. GUERMOND, *Theory and practice of finite elements*, Springer, New York, 2004.

[42] V. ERVIN, E. JENKINS, AND H. LEE, *Approximation of the Stokes–Darcy system by optimization*, Journal of Scientific Computing, 59 (2014).

[43] P. F. FISCHER, F. HECHT, AND Y. MADAY, *A Parareal in time semi-implicit approximation of the Navier-Stokes equations*, in Domain Decomposition Methods in Science and Engineering, T. J. Barth, M. Griebel, D. E. Keyes, R. M. Nieminen, D. Roose, T. Schlick, R. Kornhuber, R. Hoppe, J. Périaux, O. Pironneau, O. Widlund, and J. Xu, eds., Berlin, Heidelberg, 2005, Springer Berlin Heidelberg, pp. 433–440.

[44] L. FOLTYN, D. LUKÁŠ, AND I. PETEREK, *Domain decomposition methods coupled with Parareal for the transient heat equation in 1 and 2 spatial dimensions*, Applications of Mathematics, 65 (2020), pp. 173–190.

[45] M. J. GANDER, *Overlapping Schwarz for parabolic problems*, in Proceedings of the 9th international conference on domain decomposition methods (3-8 June 1996), P. E. Bjørstad, M. S. Espedal, and D. E. Keyes, eds., ddm.org, 1998, pp. 97–104.

[46] ———, *Optimized Schwarz methods*, SIAM J. Numerical Analysis, 44 (2006), pp. 699–731.

[47] M. J. GANDER, *50 years of time parallel time integration*, in Multiple Shooting and Time Domain Decomposition Methods, T. Carraro, M. Geiger, S. Körkel, and R. Rannacher, eds., Cham, 2015, Springer International Publishing, pp. 69–113.

[48] M. J. GANDER AND E. HAIRER, *Nonlinear convergence analysis for the Parareal algorithm*, in Domain Decomposition Methods in Science and Engineering XVII, U. Langer, M. Discacciati, D. E. Keyes, O. B. Widlund, and W. Zulehner, eds., Berlin, Heidelberg, 2008, Springer Berlin Heidelberg, pp. 45–56.

[49] M. J. GANDER AND L. HALPERN, *Absorbing boundary conditions for the wave equation and parallel computing*, Math. Comput., 74 (2005), pp. 153–176.

[50] M. J. GANDER AND L. HALPERN, *Optimized Schwarz waveform relaxation methods for advection reaction diffusion problems*, SIAM J. Numer. Anal., 45 (2007), pp. 666–697.

[51] M. J. GANDER, L. HALPERN, AND F. NATAF, *Optimal Convergence for Overlapping and Non-Overlapping Schwarz Waveform Relaxation*, in Proceedings of the 11th International Conference on Domain Decomposition Methods, C.-H. Lai, P. Bjørstad, M. Cross, and O. Widlund, eds., 1999, pp. 27–36.

[52] M. J. GANDER, L. HALPERN, AND F. NATAF, *Optimal Schwarz waveform relaxation for the one dimensional wave equation*, SIAM J. Numerical Analysis, 41 (2003), pp. 1643–1681.

[53] M. J. GANDER AND C. JAPHET, *Algorithm 932: PANG: software for nonmatching grid projections in 2D and 3D with linear complexity*, ACM Trans. Math. Software, 40 (2013), pp. Art. 6, 25.

[54] M. J. GANDER, Y. JIANG, AND B. SONG, *A superlinear convergence estimate for the Parareal Schwarz waveform relaxation algorithm*, SIAM Journal on Scientific Computing, 41 (2019), pp. A1148–A1169.

[55] M. J. GANDER, Y.-L. JIANG, AND R.-J. LI, *Parareal Schwarz waveform relaxation methods*, in Domain Decomposition Methods in Science and Engineering XX, R. Bank, M. Holst, O. Widlund, and J. Xu, eds., Berlin, Heidelberg, 2013, Springer Berlin Heidelberg, pp. 451–458.

[56] M. J. GANDER AND S. VANDEWALLE, *Analysis of the Parareal time-parallel time-integration method*, SIAM J. Scientific Computing, 29 (2007), pp. 556–578.

[57] E. GILADI AND H. KELLER, *Space-time domain decomposition for parabolic problems*, Numerische Mathematik, 93 (2002), pp. 279–313.

[58] V. GIRAULT, B. RIVIÈRE, AND M. WHEELER, *A discontinuous Galerkin method with nonoverlapping domain decomposition for the Stokes and Navier-Stokes problems*, Math. Comput., 74 (2005), pp. 53–84.

[59] R. GUETAT, *Méthode de parallélisation en temps : application aux méthodes de décomposition de domaine*, PhD thesis, UPMC Université Paris 6 et Ecole polytechnique de Tunisie, 2011.

[60] M. D. GUNZBURGER AND H. K. LEE, *An optimization-based domain decomposition method for the Navier-Stokes equations*, SIAM J. Numer. Anal., 37 (2000), pp. 1455–1480.

[61] F. HAEBERLEIN, *Méthodes de décomposition de domaine espace temps pour le transport réactif : Application au stockage géologique de CO2*, PhD thesis, Université Paris 13, 2011.

[62] L. HALPERN, *Local space-time refinement for the one-dimensional wave equation*, Journal of Computational Acoustics, 13 (2005), pp. 547–568.

[63] L. HALPERN AND F. HUBERT, *A finite volume Ventcell-Schwarz algorithm for advection-diffusion equations*, SIAM Journal on Numerical Analysis, 52 (2014), pp. 1269–1291.

[64] L. HALPERN, C. JAPHET, AND J. SZEFTEL, *Optimized Schwarz waveform relaxation and discontinuous Galerkin time stepping for heterogeneous problems*, SIAM J. Numer. Anal., 50 (2012), pp. 2588–2611.

[65] L. HALPERN AND J. SZEFTEL, *Nonlinear nonoverlapping Schwarz waveform relaxation for semilinear wave propagation*, Math. Comput., 78 (2009), pp. 865–889.

[66] F. HECHT, *New development in freefem++*, J. Numer. Math., 20 (2012), pp. 251–265.

[67] A. HEINLEIN, C. HOCHMUTH, AND A. KLAWONN, *Monolithic overlapping Schwarz domain decomposition methods with GDSW coarse spaces for incompressible fluid flow problems*, SIAM Journal on Scientific Computing, 41 (2019), pp. C291–C316.

[68] T. HOANG, J. JAFFRÉ, C. JAPHET, M. KERN, AND J. ROBERTS, *Space-Time Domain Decomposition Methods for Diffusion Problems in Mixed Formulations*, SIAM J. Numer. Anal., 51 (2013), pp. 3532–3559.

[69] T.-T.-P. HOANG, JAPHET, M. KERN, AND J. E. ROBERTS, *Space-Time Domain Decomposition for Reduced Fracture Models in Mixed Formulation*, SIAM J. Numer. Anal., 54 (2016), pp. 288–316.

[70] E. ISSMAN AND G. DEGREZ, *Non-overlapping preconditioners for a parallel implicit Navier-Stokes solver*, Future Gener. Comput. Syst., 13 (1998), pp. 303–313.

[71] C. JAPHET, *The Optimized Krylov-Ventcell method. application to convection-diffusion problems*, in Proceedings of the 9th International Conference on Domain Decomposition Methods (3-8 June 1996), P. Bjorstad, M. Espedal, and D. Keyes, eds., ddm.org, 1998, pp. 382–389.

[72] C. JAPHET, Y. MADAY, AND F. NATAF, *A new interface cement equilibrated mortar method with Ventcel conditions*, in Domain decomposition methods in science and engineering XXI, J. Erhel, M. J. Gander, L. Halpern, G. Pichot, T. Sassi, and O. Widlund, eds., vol. 98 of Lect. Notes Comput. Sci. Eng., Springer, 2014, pp. 329–336.

[73] C. JAPHET AND F. NATAF, *The best interface conditions for domain decomposition methods: absorbing boundary conditions*, Absorbing boundaries and layers, domain decomposition methods, Nova Sci. Publ.,Huntington, NY, (2001), p. 348–373.

[74] C. JAPHET, F. NATAF, AND F. ROGIER, *The Optimized Order 2 method: Application to convection–diffusion problems*, Future Generation Computer Systems, 18 (2001), pp. 17–30.

[75] S. KANG, L. NGO, H. GWON CHOI, W. CHUNG, Y.-H. YOO, AND J. YOO, *Performance comparison of parallel ILU preconditioners for the incompressible Navier-Stokes equations*, Journal of Mechanical Science and Technology, 34 (2020), pp. 1175–1184.

[76] F. KONG, Y. MA, AND A. LU, *An optimization-based domain decomposition method for numerical simulation of the incompressible Navier-Stokes flows*, Numerical Methods for Partial Differential Equations, 27 (2011), pp. 255 – 276.

[77] Y. KUZNETSOV, *Domain decomposition methods for unsteady convection-diffusion problems*, in Computing methods in applied sciences and engineering (Paris, 1990), SIAM, Philadelphia, PA, 1990, 1990, pp. 211–227.

[78] O. A. LADYZHENSKAYA, *The Mathematical Theory of Viscous Incompressible Flow*, Gordon and Breach, Sciences Publishers, 1963.

[79] E. LELARASMEE, A. E. RUEHLI, AND A. L. SANGIOVANNI-VINCENTELLI, *The waveform relaxation method for time-domain analysis of large scale integrated circuits*, IEEE Transactions on Computer-Aided Design of Integrated Circuits and Systems, 1 (1982), pp. 131–145.

[80] F. LEMARIÉ, L. DEBREU, AND E. BLAYO, *Toward an optimized global-in-time Schwarz algorithm for diffusion equations with discontinuous and spatially variable coefficients. Part 2: The variable coefficients case*, Electron. Trans. Numer. Anal., 40 (2013), pp. 170–186.

[81] E. LINDELOF, *Sur l'application des méthodes d'approximations successives à l'etude des intégrales réelles des équations difféerentielles ordinaires*, Journal de Mathematiques Pures et Appliquées, (1894), pp. 117–128.

[82] J.-L. LIONS, Y. MADAY, AND G. TURINICI, *A "Parareal" in time discretization of PDE's*, Comptes Rendus de l'Académie des Sciences - Series I - Mathematics, 332 (2001), pp. 661–668.

[83] J.-L. LIONS AND E. MAGENES, *Non-homogeneous boundary value problems and applications. Vol. I*, Springer-Verlag, New York, 1972. Translated from the French by P. Kenneth, Die Grundlehren der mathematischen Wissenschaften, Band 181.

[84] ——, *Non-homogeneous boundary value problems and applications. Vol. II*, Springer-Verlag, New York, 1972. Translated from the French by P. Kenneth, Die Grundlehren der mathematischen Wissenschaften, Band 182.

[85] P.-L. LIONS, *On the Schwarz alternating method. I*, in First International Symposium on Domain Decomposition Methods for Partial Differential Equations, M. G. A., R. Glowinski, G. G. H., and P. J., eds., Philadelphia, PA, SIAM, 1988, pp. 1–42.

[86] ——, *On the Schwarz alternating method. III: a variant for nonoverlapping subdomains*, in Third International Symposium on Domain Decomposition Methods for Partial Differential Equations, R. G. J. P. T. F. Chan and O. Widlund, eds., Philadelphia, PA, SIAM, 1990, pp. 202–223.

[87] G. LISSONI, *DDFV method : applications to fluid mechanics and domain decomposition*, PhD thesis, COMUE Université Côte d'Azur, 2019.

[88] G. LUBE, L. MÜLLER, AND H. MÜLLER, *A new non-overlapping domain decomposition method for stabilized finite element methods applied to the non-stationary Navier-Stokes equations*, Numerical Linear Algebra with Applications, 7 (2000), pp. 449–472.

[89] Y. MADAY AND G. TURINICI, *The Parareal in time iterative solver: a further direction to parallel implementation*, in Domain Decomposition Methods in Science and Engineering, T. J. Barth, M. Griebel, D. E. Keyes, R. M. Nieminen, D. Roose, T. Schlick, R. Kornhuber, R. Hoppe, J. Périaux, O. Pironneau, O. Widlund, and J. Xu, eds., Berlin, Heidelberg, 2005, Springer Berlin Heidelberg, pp. 441–448.

[90] F. MAGOULÈS, G. GBIKPI-BENISSAN, AND Q. ZOU, *Asynchronous iterations of Parareal algorithm for option pricing models*, Mathematics, 6 (2018), p. 45.

[91] V. MARTIN, *An optimized Schwarz waveform relaxation method for the unsteady convection diffusion equation in two dimensions*, Appl. Numer. Math., 52 (2005), pp. 401–428.

[92] V. MARTIN, *Schwarz waveform relaxation algorithms for the linear viscous equatorial shallow water equations*, SIAM J. Scientific Computing, 31 (2009), pp. 3595–3625.

[93] O. MULA HERNANDEZ, *Quelques contributions vers la simulation parallèle de la cinétique neutronique et la prise en compte de données observées en temps réel*, PhD thesis, UPMC Université Paris 6, 2014.

[94] J. NIEVERGELT, *Parallel methods for integrating ordinary differential equations*, Commun. ACM, 7 (1964), pp. 731–733.

[95] C. PELLETIER, *Mathematical study of the air-sea coupling problem including turbulent scale effects*, PhD thesis, Université Grenoble Alpes, 2018.

[96] E. PICARD, *Sur l'application des méthodes d'approximations successives à l'etude de certaines équations différentielles ordinaires*, Journal de Mathematiques Pures et Appliquées, (1893), pp. 217–271.

[97] A. QUARTERONI AND A. VALLI, *Domain decomposition methods for partial differential equations*, Numerical Mathematics and Scientific Computation, Oxford University Press, New York, 1999. Oxford Science Publications.

[98] A. RASHKOVAN, U. BIEDER, J. BRINSTER, L. ISHAY, AND G. ZISKIND, *Simulation of LOWMA-3 MISTRA experiment*, in Proceedings of 5th Computational Fluid Dynamics for Nuclear Reactor Safety (CFD4NRS) Workshop (Zurich, 9-11 September 2014), 2014.

[99] J. ROKICKI AND J. FLORYAN, *Domain decomposition and the compact fourth-order algorithm for the Navier-Stokes equations*, Journal of Computational Physics, 116 (1995), pp. 79 – 96.

[100] ——, *Higher-order unstructured domain decomposition method for Navier–Stokes equations*, Computers and Fluids, 28 (1999), pp. 87 – 120.

[101] E. M. RONQUIST, *A domain decomposition solver for the steady Navier-Stokes equations*, in ICOSAHOM95: Proceedings of the Third International Conference on Spectral and High Order Methods, 1995.

[102] H. A. SCHWARZ, *Gesammelte mathematische Abhandlungen. Band I, II*, Chelsea Publishing Co., New York, 1972.

[103] T. SENGUPTA, A. DIPANKAR, AND A. K. RAO, *A new compact scheme for parallel computing using domain decomposition*, Journal of Computational Physics, 220 (2007), pp. 654 – 677.

[104] P. SMOLARKIEWICZ, *The multi-dimensional crowley advection scheme*, Monthly Weather Review, 110 (1982), pp. 1968–1983.

[105] B. SONG, Y.-L. JIANG, AND X. WANG, *Analysis of two new Parareal algorithms based on the Dirichlet-Neumann/Neumann-Neumann waveform relaxation method for the heat equation*, Numerical Algorithms, 86 (2021), pp. 1685–1703.

[106] L. SONKE, *Analysis of domain decomposition for non symmetric problems : application to the Navier-Stokes equations*, ESAIM: Mathematical Modelling and Numerical Analysis - Modélisation Mathématique et Analyse Numérique, 26 (1992), pp. 289–307.

[107] J. STEINER, D. RUPRECHT, R. SPECK, AND R. KRAUSE, *Convergence of Parareal for the Navier-Stokes equations depending on the Reynolds number*, in Numerical Mathematics and Advanced Applications - ENUMATH 2013, A. Abdulle, S. Deparis, D. Kressner, F. Nobile, and M. Picasso, eds., Cham, 2015, Springer International Publishing, pp. 195–202.

[108] Y. TAKAHASHI, K. FUJIWARA, T. IWASHITA, AND H. NAKASHIMA, *Parallel finite-element method using domain decomposition and Parareal for transient motor starting analysis*, COMPEL - The international journal for computation and mathematics in electrical and electronic engineering, ahead-of-print (2019).

[109] M. TAYACHI PIGEONNAT, A. ROUSSEAU, E. BLAYO, N. GOUTAL, AND V. MARTIN, *Design and analysis of a Schwarz coupling method for a dimensionally heterogeneous problem*, International Journal for Numerical Methods in Fluids, 75 (2014), pp. 446–465.

[110] S. THÉRY, *Etude numérique des algorithmes de couplage océan-atmosphère avec prise en compte des paramétrisations physiques des couches limites*, PhD thesis, Université Grenoble Alpes (ComUE), 2021.

[111] S. THÉRY, C. PELLETIER, F. LEMARIÉ, AND E. BLAYO, *Analysis of Schwarz Waveform Relaxation for the Coupled Ekman Boundary Layer Problem with Continuously Variable Coefficients*. working paper or preprint, https://hal.inria.fr/hal-02544113, 2020.

[112] D. XIAO, C. HEANEY, I. NAVON, AND C. PAIN, *A domain decomposition method for the non-intrusive reduced order modelling of fluid flow*, Computer Methods in Applied Mechanics and Engineering, 354 (2019).

[113] X. XU, C. O. CHOW, AND S. H. LUI, *On nonoverlapping domain decomposition methods for the incompressible Navier-Stokes equations*, ESAIM: Mathematical Modelling and Numerical Analysis - Modélisation Mathématique et Analyse Numérique, 39 (2005), pp. 1251–1269.

[114] Y. Xu, *Optimized Schwarz methods with Ventcell transmission conditions for model problems with continuously variable coefficients*, Journal of Computational and Applied Mathematics, 334 (2018), pp. 97 – 110.

[115] W. Yushan, *Solving incompressible Navier-Stokes equations on heterogeneous parallel architectures.*, PhD thesis, Université Paris Sud - Paris XI, 2015.